ISAS - INTERNATIONAL SCHOOL FOR ADVANCED STUDIES

From Quantum Spins to Correlated Fermions: a New Strong Coupling Method

Thesis submitted for the degree of

"Doctor Philosophiæ"

CANDIDATE

Michela Di Stasio

SUPERVISORS

Prof. Giuseppe Morandi

Prof. Arturo Tagliacozzo

October 1993

TRIESTE

SISSA - SCUOLA INTERNAZIONALE SUPERIORE DI STUDI AVANZATI

TRIESTE

Strada Costiera 11

From Quantum Spins to Correlated Fermions: a New Strong Coupling Method

Thesis submitted for the degree of

"Doctor Philosophiæ"

CANDIDATE

Michela Di Stasio

SUPERVISORS

Prof. Giuseppe Morandi

Prof. Arturo Tagliacozzo

October 1993

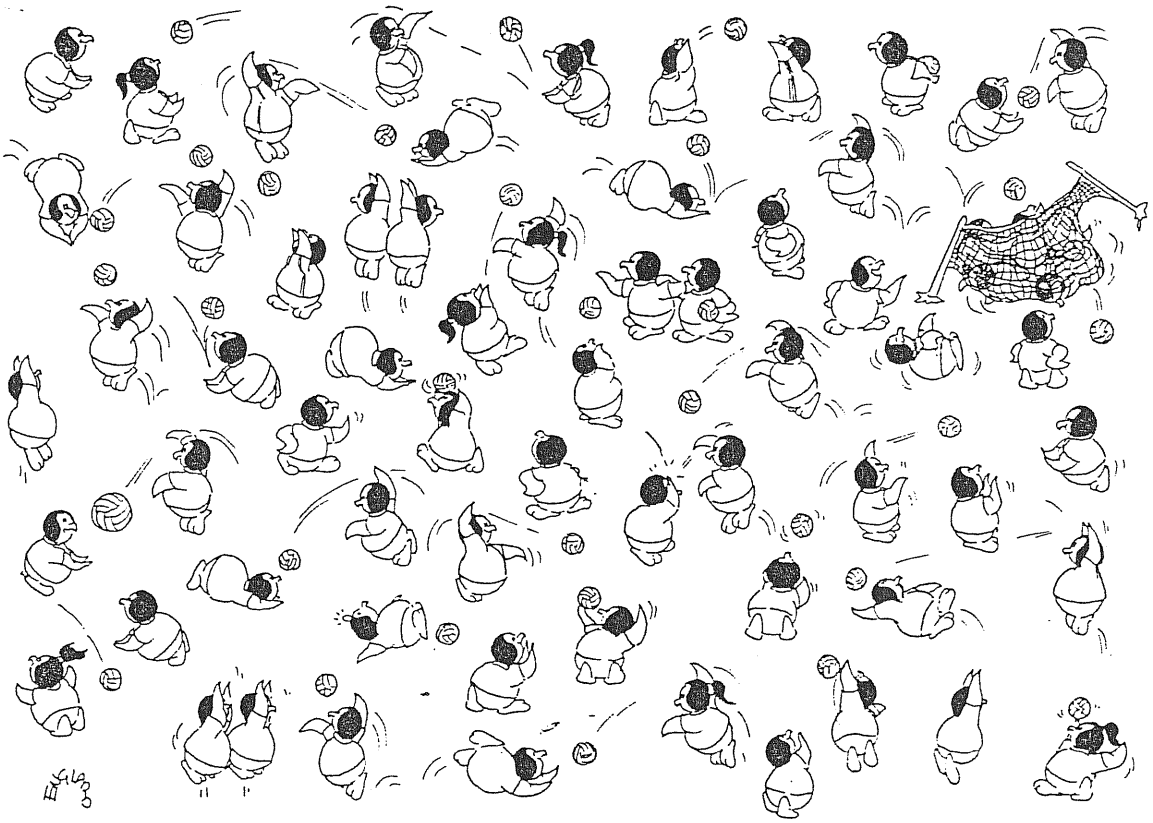

Acknowledgements

It is a pleasure for me to express my gratitude to my supervisors Arturo and Giuseppe. Not only for they have introduced me in this research field and for the helps that I have always received from them but also for their very kind hospitality in Napoli and Bologna.

I would like also to thank to all the friends and colleagues I have met here in SISSA. Especially, for the frequent friendly scientific discussions: José Lorenzana, Marta Nolasco and Michele Fabrizio. Finally, I aknowledge the friendly scientific and graphical support by Sergio Ciuchi.

Table of Contents

Chapter 1

Introduction

Theoretical investigations of strongly correlated electron systems are notoriously very difficult in particular in two and three spatial dimensions. Many fundamental questions are still open. The reasons to quote the high-T_c superconductors[1] (HTCS) enigma without addressing to any extent the superconductivity itself are essentially two.

1) After their discovery it was realized that some of the most basic problems in condensed matter physics were not yet understood. In particular, the arise of magnetic correlations as a consequence of strong interactions between electrons, the influence of mobile vacancies on such magnetic states and the effect of disorder on the correlated behavior of electrons.

2) It came up in clear evidence the need of controlled approximations to investigate the strong coupling limit of the electronic interactions. As a matter of fact the standard tools do not seems to be adequate.

These problems have triggered our attention to the search for a new method to treat strong correlations.

The cuprate compounds that undergo an HTCS transition have a very rich phase

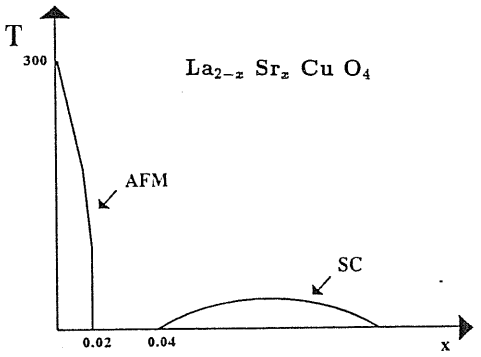

Figure 1.1: The T_c versus doping (x) schematic phase diagram of $La_{2-x}Sr_xCuO_4$.

diagram. The stoichiometric compound are antiferromagnetic (AFM) insulators. The antiferromagnetic phase is quickly destroyed by a small amount of doping. Increasing further the doping concentration they show a superconducting region with a remarkable high critical temperature. Many experiments demonstrate their 2D character[2] and the presence of strong correlations in the CuO_2 planes[3]. Up to now many of the normal state properties of these material are still not well understood.

Among the various model proposed the 2D Hubbard model [4] is widely believed to contain the essential correlations of the active electrons in the CuO_2 planes[5].

The Hubbard hamiltonian contains the kinetic energy and the on-site correlation U. In the large U limit this hamiltonian is often handled on the restricted Hilbert space of no-doubly occupied sites. What this constraint tells us is that one has to evaluate thermodynamical quantities as traces over a restricted Hilbert space for the fermions. On this space a t/U expansion can be performed, giving rise to the so called $t-J$ model[6].

At half filling this becomes the Heisenberg hamiltonian and this is believed to describe correctly the electronic properties of HTCS materials in the absence of doping or at half-filling[7].

We can summarize or extract the question:

What happens when a 2-dimensional Spin 1/2 antiferromagnet get disordered?

As one can easily see the Néel state has an unconserved order parameter ($[S^z, H] \neq 0$) with respect to the Heisenberg hamiltonian. This means that the quantum AFM phase can get disordered also at zero temperature due to quantum fluctuations. This goes in the opposite direction with respect to the classical case in which the disordering role is played by the temperature.

Moreover, we are dealing with the physical situation in which quantum fluctuations are strongly enhanced: low spatial dimensions 2D, small spin S=1/2, and eventually the presence of frustration. The understanding of quantum critical phenomena in 2D is still far from complete [8], [9]. On one hand, quantum fluctuations may here, as in 1D, be sufficiently strong to drive the system across critical points not expected from scenarios of mean field type. On the other hand, unlike the 1D case, there are few exact results available which can guide in the searching for the corresponding phases.

Our works originate from the observation that instead of evaluating directly the partition function as a trace over the restricted Hilbert space one can recover it through functional derivatives of a suitable generating functional.

In the case of the spin 1/2 Heisenberg Hamiltonians the single site occupancy constraint takes a very simple form and can be implemented exactly at all temperatures. In this restricted Hilbert space we can adopt the fermionic representation of the spin operators via the Pauli matrices. This representation is a very natural one in studying non magnetic phases such as dimerized phases or flux and chiral phases.

Within the saddle point approximation and in connection with the large N expansions (in the SU(N) symmetry group generalization of the SU(2) Heisenberg model) it was

applied by many authors [10], [11], [12] to the study of these phases.

We have shown that the inclusion of the projector together with the classical and quantum corrections gives correct thermodynamical behaviors.

Even if numerical studies[13] show that the antiferromagnetic correlations are the dominant ones in the ground state, our aim was to study, on the same footing, the AFM phase and the other non-magnetic phases at finite temperatures. We have shown that our constrained fermionization scheme reproduces first of all the well known results for the AFM phases with its spin waves corrections. The inclusion of the constraint turns out to be an essential ingredient either to reproduce the static mean field solution or to obtain a tractable Berry phase[14] from the adiabatic expansion (what is the content of paper VIII).

We have also studied the effect of the constraint on the above non magnetic phases. In absence of the constraint our one loop expansion recovers the $1/N$ corrections by Read and Sachdev[15] for the dimerized phases.

Coming back to the HTCS it was argued[16] that the dynamical frustration induced by the holes could be to some extent replaced by an effective static frustration between next nearest neighbors. Although it was shown[17] that this effective description can be inadequate when dealing with dynamical quantities it is either a first step towards the doped case or an interesting subject *per se*. In the presence of frustration the nature of the ground state is quite controversial. Among the non-magnetically ordered states proposed there are the dimer phases in which spin singlets are formed between nearest neighbor sites filling all the links in the lattice. Their generalization to Resonant Valence Bond (RVB) states have been proposed as competitive ground state for the HTCS material in their normal phase[5]. Another proposal for a possible ground state of the frustrated Heisenberg Hamiltonian was that of the flux or chiral states. The order parameter of the latter breaks

parity and time reversal and can give rise to an exotic form of superconductivity that is called anyon superconductivity[18]. Our method can be generalized to the study of any spin Hamiltonian and it has been applied to the study of the phases described above in the frustrated Heisenberg Hamiltonian.

The last Chapter of this thesis is devoted to the extension of our method away from the half-filled case. In going away from half-filling the inclusion of the projector is much more complicated. Here the projector is the Gutzwiller projector of no double occupancy of sites. The difficulties arise because the projector and the Hamiltonian do not commute. Given the Path Integral description of the partition function the projector must be implemented at each time slice of the imaginary time interval $[0, \beta]$. This very fact implies that the generating functional contains source terms that do not commute with the kinetic part of the Hamiltonian so that an explicit evaluation of the time ordering is needed. We have checked on a two-site molecule example that the limit of an infinite number of time slices converges.

Chapter 2 is an introduction to the physics of quantum spin models. In this Chapter I have tried to illustrate few other methods as the large S and large N expansion and the adiabatic expansion to allow for a comparison with our results.

Chapter 3 introduces to our method and to its application to magnetic (see paper IV,V) and non magnetic phases (see paper I,II,III,VI,VII) in the spin 1/2 Heisenberg models.

In Chapter 4 our method has been developed for the infinite U Hubbard model and applied to the toy model of a two-site system.

This thesis includes copy of the works which are listed below:

- I : "Saddle-point finite-temperature results for the infinite-U Hubbard model at half-filling" M. Di Stasio, E. Ercolessi, G. Morandi, A. Tagliacozzo and F. Ventriglia

Phys.Rev.B 45,1939 (1992)

- II : "Possible occurrence of constrained chiral phase in the frustrated Heisenberg model" M. Di Stasio Phys.Rev.B 46,9825 (1992)

- III : "Single site-occupancy constraint for the Hubbard model at finite temperature" M. Di Stasio, E. Ercolessi, G. Morandi, A. Tagliacozzo and F. Ventriglia Int. J. Mod. Phys.B 7,3281 (1993)

- IV : "Effects of quantum fluctuations in the large U Hubbard model at half-filling" M. Di Stasio, E. Ercolessi, G. Morandi and A. Tagliacozzo (submitted)

- V : " Finite temperature results from constrained fermionization in the 2D spin 1/2 Heisenberg antiferromagnet. I:the Néel phase " M. Di Stasio, E. Ercolessi, G. Morandi and A. Tagliacozzo (submitted)

- VI : " Finite temperature results from constrained fermionization in the 2D spin 1/2 Heisenberg antiferromagnet. I: dimer phases " M. Di Stasio, E. Ercolessi, G. Morandi and A. Tagliacozzo (submitted)

- VII :"Fluctuations around the magnetic and non-magnetic saddle points in the 2D spin 1/2 frustrated Heisenberg model" M. Di Stasio, E. Ercolessi, G. Morandi and A. Tagliacozzo (submitted)

- VIII :"Effective Action and Adiabatic Expansions for the 1-D and 2-D Hubbard models at half-filling" M. Di Stasio, E. Ercolessi, G. Morandi, R. Righi, A. Tagliacozzo and G.P.Zucchelli. (submitted)

Chapter 2

Approaches to Quantum Antiferromagnets

In this chapter I introduce some of the basic concepts related to quantum antiferromagnets that are described by Heisenberg hamiltonians. I present here some methods that have been used in the study of 2D quantum antiferromagnets and some of their results. The main aims are to give with simple exercises the ideas that have been developed in this field and to state the results and the methods to be compared with our results and our method. For an extensive review on the unfrustrated Heisenberg model in 2D, and its connection to the undoped HTCS materials, see Manousakis[13].

2.1 Singlets versus Néel order

The Hamiltonian we are dealing with is the antiferromagnetic ($J_{ij} > 0$) Heisenberg hamiltonian:

$$H = \sum_{(i,j)} J_{ij} \vec{S}_i \cdot \vec{S}_j \quad . \tag{2.1}$$

We refer to non frustrated case when $J_{ij} = J$ only if i , j are nearest neighbor sites on a bipartite lattice. In this case there is only one parameter in the model, the superexchange

energy J, which controls the temperature range.

In quantum mechanical spin systems, the spin $\vec{S}_i$ are vector operators. The x-,y- and z-components of the spin operator are the generators of the rotation group SU(2) and obey the commutation relations:

$$[S^\alpha, S^\beta] = i\epsilon^{\alpha\beta\gamma}S^\gamma. \tag{2.2}$$

ϵ being the totally antisymmetric 3×3 tensor. The ground state of quantum antiferromagnets is generically not known except in 1D from Bethe ansatz[19]. For bipartite lattices the classical ground state is the Néel state, where each sublattice is ferromagnetically ordered, but where the vectors on the different sublattices are antiparallel. However, in the quantum case the Néel state is not even an eigenstate of the hamiltonian.

This can be easily seen in the very simple example of a two-site system. Here we have:

$$H = \vec{S}_1 \cdot \vec{S}_2 = \frac{1}{2}(S_1^+ S_2^- + S_1^- S_2^+) + S_1^z S_2^z \tag{2.3}$$

The action of H on the Néel state is given by:

$$\vec{S}_1 \cdot \vec{S}_2 | \uparrow\downarrow> = \frac{1}{2}| \downarrow\uparrow> - \frac{1}{4}| \uparrow\downarrow> \tag{2.4}$$

thus the Néel state is not an eigenstate to H. If one prepares the system to be in the $| \uparrow\downarrow>$ state at time $t = 0$, then the time evolution operator $U(t) = \exp(iHt)$ flips the antiparallel spins up and down thus giving rise to quantum fluctuations also at temperature $T = 0$.

For the two-site system the ground state is instead given by:

$$|(12)> = \frac{1}{\sqrt{2}}(| \uparrow\downarrow> - | \downarrow\uparrow>) \tag{2.5}$$

which is an eigenstate of $\{S_{tot}^2, S_{tot}^z\}$ with eigenvalues $\{0, 0\}$.This state is a singlet.

From this simple example originate many questions for the more spins case. One wonder to know whether or not the ground state of a quantum antiferromagnet can be some sort of Néel state, if it is always a singlet and how many singlets are there.

The Marshall theorem[20] tells us that the ground state of a quantum antiferromagnet is a singlet when the lattice is bipartite and when only nearest neighbor interactions are present.

Consider a bipartite lattice and assign a valence bond like that of eq.(2.5) to each pair of a given partition[21]. Now we can define a valence bond state as the tensor product of the valence bond for each pair:

$$|VB>=\prod_{pairs}|(ij)> \tag{2.6}$$

All singlets may be constructed by a linear combination of valence bond states.

$$|Singlet>=\sum_{P}A(P)\prod_{pairs}|(i_kj_k)> \tag{2.7}$$

where $A(P)$ is the amplitude corresponding to the partition $P=\{(i_kj_k)\}$ of the lattice sites. In these states all spins are paired up in singlets. However, it is worth to notice that the valence bond states are not orthogonal and in general they cannot be linearly independent. If we consider a factorized amplitude $A(P)$ dependent only on the distance between paired sites we end up with the Resonant Valence Bond (RVB) state.

$$|RVB>=\sum_{P}\prod_{pairs}a(|i_k-j_k|)|(i_kj_k)> \tag{2.8}$$

where the optimal function $a(|i_k-j_k|)$ can be determined by a variational calculation[22]. The "resonance" comes from the fact that all the valence bond states with sites at the same relative distance enter with the same amplitude. This state has been proposed by

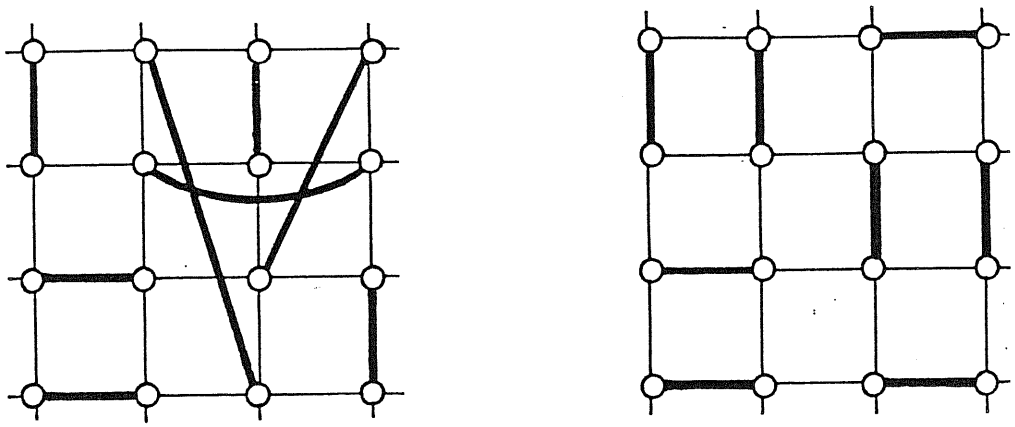

Figure 2.1: Long range and short range examples of valence bond states.

Anderson[23] as competitive ground state candidate for frustrated antiferromagnets as well as for the HTCS in their normal phase[5].

When pairs are formed only between nearest neighbor sites and all such configurations are linearly superposed with equal amplitude one gets the short range RVB state[24]. Here the configurations of valence bonds can be thought of as configurations of classical dimers that occupy the bonds.

In a 2D square lattice numerical studies[22] indicate that the RVB with fairly long range is a good approximation to the ground state while the short range version is not. It is worth to note that the long range RVB is a sort of Néel state.

A quantum Néel state is a state with a non-vanishing expectation value of the staggered magnetization. The latter is defined as:

$$M^z = < \sum_i (-1)^{R_i} S_i^z > \tag{2.9}$$

where $(-1)^{R_i} = \pm 1$ on the different sublattices. The original SU(2)symmetry of the problem is spontaneously broken in the Néel state down to a U(1) rotational symmetry

around the z axis. According to Goldstone's theorem there must be two massless modes. These are the spin waves.

The staggered magnetization that is the order parameter of the Néel state is not conserved. Its fluctuations can be strong enough to induce a quantum phase transition to a disordered state. The parameters that control this fluctuations are the dimensionality, the smallness of the spin and the presence of frustration.

For the 2D $S = 1/2$ unfrustrated Heisenberg model on a square lattice there are only numerical evidences that the ground state has antiferromagnetic long range order[25],[26],[27]. The question is still open for other lattices. Also for the frustrated case the situation is far from being clear.

Moreover, for all values of S, the LRO in 2D is unstable against thermal fluctuations as follows from the Mermin-Wagner theorem[28].

2.2 Large S expansion: spin waves

To study whether or not the Néel state can be a qualitatively correct approximation to the quantum antiferromagnet ground state may be convenient to perturb away from a limit in which the Néel state becomes exact. This occurs for a spin S Heisenberg AFM in the limit $S \to \infty$. In this limit quantum spins becomes classical because the commutator is much smaller than the square of the spin variables: $[S^\alpha, S^\beta] = i\epsilon^{\alpha\beta\gamma}S^\gamma = \mathcal{O}(S) << \mathcal{O}(S^2)$. For large spin S we expect S^z to make relatively small deviations from $\pm S$. One can formalize this idea and study the corrections to the Néel state using the Holstein-Primakov transformation[29]. We can represent spin operators in terms of bosons, say boson "a" and boson "b" on the sublattices A and B respectively, as:

$$S^z = S - a^\dagger a \;\; ; \;\; S^- = \sqrt{2S}a^\dagger(1 - a^\dagger a/2S)^{1/2} \qquad \text{on sublattice A}$$
$$S^z = -S + b^\dagger b, \;\; ; \;\; S^- = \sqrt{2S}(1 - b^\dagger b/2S)^{1/2} b \qquad \text{on sublattice B} \qquad (2.10)$$

This produces the exact commutation relations and the constraint $\vec{S}^2 = S(S+1)$. The constraint on the number of bosons on each site $n_i \leq 2S$ is also satisfied. The state with $|S^z| = S$ corresponds to the state with no bosons present. We may develop[30] a systematic expansion in $1/S$ by expanding the square root in the definitions of $S^\pm$. (Note that in this approximation the constraint $n_i \leq 2S$ is no more satisfied). Including only quadratic terms in the hamiltonian and after a Bogoliubov transformation we end up, in Fourier space, with a diagonal hamiltonian:

$$H = 2JS \sum_k \sqrt{1 - \gamma^2(k)}(c_k^\dagger c_k + d_k^\dagger d_k) \qquad (2.11)$$

The excitations created by c and d are the spin waves and for the square lattice $\gamma(k) = (\cos k_x + \cos k_y)/2$. Their spectrum is $E(k) = 2JS\sqrt{1 - \gamma^2(k)}$. Inverting the Bogoliubov transformation we can calculate the reduction in the magnetization due to quantum fluctuations:

$$M^\star = S - \frac{1}{V}\sum_k \frac{1}{2}\left(\left(1 - \gamma^2(k)\right)^{-1/2} - 1\right) \qquad (2.12)$$

For the 2D square lattice we find $M^\star \approx S - 0.28 + \mathcal{O}(1/S)$.

As one can easily see[31] in the 1D case the correction is divergent at small wave numbers. This indicates the Néel state is destabilized in 1D, no matter how large S is.

2.3 Large N expansion: dimer phases

An examination of the quantum disordered phase requires an approach which is designed explicitly to be valid in a region well separated from the Néel ordered one[32]. To this end many generalizations of the SU(2) Heisenberg model have been introduced. Here I will show in some details the bosonic SU(N) generalization. Fermionic generalizations as well have been discussed in the literature[10],[11],[15]. One can introduce a Schwinger boson representation of the spins[33],[34]. Introducing two bosons $b_{\mu,i}$ ($\mu = 1, 2$) one writes:

$$\vec{S}_i = \frac{1}{2} b^\dagger_{\mu,i} \vec{\sigma}_{\mu\nu} b_{\nu,i} \tag{2.13}$$

with the local constraint $b^\dagger_{\mu,i} b_{\mu,i} = 2S$. Where $\vec{\sigma}$ are the Pauli matrices , and summation over repeated greek indices is implied. The main advantage of this representation is that the constraint is an equality, and hence can be implemented via a Lagrange multiplier.

The hamiltonian can be rewritten (neglecting additive constants) in the form:

$$H = -\frac{J}{2} \sum_{(i,j)} (\epsilon^{\alpha\beta} b^\dagger_{i\alpha} b^\dagger_{j\beta})(\epsilon^{\gamma\delta} b_{i\gamma} b_{j\delta}) \tag{2.14}$$

($\epsilon^{+-} = -\epsilon^{-+}$, $\epsilon^{++} = \epsilon^{--} = 0$). This form makes it clear that H counts the number of singlet bonds.

We have so far described the large S expansion what makes the system more classical. In terms of the representations of the SU(2) group it corresponds to increase the dimensions of the vector space and of the three matrices (plus the identity) generators of SU(2) that becomes $(2S+1) \times (2S+1)$.

In studying the disordered phase it is convenient to introduce another parameter: the flavor index α of the bosons is allowed to run from 1 to 2N (N integer). Here we look for

the fundamental representation (dimension 2N) of the SU(2N) group of rotations in this bosonic vector space.

It is clear that the spin has a precise physical meaning only for SU(2) (from its Casimir $\vec{S}^2$), however we define here on the "spin" S through the relation:

$$2S + 1 = n_c \geq 1 \tag{2.15}$$

where n_c is the dimension of the vector space on which the realization of SU(2N) acts.

In addition we want to impose the restriction that the "spins" on a pair of sites be able to combine to form a singlet state, thus generalizing the valence bond structure of SU(2). This valence bond formation is clearly a crucial feature determining the structure of the quantum disordered phase.

In the case of SU(2), given the fundamental representation of a spin operator acting on the vector space V_2, for the two sites case the vector space becomes the tensor product of each on site representation. It turns out to be

$$V_2 \otimes V_2 = V_1 + V_3 \tag{2.16}$$

where the lower indices give the dimension of the space. This representation of SU(2) can be decomposed in a sum of irreducible representations and one of them is a singlet V_1.

It is well known[35] that such a state cannot be obtain from SU(2N) with $N > 1$. In other words there is no generalization of the antisymmetric invariant tensor ϵ to general SU(2N). The proper generalization turns out to be the symplectic group Sp(N). The Sp(N) group is defined by the set of 2N×2N unitary modular matrices U such that:

$$U^T \mathcal{I} U = \mathcal{I} \tag{2.17}$$

where

$$\mathcal{I} = \begin{pmatrix} 0 & 1 & & & \\ -1 & 0 & & & \\ & & 0 & 1 & \\ & & -1 & 0 & \\ & & & & \ddots \end{pmatrix} \tag{2.18}$$

is the generalization of the ϵ tensor to N> 1. It is clear that $Sp(\mathrm{N}) \subset \mathrm{SU(N)}$ and it is worthwhile to note that $Sp(1) \cong \mathrm{SU(2)}$.

Now the b_i^α bosons transform as the fundamental representation of $Sp(\mathrm{N})$. Valence bonds:

$$< \mathcal{I}^{\alpha\beta} b_{i\alpha}^\dagger b_{j\beta}^\dagger > \tag{2.19}$$

can be formed between any two sites and this operator is a singlet under $Sp(\mathrm{N})$ because of eq.(2.17). We can prove that it is indeed invariant under the action of a matrix U of the group:

$$\begin{aligned} &\mathcal{I}_{\beta\gamma}(U_{\beta\alpha} b_\alpha^\dagger)(U_{\gamma\delta} b_\delta^\dagger) = \mathcal{I}_{\beta\gamma}(U^T_{\alpha\beta} b_\alpha^\dagger)(U_{\gamma\delta} b_\delta^\dagger) = \\ &= U^T_{\alpha\beta} \mathcal{I}_{\beta\gamma} U_{\gamma\delta} b_\alpha^\dagger b_\delta^\dagger = \mathcal{I}^{\alpha\delta} b_\alpha^\dagger b_\delta^\dagger \ . \end{aligned} \tag{2.20}$$

The natural generalization of the Heisenberg hamiltonian to general $Sp(\mathrm{N})$ is :

$$H = -\frac{J}{2N} \sum_{(i,j)} (\mathcal{I}^{\alpha\beta} b_{i\alpha}^\dagger b_{j\beta}^\dagger)(\mathcal{I}_{\gamma\delta} b_i^\gamma b_j^\delta) \tag{2.21}$$

where $\alpha, \beta, \gamma, \delta$ runs over 1,....,2N.

This is a two parameter generalization (n_c,N) and the phase diagram for the mean field phases is shown in Fig.(2.2).

It has been shown[15] that in the large N limit at fixed n_c the ground state is quantum dimer disordered. The low energy dynamics of H is described by an effective quantum

dimer model, with each dimer configuration representing a particular pairing of the sites into valence bonds.

At leading order (N= ∞) a very large set of degenerate ground states was found for n_c=2. This limit is equivalent to the fermionic large N theory of Affleck and Marston[10].

To split the degeneracy 1/N corrections have been calculated and the lowest energy state occurs when the dimer are arranged in columns[15].

Another solvable limit is obtained by fixing the ratio of n_c and N:

$$k = \frac{n_c}{N} \tag{2.22}$$

and subsequently taking the limit of large N. In the phase diagram of Fig.(2.2) it corresponds to changing the slope of the dashed line. It was found that there exists a critical value $k = k_c$ which separates the magnetically ordered and the quantum disordered phase.

In all these mean field theories at finite N the local constraint is only satisfied in the average. Because the $N \to \infty$ limit quenches all the fluctuations the constraint is fully implemented only at N=∞. Unfortunately, the physically interesting case is at N=2. Some 1/N expansions have been performed. It has been shown, for example using the Schwinger bosons (SB) large N expansion, that if there is long range order in the mean field theory the spontaneous staggered magnetization does not vanishes to all order of the 1/N expansion[36]. The 1/N corrections are described by diagrams which include lines for the SB propagators G_o interacting via fluctuating fields. A diagram which involves L loops (traces of products of G_o) and P propagators of the fluctuating fields is of order $(1/\mathrm{N})^{P-L}$. This allows for a comparison with our calculations because even if we have worked directly at N=2 the gaussian fluctuations we have calculated are exactly the 1/N corrections at N=2 when the local constraint of single site occupancy is neglected.

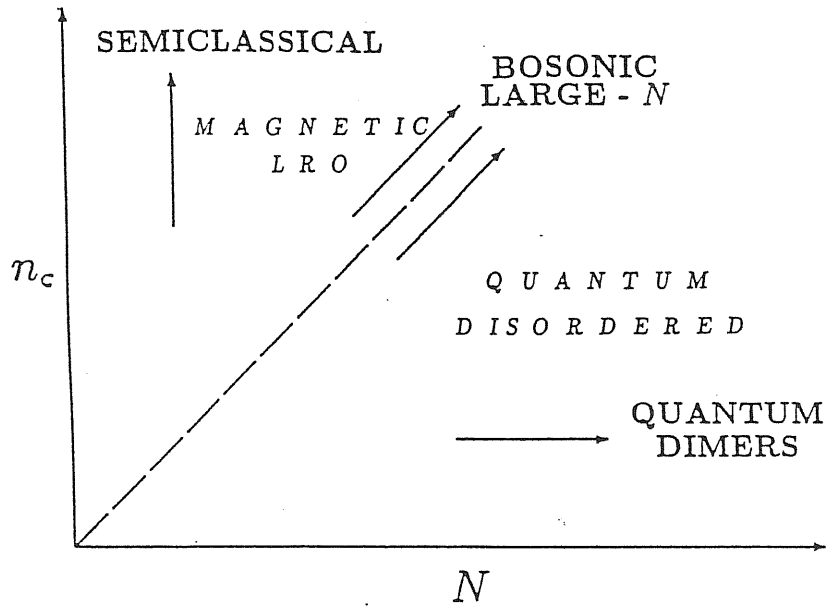

Figure 2.2: The Read and Sachdev phase diagram for generalized Heisenberg hamiltonians.

Another generalization of the Heisenberg hamiltonian to the $SU(N)$ symmetry group can be performed starting from the fermionic representation of the spin operators[10],[37]. Its asymptotic result can be located in the above phase diagram at $N \to \infty$ with n_c fix and finite. We have shown in our papers how our results can be directly compared to those results when $N = 2$. See papers IV and VI for more extensive discussions.

2.4 Adiabatic expansions

Up to now we have considered static mean field solutions and eventually the effects of including one-loop corrections around these solutions. Here we turn to the general, time-dependent case.

All the decoupling schemes of the interaction term are given in term of auxiliary fields. For example in the antiferromagnetic phase the magnetization field can be introduced as an auxiliary field to decouple the interaction term. The result is a system of spins in a

magnetization field. Now this field can be thought to be adiabatically varying. Adiabatic exchange provide a very simple way to make quantum parallel transport happen. The parallel transport of vectors is an intuitive example of anholonomy. It is a geometrical phenomenon in which non integrability causes some variables to fail to return to their original values when others, which drive them, are altered around a cycle. The variables that are cycled are parameters or auxiliary fields in the Hamiltonian of the system. If the cycling is slow, the adiabatic theorem guarantees that the system returns to its original state. However it acquires a non trivial phase that is the Berry phase[14].

A very simple example shows the appearance of the Berry phase. Consider the time dependent Hamiltonian:

$$H(t) = H\left(X(t)\right) \tag{2.23}$$

where $X(t) = \chi_k(t)$ $(k = 1, ..., N)$ and $0 \leq t \leq T$. The adiabatic theorem states that the solution of the Schrödinger equation:

$$i\partial_t \mid \psi(t) >= H(t) \mid \psi(t) > \tag{2.24}$$

are given by:

$$\mid \psi(t) >= e^{-i\int_0^t dt' E_n(X(t'))+i\gamma_n} \mid n; X(t) > \tag{2.25}$$

where $\mid n; X(t) >$ are the instantaneous eigenstates of $H(t)$:

$$H\left(X(t)\right) \mid n; X(t) >= E_n\left(X(t)\right) \tag{2.26}$$

and

$$\gamma_n = i\int_0^t d\tau \frac{d\chi_k(t)}{d\tau} < n; X(t) \mid \frac{\partial}{\partial\chi_k} n; X(t) > \tag{2.27}$$

is the Berry phase. If we have periodic boundary conditions $X(0) = X(T)$ then:

$$\begin{aligned} \gamma_n &= \oint_C d\chi_k A_k(X) \\ A_k(X) &= i < n; X(t) \mid \frac{\partial}{\partial\chi_k} n; X(t) > \end{aligned} \tag{2.28}$$

It is worth noticing, following Ref.[14], that this phase cannot be assimilated in a redefinition of the states $\mid n; X(t) >$. In fact, if we change the phase of the state $\mid n; X(t) >$ then A_k will be modified according to a local gauge transformation:

$$\mid n; X(t) > \rightarrow e^{i\theta(X(t))} \mid n; X(t) >$$
$$A_k \rightarrow A_k - \frac{\partial}{\partial \chi_k}\theta\left(X(t)\right) \quad . \tag{2.29}$$

Being γ_n a line integral (2.28), it is invariant under the local gauge transformation (2.29) and therefore cannot be neglected. The Berry phase is an intrinsic property of the parameter space $X(t)$ and that is why it is often called a geometric phase.

Coming back to spin systems, it has been shown by many authors [38], [39], [40], [41], [42] that a Berry phase can be obtained considering the magnetization to be the external time dependent field. We will call it $\phi_i^\alpha(t)$ in what follows (i labels the sites and α the space directions). The geometric part of the effective action that generalizes eq.(2.27) reads:

$$\begin{aligned} S_{geom.} &= iS\sum_{i=1}^{N}\int_0^\beta dt A_i^\alpha(t)\frac{d\phi_i^\alpha(t)}{dt} = \\ &= iS\sum_{i=1}^{N}\oint_C d\phi_i^\alpha A_i^\alpha(t) = \\ &= iS\sum_{i=1}^{N}\int_S d\sigma^\alpha \epsilon^{\alpha\beta\gamma}\frac{\partial A_i^\gamma}{\partial \phi_i^\beta} \end{aligned} \tag{2.30}$$

where the Dirac monopole A_i^α is the solution of:

$$\epsilon^{\alpha\beta\gamma}\frac{\partial A_i^\gamma}{\partial \phi_i^\beta} = \frac{\phi^\alpha}{\mid \vec{\phi}_i \mid^3} \quad . \tag{2.31}$$

This geometric part may have deep consequences in the physics and this is actually the case of the one dimensional Heisenberg chain. After the work by Haldane[38] the appearance of non trivial Berry phases in quantum spin systems is often studied in connection to the

continuum limit of the AFM effective action. Non Linear σ model provides the simplest continuum theory describing the order parameter dynamics an AFM. It has the right spectrum at long wavelengths and at low frequencies. It can be argued that the Goldstone bosons of this NLσm interact exactly as the spin waves. The velocity of light here play the role of the spin wave velocity there[43].

One can derive the NLσm from the microscopic theory assuming short range AFM correlations as shown by Haldane[38]. As an outcome of this approach a non trivial Berry phase appears in the action.

Let me briefly show how the geometric contribution to the continuum effective action brings about deep consequences in the linear chain problem. We consider the Heisenberg chain and start from the static AFM mean field solution:

$$\phi^{\alpha}_{o_i} = S(-1)^i n^{\alpha}_o \qquad (\vec{n}^2_o = 1) \tag{2.32}$$

Fluctuations around this solution are described by the fields:

$$\phi^{\alpha}_i = S(-1)^i n^{\alpha}_i \tag{2.33}$$

In the continuum limit and imaginary time[44] the geometric part of the effective action becomes:

$$\begin{aligned} S_{geom.} &= iS\sum_{i=1}^{N/2} a\Delta_x \int_0^{\beta} dt A^{\alpha}_i(\vec{n}_i)\frac{dn^{\alpha}_i}{dt} \rightarrow \\ &\rightarrow i\frac{S}{2}\int dx \int_0^{\beta} dt \left[\left(\frac{\delta A^{\alpha}_i}{\delta n^{\beta}_i} - \frac{\delta A^{\beta}_i}{\delta n^{\alpha}_i}\right)\partial_x n^{\beta}_i \partial_t n^{\alpha}_i\right] = \\ &= i\frac{S}{2}\int dx \int_0^{\beta} dt \epsilon^{\alpha\beta\gamma} n^{\alpha}(x,t)\partial_x n^{\beta}(x,t)\partial_t n^{\gamma}(x,t) = i2\pi S Q_P \end{aligned} \tag{2.34}$$

a being the lattice space so that $\sum_{i=1}^{N} a \rightarrow \int dx$ in the limit $a \rightarrow 0$ and $|\vec{n}(x,t)|^2 = 1$. The

last equality defines the Pontryagin index Q_P:

$$Q_P = \frac{1}{4\pi}\int dx \int_0^\beta dt \det \begin{pmatrix} n^1 & n^2 & n^3 \\ \partial_t n^1 & \partial_t n^2 & \partial_t n^3 \\ \partial_x n^1 & \partial_x n^2 & \partial_x n^3 \end{pmatrix} \tag{2.35}$$

that is a functional of the field n^α which assumes only integer values[45]. From an adiabatic expansion a second order time derivative in $n^\alpha(t)$ can be obtained. As an example, the total effective action for the linear chain is given by the Non Linear σ model plus the topological term:

$$S_{eff} = \frac{S}{\sqrt{2}}\int_0^\beta d^2x \, (\partial_\mu n^\alpha)^2 + i2\pi S Q_P \tag{2.36}$$

In evaluating the partition function $\mathcal{Z} = \int \mathcal{D}n^\alpha \exp(-S_{eff})$ the relevant configurations of the field n^α are those with a finite action. This means that we have to impose boundary conditions at infinity or in the lattice language we have to impose periodic boundary conditions. Therefore the space in which our order parameter is defined becomes a sphere and we call it S^2_{phys}. The order parameter is an application from S^2_{phys} to the space of configurations that is again a sphere S^2_{conf}. All the relevant configurations of the order parameter are maps: $S^2_{phys} \rightarrow S^2_{conf}$[45]. From topological theorems we know that these maps can be divided in disjoint homotopy classes. The homotopy group is: $\pi_2(S^2) = Z$[46]. It can be shown that the Pontryagin index is a number also called winding number and that it counts the number of coverings of S^2_{int} induced by the map n^α.

The linear chain problem has been solved exactly by Bethe[19]. The ground state is disordered but the AFM correlation functions show a power low decay. The absence of long range order is a consequence of the Mermin Wagner theorem [28] and is correctly accounted for by the Non Linear σ model. On the contrary the NLσm would give an exponential decay for the correlation functions. It is the presence of the geometric term the responsible of this behavior[47]. Moreover, the Haldane conjecture that integer S chains

should exhibit exponentially decaying correlation functions while half integer S chains should exhibit power law decaying has a natural explanation in term of the topological phase: $2\pi S Q_P$.

In the 2D square lattice case it has been shown that the Berry phase vanish identically [39], [40], [41].

A further step that Berry proposed[48] is the study of quantal phase corrections from adiabatic iteration. This is performed in papers VIII in imaginary time starting from our scheme for the antiferromagnetic phase with attention to some non hermiticity problems which arise.

2.5 Frustrated Antiferromagnets

The frustrated Heisenberg hamiltonian $J_1 - J_2$ we are dealing with is:

$$H = J_1 \sum_{(i,j)NN} \vec{S}_i \cdot \vec{S}_j + J_2 \sum_{(i,j)NNN} \vec{S}_i \cdot \vec{S}_j \tag{2.37}$$

The introduction of the next nearest neighbor interaction J_2 in the 2D square lattice case frustrates the classical AFM order and enhances the effects of quantum fluctuations. The 2D frustrated Heisenberg model was approached in many different ways. In the classical limit ($S \to \infty$) there exists a phase transition at $J_2/J_1 = 0.5$ below which the ground state exhibits Neél order. Using linear spin wave theory[49] it turns out that for all finite S values the Neél state and the collinear state (independent Neél order on the two sublattices) are separated by a region, $J_2/J_1 \simeq 0.5$, in which the ground state is disordered by quantum fluctuations. An upper bound estimate of the stability for the Neél state was found[50] to be $J_2/J_1 \simeq .22$ connecting the frustrated Heisenberg model to the O(3) non-linear σ model. Additional support to this scenario is given by the results of finite size scaling studies[51] ($.4 < J_2/J_1 < .65$) and by exact diagonalization studies[52], [53]. Between the

proposed phases in the intermediate range of frustration there are the dimer phases, the flux and chiral phases and also other magnetically ordered but incommensurate phases.

Our method can be directly extended to all the spin hamiltonians. In particular we have studied the possible occurrence of dimerized phases (paper VII) and of chiral or flux phases (paper II) in the 2D frustrated Heisenberg hamiltonian. In this section I review only the basic concepts regarding these latter phases.

At start we consider the bond version of the model. This can be achieved by giving the fermion representation of the spin operators:

$$\vec{S}_i = \sum_{\alpha\beta} \frac{1}{2} c^\dagger_{i\alpha} \vec{\sigma}_{\alpha\beta} c_{i\beta} \tag{2.38}$$

as we will see explicitly in the next Chapter this is a representation of the spin 1/2 operators in the restricted Hilbert space of singly occupied sites. Neglecting, for the time being, this constraint and constant terms we end up with the following hamiltonian:

$$H = -\frac{J_1}{2} \sum_{(NN)} \sum_{\alpha\beta} c^\dagger_{i\alpha} c_{j\alpha} c^\dagger_{j\beta} c_{i\beta} - \frac{J_2}{2} \sum_{(NNN)} \sum_{\alpha\beta} c^\dagger_{i\alpha} c_{j\alpha} c^\dagger_{j\beta} c_{i\beta} \tag{2.39}$$

In what follows we consider a particular form of mean field theory[10], [37] whose decoupling scheme involves an Hubbard Stratonovich factorization in terms of link variables which are complex Bose fields:

$$\chi_{ij} = \sum_{\alpha} c^\dagger_{i\alpha} c_{j\alpha} \tag{2.40}$$

A valence bond can be represented in terms of fermions in such a way. We restrict ourselves with the possibility of having bonds only between nearest neighbor and next nearest neighbor sites. We look for solution of the saddle point equations with maximal symmetry.

These bond fields are complex and can be rewritten in terms of their modulus and

phases:

$$\chi_{ij} = \rho_{ij} e^{iA_{ij}} \tag{2.41}$$

A remarkable feature of this formulation is a local U(1) gauge symmetry of the Hamiltonian in Eq.(2.39):

$$c_i \rightarrow c_i e^{i\theta_i} \qquad c_i^\dagger \rightarrow c_i^\dagger e^{-i\theta_i} \tag{2.42}$$

The auxiliary fields of eq.(2.40) are not gauge invariant and we know from the Elitzur's theorem[54] that they cannot acquire a non-zero vacuum expectation value. However we can define the states from the simplest gauge invariant order parameters that are:

$$\mathcal{P}l = \langle \prod_{plaquette} \chi_{ij} \rangle = \langle \prod_{plaquette} \rho_{ij} \rangle e^{i\Phi} \tag{2.43}$$

We require that this flux Φ that is circulation of A_{ij} around an elementary plaquette is constant:

$$\Phi = \sum_{plaquette} A_{ij} \tag{2.44}$$

In general, a non zero flux Φ violates time reversal invariance since the time reversal transformation maps $\Phi \rightarrow -\Phi$. There are two values of $\Phi = 0, \pi$ compatible with time reversal and the corresponding phases are non chiral. All the other values (mod 2π) represent a state with broken time reversal symmetry, i.e. a chiral state. For both cases ρ_{ij} assumes non zero values on the links covered by dimers.

If we consider a uniform solution for $\rho_{ij} = \rho$ and a zero flux everywhere we obtain the Baskaran Zou and Anderson solution[55]. However this solution is unstable towards a dimerized state in which ρ may have a periodic component in space.

The state with $\rho_{ij} = \rho$ constant only on the link formed by the nearest neighbor sites in the square lattice and flux $\Phi = \pi$ on each elementary plaquette is the so called flux phase[10].

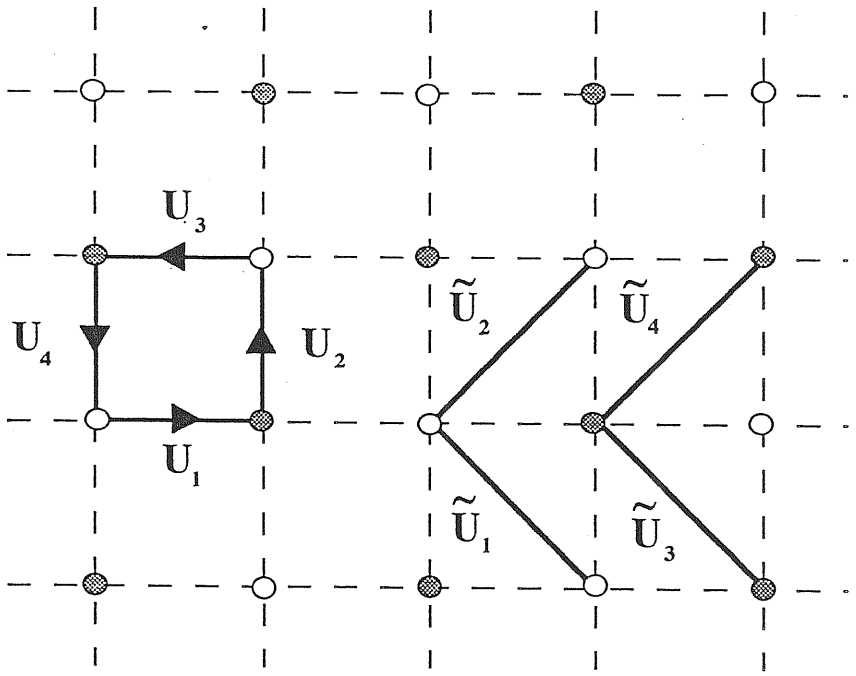

Figure 2.3: Pictorial representation of the link fields of the flux and chiral phases.

Now we consider the possibility of non-zero link diagonal fields. The chiral phase of Wen, Wilczek and Zee[12] can be obtained with the choice:

$$\begin{aligned} \chi_{ij} &= \rho e^{i\pi/4} \qquad i,j = N.N. \\ \chi_{ij} &= \tilde{\rho} \qquad\quad i,j = N.N.N. \end{aligned} \tag{2.45}$$

The chiral order parameter: $\mathcal{P}l_{\triangle}$ is proportional to the mixed product of three spin operators:

$$E_{123} = \vec{S}_1 \cdot (\vec{S}_2 \times \vec{S}_3) \tag{2.46}$$

Under time reversal $\hat{T}$ we have $\hat{T}^{-1}\vec{S}\hat{T} = -\vec{S}$ thus E_{123} is odd under time reversal. Similarly under parity $\hat{P}$, that in two space dimension is the same as reflection through a link, we have:

$$\hat{P}^{-1}E_{123}\hat{P} = E_{132} = -E_{123} \tag{2.47}$$

This feature has deep consequences[56]. The effective Lagrangian describing their low energy degrees of freedom have an extra term the so called Chern-Simon term. It follows that these systems may have low energy excitations with fractional statistic or anyons. From this point starts a novel suggested form of superconductivity, the anyon superconductivity[18].

However coming back to energetics, numerical studies[53] seems to indicate the columnar ordered dimer phase as the most favorite one. The dimer phases both in columnar and staggered order are given by isolated dimers as depicted in Fig.(2.4). These phases do not break time-reversal symmetry. The large-N expansion (in the SU(N) symmetry group) gives evidence for the stability of a dimerized phase in columnar order and does not give any evidence for chiral ordered or spin-nematic states.

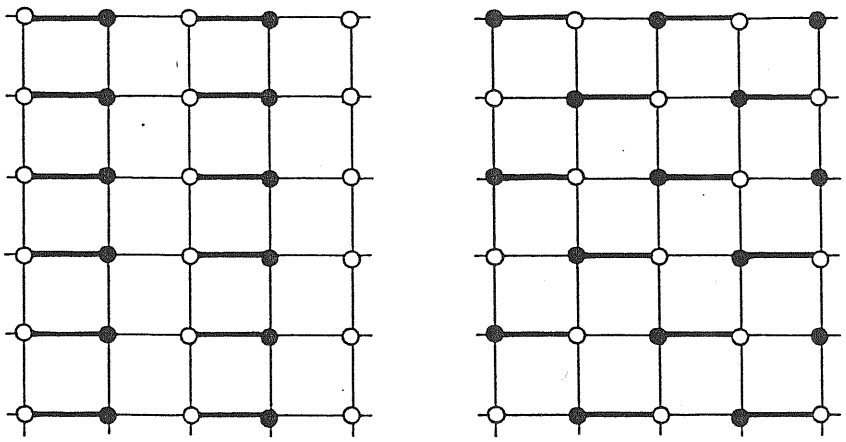

Figure 2.4: Pictorial representation of the link fields for the columnar (a) and staggered (b) dimer phases.

Chapter 3

Constrained Fermionization in the Heisenberg model

In this chapter I present our method and some of the results we have obtained studying the magnetic and non-magnetic phases of Heisenberg Hamiltonians. The fermionic representation of the spin operators is exact if the fermionic operators act on the restricted Hilbert space of singly occupied sites. Many thermodynamical quantities can be deduced from the partition function. The latter is expressed as a trace over the restricted Hilbert space. In evaluating the partition function, we have implemented the single site occupancy constraint through appropriate derivatives of a suitable generating function. This idea can be applied, in principle, to implement any projector. Here it has been applied to the study of 2D quantum spin (S=1/2) systems described by AFM Heisenberg Hamiltonians. Because the single site occupancy projector commutes with the hamiltonian, it can be implemented exactly at all temperatures. The first Section is meant to review this procedure applying it to the well known and standard case of the antiferromagnetic phase in the unfrustrated case. The second Section deals with the results for the AFM phase. At the saddle point approximation level the constraint is implemented exactly and we recover the mean field results of other pure spin methods. Including the one-loop correction to the static saddle

point we have obtained the well known spin waves corrections. More details can be found in Paper V. For order parameter configurations that are slowly varying in time a systematic adiabatic expansion can be developed starting from our scheme as shown in paper VIII and Berry's phase contributions arise quite naturally.

By means of constrained fermionization of the spin operators one can describe the magnetic and non magnetic phases on the same footing. In the third and fifth Section I report our results for the dimer phases both in columnar and staggered orders and for the flux and chiral phases respectively. Classical and quantum fluctuations allow us to construct an approximate free energy which shows the correct low temperature thermodynamical behavior.

From numerical calculations the dimer phase in columnar order seems to be a good candidate for the ground state when disorder is introduced in the pure nearest neighbor AFM interactions. I will show in the fourth Section how our method can be directly extended to study the frustrated Heisenberg hamiltonian and report the results on the effects of quantum fluctuations.

3.1 The projecting technique

Here we are dealing with the Heisenberg hamiltonian:

$$H = \sum_{(i,j)} J_{ij} \vec{S}_i \cdot \vec{S}_j \tag{3.1}$$

where the parenthesis ( ) indicates not repeated pairs of sites. We will consider:

$$J_{ij} = \begin{cases} J_1 & \text{if } i,j \text{ are nearest neighbors} \\ J_2 & \text{if } i,j \text{ are next nearest neighbors} \\ 0 & \text{otherwise} \end{cases} \tag{3.2}$$

Fermionization of the spin 1/2 operators, in terms of creation and annihilation operators $(c^\dagger, c)$ and Pauli matrices $\vec{\sigma}$, according to:

$$\vec{S}_i = \frac{1}{2} c^\dagger_{i\alpha} \vec{\sigma}_{\alpha\beta} c_{i\beta} \tag{3.3}$$

is exact if the Hilbert space is restricted to states with single site occupancy.

This can be shown with a very simple exercise:

If we consider a single site there are two possible realizations of SU(2) in terms of fermion operators:

a)

$$S_+ = c^\dagger_\uparrow c_\downarrow \;\; ; \;\; S_- = (S_+)^\dagger \;\; ; \;\; S_z = \frac{1}{2}(\hat{n}_\uparrow - \hat{n}_\downarrow) \tag{3.4}$$

b)

$$S'_+ = c^\dagger_\uparrow c^\dagger_\downarrow \;\; ; \;\; S'_- = (S'_+)^\dagger \;\; ; \;\; S'_z = \frac{1}{2}(\hat{n} - 1) \tag{3.5}$$

The Fock space has 4 dimensions and is:

$$\mathcal{H} = \mathcal{H}_1 \oplus \mathcal{H}_2$$

$$\mathcal{H}_1 = span\{|\uparrow>, |\downarrow>\} \quad \mathcal{H}_2 = span\{|0>, |\uparrow\downarrow>\} \tag{3.6}$$

The realizations a) and b) commute. The first one acts irreducibly on $\mathcal{H}_1$ and reducibly on $\mathcal{H}_2$. The reverse holds for the second realization. Moreover, given: $\vec{S}^2 = S(S+1)$ and $\vec{S}'^2 = S'(S'+1)$, we have: on $\mathcal{H}_1$: $S = 1/2$, $S' = 0$ and on $\mathcal{H}_2$: $S = 0$, $S' = 1/2$.

Therefore, going to the lattice case and choosing the realization a), thermal averages should include the projector which restricts the Hilbert space:

$$P_{hf} = \prod_i n_i(2 - n_i) \tag{3.7}$$

$(n_i = n_{i\uparrow} + n_{i\downarrow}; n_{i\sigma} = c^\dagger_{i\sigma} c_{i\sigma}, \sigma = \uparrow, \downarrow)$.

We can write the Heisenberg hamiltonian in terms of fermion operators as:

$$H = P_{hf}\left(-\frac{1}{2}\sum_{(i,j)} J_{ij} c^{\dagger}_{i\alpha} c_{j\alpha} c^{\dagger}_{j\beta} c_{i\beta}\right) P_{hf} - \frac{1}{4}\sum_{(ij)} J_{ij} \tag{3.8}$$

where summation over repeated spin indices is implicitly stated. The partition function and all the thermodynamical quantities should be calculated as traces over the restricted Hilbert space as:

$$Z = Tr\{e^{-\beta H} P_{hf}\} \tag{3.9}$$

To implement this projector we add a source term to the Hamiltonian H:

$$H' = H - \frac{1}{\beta}\sum_i z_i n_i \tag{3.10}$$

here the z_i's are real variables which we can think of as local chemical potentials.

Due to the fact that n_i and H commute, we can define the generating function:

$$\mathcal{Z}[z_i] = Tr\{\exp(-\beta H + \sum_i z_i n_i)\} \tag{3.11}$$

The original partition function is recovered performing the following derivatives:

$$\mathcal{Z} = \prod_i \frac{\partial}{\partial z_i}(2 - \frac{\partial}{\partial z_i})\mathcal{Z}[z_i]\Big|_{z_i=0} . \tag{3.12}$$

First of all due to the commuting properties of the Heisenberg hamiltonian with the occupation number operator (or$[H, P_{hf}] = 0$) the evolution operator will not bring the system out of the restricted Hilbert space. Henceforth we will disregard the projectors in the exponential. This is the major simplification that occurs when dealing with spin hamiltonians.

Everything is exact up to now and we can take advantage of the fact that the evaluation of $\mathcal{Z}[z_i]$ only requires standard techniques because the trace is an unrestricted trace.

It is a standard procedure to express the generating function $\mathcal{Z}[z_i]$ as a Path Integral over Grassman variables[57]:

$$\mathcal{Z}[z_i] = \int \prod_{i,\alpha} \mathcal{D}\psi^{\star}_{i\alpha}(\tau)\mathcal{D}\psi_{i\alpha}(\tau) \exp\left\{ \int_0^1 d\tau \sum_{i,\alpha} \psi^{\star}_{i\alpha}(\tau)(\partial_\tau - z_i)\psi_{i\alpha}(\tau) + \right.$$
$$\left. -\beta \sum_{(i,j)} J_{ij} \int_0^1 d\tau \vec{S}_i(\tau)\cdot\vec{S}_j(\tau) \right\} \tag{3.13}$$

where: $\vec{S}_i(\tau) = \psi^{\star}_{i\alpha}(\tau)\vec{\sigma}_{\alpha\beta}\psi_{i\beta}(\tau)$. Here τ is a scaled imaginary time variable ranging from 0 to 1, the ψ's are Grassmann variables obeying antiperiodic boundary conditions in τ at the extrema of the interval $[0,1]$.

In evaluating this generating function we can use Hubbard-Stratonovich decouplings to integrate out exactly the fermions. The price to be paid is the presence of multidimensional integrals over the Hubbard Stratonovich auxiliary fields.

Performing the derivatives as in Eq.(3.12) we implement the projector exactly. We end up with an effective action in terms of the auxiliary fields.

Obviously it is not possible to evaluate exactly this multidimensional path integral. The standard procedure is to evaluate it at the saddle point and then to add corrections. In all the forthcoming approximations we will treat the constraint term on the same footing as the other terms. Different phases are studied choosing different saddle points. The choice of the auxiliary fields will drive towards magnetic or non-magnetic saddle point solutions.

I will discuss here the well known case of the antiferromagnetic phase for the unfrustrated Heisenberg Hamiltonian. This Hamiltonian can be written in Fourier space:

$$H = J \sum_{(q)} \gamma(q)\vec{S}(q)\cdot\vec{S}(-q) \tag{3.14}$$

where $\gamma(q) = \cos q_x + \cos q_y$.

The Hubbard-Stratonovich decoupling gives:

$$e^{-\beta J\ \gamma_q \vec{S}(q,\tau)\cdot\vec{S}(-q,\tau)} = \\ = \int \mathcal{D}^2\vec{\mathcal{M}}(q,\tau) e^{-\int_0^1 d\tau\ \{\pi|\vec{\mathcal{M}}(q,\tau)|^2 + \sqrt{-\pi\beta J\gamma_q}(\vec{\mathcal{M}}(q,\tau)\cdot\vec{S}(q)+c.c.)\}} \tag{3.15}$$

where the auxiliary fields $\vec{\mathcal{M}}(q,\tau)$ obey periodic boundary conditions in τ. It is useful to introduce the Fourier transforms of the fields, i.e.:

$$\begin{aligned} \psi_{i\alpha}(\tau) &= \sum_{n=-\infty}^{\infty} e^{-i\omega_n\tau}\psi_{i\alpha}(\omega_n) \\ \vec{\mathcal{M}}(q,\tau) &= \sum_{m=-\infty}^{\infty} e^{-i\Omega_m\tau}\vec{\mathcal{M}}(q,\Omega_m) \end{aligned} \tag{3.16}$$

where on account of the boundary conditions: $\omega_n = (2n+1)\pi$ and $\Omega_m = 2m\pi$.

Having integrated out exactly the fermions we get:

$$\mathcal{Z}[z_i] = \mathcal{N}\int \prod_{q,m} \mathcal{D}^2\vec{\mathcal{M}}(q,\Omega_m) \exp\left\{-\pi\sum_{q,m} \mid \vec{\mathcal{M}}(q,\Omega_m)\mid^2 - S_{eff}[\tilde{\mathcal{A}}]\right\} \tag{3.17}$$

The effective action is:

$$S_{eff}[\tilde{\mathcal{A}}] = -Tr\ln[1+G_o\tilde{\mathcal{A}}] \tag{3.18}$$

with:

$$\tilde{\mathcal{A}}^{nn'}_{\alpha\beta}(i,j) = \delta_{i,j}\left\{z_i\delta_{n,n'}\delta_{\alpha,\beta} - 2\sum_q e^{iqR_i}\left(\frac{-\pi\beta J\gamma_q}{N}\right)^{1/2}\vec{\mathcal{M}}(q,\Omega_m)\cdot\vec{\sigma}_{\alpha\beta}\right\} \tag{3.19}$$

We have defined here the free electronic Green function $(G_o)^{nn'}_{\alpha\beta}(i,j) = (i\omega_n)^{-1}\delta_{i,j}\delta_{n,n'}\delta_{\alpha,\beta}$. The normalization factor is: $\mathcal{N} = \exp(Tr\ln G_o^{-1}) = 4^N$. The derivatives appearing in

eq.(3.12) lead to the partition function. The resulting extra factors can be exponentiated to give:

$$\mathcal{Z} = \int \prod_{q,m} \mathcal{D}^2 \vec{\mathcal{M}}(q,\Omega_m) \exp\left\{ -\pi \sum_{q,m} \mid \vec{\mathcal{M}}(q,\Omega_m) \mid^2 - S_{eff}[\mathcal{A}] + \sum_i \ln 4 B_i[\mathcal{A}] \right\} \quad . \quad (3.20)$$

The matrix $\mathcal{A}$ that is $\tilde{\mathcal{A}}_{z_i=0}$ depends only on $\omega_{n'} - \omega_n = \Omega_m$ Here the contribution of the constraint is:

$$\begin{aligned} B_i[\mathcal{A}] &= \left[\frac{\partial^2 S_{eff}}{\partial z_i^2} - 2\frac{\partial S_{eff}}{\partial z_i} - \left(\frac{\partial S_{eff}}{\partial z_i} \right)^2 \right]_{z_i=0} \\ &= Tr\left\{ [\chi P_i]^2 \right\} + 2Tr\left\{ \chi P_i \right\} - \left(Tr\left\{ \chi P_i \right\} \right)^2 \end{aligned} \quad (3.21)$$

We have defined the projector P_i, onto the $i-th$ site of the lattice, whose matrix elements in the Wannier representation are $(P_i)_{jk} = \delta_{jk}\delta_{ij}$ and the operator $\chi = (G_o^{-1} + \mathcal{A})^{-1}$.

Note that up to this point everything is exact.

To isolate the static saddle point corresponding to the antiferromagnetic phase we choose $\vec{\mathcal{M}}(q,m) = \hat{z}\mathcal{M}^z(\vec{\pi},0)\delta_{m,0}\delta_{q,\vec{\pi}}$ and look for the self-consistency equation. Here the q vector doubling the unitary cell is $\vec{\pi} \equiv (\pi,\pi)$. In the next Section I report the results. Now I want to go a step further giving the main ingredients for the one-loop corrections. The total effective action of eq.(3.20), evaluated at the stationary point gives a poor approximation to the free energy. By including the so called "one loop corrections " in the estimation of the path integral, we take into account the field configurations which allow for fluctuations of the order parameter around its mean field value, at the gaussian level. We write:

$$\vec{\mathcal{M}}(q,\Omega_m) = \mathcal{M}^z(\pi,0)\hat{z} + \delta\vec{\mathcal{M}}(q,\Omega_m) \quad (3.22)$$

This changes $\mathcal{A}$ into $\mathcal{A}+\delta\mathcal{A}$. The effective action can be written as: $\mathcal{F}=\mathcal{F}^0+\mathcal{F}^{(2)}$ with $S_{eff}=S^0_{eff}+S^{(2)}_{eff}$, where the superscript (0) denotes the mean field value and the superscript (2) the second variation.

Understanding χ as the one evaluated at the saddle point ($\chi=(G_o^{-1}+\mathcal{A})^{-1}$), we get:

$$S^{(2)}_{eff}=\frac{1}{2}Tr\{[\chi\delta\mathcal{A}]^2\}. \tag{3.23}$$

which is depicted in Fig.(3.1(a)). The second variation $\mathcal{F}^{(2)}$ is:

$$\beta\mathcal{F}^{(2)}=\pi Tr\{\mid\delta\vec{\mathcal{M}}\mid^2\}+S^{(2)}_{eff}-\frac{1}{2}\sum_i\left(\frac{\delta^2B_i}{B_i}-\frac{(\delta B_i)^2}{B_i^2}\right) \tag{3.24}$$

where:

$$\delta B_i=2Tr\{\chi P_i\chi P_i\chi\delta\mathcal{A}\} \tag{3.25}$$

and

$$\delta^2B_i=4Tr\{\chi P_i\chi P_i\chi\delta\mathcal{A}\chi\delta\mathcal{A}\}+2Tr\{\chi P_i\chi\delta\mathcal{A}\chi P_i\chi\delta\mathcal{A}\} \tag{3.26}$$

The first term of the constraint contribution, δ^2B_i, is represented diagrammatically as in Fig.(3.1(b)) and the second term $(\delta B_i)^2$ is depicted in Fig.(3.1(c)).

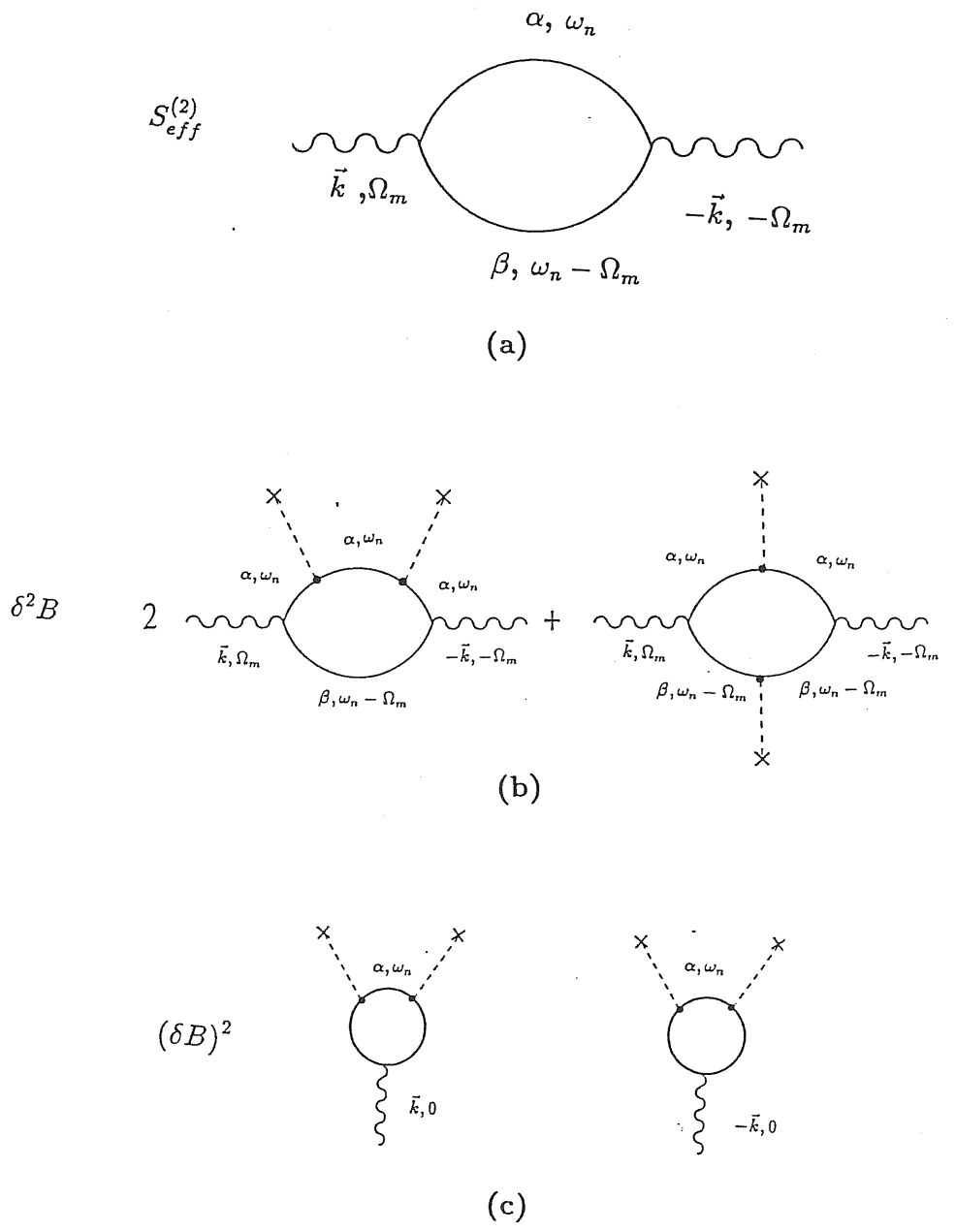

Figure 3.1: Diagrammatic representation of: (a)$\delta^2 S_{eff}$ (b)$\delta^2 B_i$ (c) $(\delta B_i)^2$. The wiggly lines represent the fluctuating fields $\delta\vec{\mathcal{M}}(\mathbf{Q})$, the full lines the χ functions while the broken lines represent the effect of the projector viewed as an external perturbation.

3.2 Antiferromagnetic phase

We have introduced the rescaled order parameter $M = \sqrt{\frac{\pi}{2N\beta J}}\mathcal{M}^z$.

The saddle point approximation to the free energy which should be derived from the logarithm of the partition function of eq.(3.20), is:

$$f^0_{eff} = \mathcal{F}/NJ = 2M^2 - 2t \ln \cosh M/t - t \ln B \tag{3.27}$$

where the constraint B which turns out to be site independent, reads:

$$B = 1 - \frac{1}{2\cosh^2 M/t} \tag{3.28}$$

So that the final result becomes:

$$f^0_{eff} = 2M^2 - t \ln \cosh 2M/t + t \ln 2 \tag{3.29}$$

Minimization of this expression yields the mean field magnetization:

$$M = \frac{1}{2} \tanh \frac{2M}{t} \tag{3.30}$$

with critical temperature $t_c = 1$ and $f^0_{eff}(t = 0) = -1/2$. This is exactly what found in the mean field approach to the Heisenberg and/or Ising model, when traces are performed over spin states. In fact, the constraint is satisfied at all temperatures at the mean field level, what comes from the fact that $< n_i >= 1$ and $< n_i^2 >= 1$ at all temperatures.

A crucial check of our method to include the single site-occupancy constraint is the evaluation of the mean occupation number $< n_i >$ and of its mean square fluctuation $< n_i^2 >$. It can be easily proved that $< n_i >= 1$ at all temperatures (see paper III), but we cannot in general prove the corresponding relation: $< n_i^2 >= 1$. Here we show that, at

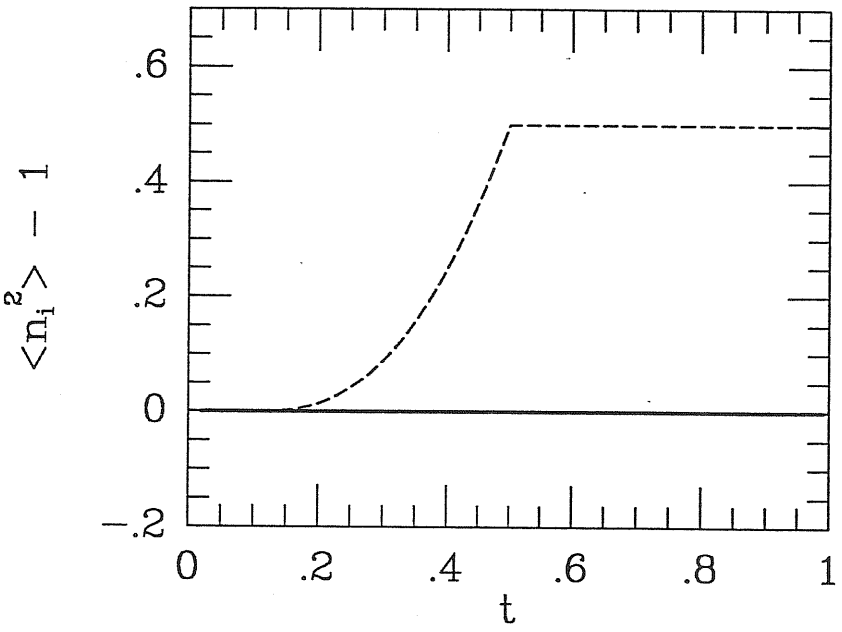

Figure 3.2: $< n_i^2 >$ versus temperature.

the saddle point, when the constraint is taken into account, the mean square occupation number $< n_i^2 >_{s.p.}$ is exactly equal to one.

According to eq.(3.20) we write symbolically this quantity as:

$$< n_i^2 >_{s.p.} = \left\langle \frac{\partial^2}{\partial z_i^2} e^{-\Sigma(z_i)} \Big|_{z_i=0} \right\rangle_{s.p.} \tag{3.31}$$

where

$$\Sigma(z_i) = S_{eff}(z_i) - \sum_i \ln 4B_i(z_i). \tag{3.32}$$

Note that $\frac{\partial S_{eff}}{\partial z_i}\Big|_{z_i=0} = -1$ and that $\frac{\partial^2 S_{eff}}{\partial z_i^2}\Big|_{z_i=0} = Tr\{\chi P_i \chi P_i\}$.

In the absence of the constraint we have:

$$< n_i^2 >^0_{s.p.} = 1 - \langle \frac{\partial^2 S_{eff}}{\partial z_i^2} \rangle \Big|_{z=0} = 1 + \frac{1}{\cosh^2 M/t} \tag{3.33}$$

$< n_i^2 >$ is one only at zero temperature because the saddle point satisfies the constraint

and no classical (static) fluctuations survive. At the critical temperature, when M is zero, it reaches the value 3/2 due to the equiprobability of occupations. When the constraint is ignored the mean field critical temperature is $t_c^0 = 0.5$ and the equation for the magnetization is: $M = \frac{1}{2}\tanh\frac{M}{t}$. This result is plotted in Fig.(3.2) broken curve. Including the constraint we have shown (see Paper V) that:

$$< n_i^2 >_{s.p.} = 1 - \left\langle \left(\frac{\partial^2 S_{eff}}{\partial z_i^2} - \sum_j \frac{1}{B_j} \frac{\partial^2 B_j}{\partial z_i^2} \right) \Bigg|_{z=0} \right\rangle_{s.p.} = 1 \ . \tag{3.34}$$

See Fig.(3.2).

One loop corrections

By including the so called "one loop corrections " in the estimation of the path integral, we take into account the field configurations which allow for fluctuations of the order parameter around its mean field value, at the gaussian level. We write:

$$\vec{\mathcal{M}}(q, \Omega_m) = \mathcal{M}^z(\pi, 0)\hat{z} + \delta\vec{\mathcal{M}}(q, \Omega_m) \tag{3.35}$$

We have found that, while the longitudinal fluctuation modes ($\|$ to $\hat{z}$) are decoupled, the quadratic form for $\mathcal{F}^{(2)}$ relative to the transverse fluctuations consists of four equal 2×2 blocks mixing the real and imaginary components of $\delta\mathcal{M}^x$ and $\delta\mathcal{M}^y$ at q and $q + \pi$ in pairs. We denote its eigenvalues by λ_+ and λ_-. They are:

$$\lambda_\pm = \pi \left[-1 \pm \frac{\beta J \gamma_q 2M}{\sqrt{(\Omega_m^2 + (4M/t)^2}} \right] \tag{3.36}$$

They vanish at $\Omega_m = 0$ when is $q = 0$ and $q = (\pi, \pi) = \vec{\pi}$. They are the Goldstone modes (spin waves) corresponding to the broken symmetry of the AFM state.

The collective excitation spectrum is recovered by the analytical continuation of the product $\lambda_+^{AF} \cdot \lambda_-^{AF}$ for $i\Omega_m \to \beta\omega + i0$ and looking for the zeros. The result is the usual spin waves dispersion that is:

$$\omega_q = 2MJ\sqrt{(1-(\gamma_q/2)^2)}. \tag{3.37}$$

which is affected by the constraint only through the temperature dependence of $M(t)$. It is remarkable that no other contribution to the longitudinal modes arises from terms of the constraint with $\Omega_m \neq 0$. This implies that there are no quantum corrections (i.e. at zero temperature) due to the constraint.

The zero temperature the energy is:

$$f(t=0) = f^0 + \frac{2}{N}\sum_q^{RBZ}\left[\sqrt{(1-(\gamma_q/2)^2)}-1\right] \tag{3.38}$$

where $f^0 = 2(M^2 - M) = -0.5$, $(M = 1/2)$ and the correction due to the fluctuations is -0.158. This is the well known result of the first $(1/S)$ correction.

The presence of the constraint affects the finite temperature dependence of the free energy as one can see in Fig.(3.3) which reports the specific heat divided by the temperature versus temperature. Thermal fluctuations are strongly depressed by the constraint while the low temperature behavior $C_V \sim at^2$ remains exactly the same.

3.3 Dimer phases

Dimer phases are bond centered charge density waves in which each site forms a spin singlet with one of its nearest neighbor and in fact breaks the original translational symmetry. The dimer phases we have considered are the the staggered one in which translational symmetry along the diagonals of the lattice is preserved and the columnar one in which the elementary cell is doubled in one direction. See Fig.(3.4).

In studying these non magnetic phases the fermionization of spin operators is a very natural tool.

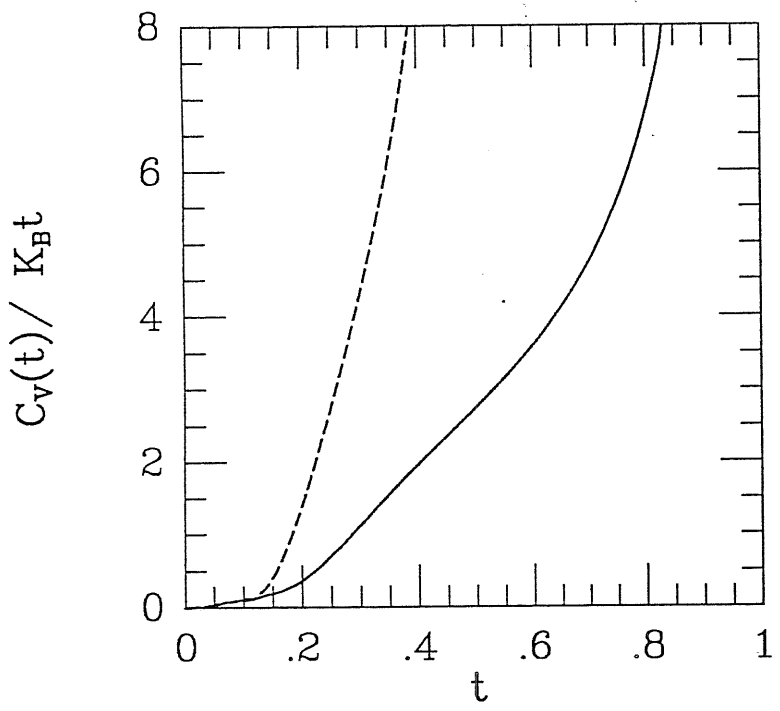

Figure 3.3: Specific heat versus temperature. In the presence (full curve) and in the absence (broken curve) of the constraint.

The Heisenberg Hamiltonian can be rewritten as:

$$H = P_{hf}\left(-\frac{J}{2}\sum_{(i,j)} c^{\dagger}_{i\alpha}c_{j\alpha}c^{\dagger}_{j\beta}c_{i\beta}\right)P_{hf} - N\frac{J}{2} \tag{3.39}$$

with $P_{hf} = \prod_i n_i(2-n_i)$, the single site-occupancy projector.

In the path integral representation of the generating function $\mathcal{Z}[z_i]$ we perform a different Hubbard Stratonovich decoupling. Now we choose link auxiliary fields:

$$\mathcal{U}_{ij}(\tau) = \sum_{\alpha} \psi^{*}_{i\alpha}(\tau)\psi_{j\alpha}(\tau) \tag{3.40}$$

Assuming that the $\mathcal{U}_{ij}$'s break the translational symmetry as less as possible we have the two possible bipartite lattices as in Fig.(3.4). The saddle point choice $\mathcal{U}_1 = U(V)$ and

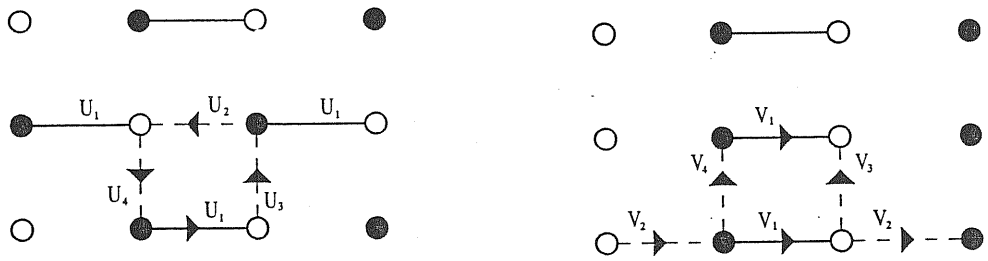

Figure 3.4: Pictorial representation of the link order parameters. (a) Staggered dimer phase (periodicity is along the diagonals) (b) Columnar dimer phase (periodicity is doubled along the x axis).

$\mathcal{U}_2 = \mathcal{U}_3 = \mathcal{U}_4 = 0$ corresponds to the staggered (columnar) dimer phase. At the saddle point level the two dimer phases we have studied are degenerate. A very important check of our method is the evaluation of the mean square fluctuations of the on-site occupation number. It turns out that at the saddle point it deviates from the exact result as a function of temperature less then 10% (see paper III).

We call this saddle point phases "generalized mean field phases". In fact, the classical result in the theory of Path Integrals [58] that says that the saddle point evaluation of the path integral yields the value of the free energy that one would obtain by performing a mean field (Hartree) approximation on the original Hamiltonian does not hold true in the case of constrained path integrals. This is exactly our case. Here the variational principle does not help us and we are not allowed to refer to the saddle point evaluation of the exponent in the path integral as to an approximation to the free energy.

As a matter of fact we have found that the saddle point approximation to the free

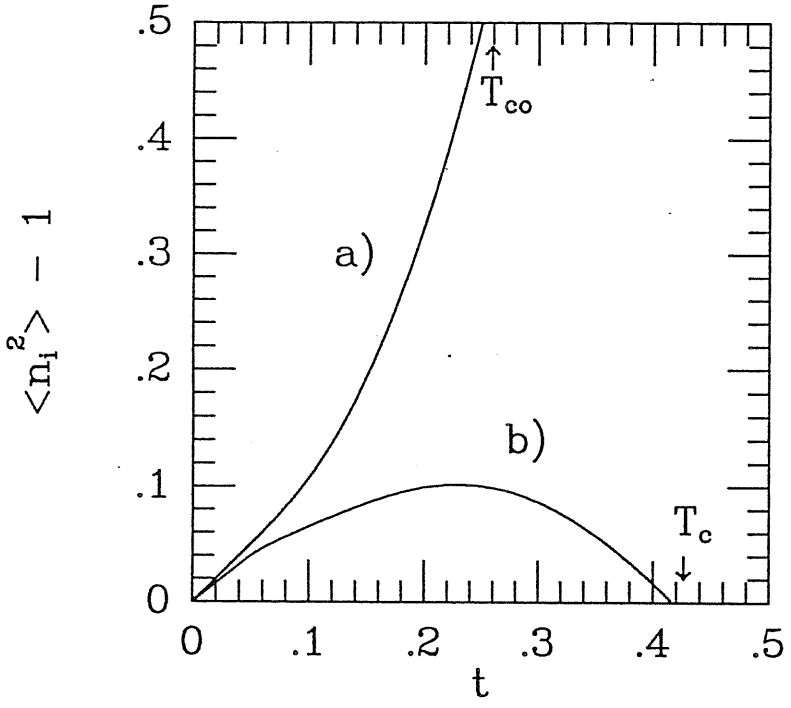

Figure 3.5: $< n_i^2 >$ vs. temperature for the staggered dimer phase. Curve b) is for the constrained case while the curve a) refers to the unconstrained case.

energy is a very poor approximation. The restriction due to the constraint are even too strong. It reduces the entropy so much that at low temperature the specific heat becomes negative (see Fig.(3.6)).

We have shown that to overcome the drawbacks of the constrained fermionization the inclusion of quantum fluctuations together with a careful analysis of the zero modes are needed. (See papers IV,VI for a detailed analysis and discussion). They follow from the spontaneous breaking of the residual U(1) symmetry and are affected by the constraint also at zero temperature. We have shown that there are two more flat directions in the second variation of the action around the columnar phase saddle point, which eventually cause this phase to be lower in energy with respect to the staggered one. Because these

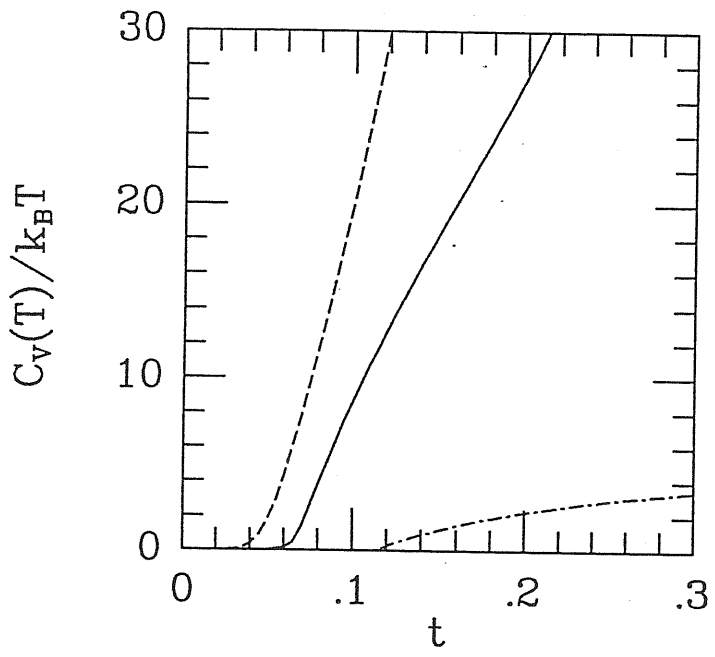

Figure 3.6: Specific heat vs. temperature. The full curve is in presence of the constraint and including quantum fluctuations, the broken curve in its absence and with quantum corrections, the dashed-dotted curve is in the presence of the constraint but without including the quantum corrections

modes are dispersionless at zero energy and the other excitations are at energy $2d$ the temperature dependence of the specific heat is governed by the gap $2d$.

The results concerning the thermodynamical behavior is summarized in Fig.(3.6) where the specific heat vs. temperature is plotted. The constraint strongly reduces the thermal fluctuations and together with the one-loop corrections gives a correct thermodynamical behavior for the specific heat.

Concerning the zero temperature results they are summarized in Table 3.1.

It is worth noticing that adding back the extra constant term appearing in the Hamiltonian, then the constraint is satisfied only in the average the saddle point free energy becomes: $f^0_{dimers} = -3/4$. Because $B \to 1$ in the zero temperature limit the unconstraint

$T = 0$ Energies	f^{MF}	f
COLUMNAR CONSTRAINED	-0.375	-0.771
STAGGERED CONSTRAINED	-0.375	-0.668
COLUMNAR	-0.75	-1.198
STAGGERED	-0.75	-1.095

Table 3.1: Zero temperature results for the energies of the columnar and staggered dimer phases. f^{MF} is the saddle point free energy, f is the free energy when added the quantum corrections.

result is not changed at the mean field level at $t = 0$. This is because the saddle point satisfies the constraint in the average automatically. However this does not correspond to strictly projecting out empty and doubly occupied sites. At zero temperature this can be done by hand[10], noticing that the independent dimers of the mean field configuration, when projected become a collection of spin singlet with a total energy per particle: $f^0_{singlets} = -S(S+1)/2 = -3/8$.

While numerical calculations [25], [26], [27] give strong evidence that ground state of the square lattice unfrustrated Hisenberg model has AFM correlations with an estimation of the energy per particle ~ -0.69, our method would still favor the columnar dimer phase even if much less then in the unconstrained case. By including the constraint of single site-occupancy at the one-loop level of approximation, we are unable to completely overcome the drawbacks of unconstrained fermionization which makes the estimate of the ground state energies unsatisfactory. The reasons why dimer phases result to be lower in energy at $T = 0$ than the antiferromagnetic one within our method is basically in the strong effects of quantum fluctuations on these non-magnetic phases. Fluctuations give a

consistent contribution to the ground state energy, what makes this problem intrinsically difficult. We believe that in order to compare the ground states energy of magnetic versus non-magnetic phases one should go beyond the one-loop approximation to the saddle point result. The depression of fluctuations due to the constraint should be even stronger in further approximations.

3.4 Effects of frustration

We are dealing with the frustrated Heisenberg hamiltonian:

$$\begin{aligned} H &= J_1 \sum_{(i,j)NN} \vec{S}_i \cdot \vec{S}_j + J_2 \sum_{(i,j)NNN} \vec{S}_i \cdot \vec{S}_j \\ &= J_1 \sum_q \bar{\gamma}(q) \vec{S}(q) \cdot \vec{S}(-q) \end{aligned} \tag{3.41}$$

where $\bar{\gamma}(q) = \gamma(q) + 2\frac{J_2}{J_1} \cos q_x \cos q_y$.

We can straightforwardly extend our method of including the single site-occupancy projector needed to represent the spin operators in terms of fermionic operators and Pauli matrices because P_{hf} and H still commute.

As one can see from paper VII our results are again the spin wave results for the AFM phase with one loop quantum corrections. The corrections to the free energy show an instability for $J_2/J_1 \geq 0.5$. Including the corrections to the magnetization order parameter one would find the instability (i.e.$M^\star \to 0$) for $J_2/J_1 \geq 0.42$.

In presence of frustration it seems that numerical exact diagonalization [53], [51] favors the dimerized phases in columnar order. In this case while the saddle point free energies do not depend on the frustration parameter $\alpha^2 = J_2/J_1$, the addition of the fluctuating diagonal link fields lower the energy substantially. As one can see from Fig.(3.8) in the extremely frustrated limit of $\alpha^2 = 1$ they recover the degeneracy they have within the saddle point approximation.

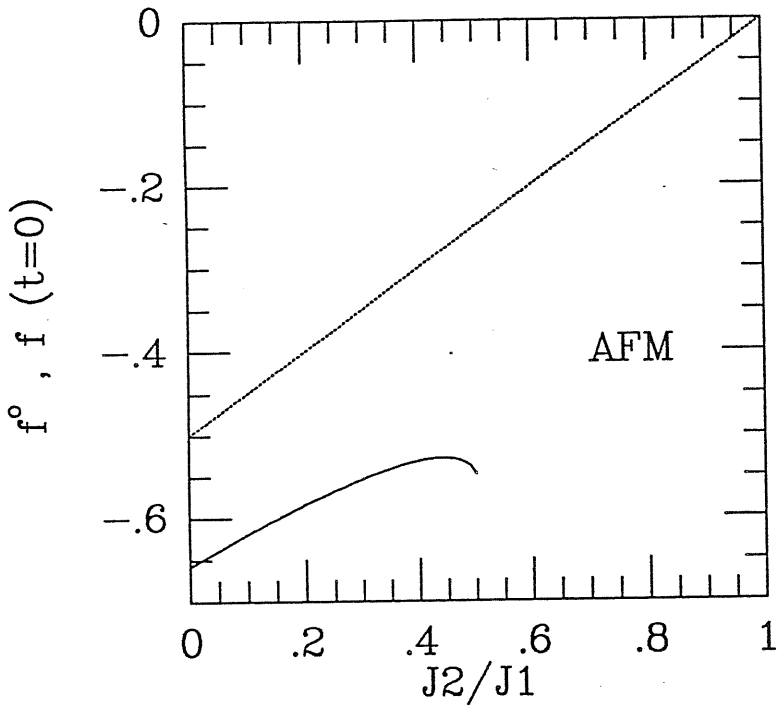

Figure 3.7: Antiferromagnetic phase. Mean field energy (broken curve) and total free energy (full curve) as a function of the frustration parameter J_1/J_2.

In contrast the free energy of the Néel phase increases in the presence of frustration also at the saddle point level of approximation. Moreover, the spin wave corrections drive the AFM system towards instability as α^2 increases.

Actually, a quantitative comparison between the AFM phase and the Dimer phases which arise from our calculation is believe to be far from reality. In fact while numerical studies strongly suggest an AFM ground state in the unfrustrated case ($J_2 = 0$) we have found lower energies for the dimer phases. This is because of the approximated way in which the constraint contributions have been calculated. Even if the $\ln B$ term in the effective action strongly depresses the fluctuations, one-loop corrections are not enough to provide a reliable estimate of the relative ground state energies when different decouplings

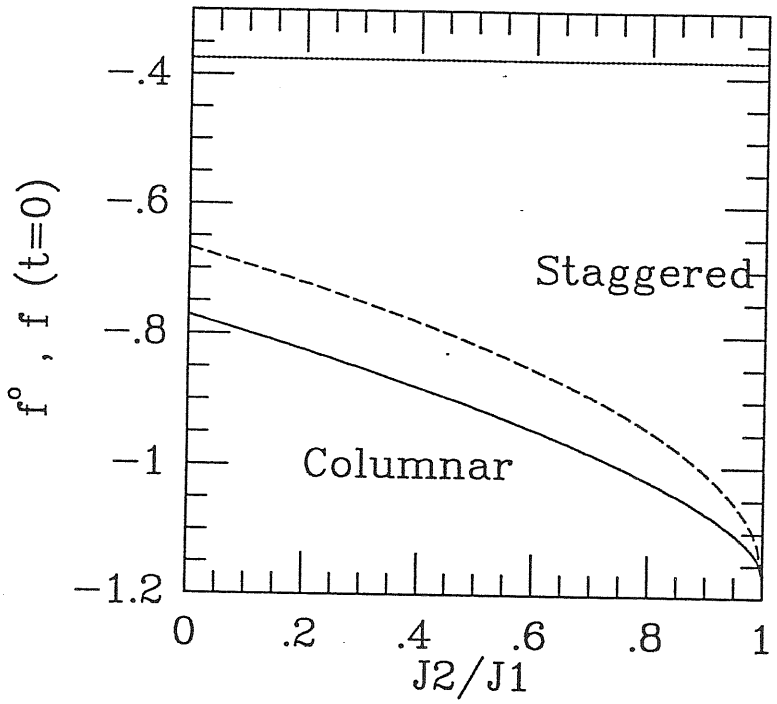

Figure 3.8: Columnar and staggered dimer phases. Mean field energy (dotted curve) and total free energies (broken curve is for the staggered and full curve for the columnar order) as a function of the frustration parameter J_1/J_2.

are adopted. From the mean field Hamiltonians corresponding to the unconstrained saddle point one can argue the origin of this difference. In fact, in the case of the link auxiliary fields the mean field hamiltonian would be an hopping hamiltonian which changes easily the site occupation numbers. In presence of the constraint, at the saddle point level, we have found that the mean square fluctuations of the occupation number ($< n_i^2 > -1$) are constrained but only up 10%. On the contrary, taking a magnetic decoupling scheme, the order parameter is a local one and we have found that also at the saddle point level the constraint is fully implemented giving zero fluctuations of the occupation number.

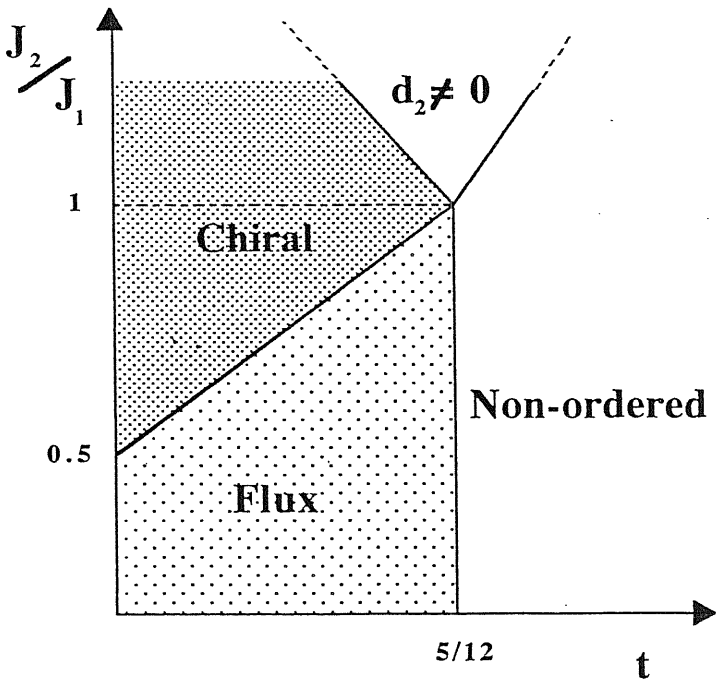

Figure 3.9: Relative mean field phase diagram between flux and chiral phases as a function of frustration and temperature.

3.5 Flux and Chiral phases

The interest in flux and chiral spin states is related to the claim that such a background could lead to an U(1) lattice gauge theory which include a Cern-Simon term when the original gauge invariance is violated. These theories may give rise to exotic anyon superconductivity. The reason is that parity and time reversal must be violated. The chiral phase of the $J_1 - J_2$ hamiltonian is a spin liquid state whose local order parameter breaks P and T as we have shown in the second Section of this thesis.

In papers II,III we have studied these phases within our constrained fermionization

scheme at the mean field level.

Here I discuss only the relative mean field phase diagram.

We have found that the chiral phase exists as a saddle point solution also in the presence of the constraint if $J_2/J_1 > 0.5$. Whenever the chiral phase exists it has a mean field free energy always lower that that of the flux phase that is independent of J_2 and has a mean field critical temperature $t_c = 5/12$. The zero temperature energy of the chiral phase runs between -0.229 for $J_2 = 0.5$ that coincides with the energy of the flux phase to -0.25 when $J_2/J_1 = 1$ that is the energy of the dimer phase. Going to the extremely frustrated limit $J_2 > J_1$ the energy of the chiral phase becomes even lower than that of the dimer phase.

In the absence of frustration we have studied the effects of classical fluctuations around the flux phase saddle point in comparison with those around a dimer saddle point. Allowing for variations of the the auxiliary fields $\mathcal{U}_i$'s around their stationary values, we have considered only fluctuations of the same space periodicity as our saddle point solutions. This provides a qualitative measure of the stability of the saddle point solutions, with respect to this type of fluctuations.

Because of the chosen symmetry for the random auxiliary fields $\mathcal{U}_i$, the order parameter has four complex components. Therefore, the dynamical matrix around the stationary point solutions is an 8X8 matrix. Its diagonalization gives eight normal modes.

The global symmetries of the action are found as zero eigenvalues of the $8X8$ curvature matrix. These zero modes correspond to the residual gauge symmetries which are not broken by the mean field solutions (see paper III).

Non zero modes give the collective excitations. We have also evaluated the mean square fluctuations of the order parameter corresponding to the eigenvalues which give

the most divergent fluctuations as a function of temperature and compare it in presence and in absence of the constraint.

These mean square fluctuations give the temperatures, according to the Ginzburg Landau criterion, at which there is the breakdown for mean field solutions and the onset of criticality. We have found that the temperature destabilizes the flux phase more than it does with the dimer phase, especially due to the constraint, which does not suppress phase fluctuating modes, provided the flux is conserved.

In the absence of the constraint the single particle excitation spectrum, in the Flux phase, as deduced from the energies $E_k = \pm\sqrt{\cos k_x^2 + \cos k_y^2}$. is gauge dependent. This gauge dependence does not lead to any inconsistencies since the physical excitations consist of particle-hole pairs confined together on the same site. In presence of the constraint, it is no more obvious how to isolate quasiparticle energies from the free energy. In this case one should evaluate the single particle Green functions and identify single particle energies from their poles. In the absence of the constraint, we can construct a gauge invariant quantity out of the $\pm E_k$'s that is the single particle (particle-hole) excitation spectrum given by:

$$\omega_q = \{E_{k+q} + E_k; k, k+q \in RBZ\} \tag{3.42}$$

where:

$$E_{k+q} + E_k = 2\ d\ \sqrt{\cos^2(k_x + q_x) + \cos^2(k_y + q_y)}\sqrt{\cos^2 k_x + \cos^2 k_y} \tag{3.43}$$

The excitation spectrum has zero energy modes at $q = (0,0)$, $(0,\pi)$, $(\pi,0)$ and $q = (\pi,\pi)$ and has a linear dispersion at low energy.

Chapter 4

The projected Fermi gas

The limit if infinite U in the Hubbard model[4] can be thought of as that of a Fermi gas of mutually avoiding particles. The restriction to states without double site occupancies is called the projected Fermi gas.

Without attempting to review the various methods by which the strong coupling limit ($U \to \infty$) of the Hubbard model has been approached [59],[60] I introduce briefly the problems connected with it and present our method to deal with the Gutzwiller projector[61] of no doubly occupied sites. Finally I will show how the method works on a toy model of a two-site system.

4.1 The model and the projector

The Hubbard hamiltonian is:

$$H = H_{kin} + H_I$$

$$H_{kin} = -t \sum_{\sigma} \sum_{(i,j)} (c^{\dagger}_{i,\sigma} c_{j\sigma} + h.c.) = \sum_{k,\sigma} \epsilon(k) n_{k\sigma}$$

$$H_I = U \sum_i n_{i\uparrow} n_{i\downarrow} \tag{4.1}$$

it consists of two parts. H_{kin} is the kinetic part which is of purely quantum mechanical origin, and H_I is the interaction part, $U = 0$ being the non interacting limit. One refers to the weak-coupling limit when $U/t << 1$ and to the strong-coupling limit when $U/t >> 1$. While the kinetic energy of non interacting particles is simple in momentum space, the physical origin of the interaction usually implies that this term is simple in position space. Therefore, the generic case is $[H_{kin}, H_I] \neq 0$ and this implies a non trivial competition between the two terms. While in the weak-coupling limit the "band" aspect dominates, in the strong-coupling the main difficulties arises because the interaction term tends to favor localization.

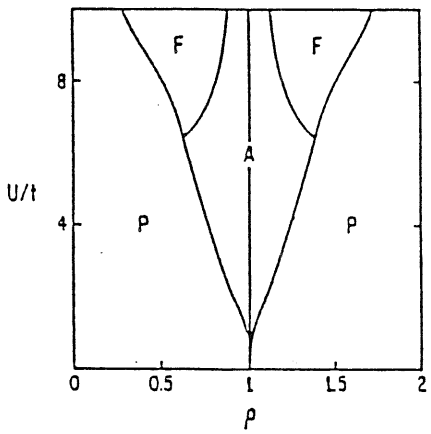

Figure 4.1: Phase diagram for the 2D Hubbard model on a square lattice in mean-field theory. A= antiferromagnet; P= paramegnetic; F= ferromagnetic

The first feasible step is to perform an Hartree-Fock decoupling of the interaction term (see Ref.[62] for the 3D case and Ref.[63] for the 2D case). The original Hamiltonian becomes:

$$H = -t \sum_\sigma \sum_{(i,j)} (c^\dagger_{i,\sigma} c_{j\sigma} + h.c.) + \frac{1}{2} U \sum_{i,\sigma} < n_{i\sigma} > n_{i\bar{\sigma}} - U \sum_i < n_{i\uparrow} >< n_{i\downarrow} > \quad . \tag{4.2}$$

Here the expectation values $< n_{i\sigma} >$ have to be calculated self-consistently. The high non linearity of the self-consistency equation leads to a rich variety of magnetic and/or

non-magnetic behaviors of the models as the parameter U/t is varied. The results are summarized in the well known fig.(4.1). In particular one can see that, from small values of U/t onwards, the system is an antiferromagnetic insulator at half-filling. This is in agreement with the prediction of a Mott transition in the strong coupling limit and at half-filling.

In the weak-coupling limit ($U << t$) the starting point is the Fermi gas in k-representation and in principle a perturbation expansion in U/t can be performed using standard techniques.

On the other hand, in the strong coupling limit, where double occupancy of lattice sites is suppressed, a real space picture is more helpful. Here the Hilbert space for the Hubbard model may be simply written as a tensor product over the four possible states at lattice sites i:

$$\mathcal{H} = \otimes_i span\{|0>, |\uparrow>, |\downarrow>, |\uparrow\downarrow>\}_i \tag{4.3}$$

The difficulties of the strong-coupling limit $U = \infty$ are caused by the structure of the Hubbard interaction. In fact at $U = \infty$ the ground state has an infinite degeneracy (2^L in the case of a half filled band N=L). The ground state cannot be obtained by degenerate perturbation theory in t/U because the exact solution of the effective hamiltonian for $U >> t$ i.e. the $t - J$ model in not simple at all[64], [65], [66], [6].

It is necessary to work with a restricted Hilbert space $\mathcal{H}^{restr}$, where doubly occupied sites are excluded. However difficulties are due to the fact that projected operators usually do not obey canonical commutation relations and do not commute with the hamiltonian. We will come back to this point in the next Section.

4.2 The generating functional: our method

The infinite U limit of the one band Hubbard model away from half-filling is given by the hopping hamiltonian:

$$\tilde{H} = \mathbf{P}(-t \sum_{(i,j),\sigma} c^{\dagger}_{i,\sigma} c_{j,\sigma} + h.c.)\mathbf{P} = \mathbf{P}H\mathbf{P} \tag{4.4}$$

where the fermion operators act on the restricted Hilbert space of no doubly occupied sites. This constraint is given by the Gutzwiller projector:

$$P = \prod_{i}(1 - n_{i\uparrow}n_{i,\downarrow}) \tag{4.5}$$

Our aim is to evaluate the partition function:

$$Z = Tr\{e^{-\beta PHP}P\} \tag{4.6}$$

using appropriate derivatives of a suitable generating functional. At great difference with the half-filled case (Heisenberg hamiltonian and the single-site occupancy projector) here we have:

$$[H, n_{i,\sigma}] \neq 0 \tag{4.7}$$

In order to proceed further in this direction we can use the Trotter formula[57] to divide the imaginary time interval $[0, \beta]$ into n equal subintervals ($\epsilon = \beta/n$) and write the partition function as:

$$\begin{aligned} Z &= \lim_{n\to\infty} Tr\left\{\left(e^{-\frac{\beta}{n}PHP}\right)^n P\right\} = \lim_{n\to\infty} Tr\left\{\left(e^{-\frac{\beta}{n}PHP}P\right)^n\right\} = \\ &= \lim_{n\to\infty} Tr\left\{\left(e^{-\frac{\beta}{n}H}P\right)^n\right\} \end{aligned} \tag{4.8}$$

When n is finite the last equality is to order $\mathcal{O}(1/n^2)$.

We can rewrite the previous expression by introducing the variable $\tau_k = \frac{\beta}{n}k$; $k = 1, ..., n$ and the Heisenberg representation of the projector $P(\tau_k) = e^{\tau_k H} P e^{-\tau_k H}$ as:

$$\begin{aligned} Z &= \lim_{n\to\infty} Tr\left\{\left(e^{-(\tau_n-\tau_{n-1})H}P\right)\left(e^{-(\tau_{n-1}-\tau_{n-2})H}P\right).....\left(e^{-\tau_1 H}P\right)P\right\} \\ &= \lim_{n\to\infty} Tr\left\{e^{-\tau_n H}P(\tau_n)P(\tau_{n-1}).....P(0)\right\} = \lim_{n\to\infty} Tr\left\{e^{-\beta H}\prod_{i=1}^{n}P(\tau_i)\right\} \end{aligned} \quad (4.9)$$

We propose to evaluate the auxiliary generating functional:

$$Z[z_{i,\sigma}(\tau)] = Tr\{e^{-\beta H}T_\tau e^{\int_0^\beta d\tau \sum_{i,\sigma} z_{i,\sigma}(\tau)n_{i,\sigma}(\tau)}\} \quad (4.10)$$

where we have added a source term to the hamiltonian. The time ordering T_τ is required because $n_{i\sigma}$ and H do not commute. Note that this is an unrestricted trace. The time ordered exponential must be explicitly evaluated via series expansion. When $Z[z_{i,\sigma}(\tau)]$ is known the original partition function can be obtained by derivation:

$$Z = \lim_{n\to\infty}\prod_{i,\tau_i}(1 - \frac{\partial^2}{\partial z_{i,\uparrow}(\tau_i)\partial z_{i,\downarrow}(\tau_i)})Z[z_i]\Big|_{z_i=0} \quad (4.11)$$

Under reserve of convergence eq.(4.11) is exact. In the next Section I show that this is indeed the case for the toy model of a two-site system.

Expliciting the Time ordering operator in Eq.(4.10), for each spin index as:

$$\begin{aligned} &T_\tau\left[\exp\left(-\int_0^1 d\tau \sum_i z_i(\tau)n_i(\tau)\right)\right] = 1 + \\ &+\sum_{n=1}^{\infty}(-1)^n\int_0^1 d\tau_n...\int_0^{\tau_2} d\tau_1 \sum_{\{a_1,...a_n\}}[z_{a_n}(\tau_n)...z_{a_1}(\tau_1)][n_{a_n}(\tau_n)...n_{a_1}(\tau_1)] \end{aligned} \quad (4.12)$$

The sum is over all possible collection of n site indices $a_1...a_n$. It is clear that the formal expression of the generating functional requires the evaluation of the correlation functions:

$$<< n_{a_n}(\tau_n) n_{a_{n-1}}(\tau_{n-1}) .... n_{a_1}(\tau_1) >> \tag{4.13}$$

of the non interacting system. The average in the above equation can be related to the n-particles Green function and rewritten via the Wick theorem in terms of the single particle Green functions for the non interacting system. As shown in Refs.[67],[68], in the case of equal time correlation functions, one can give a diagrammatic representation of these contractions and a linked cluster theorem allows to neglect the disconnected diagrams. The main difficulties in the evaluation of the first projector, $\mathbf{P}(0)$, are essentially the same as found in references [68], [69] where the authors dealt with the Gutzwiller correlations at equal time. They have found an analytical expression in the one dimensional case but the problem is still unsolved for higher dimensions.

4.3 Two-site example

We have tested the procedure outlined in the previous Section on a simple model of a two-site molecule. Our aim in solving this toy model is to check the convergence of the limit in eq.(4.11) and to see how the projectors act at each time slice. From this example we will also extract useful hints to address the general problem for the infinite system.

Here we are dealing with two sites:"c" and "d". We call $c(c^\dagger)$ and $d(d^\dagger)$ the creation (annihilation) operators on the sites c and d respectively. For future convenience we introduce also a chemical potential μ. The Hamiltonian of the system is:

$$H = \mathbf{P}(\sum_\sigma \tilde{H})\mathbf{P} = \mathbf{P}(\sum_\sigma -t(c^\dagger_\sigma d_\sigma + h.c.) - \mu(n_{c\sigma} + n_{d\sigma}))\mathbf{P} \ . \tag{4.14}$$

It is obviously very easy to evaluate the true partition function of this model in the restricted (9 dimensional) Hilbert space.

First of all let us state the results that come from direct evaluations of the traces. Call Z_o the unrestricted partition function and Z_r the restricted one. We introduce the definitions: $z = e^{\beta\mu}$ and $x = \cosh \beta t$. We have:

$$Z_o = [1 + z^2 + 2zx]^2 = \tilde{Z}_0^{\uparrow} \tilde{Z}_0^{\downarrow} \tag{4.15}$$

and

$$Z_r = 1 + 4z^2 + 4zx \tag{4.16}$$

Our method consists in evaluating Z_r as:

$$Z_r = \lim_{n\to\infty} \prod_{i=0,n} \mathrm{P}(\tau_i) Z[z_{i\sigma}(\tau_i)] \Big|_{z_{i\sigma}=0} \tag{4.17}$$

To proceed further we need a formal solution for the generating functional. Instead of the four sources $z_{i\sigma}(\tau)$ that were coupled with $n_{i\sigma}(\tau)$ we will use the sources $\xi_\sigma(\tau)$ and μ_σ that are coupled to the combinations $n_\sigma^- = n_{c\sigma} - n_{d\sigma}$ and $n_\sigma^+ = n_{c\sigma} + n_{d\sigma}$ respectively. The simplification comes from the fact that the last term is a conserved quantity and is therefore time independent. The price to be payed is a more complicated form of the projector:

$$P = 1 - \frac{1}{2}[n_\uparrow^+ n_\downarrow^+ + n_\uparrow^- n_\downarrow^-] + \frac{1}{16}[(n_\uparrow^+ n_\downarrow^+ + n_\uparrow^- n_\downarrow^-)^2 - (n_\uparrow^+ n_\downarrow^- + n_\uparrow^- n_\downarrow^+)^2] \tag{4.18}$$

The generating functional reads:

$$\mathcal{Z}[\mu, \xi(\tau)] = Tr\left\{ e^{-\beta H - \mu N} T_\tau \left[\exp\left(- \int_0^1 d\tau \sum_\sigma \xi_\sigma(\tau)(n_{c\sigma} - n_{d\sigma})(\tau) \right) \right] \right\} \tag{4.19}$$

which is a separate product for the two spin components.

In computing Z_o we can consider only one spin direction omitting the spin index henceforth. Written in the basis $X^\dagger = (c^\dagger, d^\dagger)$ the hamiltonian is:

$$\tilde{H} = -tX^{\dagger}\sigma_1 X - \mu X^{\dagger}X \tag{4.20}$$

σ_i being the Pauli matrices. Defining: $\zeta = (c+d)/\sqrt{2}$ and $\eta = (d-c)/\sqrt{2}$ the hamiltonian can be rewritten in diagonal form as: $\tilde{H} = -t(\zeta^{\dagger}\zeta - \eta^{\dagger}\eta) - \mu(\zeta^{\dagger}\zeta + \eta^{\dagger}\eta)$. Given the Hilbert space $|n_c, n_d>$, $\tilde{H}$ is diagonal in the basis:

$$|0>=|00> \ , \ |0'>=|11> \ , \ |+>=\frac{1}{\sqrt{2}}(|10>+|01>) \ , \ |->=\frac{1}{\sqrt{2}}(|10>-|01>) \tag{4.21}$$

with eigenvalues 0 , 0 , $+t$, $-t$.

Let us introduce a spin algebra:

$$S_+ = \zeta^{\dagger}\eta \ , \ S_- = \eta^{\dagger}\zeta \ , \ S_z = \frac{1}{2}(n_\zeta - n_\eta) \tag{4.22}$$

so that $H = -2tS_z$ and $S_x(\tau) = (n_{c\sigma} - n_{d\sigma})(\tau)$. From the Heisenberg equations of motion we have:

$$S_x(\tau) = \frac{1}{2}(S_+ e^{-2t\tau} + S_- e^{2t\tau}) \tag{4.23}$$

Then, for one spin direction, the generating functional can be written as:

$$\begin{aligned}
&\mathcal{Z}_\sigma[\mu, \xi(\tau)] = Tr\left\{e^{2\beta t S_z + \beta\mu N} T_\tau \left[\exp\left(2\int_0^1 d\tau \xi(\tau) S_x(\tau)\right)\right]\right\} = \\
&= Tr\left\{e^{2\beta t S_z + \beta\mu N}\left[1 + \sum_{n=1}^{\infty}\int_0^1 d\tau_n \int_0^{\tau_n} d\tau_{n-1} \ldots \int_0^{\tau_2} d\tau_1 [\xi(\tau_n)\ldots\xi(\tau_1)]\cdot\right.\right. \\
&\left.\left.\cdot[S_+ e^{-2t\tau_n} + S_- e^{2t\tau_n}]\ldots[\ldots]\ldots[S_+ e^{-2t\tau_1} + S_- e^{2t\tau_1}]\right]\right\}
\end{aligned} \tag{4.24}$$

Because $S_\pm|0>=S_\pm|0'>=0$ we have:

$$\mathcal{Z}_\sigma[\mu,\xi(\tau)] = \mathcal{Z}_\sigma[\mu,0] + ze^{\beta t}\sum_{n=1}^{\infty} < +|A_n|+ > + ze^{-\beta t}\sum_{n=1}^{\infty} < -|A_n|- > \qquad (4.25)$$

with

$$A_n = \int_0^1 d\tau_n \xi(\tau_n)[S_+ e^{-2t\tau_n} + S_- e^{2t\tau_n}] \ldots \int_0^{\tau_2} d\tau_1 \xi(\tau_1)[S_+ e^{-2t\tau_1} + S_- e^{2t\tau_1}] \quad . \qquad (4.26)$$

Note that the only terms that survive in the sum are those with even n and their matrix elements are:

$$\begin{aligned} < +|A_{2n}|+ > &= \int_0^1 d\tau_{2n}\xi(\tau_{2n}) \ldots \int_0^{\tau_2} d\tau_1 \xi(\tau_1) e^{-2t\tau_{2n}} \ldots e^{-2t\tau_2} e^{2t\tau_1} \\ < -|A_{2n}|- > &= \int_0^1 d\tau_{2n}\xi(\tau_{2n}) \ldots \int_0^{\tau_2} d\tau_1 \xi(\tau_1) e^{2t\tau_{2n}} \ldots e^{2t\tau_2} e^{-2t\tau_1} \quad . \end{aligned} \qquad (4.27)$$

Eq.(4.25) and (4.27) are the formal solution for $\mathcal{Z}_\sigma$ for any choice of $\xi(\tau)$. Now we can apply the projectors at time each time slice.

The first step is the evaluation of the effects of the projector at $\tau = 0$:

$$\mathrm{P}(0) Z[z_i(\tau_i)]|_{z_i=0} = 1 + 2z^2 + 2z^2x^2 + 4zx \quad . \qquad (4.28)$$

As one can see, applying the first projector $\mathrm{P}(0)$ at the time $t = 0$, the z^3 and z^4 terms that are present in eq.(4.15) disappear. These are the terms that come from the mixing of at least one doubly occupied site.

The second step consists in the application of two projectors at two consecutive times. We get:

$$\mathrm{P}(\tau_1)\mathrm{P}(0) Z[z_i(\tau_i)]|_{z_i=0} = \frac{1}{2}\,\mathrm{P}(0) Z[z_i]|_{z_i=0} - \frac{1}{2} + \frac{1}{2}\sum_\sigma \tilde{Z}_0^\sigma + \frac{1}{2}(2z^2)\cosh^2\beta t(1-2\tau_1) \qquad (4.29)$$

This is in the form we want to generalize. It is worth noticing that "time" correlations are going to appear in the argument of the hyperbolic cosine function.

Now we go to the third step:

$$\begin{aligned}
&\mathbf{P}(\tau_2)\mathbf{P}(\tau_1)\mathbf{P}(0)Z[z_i(\tau_i)]\|_{z_i=0} = \\
&= \frac{1}{2^2}\mathbf{P}(0)Z[z_i] - (\frac{1}{4}+\frac{1}{2}) + (\frac{1}{4}+\frac{1}{2})\sum_\sigma \tilde{Z}_0^\sigma + \\
&+\frac{1}{2^2}(2z^2)(\sum_{i=1,2}\cosh^2\beta t(1-2\tau_i) + \cosh^2\beta t(1-2(\tau_2-\tau_1)))
\end{aligned} \tag{4.30}$$

Here a two-time correlation comes in. At this point it is easy to give the recursive form in which all the time correlations appear:

$$\begin{aligned}
&\mathbf{P}(\tau_n).....\mathbf{P}(0)Z[z_i(\tau_i)]\|_{z_i=0} = \\
&= \frac{1}{2^n}\mathbf{P}(0)Z[z_i] - \sum_{l=1}^{n}\frac{1}{2^l} + \sum_{l=1}^{n}\frac{1}{2^l}\sum_\sigma \tilde{Z}_0^\sigma + \\
&+\frac{1}{2^n}(2z^2)(\sum_{i=1}^{n}\cosh^2\beta t(1-2\tau_i) + \sum_{i<j}\cosh^2\beta t(1-2(\tau_j-\tau_i)) + \\
&+ \sum_{i<j<k}\cosh^2\beta t(1-2(\tau_j-\tau_i)-2\tau_k) + ...)
\end{aligned} \tag{4.31}$$

Finally in the limit $n \to \infty$, knowing that $\sum_{l=1}^{\infty} 1/2^l = 1$, we have:

$$\begin{aligned}
Z_r \;=\; &\sum_\sigma \tilde{Z}_0^\sigma - 1 + 2z^2 \lim_{n\to\infty}\frac{1}{2^n}(\sum_{i=1}^{n}\cosh^2\beta t(1-2\tau_i) + \sum_{i<j}\cosh^2\beta t(1-2(\tau_j-\tau_i)) + \\
&+ \sum_{i<j<k}\cosh^2\beta t(1-2(\tau_j-\tau_i)-2\tau_k) + ...)
\end{aligned} \tag{4.32}$$

We can show that the limit converges in the case $t = 0$ in which all the $\cosh^2$ are equal to one. In fact the last term becomes:

$$\frac{1}{2^n}\sum_{k=0}^{n}\binom{n}{k} - 1 \simeq \frac{1}{2^n}(1+1)^n = 1 \tag{4.33}$$

Moreover, for any $t \neq 0$ the $\cosh^2$ in the sums are less then a given constant and the same argument holds true. This is because the argument of $\cosh^2$ is always less then $2\beta t$.

In the limit $n \to \infty$ we can rewrite the sums as integrals introducing an opportune measure that preserves the convergence of the result. In the case $t = 0$ it is easy to see that the last in Eq.(4.32) becomes:

$$\frac{1}{2^n}\sum_{k=1}^{n}\alpha^k\int_0^1 d\tau_k\cdots\int_0^{\tau_2}d\tau_1 = \frac{1}{2^n}\sum_{k=1}^{n}\frac{\alpha^k}{k!} = \frac{e^\alpha}{2^n} - \frac{1}{2^n} \tag{4.34}$$

what converges to the right result if the integral measure α is taken to be $n\ln 2$. At finite n a numerical text gives good results.

Now we came back to the general case. Remembering that $2\tilde{Z}_0^\sigma = 2 + 2z^2 + 4zx$, and transforming ordered sums into ordered integrals with the opportune measure discussed above, we have:

$$Z_r = 1 + 2z^2 + 4zx + +2z^2\lim_{n\to\infty}\frac{1}{2^n}\sum_{k=1}^{n}\alpha^k\int_0^1 d\tau_k\cdots\int_0^{\tau_2}d\tau_1\cosh^2 2\beta t(\frac{1}{2} - \sum_{l=1}^{k}(-1)^{k-l}\tau_l) \tag{4.35}$$

Finally, we have the right result if the last term in eq.(4.35) converges to $2z^2$.

Using the relation:

$$\cosh^2 2\beta t(\frac{1}{2} - \sum_{l=1}^{k}(-1)^{k-l}\tau_l) = \frac{1}{2}\cosh 4\beta t(\frac{1}{2} - \sum_{l=1}^{k}(-1)^{k-l}\tau_l) + \frac{1}{2} \tag{4.36}$$

the second term will give half of the desired result. Now we have to prove that the first term, inserted in Eq.(4.35), i.e.:

$$\mathcal{L} = \frac{1}{2}\lim_{n\to\infty}\frac{1}{2^n}\sum_{k=1}^{n}\alpha^k\int_0^1 d\tau_k\cdots\int_0^{\tau_2}d\tau_1\cosh 4\beta t(\frac{1}{2} - \sum_{l=1}^{k}(-1)^{k-l}\tau_l) \tag{4.37}$$

converges to $\frac{1}{2}$.

We define the function[70]:

$$F_a(y) = 1 + \sum_{k=1}^{n} \alpha^k \int_0^y d\tau_k \cdots \int_0^{\tau_2} d\tau_1 e^{-a\sum_{l=1}^{k}(-1)^{k-l}\tau_l} \tag{4.38}$$

which satisfy the differential equation:

$$F_a''(y) = aF_a'(y) - \alpha^2 F_a(y) = 0 \tag{4.39}$$

Given the boundary conditions: $F_a(0) = 1$, $F_a'(0) = \alpha$ we have the solution:

$$F_a(y) = e^{-\frac{a}{2}y}\left\{\cosh\frac{Xy}{2} + \frac{a}{X}\sinh\frac{Xy}{2} + \frac{2\alpha}{X}\sinh\frac{Xy}{2}\right\} \tag{4.40}$$

where $X = [a^2 + 4\alpha^2]^{1/2}$. In the limit $\alpha(n) \to \infty$: $F_a(y) \simeq e^{-\frac{a}{2}y}e^{\alpha y}$.

Now we can rewrite $\mathcal{L}$ in terms of $F_a(y)$ (with $a = \pm 4\beta t$, $y = 1$, $\alpha = n\ln 2$) as:

$$\mathcal{L} = \frac{1}{2}\lim_{n\to\infty}\frac{1}{2^n}\left\{\frac{e^{2\beta t}}{2}[F_{4\beta t}(1) - 1] + \frac{e^{-2\beta t}}{2}[F_{-4\beta t}(1) - 1]\right\} \tag{4.41}$$

Using the asymptotic expression for $F_a(y)$ we get:

$$\mathcal{L} = \frac{1}{2}\lim_{n\to\infty}\frac{1}{2^n}\left\{\frac{e^{2\beta t}}{2}e^{-2\beta t}\left[e^{n\ln 2} - 1\right] + \frac{e^{-2\beta t}}{2}e^{2\beta t}\left[e^{n\ln 2} - 1\right]\right\} = \frac{1}{2} \tag{4.42}$$

This complete the proof.

From the lesson of the two-site example one expects that further applications of the projector at subsequent times allows for an iteration procedure. The main problems in proceeding are the following.

First, one has to cope with the difficulties connected with the series of many sites correlations which are all there. However this refers to the evaluation of the generating functional of Eq.(4.10) which requires averages with respect to the non interacting Hamiltonian if the projected Fermi gas is studied. In particular the claim that the application of the Hamiltonian on a projected state does not add too many extra components out of the restricted Hilbert space, implies that P and H almost commute, so that the time dependence of the source $z_{i\sigma}(\tau)$ could be dealt with within an adiabatic scheme.

The second difficulty is the limit to infinite time steps of the partition function which is expected to be non trivial.

Bibliography

[1] J.G.Bednorz, K.A.Müller Z.Phys.B 64 189 1986

[2] T.Ito, K.Takenaka, S.Uchida Phys.Rev.Lett. **70**,3995 (1993)

[3] M.A.Van Veenendaal, R.Schlatmann, G.A.Sawatzky, W.A.Groen Phys.Rev.B **47**,446 (1993)

[4] J.Hubbard Proc.Roy.Soc.A **276**,238 (1964); Proc.Roy.Soc.A **285**,542 (1965)

[5] P.W.Anderson Science **235**,1196 (1987)

[6] F.C.Zhang, T.M.Rice Phys.Rev.B **37**,3759 (1988)

[7] G.Shirane et al. Phys.Rev.Lett. **59**,1613 (1987)

[8] A.Chubukov, S.Sachdev, J.Ye (preprint)

[9] R.Shankar Rev.Mod.Phys.(1993)

[10] I.Affleck, J.B.Marston Phys.Rev.B **37**,3774 (1988), J.B.Marston, I.Affleck Phys.Rev.B **39**,11538 (1989)

[11] N.Read, S.Sachedv Phys.Rev.Lett. **66**,1773 (1991)

[12] X.G.Wen, F.Wilczek, A.Zee Phys.Rev.B **39**,11413 (1989)

[13] E.Manousakis Rev.Mod.Phys. **63**,1 (1991)

[14] M.V.Berry Proc.Roy.Soc. **A392**,45 (1984)

[15] N.Read, S.Sachdev Nucl.Phys.B **316**,609 (1989)

[16] M.Inui,S.Doniach,M.Gabay Phys.Rev.B **38**,6631 (1988)

[17] F.Nori,E.Gagliano,S.Bacci Phys.Rev.Lett. **68**,240 (1992)

[18] A.P.Balachandran, E.Ercolessi, G.Morandi, A.M.Srivastava Int. Jou. of Mod. Phys.B 4,2057 (1990)

[19] H.Bethe Z.Physik **71**,205 (1931)

[20] W.Marshall Proc.Roy.Soc.A **232**,48 (1955)

[21] E.Fradkin "Field theories of condensed matter systems" Addison-Wesley Ed. (1991)

[22] S.Liang, B.Doucçt, P.W.Anderson Phys.Rev.Lett. **61**, 2585 (1988)

[23] P.W.Anderson Mat.Res.Bull. **8**,153 (1973)

[24] S.Kivelson, D.Rokhsar, J.P.Sethna Phys.Rev.B **35**,865 (1987)

[25] J.D.Reger, A.P.Young Phys.Rev.B **37**,5978 (1988)

[26] N.Trivedi, D.Ceperly Phys.Rev.B **40**,2737 (1989)

[27] B.Bernu, C.Lhuillier, L.Pierre Phys.Rev.Lett. **69**,2590 (1992)

[28] N.D.Mermin, H.Wagner Phys.Rev.Lett. **17**,1133 (1966)

[29] T.Holstein, H.Primakoff Phys.Rev. **58**,1098 (1940)

[30] P.W.Anderson Phys.Rev. **86**,694 (1952)

[31] I.Affleck Lecture notes of the Les Houches summer school on "Field theory methods and quantum critical phenomena" E.Brezin and J.Zinn-Justin eds.(1989)

[32] S.Sachdev Lecture notes for the summer course on: Low dimensional quantum field theories for condensed matter physicists. (ICTP-trieste 1992)

[33] A.Auerbach, D.P.Arovas Phys.Rev.lett. **61**,617 (1988)

[34] D.P.Arovas, A.Auerbach Phys.Rev.B **38**,316 (1988)

[35] M.Hamermesh "Group theory and its application to physical problems" Addison-Wesley Publ.Co. (1964)

[36] M.Raykin, A.Auerbach (preprint: "The 1/N expansion and long range antiferromagnetic order")

[37] G.Kotliar Phys.Rev.B **37**,3664 (1988)

[38] F.D.M.Haldane Phys.Rev.Lett. **61**,1029 (1988)

[39] E.Fradkin, M.Stone Phys.Rev.B **38**,7215 (1988)

[40] L.B.Ioffe, A.I.Larkin Int.J.Mod.Phys.B **2**,203 (1988)

[41] A.Angelucci, G.Jug Int.J.Mod.Phys.B **3**,1069 (1989)

[42] A.Parola Phys.Rev.B **40**,7109 (1989)

[43] S.Chakravarty, B.I.Halperin, D.R.Nelson Phys.Rev.B **39**,2344 (1989)

[44] A.Angelucci, Ph.D.Thesis (Trieste University 1990)

[45] R.Rajaraman "Solitons and instantons" (North- Holland, Amsterdam 1982)

[46] C.Nash , S.Sen "Topology and geometry for physicists" (Academic Press, London 1989)

[47] I.Affleck, F.D.H.Haldane Phys.Rev.B **36**,5291 (1985)

[48] M.V.Berry Proc.Roy.Soc. **A414**,31 (1987)

[49] P.Chandra,B.Ducot Phys.Rev.B **38**,9335 (1988)

[50] T.Einarsson,H.Johannesson Phys.Rev.B **43**,5867 (1991)

[51] H.J.Schulz, T.A.L.Ziman Europh.Lett. **18**,355 (1992)

[52] E.Dagotto, A.Moreo Phys.Rev.Lett. **63**,2148 (1989)

[53] D.Poilblanc, E.Gagliano, S.Bacci, E.Dagotto Phys.Rev.B **43**,10970 (1991)

[54] S.Elitzur Phys.Rev.D **12**,3978 (1975)

[55] G.Baskaran, Zou, P.W.A. Anderson Solit State Comm. **63**,937(1987)

[56] Z.Zou,R.B.Laughlin Phys.Rev.B **42**,4073 (1990)

[57] J.W.Negele, H.Orland "Quantum many-particle systems" Addison-Wesley Ed. (1988)

[58] J.Hubbard Phy.Rev.Lett. **3**,77 (1959)

[59] D.Vollhardt Lecture notes for the international school of physics "Enrico Fermi" on "Perspectives in Many-particle physics" Varenna (1992)

[60] P.Fulde "Electron correlations in molecules and solids" Springer-Verlag (1991)

[61] M.C.Gutzwiller Phys.Rev.Lett. **10**,159 (1963)

[62] M.Cyrot J.Phys. (Paris) **33**,125 (1972)

[63] J.E.Hirsh Phys.Rev.B **28**,4059 (1983) ; J.E.Hirsh Phys.Rev.B **31**,4403 (1985)

[64] W.Kohn Phys.Rev.A **133**,171 (1964)

[65] K.A.Chao, J.Spalek, A.M.Oles J.Phys.C **10**,L271 (1977)

[66] C.Gros, R.Joynt, T.M.Rice Phys.Rev.B **36**,381 (1987)

[67] P.Horsch, P.Fulde Z.Phys. B **36**,23 (1979)

[68] W.Metzner, D.Vollhardt Phys.Rev.B **37**,7382 (1988)

[69] F.Gebhard, D.Vollhardt Phys.Rev.Lett. **59**,1472 (1987)

[70] N.River, T.J.Coe J.Phys.C **10**,4471 (1977)

Paper I

RAPID COMMUNICATIONS

PHYSICAL REVIEW B VOLUME 45, NUMBER 4 15 JANUARY 1992-II

Saddle-point finite-temperature results for the infinite-U Hubbard model at half filling

M. Di Stasio
Scuola Internazionale Superiore di Studi Avanzati, International School for Advanced Studies, v. Beirut 2, I-34100 Miramare, Trieste, Italy

E. Ercolessi
Physics Department, Syracuse University, Syracuse, New York 13244-1130

G. Morandi
Dipartimento di Fisica, Universitá di Bologna, v. Irnezio 46, I-40126 Bologna, Italy

A. Tagliacozzo and F. Ventriglia
Dipartimento di Scienze Fisiche, Universitá di Napoli, Mostra d'Oltremare Pad. 19, I-80125 Napoli, Italy
(Received 17 June 1991; revised manuscript received 7 October 1991)

We implement the constraint of no-double-site occupancy exactly, in the spin-$\frac{1}{2}$ Hubbard-Heisenberg model at half filling. The staggered Peierls and the flux phase are again found to be saddle points for the effective action, also at finite temperature. The mean-field critical temperatures are higher when the occupancy restriction is taken into account. Gaussian fluctuations of the auxiliary field are reasonably small for a large temperature range, but have to be necessarily included, when extending the free energy to finite temperatures.

Increasing efforts have been concentrated in past years in characterizing the ground state and the low-lying excitations of the Hubbard model close to half filling in the large-U limit. This model could be relevant to the copper oxide high-T_c superconducting materials.[1]

We are concerned here with the case of half filling (one electron per site) on a square lattice. It is known that, for any space dimension, the Hubbard model can be mapped, in the strong-coupling limit and at half filling, into an antiferromagnetic (AFM) Heisenberg model.

The question is still open, whether long-range Néel[2-4] order occurs, or other phases are present, as suggested by mean-field theory, for instance, the dimerized phase (Peierls phase) or the flux phase.[5-7] The latter is particularly relevant because of gapless particle-hole excitations at special points of the Brillouin zone (BZ) with linear dispersion, giving rise to an approximate (2+1)-dimensional (massless) relativistic free-fermion quantum field theory. This could be the starting point[8] (by inclusion of frustration) for the so-called "anyon" superconductivity.[9]

Recently, the flux phase has been found to be unstable,[10] but could be stabilized by adding further interactions (Ref. 11, hereafter denoted by MA). The most popular approach to the ground state of the Heisenberg model at half filling is to investigate its generalizations to SU(N) antiferromagnets:[12,13] The saddle-point approximation becomes exact in the limit of N going to infinity.

Also the $1/N$ corrections have been calculated to include the quantum Gaussian fluctuations. An auxiliary field is introduced in the N-component Lagrangian to account for the average site occupancy of $N/2$. The large-N limit quenches the fluctuations of this occupation number regardless of the value of U ($U>0$) (MA). This also happens when the constraint is handled within the slave boson method.[14]

At finite N, the infinite-U limit should completely suppress the fluctuations which could possibly arise. However, this feature is hard to reproduce. Numerical methods are being developed,[15-17] while the slave boson technique is expected not to give reliable results at finite temperature.

At zero temperature, the constraint of single-site occupancy ($U\rightarrow\infty$, $N=2$) has been implemented in recent calculations by means of the Gutzwiller projection, and the resulting ground state has been found to have good variational energy.[18]

Our work moves from the observation that, when $N=2$, the constraint of half filling takes a very simple form and can be implemented exactly at any temperature. Therefore, the compromise choice we have made was to project properly onto the restricted subspace in evaluating the fermion trace with $N=2$, and to perform the saddle-point approximation, with no pretention of it being exact in some limit. In this way we are able to study the effect of the constraint at any temperature on the partition function, at least within the saddle-point approximation.

According to the usual procedure, we introduce an auxiliary link field U_{ij}, which we keep static together with its small variations. This amounts to include classical Gaussian fluctuations only around the mean-field configuration. In this limit we find that the results do not change at $T=0$, with respect to the ones already present in the literature. However, the inclusion of the constraint acts as an effective reduction of the entropy of the system at finite temperature. In the spirit of the MA work we consider here only phases with periodicity along the lattice diagonals. Their Peierls and the flux phase are still extrema of the free energy and, because the correction has the role of inhibiting classical fluctuations, the mean-field transition

temperatures are increased. We report here the temperature dependence of the free energy for the Peierls phase and leave the free energy of the flux phase to further work. Preliminary results show that the former remains the state lower in energy also at finite temperature, and the most stable one.

It has been shown in Ref. 13 that special quantum fluctuations which are only present when the spin-Peierls dimers are arranged into columns (2×1 unit cell) stabilize this columnar phase with respect to the staggered one ($\sqrt{2}\times\sqrt{2}$ unit cell), which we consider here. The fluctuations we include preserve the $\sqrt{2}\times\sqrt{2}$ periodicity so that the columnar phase would require additional analysis.

In the limit of infinite U the Hubbard Hamiltonian can be mapped at half filling onto the Heisenberg model,

$$H_0=-\frac{J}{2}\sum_{(i,j)}\chi_{ij}^{\dagger}\chi_{ij}\,,$$

provided that no double occupancy of the sites is allowed.

Here $\chi_{ij}=\sum_{\alpha}c_{i\alpha}^{\dagger}c_{j\alpha}=\chi_{ji}^{\dagger}$ and $c_{i\alpha}(c_{i\alpha}^{\dagger})$ are fermion operators for electrons at site i having spin $\alpha=1,2$. Note that labels i,j $(i\neq j)$ should be counted only once, which we denote by the brackets.

As the particle number is fixed, we evaluate the partition function within the canonical ensemble:

$$Z=\mathrm{Tr}\{e^{-\beta H_0}\mathcal{P}\}\,,$$

where the half filling projector $\mathcal{P}$ is given by ($\hat{n}_i=\chi_{ii}$):

$$\mathcal{P}=\prod_i\hat{n}_i(2-\hat{n}_i)\,.$$

Because $\hat{n}_i$ and H_0 commute, Z can be obtained from the generating function, $\mathcal{Z}[z]=\mathrm{Tr}\{\exp[-\beta H_0+\sum_i z_i\hat{n}_i]\}$, by derivation with respect to the real parameters z_i, as follows:

$$Z=\prod_i\frac{\partial}{\partial z_i}\left(2-\frac{\partial}{\partial z_i}\right)\mathcal{Z}[z]\Big|_{z=0}\,. \tag{1}$$

The representation of $\mathcal{Z}[z]$ in terms of Grassman fields $\psi_{i\alpha}(\tau)$ is

$$\mathcal{Z}[z]=\int\prod_{i\alpha}\mathcal{D}\psi_{i\alpha}^{*}\mathcal{D}\psi_{i\alpha}\exp\left\{-\int_0^1 d\tau\sum_{i\alpha}\psi_{i\alpha}^{*}(\tau)(\partial_\tau-z_i)\psi_{i\alpha}(\tau)+\frac{\beta J}{2}\sum_{(i,j)}\int_0^1 d\tau\,\psi_{i\alpha}^{*}(\tau)\psi_{j\beta}^{*}(\tau)\psi_{i\beta}(\tau)\psi_{j\alpha}(\tau)\right\}. \tag{2}$$

The usual Hubbard-Stratonovich (HS) procedure allows for the integration of the fermion fields, yielding

$$\mathcal{Z}[z]=\int\prod_{(i,j)}\mathcal{D}U_{ij}\exp\left\{-\pi\sum_{(i,j)}\sum_m|U_{ij}(\Omega_m)|^2+2\,\mathrm{Tr}\ln A\right\}, \tag{3}$$

where $U_{ij}(\Omega_m)$ is the frequency-transformed auxiliary-boson field chosen as $U_{ij}(\tau)=\sum_\beta\psi_{j\beta}^{*}(\tau)\psi_{i\beta}(\tau)$. The factor 2 comes from the spin and the matrix A has elements $A_{ij}^{nn'}=(i\omega_n+z_i)\delta_{ij}\delta_{nn'}-cU_{ij}(\omega_n-\omega_{n'})$. Here, $\omega_n=(2n+1)\pi$ and $c=(\pi\beta J/2)^{1/2}$.

This result can be rewritten in terms of the single-particle Green's function G_0, for $J=0$, whose matrix elements are $(G_0)_{ij}^{nn'}=(i\omega_n)^{-1}\delta_{ij}\delta_{nn'}$, and of the matrix $(\tilde{U})_{ij}^{nn'}=z_i\delta_{ij}\delta_{nn'}-cU_{ij}(\omega_n-\omega_{n'})$; that is,

$$\mathcal{Z}[z]=\mathcal{N}\int\prod_{(i,j)}\mathcal{D}U_{ij}\exp\left\{-\pi\sum_{(i,j)}\sum_m|U_{ij}(\Omega_m)|^2+2\,\mathrm{Tr}\ln[1+G_0\tilde{U}]\right\}. \tag{4}$$

The normalization factor is $\mathcal{N}=\exp[2\,\mathrm{Tr}\ln G_0^{-1}]=4^N$, where N is the number of sites.

An effective action can be introduced:

$$\begin{aligned}S_{\mathrm{eff}}[\tilde{U}]&=-2\,\mathrm{Tr}\ln[1+G_0\tilde{U}]\\&=-\sum_i z_i+2\,\mathrm{Sp}[\ln\cosh(\tilde{U}/2)]\,.\end{aligned} \tag{5}$$

In the last expression the HS field has been assumed to be static and the notation "Sp" denotes traces over the site indices alone.

According to Eq. (1), the partition function becomes

$$Z=\int\prod_{(i,j)}\mathcal{D}U_{ij}\exp\left\{-\pi\sum_{(i,j)}|U_{ij}|^2-S_{\mathrm{eff}}[U]+\sum_i\ln(4B_i[U])\right\}, \tag{6}$$

where the last term arises from the constraint of half filling, with

$$B_i[U]=\left[\frac{\partial^2 S_{\mathrm{eff}}[U]}{\partial z_i^2}-2\frac{\partial S_{\mathrm{eff}}[U]}{\partial z_i}-\left(\frac{\partial S_{\mathrm{eff}}[U]}{\partial z_i}\right)^2\right]\Big|_{z=0}. \tag{7}$$

From now on we shall discuss the case of a square lattice and nearest-neighbor interactions. Then we find $\partial S_{\mathrm{eff}}/\partial z_i|_{z=0}=-1$. For the vanishing interaction $(J\to0)$, $\partial^2 S_{\mathrm{eff}}/\partial z_i^2|_{z=0}=-\frac{1}{2}$ and S_{eff} itself vanishes so that only the configurational entropy is left to the free energy, which is equal to $N\ln2$. This should be compared to the value $N\ln4$, which one gets when double occupancy of each site is not forbidden.

The full expression for B_i is

$$B_i=1+2\sum_n\mathrm{Sp}\left[\frac{1}{i\omega_n-cU}P_i\frac{1}{i\omega_n-cU}P_i\right],$$

where P_i is the projector on the state localized on the ith site of the lattice $[(P_i)_{jk}=\delta_{ij}\delta_{jk}]$.

Thus, the half filling constraint reduces the entropy term in the effective free energy:

$$\beta\mathcal{F}_{\mathrm{eff}}[U]=\pi\sum_{(i,j)}|U_{ij}|^2+S_{\mathrm{eff}}[U]-\sum_i\ln(4B_i[U]). \tag{8}$$

Following MA, we restrict now the discussion to random fields U_{ij} that are translationally invariant along the diagonals of the square lattice of spacing a. The matrix U^2 is diagonal in reciprocal space and its elements are $|\lambda(k)|^2$,

with

$$\lambda(k)=U_1e^{ik_xa}+U_2^*e^{-ik_ya}+U_3e^{-ik_xa}+U_4^*e^{ik_ya} \tag{9}$$

defined in terms of the four complex numbers U_i and k, spanning the reduced Brillouin zone (RBZ).

Setting $cU_i=\beta\Delta_i$ and $c|\lambda(k)|=\beta\Delta_k$, the B_i's turn out to be site independent, and the effective free energy reads

$$\beta\mathcal{F}_{\rm eff}[U_i]=N\beta\sum_i\frac{|\Delta_i|^2}{J}-4\sum_k\ln\cosh(\tfrac{1}{2}\beta\Delta_k)-N\ln(4B)\,, \tag{10}$$

with

$$B=1-\frac{1}{\beta}\left(\frac{2}{N}\right)^2\sum_{k,k'}\frac{\Delta_k\tanh(\frac{1}{2}\beta\Delta_k)-\Delta_{k'}\tanh(\frac{1}{2}\beta\Delta_{k'})}{\Delta_k^2-\Delta_{k'}^2}\,. \tag{11}$$

Again, when $J\to 0$ and Δ vanishes, then $B\to\frac{1}{2}$ for any temperature. On the other hand, at zero temperature, when $\Delta\neq 0$, $B=1$. Therefore, B decrease smoothly from $B=1$ at zero temperature to the value $B=\frac{1}{2}$ at high temperature.

While the path integral in Eq. (6) is unavoidable, the field configurations which minimize the effective free energy are easily found. The most studied phases, since the work by MA, are the Peierls phase and the flux phase.[5]

The dimensionless temperature will be denoted by $t=(\beta J)^{-1}$ and $d=\Delta/J$ is the magnitude of the order parameter. In the following, the two saddle points are described.

a. Staggered Peierls phase. $d_1=d$, $d_2=d_3=d_4=0$. Using Eq. (11), Eq. (10) becomes

$$f_{\rm eff}^0=\frac{\mathcal{F}_{\rm eff}^0}{NJ}=d^2-2t\ln(\cosh d/2t)-t\ln(4B_P)(d/2t)\,. \tag{12}$$

$$B_P(x)=1-\frac{1}{4}\left\{\frac{\tanh x}{x}+\frac{1}{\cosh^2 x}\right\}. \tag{13}$$

The self-consistency equation for the order parameter is

$$2d=\tanh\frac{d}{2t}+\frac{1}{2}\frac{\partial}{\partial x}\ln B_P\Big|_{x=d/2t}\,, \tag{14}$$

where $d(t=0)=\frac{1}{2}$ and $f_{\rm eff}^0(t=0)=-\frac{1}{4}$. The mean-field transition temperature is found to be higher ($t_c=\frac{5}{12}$) than that found in the absence of the constraint ($t_{c0}=\frac{1}{4}$).

b. Flux phase. $d_i=de^{i\pi/4}$ and $d_k=2d|\cos k_x-i\cos k_y|$ ($a=1$). Then,

$$f_{\rm eff}^0=4d^2-2d\bar{\varepsilon}-2t\int\frac{d^2k}{2\pi^2}\ln(1+e^{-2d\varepsilon_k/t})-t\ln B\,,$$

where $\bar{\varepsilon}=\int d^2k\,\varepsilon_k/2\pi^2=0.918$, $\varepsilon_k=(\cos k_x^2+\cos k_y^2)^{1/2}$, and B is given by Eq. (11). One finds $d(t=0)=\bar{\varepsilon}/4$ and $f_{\rm eff}^0(t=0)=-\bar{\varepsilon}^2/4=-0.2295$.

The magnitude of the order parameter satisfies the equation

$$4d=\int\frac{d^2k}{2\pi^2}\varepsilon_k\tanh\frac{d\varepsilon_k}{t}+\frac{t}{2}\frac{\partial}{\partial d}\ln B\,. \tag{15}$$

The transition temperature is found to be equal to that of the Peierls phase, both in the presence and absence of the constraint.

Proceeding now to the comparison between the saddle-point free energies of the two phases, we find that their temperature dependence turns out to be unphysical, when the limitation of single-site occupancy is introduced.

In fact, due to the limited contribution coming from the entropy of the saddle-point configuration, appearing in the free energy, the latter is found to increase with the temperature in a small range, which would yield a negative entropy at those temperatures.

This implies that the bare saddle-point contribution to the free energy is not enough and Gaussian fluctuations should be also included, at least. We report here the results for the Peierls phase only, leaving the comparison with the flux phase to a forthcoming publication.

The contribution of the Gaussian fluctuations is obtained from the second variation of the exponent given by the curly bracket in Eq. (6). Starting from the effective action of Eq. (5), we obtain

$$\delta^2S_{\rm eff}=2c^2\sum_n{\rm Sp}\left[\frac{1}{i\omega_n-cU}\delta U\frac{1}{i\omega_n-cU}\delta U\right]. \tag{16}$$

The trace can be performed in Fourier space as always and the summation on the Matsubara frequencies gives us a closed expression for the second variation of the effective free energy in absence of the constraint:

$$\frac{1}{NJ}\delta^2\mathcal{F}_{\rm eff}=\frac{1}{NJ}\left(\pi N\sum_{i=1}^4|\delta U_i|^2+\delta^2S_{\rm eff}\right)=\frac{4}{N}\sum_k\left\{|\delta d_k|^2[1+Q(|d_k|)]+{\rm Re}\left[\delta d_k\left(\frac{d_k^*}{|d_k|}\right)^2q(|d_k|)\delta d_k\right]\right\}, \tag{17}$$

$$Q(|d_k|)=-\frac{1}{4|d_k|}\tanh\frac{|d_k|}{2t}-\frac{1}{8t\cosh^2(|d_k|/2t)}\,,\quad q(|d_k|)=\frac{1}{4|d_k|}\tanh\frac{|d_k|}{2t}-\frac{1}{8t\cosh^2(|d_k|/2t)}\,. \tag{18}$$

We analyze now the fluctuations around the Peierls phase. The second variation of the effective free energy becomes

$$\frac{1}{NJ}\delta^2\mathcal{F}_{\rm eff}=\left[1-\frac{1}{4t\cosh^2(d/2t)}-\alpha\right]\sum_{i=2}^4|\delta d_i|^2+\left[1-\frac{1}{4t\cosh^2(d/2t)}-\alpha-\frac{D_B}{4d}+\frac{D_B^2}{32t}\right]2({\rm Re}\{\delta d_1\})^2. \tag{19}$$

The contribution coming from the constraint is in the terms containing the quantities α and D_B given by

$$\alpha=\frac{1}{4tB_P\cosh^2(d/2t)}\left(\frac{1-2\sinh^2(d/2t)}{6\cosh^2(d/2t)}+\frac{t^2}{d^2}[1-(t/d)\sinh(d/t)]\right),\quad D_B=\frac{\partial}{\partial x}\ln B_P\Big|_{x=d/2t}\,. \tag{20}$$

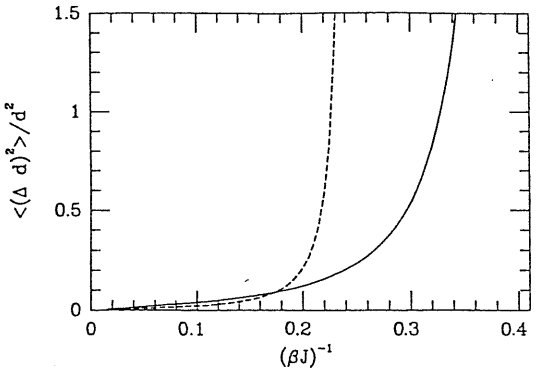

FIG. 1. The relative mean-square fluctuation of the order parameter vs reduced temperature (see text). Dashed curve: Peierls phase without the single occupancy constraint. Solid curve: Peierls phase including the constraint.

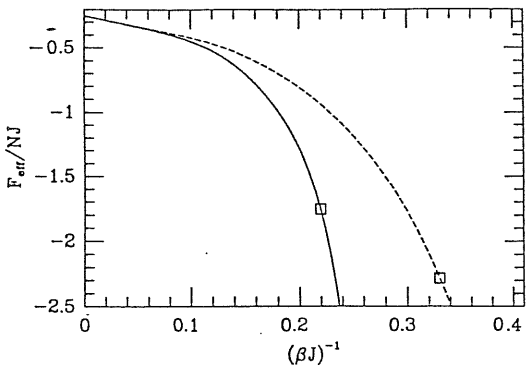

FIG. 2. Reduced free energy per particle vs reduced temperature (including Gaussian fluctuations around the saddle point), for the Peierls phase without (dashed curve) and with (solid curve) the constraint.

When these terms are neglected, Eq. (19) becomes the generalization of the MA result to finite temperatures.

As first pointed out in MA, one zero eigenvalue is found in the diagonalization of the curvature matrix around the saddle point due to the gauge invariance that leaves the phase of d_1 undetermined. This is immediately seen in absence of constraint because, due to Eq. (14), the first term in Eqs. (18) is equal to $\mp\frac{1}{2}$, respectively. This implies that the imaginary part of d_1 disappears from Eq. (17). Note that the curvature vanishes at the critical temperature t_c as it should. The curvature itself, for displacements around the mean-field configuration, provides a qualitative measure of the stability of the mean-field result, with respect to fluctuations of the same space periodicity.

Variations of the complex variables U_i $(i=1,\ldots,4)$ around their equilibrium values, change the free energy according to an 8×8 curvature matrix, which has one zero eigenvalue corresponding to the Goldstone mode, one nondegenerate eigenvalue λ_1, and one 6 times degenerate eigenvalue $\lambda_2=\lambda_1/2$.

In Fig. 1, we plot the relative mean-square fluctuations of the order parameter, corresponding to the eigenvalues that give the most divergent fluctuations, i.e., $\langle(\Delta d)^2\rangle/d^2=t/4\lambda_2 d^2$, as a function of temperature and compare it to the one in absence of the constraint (dashed line). Of course, these quantities diverge when the critical temperature is approached, because the free energy becomes flat at that temperature around the mean-field configuration.

Performing the functional integral of Eq. (6), within the Gaussian approximation, is straightforward,[13] except that, due to the broken gauge symmetry $(d\rightarrow d\exp i\gamma)$, the zero mode has to be excluded:[19]

$$\beta\mathcal{F}_{\rm eff}=\beta\mathcal{F}^0_{\rm eff}-\frac{N}{2}\ln\left(\frac{d^2}{\lambda_1\lambda_2^6}\right), \tag{21}$$

with $\mathcal{F}^0_{\rm eff}$ given by Eq. (12). The result is plotted in Fig. 2. The squares are located at temperatures at which $\langle(\Delta d)^2\rangle/d^2$ becomes of order 1, signaling the breakdown of mean-field theory and the onset of critical behavior.

In the case of the flux phase, three zero eigenvalues are found. They are the three Goldstone phase modes corresponding to the residual gauge symmetries discussed in Ref. 7. When following the same steps as above, we find that the free energy of the flux phase is definitely higher than that of the staggered dimerized phase. More complete results will be reported elsewhere.

We are indebted to E. Tosatti and G. P. Zucchelli for discussions and suggestions. This work was partly supported by GNSM (CNR), INFM, European Research Office U.S. Army, and CINECA.

[1]P. W. Anderson, Science **235**, 1196 (1987).
[2]M. Gross, E. Sanchez Velasco, and E. Siggia, Phys. Rev. B **39**, 2484 (1989).
[3]N. Read and S. Sachdev, Phys. Rev. Lett. **62**, 1694 (1989).
[4]J. B. Marston, Phys. Rev. B **42**, 10804 (1990).
[5]I. Affleck and J. B. Marston, Phys. Rev. B **37**, 3774 (1988).
[6]G. Kotliar, Phys. Rev. B **37**, 3664 (1988).
[7]A. P. Balachandran, E. Ercolessi, G. Morandi, and A. M. Srivastava, Int. J. Mod. Phys. B **4**, 2057 (1990).
[8]X. G. Wen, F. Wilczeck, and A. Zee, Phys. Rev. B **39**, 11413 (1989).
[9]R. B. Laughlin, Science **242**, 525 (1988).
[10]T. Dombre and G. Kotliar, Phys. Rev. B **39**, 855 (1989).
[11]J. B. Marston and I. Affleck, Phys. Rev. B **39**, 11538 (1989).
[12]D. P. Arovas and A. Auerbach, Phys. Rev. B **38**, 316 (1988).
[13]N. Read and S. Sachdev, Nucl. Phys. **B316**, 609 (1989).
[14]G. Kotliar and J. Liu, Phys. Rev. B **38**, 5142 (1988).
[15]C. Gros, Ann. Phys. (N.Y.) **189**, 53 (1989).
[16]E. Manousakis and R. Salvador, Phys. Rev. Lett. **60**, 840 (1988).
[17]N. Trivedi and D. Ceperly, Phys. Rev. B **41**, 4552 (1990).
[18]C. Gros, Phys. Rev. B **42**, 6838 (1990).
[19]J. W. Negele and H. Orland, *Quantum Many Particle Systems* (Addison-Wesley, New York, 1988), p. 214.

Paper II

PHYSICAL REVIEW B VOLUME 46, NUMBER 15 15 OCTOBER 1992-I

Possible occurrence of constrained chiral phase in the frustrated Heisenberg model

M. Di Stasio
International School of Advanced Studies, SISSA, via Beirut 4, I-34014 Miramare Trieste, Italy
(Received 15 June 1992)

The partition function of the frustrated Heisenberg Hamiltonian allows for nonmagnetic stationary points. These are found in the subspace of singly occupied sites in which a fermion representation of the spin operators can be adopted. Here we discuss the competition between the flux and the chiral phase. A saddle-point phase diagram is pictured for the relative stability of the flux and chiral phases as a function of frustration and temperature.

I. INTRODUCTION

The discovery of high-temperature superconductivity in doped La_2CuO_4 and related compounds renewed considerable interest in searching for exotic superconductivity. Anyon superconductivity, in particular, requires that the ground state violates the discrete symmetries P and T, so that its single-particle excitations obey fractional statistics. Indeed the chiral spin state, as defined in Ref. 1, is a spin liquid and its local order parameter breaks P and T symmetry. This state is a possible mean-field solution of the frustrated Heisenberg model in two-space dimensions but it has also been studied in the context of the t-J Hamiltonian.[2]

To apply similar ideas to the metallic oxide layers of high-temperature superconductors the first step is to consider the strong-correlation regime of the Hubbard Hamiltonian. It is well known that in presence of strong on-site Coulomb repulsion and for the half-filled band case the Hubbard Hamiltonian can be canonically transformed into a Heisenberg Hamiltonian (J_1 antiferromagnetic interaction between nearest neighbors) acting on a restricted Hilbert space of singly occupied sites.

When holes are introduced in the cuprate compounds some authors[3] speculate that the dynamical frustration induced by the holes could be to some extent replaced by an effective static frustration (J_2) between next nearest neighbors (NNN) in the original Heisenberg Hamiltonian, again in the presence of the single-occupancy constraint. Although it was shown[4] that this effective description can be inadequate when measuring several physical quantities, nonetheless we will adopt here the J_1-J_2 model Hamiltonian as a starting point. Here we are mainly interested in the possible existence of a chiral spin state in the presence of the constraint.

Including the constraint allows us to use the irreducible representation of the spin operator algebra in terms of fermion operators and Pauli matrices.[6]

The two-dimensional (2D) frustrated Heisenberg model has been approached in many different ways. In the classical limit ($S \to \infty$) there exists a phase transition at $J_2/J_1 = 0.5$ below which the ground state exhibits Néel order. Using linear spin-wave theory[7] it turns out that for all finite S values the Néel state and the collinear state (independent Néel order on the two sublattices) are separated by a region, $J_2/J_1 \simeq 0.5$, in which the ground state is disordered by quantum fluctuations. A different range of stability for the Néel state was found[8] connecting the frustrated Heisenberg model to the O(3) nonlinear σ model. The authors[8] found $J_2/J_1 \simeq 0.22$ as an upper bound estimate to the stability region of the Néel state. Additional support to this scenario is given by the results of finite-size scaling studies[10] ($0.4 < J_2/J_1 < 0.65$) and by exact diagonalization studies[11] on the chiral phase. On the contrary large-N expansion [in the SU(N) symmetry group] does not give any evidence for chiral-ordered or spin-nematic states.[9]

Here the question of the possible existence of a chiral state in the frustrated Heisenberg model in presence of the single-occupancy constraint is addressed from another point of view. Our work[5] originates from the observation that when N =2 and $S = \frac{1}{2}$ the single-occupancy constraint takes a very simple form and can be implemented exactly at any temperature. In this restricted Hilbert space we can adopt the fermion representation of the spin operators via the Pauli matrices. Therefore the compromising choice we have made was to project properly onto the restricted subspace when evaluating the fermion trace and to perform the saddle-point approximation on the path-integral expression for the partition function, with no pretension of it being exact in some limit (Sec. I). It is worth noticing that the saddle-point approximation of a constrained path integral does not give the same free energy as one obtains from a Hartree-Fock approximation on the original Hamiltonian. Results for the chiral phase that is still an extrema of the total action in the presence of the constraint are reported in Sec. II. The last section contains discussions of the results given by this method, the relative phase diagram between flux, chiral, and nonordered phases, and some speculations on possible future extensions and applications.

II. CONSTRAINED PATH-INTEGRAL EXPRESSION FOR THE PARTITION FUNCTION

Here we are dealing with a frustrated Heisenberg Hamiltonian

$$H = J_1 \sum_{(i,j)_{\rm NN}} \mathbf{S}_i \cdot \mathbf{S}_j + J_2 \sum_{(i,j)_{\rm NNN}} \mathbf{S}_i \cdot \mathbf{S}_j \tag{1}$$

acting on a restricted Hilbert space of singly occupied sites whose projector is

$$\mathbb{P} = \prod_i n_i(2 - n_i). \tag{2}$$

In this restricted Hilbert space we can adopt the irreducible representation of the spin operator in terms of fermion operators:

$$\mathbf{S}_i = c^\dagger_{i\alpha} \boldsymbol{\sigma}_{\alpha\beta} c_{i\beta}, \tag{3}$$

where $\boldsymbol{\sigma}$ are the Pauli matrices. Since $\mathbb{P}$ and H commute, the true partition function

$$Z = \mathrm{Tr}\{e^{-\beta H}\mathbb{P}\} \tag{4}$$

can be exactly calculated performing the appropriate derivatives of the generating function

$$Z[z] = \mathrm{Tr}\{e^{-\beta H + \sum_i z_i n_i}\}, \tag{5}$$

$$Z = \prod_i \frac{\partial}{\partial z_i}\left(2 - \frac{\partial}{\partial z_i}\right) Z[z]\Big|_{z_i=0}. \tag{6}$$

The generating function $Z[z]$ can be evaluated with the usual techniques for an unconstrained path integral introducing the anticommuting Grassmann fields $\psi^*_{i\alpha}(\tau)$ and $\psi_{i\alpha}(\tau)$,

$$Z[z] = \int \prod_{i\alpha} \mathcal{D}\psi_{i\alpha} \exp\Bigg\{ - \int_0^1 d\tau \sum_{i\alpha} \psi^*_{i\alpha}(\partial_\tau - z_i)\psi_{i\alpha} + \sum_{\alpha\beta}\left(\frac{\beta J_1}{2} \sum_{(ij)_{\rm NN}} \psi^*_{i\alpha}\psi^*_{j\beta}\psi_{i\beta}\psi_{j\alpha} + \frac{\beta J_2}{2} \sum_{(ij)_{\rm NNN}} \psi^*_{i\alpha}\psi^*_{j\beta}\psi_{i\beta}\psi_{j\alpha} \right)\Bigg\}. \tag{7}$$

Next step is the introduction of Hubbard-Stratonovich link fields[1,12] to decouple the four fermion terms:

$$\begin{aligned} \mathcal{U}_{ij}(\tau) &= \sum_\alpha \psi^*_{i\alpha}(\tau)\psi_{j\alpha}(\tau) \quad \text{if } i,j \text{ are NN}, \\ \tilde{\mathcal{U}}_{ij}(\tau) &= \sum_\alpha \psi^*_{i\alpha}(\tau)\psi_{j\alpha}(\tau) \quad \text{if } i,j \text{ are NNN}. \end{aligned} \tag{8}$$

Note that $\mathcal{U}^*_{ij}(\tau) = \mathcal{U}_{ji}(\tau)$ and $\mathcal{U}_{ij}(0) = \mathcal{U}_{ji}(1)$ to obey periodic boundary conditions. The two terms in the Hamiltonian commute so that we can use twice the usual Hubbard-Stratonovich identity. After Fourier transforming in frequency space we can integrate out exactly the fermions at the cost of introducing multidimensional integrals over these auxiliary bosonic fields. We end up with

$$Z[z] = \int \prod_{kl,m} \mathcal{D}\mathcal{U}_{kl}(\Omega_m) \exp\left\{ -\pi \sum_{(ij)_{\rm NN},m} |\mathcal{U}_{ij}(\Omega_m)|^2 - \pi \sum_{(ij)_{\rm NNN},m} |\tilde{\mathcal{U}}_{ij}(\Omega_m)|^2 + 2\,\mathrm{Tr}\ln A \right\}, \tag{9}$$

where Ω_m are bosonic Matsubara frequencies. The matrix A resulting from the fermion integration has matrix elements

$$A^{n,n'}_{i,j} = (i\omega_n + z_i)\delta_{i,j}\delta_{n,n'} - c_1\mathcal{U}_{ij}(\omega_n - \omega_{n'}) - c_2\tilde{\mathcal{U}}_{ij}(\omega_n - \omega_{n'}) = i\omega_n\delta_{i,j}\delta_{n,n'} + [\hat{U}(z)]^{n,n'}_{i,j}. \tag{10}$$

The last equality defines the matrix $\hat{U}(z)$. According to Eq. (6) the partition function reads

$$Z = \int \prod_{kl,m} \mathcal{D}\mathcal{U}_{kl}(\Omega_m) \exp\left\{ -\pi \sum_{(ij)_{\rm NN},m} |\mathcal{U}_{ij}(\Omega_m)|^2 - \pi \sum_{(ij)_{\rm NNN},m} |\tilde{\mathcal{U}}_{ij}(\Omega_m)|^2 - S_{\rm eff}[\hat{U}(0)] + \sum_i \ln 4B_i[\hat{U}(0)] \right\}, \tag{11}$$

where $S_{\rm eff}[\hat{U}(z)] = -2\,\mathrm{Tr}\ln[1 + G_o\hat{U}(z)]$ and G_o is the single free-particle Green's function. The effect of the constraint is entirely contained in the functionals $B_i[\hat{U}(0)]$ given by

$$B_i[\hat{U}(0)] = \left[\frac{\partial^2 S_{\rm eff}[\hat{U}(z)]}{\partial z_i^2} - 2\frac{\partial S_{\rm eff}[\hat{U}(z)]}{\partial z_i} - \left(\frac{\partial S_{\rm eff}[\hat{U}(z)]}{\partial z_i} \right)^2 \right]\Bigg|_{z=0}. \tag{12}$$

What we get at the end is a total effective action that explicitly contains a term coming from the constraint inclusion. We are now in position to generalize the saddle-point results present in literature[12,1] in the presence of the single-occupancy constraint and to discuss its effect at least at the same approximation level.

III. SADDLE-POINT STATIC PHASES: RESULTS FOR THE CONSTRAINED CHIRAL PHASE

The static approximation amounts to restricting the integral to paths that are constant in "time," i.e., that satisfy $\mathcal{U}_{ij}^{n,n'} = \mathcal{U}_{ij}\delta_{n,n'}$. This brings about a great simplification of the formalism. Following Refs. 1 and 12 we restrict the random fields $\mathcal{U}_{ij}$ to be translationally invariant along the diagonals of the square lattice. The resulting bipartite lattice will have a corresponding halved Brillouin zone (RBZ). Working in the reciprocal space we can introduce a basis $|\mathbf{k},\alpha\rangle$ with $\alpha = e, o$ being even or odd. The complex fields $\mathcal{U}_i$ (i=1,8) are diagonal in $\mathbf{k}$ and their matrix elements are

$$\begin{aligned}
\langle \mathbf{k},o|\mathcal{U}|\mathbf{k},o\rangle &= 2\,\mathrm{Re}\{\tilde{\mathcal{U}}_2 e^{i(k_x+k_y)} + \tilde{\mathcal{U}}_1 e^{i(k_x-k_y)}\} \\
&= \lambda_{oo}(\mathbf{k}), \\
\langle \mathbf{k},e|\mathcal{U}|\mathbf{k},e\rangle &= 2\,\mathrm{Re}\{\tilde{\mathcal{U}}_4 e^{i(k_x+k_y)} + \tilde{\mathcal{U}}_3 e^{i(k_x-k_y)}\} \\
&= \lambda_{ee}(\mathbf{k}), \\
\langle \mathbf{k},o|\mathcal{U}|\mathbf{k},e\rangle &= \mathcal{U}_1 e^{ik_x} + \mathcal{U}_2^* e^{-ik_y} + \mathcal{U}_3 e^{-ik_x} + \mathcal{U}_4^* e^{ik_y} \\
&= \lambda(\mathbf{k}), \\
\langle \mathbf{k},e|\mathcal{U}|\mathbf{k},o\rangle &= \lambda^*(\mathbf{k}).
\end{aligned} \tag{13}$$

The diagonalization of the matrix $c_1\mathcal{U}_{ij} + c_2\tilde{\mathcal{U}}_{ij}$ in the sublattice indices $\alpha = e, o$ yields the eigenvalues

$$a_\pm(k) = \frac{\lambda_{oo}+\lambda_{ee}}{2} \pm \sqrt{(\lambda_{oo}-\lambda_{ee})^2 c_2^2 + |\lambda|^2 c_1^2}. \tag{14}$$

The effective action can now be evaluated and reads

$$S_{\mathrm{eff}}[\hat{U}] = -2\sum_{k\in \mathrm{RBZ}} \left(\ln\cosh\frac{a_+(k)}{2} + \ln\cosh\frac{a_-(k)}{2}\right). \tag{15}$$

That is all one would need in the absence of the constraint to find saddle-point solutions. The chiral saddle-point solution corresponds to the order parameter choice (see Fig. 1):

$$\begin{aligned}
&\mathcal{U}_i = f e^{i\pi/4}, \quad i = 1,4, \\
&\tilde{\mathcal{U}}_1 = \tilde{\mathcal{U}}_4 = -\tilde{\mathcal{U}}_2 = -\tilde{\mathcal{U}}_3 = g
\end{aligned} \tag{16}$$

with f and g real. The simplest gauge invariant order parameter is

$$\mathcal{P}l_\triangle = \langle \mathcal{U}_1\mathcal{U}_2\tilde{\mathcal{U}}_2\rangle = f^2 g e^{i\pi/2} = f^2 g e^{i\Phi}, \tag{17}$$

where the fields circle a closed triangle or a plaquette. P violation is apparent because the expectation values for plaquettes transversed in opposite directions are different. Moreover in Eq. (17) the phase Φ can be interpreted as the flux through the plaquette of a magnetic field such that $\Phi = \int_\triangle \mathbf{A}\cdot d\mathbf{l}$.

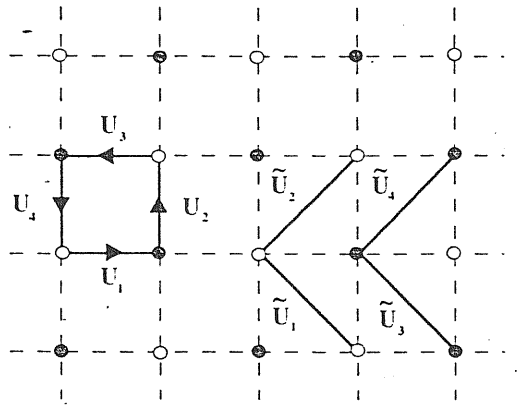

FIG. 1. Definitions of the auxiliary fields in the bipartite lattice.

With these assumptions for the fields, which imply that $a_+(k) = -a_-(k) = a(k)$, the constraint term is

$$B[f,g] = 1 - \left(\frac{2}{N}\right)^2 \sum_{k,q} \frac{a(k)\tanh\frac{a(k)}{2} - a(q)\tanh\frac{a(q)}{2}}{a^2(k)-a^2(q)}. \tag{18}$$

Introducing the dimensionless order parameters $d_1 = \frac{c_1}{\beta J_1} f$ and $d_2 = \frac{c_2}{\beta J_2} g$, the reduced temperature $t = 1/\beta J_1$, and the frustration parameter $J_{21} = J_2/J_1$, the total effective action per particle and in units of J_1 is

$$S^{\mathrm{tot}} = 4(d_1^2 + J_{21} d_2^2) - 2t\left(\frac{2}{N}\right)\sum_k \ln\cosh\frac{a(k)}{2} - t\ln 4B. \tag{19}$$

The self-consistency equations for d_1 and d_2 are two-coupled integral equations that we have solved numerically. These equations allow different solutions: (a) $d_1 \neq 0$, $d_2 \neq 0$ is the chiral phase, (b) $d_1 \neq 0$, d_2=0 is the flux phase[12] whose simplest order parameter is a plaquette expectation value $\mathcal{P}l_\square = \langle \mathcal{U}_1\mathcal{U}_2\mathcal{U}_3\mathcal{U}_4\rangle = d_1^4 e^{i\pi}$, (c) $d_1 = 0$, $d_2 \neq 0$, and, finally (d) $d_1 = d_2 = 0$ is a nonordered phase.

The resulting relative phase diagram is shown in Fig. 2. It is worth noticing that finite critical temperatures should be expected because we are dealing with a generalized mean-field approximation. We found that the chiral phase ($d_1, d_2 \neq 0$) exists as a saddle-point solution also in the presence of the constraint if $J_{21} > 0.5$. Whenever the chiral phase exists it has a mean-field free energy always lower than that of the flux phase that is independent of J_2 and with a critical temperature $t_c = \frac{5}{12}$.[13] (More exhaustive results on the latter phase are reported in Ref. 14.) The $t = 0$ free energy of the chiral phase runs between -0.229 for $J_{21} = 0.5$ that coincides with the free energy for the flux phase to -0.25 when $J_{21} = 1$ that is the free energy of the dimer or Peierls phase.[12,5] Going to the extreme limit $J_2 > J_1$ the $t = 0$ free energy of the chiral phase becomes even lower than that of the Peierls phase.

This scenario holds also in absence of the constraint but with lower critical temperatures [e.g., t_c^0(flux

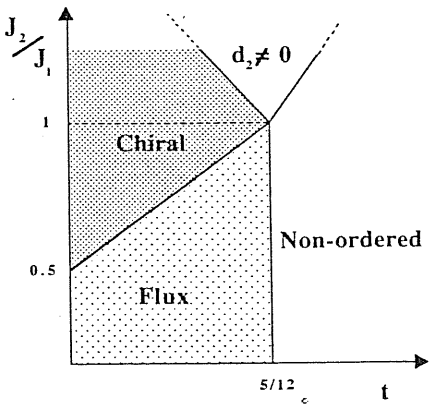

FIG. 2. Relative phase diagram between flux, chiral, and nonordered phases.

phase)$=\frac{1}{4}$]. At this level of approximation, the constraint acts as an entropy reductor. The function $B(t)$ goes from 1 to $\frac{1}{2}$ as t runs from 0 to t_c lowering the configurational entropy from $N\ln 4$ to $N\ln 2$, which gives the correct counting of allowed states. Another crucial check of our method of including the single-occupancy constraint is the evaluation of the mean occupation number and its fluctuations. We found that $\langle n_i \rangle$ is always exactly 1 and $\langle n_i^2 \rangle$ evaluated at the saddle point deviates from 1 by less than 10% (see Ref. 14). However when evaluating the temperature dependence of the saddle-point free energy we found that it shows a wrong behavior (t increasing) at low temperatures. At this level of approximation we think that the entropy reduction given by the constraint inclusion is even too strong. Adding classical and quantum fluctuations should take care of this low-temperature behavior.[15]

IV. DISCUSSION AND CONCLUSIONS

Here we have presented a method of including the single-occupancy constraint in the path-integral expression for the partition function of the frustrated Heisenberg model. Within the saddle-point approximation we studied the possible existence of the chiral phase as a function of the frustration parameter J_{21} and of the reduced temperature. The self-consistency equations allow different solutions: the chiral phase ($d_1, d_2 \neq 0$), the flux phase ($d_1 \neq 0, d_2 = 0$), the phase with $d_2 \neq 0$ and $d_1 = 0$, and the nonordered phase ($d_1 = d_2 = 0$). The relative stability of these phases is reported in Fig. 2 when adding the constraint. Here it is shown that the saddle-point chiral solution still exists and its critical temperature is higher when including the constraint correction. This correction is effective also within the saddle-point approximation of what can be seen by the strong reduction of $\langle n_i^2 \rangle_{sp} - 1$ to less than 10%.

From the temperature dependence of the saddle-point free energy we pointed out the need of including classical and quantum fluctuations to get a physically reliable approximation to the free energy in the presence of the constraint in the low-temperature region. In fact, large quantum fluctuations are expected.

Even if the saddle-point approximation is inadequate to determine which, if any, of the mean-field solutions describe the ground state we show that, also in presence of the constraint, the chiral spin state can be considered as a good candidate for the ground state of the frustrated 2D Heisenberg Hamiltonian in the strong frustration region. In fact the $t = 0$ mean-field free energies of the Néel state (for $0 < J_{21} < 0.5$) of the collinear antiferromagnetic state (for $0.5 < J_{21} < 1$) and of the Dimer state are all equal to -0.25 and the chiral state (for $J_{21} > 0.5$) has a free energy very close to this value and even lower in the extreme case $J_{21} > 1$.

What would be very interesting is a comparison between the quantum fluctuations of the two antiferromagnetic phases and of the chiral phase. This will be discussed at a later date.

ACKNOWLEDGMENTS

I am especially grateful to Professor G. Morandi and Professor A. Tagliacozzo for discussions, suggestions, and a careful reading of the manuscript.

[1]X.G. Wen, F. Wilczek, and A. Zee, Phys. Rev. B **39**, 11 413 (1989).
[2]Z. Zou and R.B. Laughlin, Phys. Rev. B **42**, 4073 (1990).
[3]M. Inui, S. Doniach, and M. Gabay, Phys. Rev. B **38**, 6631 (1988).
[4]F. Nori, E. Gagliano, and S. Bacci, Phys. Rev. Lett **68**, 240 (1992).
[5]M. Di Stasio, E. Ercolessi, G. Morandi, A. Tagliacozzo, and F. Ventriglia, Phys. Rev. B **45**, 1939 (1992).
[6]E. Ercolessi, G. Morandi, and F. Ortolani, Mod. Phys. Lett. B **6**, 77 (1992).
[7]P. Chandra and B. Ducot, Phys. Rev. B **38**, 9335 (1988).
[8]T. Einarsson and H. Johannesson, Phys. Rev. B **43**, 5867 (1991).
[9]N. Read and S. Sachedv, Phys. Rev. Lett. **66**, 1773 (1991).
[10]H.J. Schulz and T.A.L. Ziman, Europhys. Lett. **18**, 355 (1992).
[11]D. Poilblanc, E. Gagliano, S. Bacci, and E. Dagotto, Phys. Rev. B **43**, 10 970 (1991).
[12]I. Affleck and J.B. Marston, Phys. Rev. B **37**, 3774 (1988).
[13]Due to the Mermin and Wagner theorem [N.D. Mermin and H. Wagner, Phys. Rev. Lett. **17**, 1133 (1966)] no true finite-temperature transitions are expected in the two-dimensional Heisenberg model. For this reason, the mean-field finite-temperature "transitions" should be interpreted as crossovers signaling the appearance of a large, but finite, correlation length. Weak three-dimensional coupling is sufficient to induce true long-range order and true finite-temperature transition in the mean-field phases here discussed.
[14]M. Di Stasio, E. Ercolessi, G. Morandi, A. Tagliacozzo, and F. Ventriglia (unpublished).
[15]M. Di Stasio, E. Ercolessi, G. Morandi, A. Tagliacozzo, and F. Ventriglia (unpublished). We have shown, studying the Peierls phase, that quantum fluctuations are necessary to get reliable results for the free energy in the low-temperature region. Adding these contributions we get either the right entropy behavior or a correct specific-heat behavior.

Paper III

International Journal of Modern Physics B, Vol. 7, No. 18 (1993) 3281–3311

SINGLE SITE-OCCUPANCY CONSTRAINT FOR THE HUBBARD MODEL AT FINITE TEMPERATURE

M. DI STASIO*, E. ERCOLESSI†, G. MORANDI[b],
A. TAGLIACOZZO*,# and F. VENTRIGLIA#

*International School for Advanced Studies,
via Beirut 2, I-34100 Miramare, Trieste, Italy

†Physics Dept., Syracuse University, Syracuse, NY 13244-1130, USA

[b]Dipartimento di Fisica, Università di Bologna,
CISM and INFN, via Irnerio 46, I-40126 Bologna, Italy

#Dipartimento di Scienze Fisiche, CISM, Università di Napoli,
Mostra d'Oltremare Pad.19, I-80125 Napoli, Italy

Received 24 February 1993

We show how it is possible to include the constraint of single site-occupancy in the large U limit of the Hubbard model at half-filling by means of a local chemical potential. The formalism which is in principle exact allows for finite temperature mean field results satisfying the constraint within 10%. The method is here applied to the dimerized phase and the commensurate flux phase which are still found as local saddle points of the action. The symmetry properties of these actions have been studied. One loop static corrections have been added to obtain an effective free energy and an estimate of the specific heat. In the limit of zero temperature our results reproduce those of the conventional mean field theory of these phases, because quantum fluctuations have not been included. We find that the temperature destabilizes the flux phase more than it does with the dimer phase, especially due to the constraint, which does not suppress phase fluctuating modes, provided the flux is conserved.

1. Introduction

One of the puzzles about the appearance of high-temperature superconductivity in copper oxide materials is the role played by the antiferromagnetic (AF) interactions in the CuO planes which are believed to be dominant, particularly at low doping. As a matter of fact this is confirmed by neutron scattering and NMR experiments.[1]

Since Anderson's suggestion,[2] the Hubbard model in two dimensions, is widely studied in this context, assuming the on site repulsion U to be much greater than the hopping integral t.[3]

Monte Carlo simulations and finite size scaling show that at half-filling the ground state of the repulsive U Hubbard model has long range antiferromagnetic order.[4]

PACS Nos.: 71.10.+x; 75.10.Jm; 74.20.-z.

In the infinite U-limit the model maps onto the so-called "t-J" model, provided that the space of states is restricted to configurations in which no double occupancy is allowed. This is approached by means of a large variety of methods, among which exact small cluster diagonalization,[5] mean field within the slave boson technique or Gutzwiller projection.[6,8,22] For zero doping (half-filling) the kinetic energy term drops out and the model becomes the 2D AF Heisenberg model which is again widely studied.[9] Besides numerical methods and simulations, a modified spin wave theory has been developed, starting from an AF ordered ground state,[10] the renormalization group based on the nonlinear σ model,[11] Monte Carlo simulations,[12,13] large N expansion.[14,15]

In a square lattice with n.n. interactions several mean field phases have been suggested. Simultaneously with the "s+id" phase found by Kotliar,[16] Affleck and Marston[17] (AM) showed the local stability of the Peierls or dimerized phase and of the commensurate flux phase, in which half a flux quantum per plaquette is spontaneously generated. While these two phases double the lattice periodicity, the spin Peierls phase could have different periodicity as is the case of the columnar phase, which is found to be even lower in energy in a large N expansion.[8] Spin Peierls phases seem also to be relevant when frustration is introduced.[19]

Because there is wide consensus that the square lattice spin 1/2 is Néel ordered at $T = 0$, the dimer phase or the staggered flux phase can only be higher saddle points of the free energy. Away from half-filling these phases seem to be only stable for small values of t/J.

On the other hand the flux phase was found to be equivalent to the RVB phase.[20] It has been pointed out that this phase is actually unstable with respect to umklapp fluctuations in the amplitude,[21] but higher order terms in the free energy could stabilize it. A staggered magnetization in a flux phase background seems to be a good starting point for variational Monte Carlo calculations.[22,23]

Besides, the interest in the flux phase and in the chiral spin states[24,25] is also related to the claim that such a background could lead to an $U(1)$ lattice gauge theory which includes a Chern Simons term when gauge invariance is violated because of the doping.[26,27]

On the other hand, if one wants to consider the spin-1/2 Heisenberg model as the limit of the t-J model at half-filling single occupancy of each site should be enforced. This constraint happens to be satisfied in the extension to the $SU(N)$ Heisenberg model for $N \to \infty$, when the saddle point approximation to the partition function becomes exact. In fact, the large N limit quenches the fluctuations of the occupation number of each site, regardless of the value of $U(U > 0)$. Nothing can be said, however, about the analytical continuation of the results to the desired value of $N = 2$ At zero temperature the Gutzwiller projector has been implemented in numerical calculations.[28] An interesting approximate scheme to include the constraint variationally within mean field at zero temperature can be found in Ref. 29. Slave bosons have been applied to study the phase diagram with tem-

perature, also away from half-filling, but fluctuations have not been investigated.[30] One expects that the ones related to site-occupancy are difficult to control at finite temperature.

In this work we report on a novel method to include the constraint of single site-occupancy at finite temperature. To check this method it is applied to the study of the temperature dependence of the dimer and flux phase of AM at half-filling within mean field. One loop corrections are also included for static field configurations, which allow for an estimate of the entropy. Fluctuations in the site occupancy of at most 10% from the value of one is found, giving some confidence to the mean field treatment of the constraint. A first report of this work, which was limited to the dimer phase, was given in Ref. 31. Quantum fluctuations are not included and will be discussed elsewhere.[32]

The two phases are still local minima of the action and the dimer phase is favoured, as expected. In these phases the Fermi surface is depleted: a gap is opened in the case of the dimer phase while the Fermi surface is reduced to points in the flux phase. Therefore an energy barrier is expected to be present with respect to fluctuations towards the Néel ordered state. The effect of the constraint on thermal fluctuations both in amplitude and phase is investigated around these local minima. We find that thermal fluctuations are reduced on the average by the constraint, so that the mean field transition temperature is found to be higher ($T_c = 5/12\,J$).

An interesting outcome of the analysis is that relative mean square fluctuations of the order parameter for the flux phase are much larger than those for the dimer phase, so that the stability of the former is more sensitive to the increase of temperature. In any case we are able to estimate the critical region: mean field turns out to be a rather poor approximation over a wide range of temperatures ($T_c - T^* \sim 0.09J$ (dimer phase), $T_c - T^* \sim 0.34J$ (flux phase)). Examining one-loop corrections, we find that, when temperature is lowered below $T \sim 0.08J$ quantum corrections to the free energy of the dimer and flux phase should not be neglected any longer.

In Sec. 2 we show the method by which the constraint can be included also at finite temperature. The interest of our approach is in that it can be extended away from half-filling. However, the formal set-up is here presented and tested just for the half-filling case.

In Sec. 3 the saddle-point approximation is used which leads to the usual mean field solutions. These are described in Sec. 4, together with the corresponding fluctuation modes that are involved in adding one-loop corrections to the free energy.

In Sec. 5 the mean occupation number is evaluated together with its mean square fluctuations, to check which extent the requirement of single site-occupancy is satisfied within our approximations at finite temperatures. The encouraging result is plotted in Fig. 1.

In Sec. 6 we discuss the results.

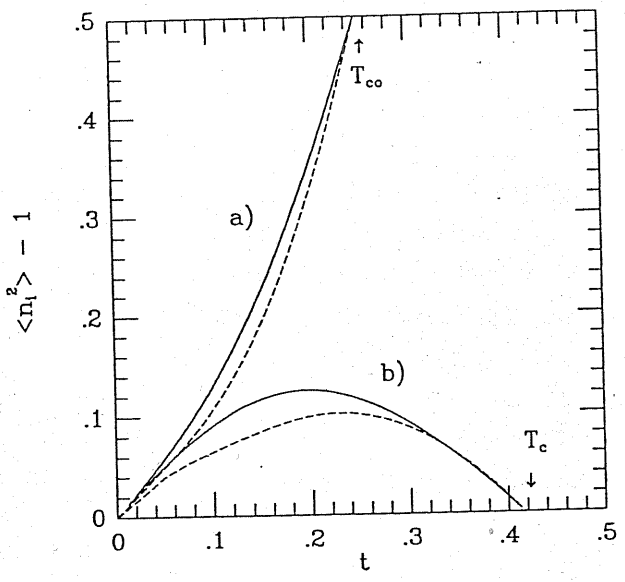

Fig. 1. Mean square fluctuations $\langle n_i^2 \rangle - \langle n_i \rangle^2$ as a function of temperature $t = (\beta J)^{-1}$ for the dimer phase (broken line) and the flux phase (full line), with the constraint included (b) and without the constraint (a).

2. Path Integral Expression for the Partition Function

It is well known that the large U Hubbard model maps at half-filling onto the spin-1/2 antiferromagnetic Heisenberg model, provided that the hamiltonian only acts on states which do not imply double occupancy of sites. In turn the spin-1/2 Heisenberg hamiltonian can be rewritten using the fermion representation for the spins provided that all sites are singly occupied.

We show in this section how the constraint can be implemented in the evaluation of thermal averages.

At half-filling, i.e. when it is projected onto the subspace of the total Hilbert space containing only states with exactly one electron per lattice site, the Hubbard hamiltonian maps[27] into an AFM Heisenberg hamiltonian. Up to additive constants, the latter can be rewritten as

$$H_o = -\frac{1}{2} \sum_{(i,j)} \sum_{\alpha\beta} J_{ij} c^{\dagger}_{i,\alpha} c_{j,\alpha} c^{\dagger}_{j,\beta} c_{i,\beta} \tag{1}$$

where $J_{ij} = 4|t_{ij}|^2/U$, t_{ij} are the n.n. hopping matrix elements, and $\sum_{(i,j)}$ stands for a sum over ordered n.n. sites in the lattice. Altogether there will be $2N$ such pairs for a 2D square lattice with N sites. The operators $c_{i\alpha}$ annihilate electrons of spin α at site i of the lattice. From now on we will set $J_{ij} = \text{const} = J \neq 0$ only for n.n. sites. In principle one should consider in the full Hilbert space the projected hamiltonian

$$H = \mathcal{P}_{hf} H_o \mathcal{P}_{hf} \tag{2}$$

where $\mathcal{P}_{hf}$ is the projector onto the subspace of singly-occupied sites, i.e.

$$\mathcal{P}_{hf} = \prod_i n_i(2 - n_i) \tag{3}$$

($n_i = n_{i\uparrow} + n_{i\downarrow}; n_{i\sigma} = c^\dagger_{i\sigma} c_{i\sigma}$, $\sigma = \uparrow, \downarrow$). Therefore, the partition function in the restricted Hilbert space should be written as

$$\mathcal{Z} = \mathrm{Tr}\{\mathcal{P}_{hf} \exp(-\beta H)\} \,. \tag{4}$$

However, it can be easily checked that H and $\mathcal{P}_{hf}$ commute so that Eq. (4) can be immediately shown that the partition function can be rewritten, in a much simpler way, as

$$\mathcal{Z} = \mathrm{Tr}\{\mathcal{P}_{hf} \exp(-\beta H_o)\} \tag{5}$$

Below half-filling, i.e. when one wants to allow not exactly one but at most one electron per site, the Hubbard hamiltonian maps instead onto the full t-J hamiltonian, which contains, besides H_o, the hopping term of the original hamiltonian (a three-site hopping term arising in the restriction process[27] is usually neglected), and the relevant projector becomes the well-known Gutzwiller projector

$$\mathcal{P}_G = \prod_i (1 - n_{i,\uparrow} n_{i,\downarrow}) \,. \tag{6}$$

The main difficulty now is that $\mathcal{P}_G$ doesn't commute with the t-J hamiltonian anymore. This point will be discussed in more detail in Sec. 6.

Going back to the half-filled case which we want to discuss here, our strategy is to evaluate the auxiliary generating function

$$\mathcal{Z}[z] = \mathrm{Tr}\{\exp(-\beta H)\} \tag{7}$$

where we have added a source term to the Hamiltonian H_o

$$H[z_i] = H_o - \frac{1}{\beta} \sum_i z_i n_i \tag{8}$$

(the z_i's are real variables). Once $\mathcal{Z}[z]$ is known, the original partition function can be easily obtained by derivation

$$\mathcal{Z} = \prod_i \frac{\partial}{\partial z_i} (2 - \frac{\partial}{\partial z_i}) \mathcal{Z}[z] \Big|_{z=0} \,. \tag{9}$$

The advantage is that the evaluation of Eq. (7) only requires standard techniques because the trace is unrestricted and the source term commutes with H_o. Therefore we write $\mathcal{Z}[z]$ as

$$\mathcal{Z}[z] = \int \prod_{i,\alpha} \mathcal{D}\psi^{\star}_{i,\alpha} \mathcal{D}\psi_{i,\alpha} \exp\left\{ - \int_0^1 d\tau \sum_{i,\alpha} \psi^{\star}_{i,\alpha}(\tau)(\partial_\tau - z_i)\psi_{i,\alpha} + \frac{\beta J}{2} \sum_{(i,j)} \sum_{\alpha,\beta} \int_0^1 d\tau \psi^{\star}_{i,\alpha}(\tau)\psi^{\star}_{j,\beta}(\tau)\psi_{i,\beta}(\tau)\psi_{j,\alpha}(\tau) \right\} . \tag{10}$$

Here τ is a scaled imaginary time variable ranging from 0 to 1, and the ψ's and $\psi^{\star}$'s are Grassmann fields obeying antiperiodic boundary conditions in τ at the extremes of the interval [0, 1]. In view of discussing the non-uniform phases first introduced by AM[17] we single out the operator

$$\mathcal{U}_{ij}(\tau) = \sum_{\beta} \psi^{\star}_{j,\beta}(\tau)\psi_{i,\beta}(\tau) \tag{11}$$

and use the Hubbard Stratonovich decoupling

$$\exp\left\{ \frac{\beta J}{2} \sum_{\alpha,\beta} \int_0^1 d\tau \psi^{\star}_{i,\alpha}(\tau)\psi^{\star}_{j,\beta}(\tau)\psi_{i,\beta}(\tau)\psi_{j,\alpha}(\tau) \right\}$$
$$= \int \mathcal{D}\mathcal{U}_{ij} \exp\left\{ - \int_0^1 d\tau \left(\pi |\mathcal{U}_{ij}(\tau)|^2 + \sqrt{\frac{\pi\beta J}{2}} \sum_{\alpha} (\psi^{\star}_{i,\alpha}(\tau)\mathcal{U}_{ij}(\tau)\psi_{j,\alpha}(\tau) + \text{c.c.}) \right) \right\} . \tag{12}$$

Here the symbol $\int \mathcal{D}\mathcal{U}_{ij}$ represents the integrals over the real and imaginary parts of the auxiliary boson fields $\mathcal{U}_{ij}$: $\int d\Re e\{\mathcal{U}_{ij}\} d\Im m\{\mathcal{U}_{ij}\}$.

These obey periodic boundary conditions in τ, and their matrix is hermitian: $\mathcal{U}^{\star}_{ij}(\tau) = \mathcal{U}_{ji}(\tau)$.

Moving to Fourier space the generating function is

$$\mathcal{Z}[z] = \int \prod_{(i,j)} \mathcal{D}\mathcal{U}_{ij} \prod_{i,\alpha} \mathcal{D}\psi^{\star}_{i,\alpha} \mathcal{D}\psi_{i,\alpha} \exp\left\{ -\pi \sum_{(i,j)} \sum_{m} \left(|\mathcal{U}_{ij}(\Omega_m)|^2 + \sum_{\langle ij \rangle} \sum_{(n,n')} \sum_{\alpha} \psi^{\star}_{i,\alpha}(\omega_n) \left[(G_o^{-1})^{nn'}_{ij} + (\tilde{\mathcal{U}})^{n,n'}_{ij} \right] \psi_{j,\alpha}(\omega'_n) \right\} \tag{13}$$

where now $\sum_{\langle ij \rangle}$ stands for a sum over unordered pairs, and $\omega_n = (2n+1)\pi$, $\Omega_m = \omega_n - \omega_{n'}$ are Fermi and Bose Matsubara frequencies respectively. We have defined here $(G_o)^{n,n'}_{ij} = (i\omega_n)^{-1}\delta_{i,j}\delta_{n,n'}$, and $(\tilde{\mathcal{U}})^{n,n'}_{ij} = z_i\delta_{i,j}\delta_{n,n'} - c\mathcal{U}_{ij}(\omega_n - \omega_{n'})$ with $c = \sqrt{\pi\beta J/2}$.

Note that $\tilde{\mathcal{U}}_{ij}^{n,n'}$ is hermitian when considered as a matrix in the site and the fermion frequency indices (i.e. $\tilde{\mathcal{U}}_{ij}^{n,n'} = (\tilde{\mathcal{U}}_{ji}^{n',n})^{\star}$) or, when rewritten in terms of Ω_m: $\tilde{\mathcal{U}}_{ij}(\Omega_m) = \tilde{\mathcal{U}}_{ji}^{*}(-\Omega_m)$.

Integrating out the fermion fields, we obtain the well known result

$$\mathcal{Z}[z] = \mathcal{N} \int \prod_{(i,j)} \mathcal{D}\mathcal{U}_{ij} \exp\{-\pi \sum_{(i,j)} \sum_{m} |\mathcal{U}_{ij}(\Omega_m)|^2\} \times \exp\{2\mathrm{Tr}\, \ln[1 + G_o\tilde{\mathcal{U}}]\} \,. \tag{14}$$

The normalization factor is $\mathcal{N} = \exp[2\mathrm{Tr}\, \ln G_o^{-1}] = 4^N$ and the factor of 2 comes from the summation over spin indices.

Equation (14) defines the effective action in the absence of the constraint

$$S_{\mathrm{eff}}[\tilde{\mathcal{U}}] = -2\mathrm{Tr}\, \ln[1 + G_o\tilde{\mathcal{U}}] \tag{15}$$

as a function of the Gaussian random fields $\mathcal{U}$. At this stage we can include the condition of single occupancy by taking the appropriate derivatives with respect to the z_i's according to Eq. (9). The partition function $\mathcal{Z}$ that we obtain when the variables z_i are set equal to zero is

$$\mathcal{Z} = \int \prod_{(i,j)} \mathcal{D}\mathcal{U}_{ij} \exp\left\{-\pi \sum_{(i,j)} \sum_{m} |\mathcal{U}_{ij}(\Omega_m)|^2 - S_{\mathrm{eff}}[c\mathcal{U}] + \sum_i \ln 4B_i[\mathcal{U}]\right\} \tag{16}$$

with S_{eff} given by Eq. (15) and

$$B_i[\mathcal{U}] = \left(\frac{\partial^2 S_{\mathrm{eff}}[\tilde{\mathcal{U}}]}{\partial z_i^2} - 2\frac{\partial S_{\mathrm{eff}}[\tilde{\mathcal{U}}]}{\partial z_i} - \left(\frac{\partial S_{\mathrm{eff}}[\tilde{\mathcal{U}}]}{\partial z_i}\right)^2\right)\Bigg|_{z=0} . \tag{17}$$

The derivatives of the effective action in Eq. (17) can be expressed in terms of the projector P_i, onto the ith site of the lattice, whose matrix elements in the Wannier representation are $(P_i)_{jk} = \delta_{jk}\delta_{ij}$. We have

$$\left.\frac{\partial S_{\mathrm{eff}}}{\partial z_i}\right|_{z=0} = -2\mathrm{Tr}\left\{(1 - cG_o\mathcal{U})^{-1} G_o P_i\right\} \tag{18}$$

and

$$\left.\left(\frac{\partial^2 S_{\mathrm{eff}}}{\partial z_i^2}\right)\right|_{z=0} = 2\mathrm{Tr}\left\{\left[(1 - cG_o\mathcal{U})^{-1} G_o P_i\right]^2\right\} . \tag{19}$$

In the next section we evaluate the function $B_i[\mathcal{U}]$ of Eq. (17) for static fields $\mathcal{U}$.

The crudest way to estimate the integral over configurations of the link field $\mathcal{U}_{ij}$ is the saddle point approximation.

Static field configurations which minimize the action are discussed in the next two sections. Then, the exponent in curly brackets in Eq. (16), when evaluated at these configurations, can be interpreted as an effective free energy $\beta\mathcal{F}_{\text{eff}}$. In this context the term in the logarithm of B_i appearing in Eq. (16) plays the role of a correction to the entropy of the system which is reduced because single occupancy of sites has been enforced.

3. Static Approximation and Saddle Point Solutions

The search for static saddle point configurations is the first step to give an estimate of the partition function of Eq. (16). The static approximation brings about a great simplification of the formalism since all the frequency sums decouple from those over site indices (which we shall denote by "Sp" henceforth). In fact, the matrix elements of the mean field $\mathcal{U}(\Omega_m)$ are chosen as $\mathcal{U}_{ij}^{n,n'} = \mathcal{U}_{ij}\delta_{n,n'}$, where the matrix $\mathcal{U}$ is hermitian in the site indices.

The explicit expression for S_{eff} of Eq. (15) becomes:

$$\begin{aligned} S_{\text{eff}}[\tilde{\mathcal{U}}] &= 2\sum_{k=1}^{\infty}\frac{(-1)^k}{k}\text{Tr}\{(G_o\tilde{\mathcal{U}})^k\} \\ &= -\sum_{i=1}^{N} z_i + 2\sum_{k=2}^{\infty}\frac{(-1)^k}{k}\gamma_k Sp[(\tilde{\mathcal{U}})^k] \end{aligned} \tag{20}$$

where $\gamma_k = \sum_n (\frac{1}{i\omega_n})^k$ and $\gamma_{2k+1} = 0$.

Its first derivative with respect to z_i which was formally given by Eq. (18) becomes

$$\frac{\partial S_{\text{eff}}[\tilde{\mathcal{U}}]}{\partial z_i} = -1 + \sum_{k=1}^{\infty} 2\gamma_{2k} Sp[\tilde{\mathcal{U}}^{2k}\tilde{\mathcal{U}}^{-1}P_i] \,. \tag{21}$$

For a square lattice and only nearest neighbour interactions $\left.\frac{\partial S_{\text{eff}}}{\partial z_i}\right|_{z=0} = -1$. In fact the trace over site indices of powers of the auxiliary bosonic field $\mathcal{U}$ corresponds to building up loops of appropriate length in the lattice. In this case only loops with an even number of sites will be allowed and hence only even powers of $\mathcal{U}$ would survive when taking the trace.

The second derivative of the effective action corresponding to Eq. (19), is given by

$$\frac{\partial^2 S_{\text{eff}}}{\partial z_i^2} = 2\sum_{k=0}^{\infty}\gamma_{2(k+1)}\sum_{q=0}^{k} Sp[(\tilde{\mathcal{U}})^{2q}P_i(\tilde{\mathcal{U}})^{2(k-q)}P_i] \,. \tag{22}$$

If the local variables z_i are still kept, Eqs. (21) and (22) can be inserted in the generating functional of Eq. (14), to calculate the average occupancy at site i, $\langle n_i \rangle$ and other more general averages of products of n_i operators. The technique to calculate them within the static approximation is reported in Appendix C. In the case of a square lattice it is easy to prove that the average occupancy is exactly one at any temperature (see Sec. 5).

The mean square fluctuations of n_i should also vanish, of course, but this result can not be expected to hold, if any approximation is involved in evaluating the average. In fact, we were only able to evaluate these averages within the mean field approximation, for the dimer and the flux phases and details can be found in Sec. 5, where the result is discussed. As shown in Fig. 1, the fluctuations float with temperature within 10%, what can be taken as a check of the reliability of the approximation itself.

To proceed further in calculating Eqs. (20), (21) and (22), one has to specify the space dependence of the U field. We have used the configurations for the field U which lead to the non-uniform phases of AM.

These are mean field solutions which are translationally invariant along the diagonals of the square lattice. The resulting bipartite lattice gives rise to the doubling of the unit cell and consequently the Brillouin zone is halved (RBZ).

Once this choice is made, the representation of the fields U_{ij} and of the projectors P_i in Fourier space will considerably simplify the calculations.

Let us denote a suitable basis by $|\alpha, k\rangle$, where k is in the RBZ and α takes the two values even or odd ($\alpha = e, o$), labeling the two sublattices respectively. These single particle states are eigenfunctions of the translation operators $T_{\vec{a}(\vec{b})}$ along the diagonals $\vec{a} = \vec{x} + \vec{y}$, $\vec{b} = \vec{x} - \vec{y}$

$$T_{\vec{a}(\vec{b})}|\alpha, k\rangle = e^{-i\vec{k}\vec{a}(\vec{b})}|\alpha, k\rangle \ . \tag{23}$$

Their projection onto the Wannier states labeled by the site index i is

$$\langle i|\alpha, k\rangle = \sqrt{\frac{2}{N}} e^{-i\vec{k}\cdot\vec{R}_i}\delta_{i,\alpha} \ . \tag{24}$$

The matrix elements of U in this basis are

$$\langle o, \vec{k}|U|\vec{\ }|, \vec{\langle}\rangle = \delta_{\vec{\|}, \vec{\ }'}\lambda(\vec{\|}) \tag{25}$$

where

$$\lambda(\vec{k}) = U_1 e^{ik_x} + U_2^\star e^{-ik_y} + U_3 e^{-ik_x} + U_4^\star e^{ik_y} \ . \tag{26}$$

Here we follow the notations of Ref. (17). The U_l are complex (oriented) link variables as depicted in Fig. 2. Complex conjugation correspond to reverse the

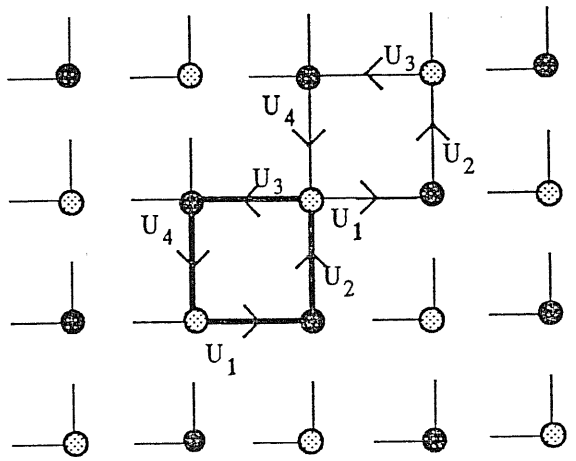

Fig. 2. Pictorial representation of the link order parameter in terms of $\mathcal{U}_1, \mathcal{U}_2, \mathcal{U}_3, \mathcal{U}_4$. Periodicity is along the diagonals. Reversing the arrows implies complex conjugation. Black filled sites are named "even" in the text.

arrow of the link. The lattice constant is taken to be unity. Note that the matrix $\mathcal{U}^2$ is diagonal with doubly degenerate eigenvalues: $E^2(\vec{k}) = |\lambda(\vec{k})|^2$.

Similarly the matrix elements of the projector P_i are

$$\langle \alpha, \vec{k}|P_i|\beta, \vec{h}\rangle = \frac{2}{N} e^{i(\vec{h}-\vec{k})R_i} \delta_{\alpha,\beta}\delta_{\alpha,i} \tag{27}$$

that is, they are diagonal in the α indices.

Within this scheme, the effective action of Eq. (15), evaluated at $z_i = 0$, becomes

$$S_{\text{eff}}[\mathcal{U}] = -4 \sum_k \ln \cosh\left(\frac{cE(k)}{2}\right) . \tag{28}$$

It is straightforward to show that the constraint of Eq. (17) becomes

$$\begin{aligned} B &= 1 + 2 \sum_n Sp\left[\frac{1}{i\omega_n - c\mathcal{U}} P_i \frac{1}{i\omega_n - c\mathcal{U}} P_i\right] \\ &= 1 - \left(\frac{2}{N}\right)^2 \sum_{k,k'} \frac{x_k \tanh(x_k/2) - x_{k'} \tanh(x_{k'}/2)}{x_k^2 - x_{k'}^2} \end{aligned} \tag{29}$$

which is independent of site i. Here the dimensionless variables $d_i = \frac{c}{\beta J}\mathcal{U}_i$, $d_k = \frac{c}{\beta J}\lambda(k)$ and $x_k = cE(k)$ have been used. Finally

$$\mathcal{Z} = \left(\int \prod_{i=1}^{4} \mathcal{D}\mathcal{U}_i \exp\{-\frac{2}{N}\beta \mathcal{F}_{\text{eff}}[\mathcal{U}]\}\right)^{N/2} \tag{30}$$

where

$$f_{\text{eff}} = \frac{\mathcal{F}_{\text{eff}}}{NJ}$$
$$= \sum_i |d_i|^2 - \frac{2}{\beta J}\frac{2}{N}\sum_k \ln\cosh(x_k/2) - \frac{1}{\beta J}\ln 4B \tag{31}$$

is the effective total action depending on the values of d_i $(i = 1, \ldots, 4)$. Trivial limiting cases can be explored.

In the case of non interacting gas of N particles the only effect of the constraint of single site occupancy is to reduce the configurational entropy to $N \ln 2$. In fact, when $J \to 0$, then $x_k \to 0$ and $B \to 1/2$ for any temperature. On the other hand, at zero temperature, we have $B = 1$ no matter what d is. This is a limitation due to including the constraint within the static approximation only. In fact $\overline{n_i^2} = 1$ at zero temperature and no extra contribution due to the constraint arises within static fluctuations in this limit.

It is readily seen that B decreases smoothly from 1 to 1/2 when the temperature increases. This means that, for any configuration, the effect of the constraint is to reduce the entropy term in the total effective action.

Minimization of the effective total action of Eq. (31) yields the mean field configurations for the order parameters d_k. In fact the stationarity of the action implies that $(l = 1, \ldots, 4)$

$$\frac{\partial \beta \mathcal{F}}{\partial \mathcal{U}_l^\star} = \pi \frac{N}{2}\mathcal{U}_l - 2\sum_k \frac{\partial x_k}{\partial \mathcal{U}_l^\star}\cdot \mathcal{D}_k = 0\ . \tag{32}$$

Here

$$\mathcal{D}_k = \tanh(x_k/2) - \frac{4}{NB}\sum_{k'} C(x_k, x_{k'}) \tag{33}$$

with the function C, which is the derivative of B of Eq. (29) with respect to x_k, given by

$$C(x, y) = \frac{1}{(x^2 - y^2)^2}\left(\frac{x(x^2 - y^2)}{2\cosh^2(x/2)} + \right.$$
$$\left. - (x^2 + y^2)\tanh(x/2) + 2xy\tanh(y/2)\right)\ . \tag{34}$$

The self-consistency equation for the order parameters $d_{\tilde{q}}$, derived from Eq. (32) is $(t = 1/\beta J)$

$$d_{\tilde{q}} = t\frac{2}{N}\sum_k (\cos(q_x - k_x) + \cos(q_y - k_y))\frac{\mathcal{D}_k}{x_k}\cdot d_k\ . \tag{35}$$

The mean field phases of AM arise from Eq. (35). The breaking of the local gauge symmetry that follows from the choice of our order parameters is forbidden by the Elitzur theorem[33] and is an artifact of the way in which we construct the mean field approximation by fixing a particular gauge at the outset, which allows us to satisfy the consistency equation of Eq. (35). Once this breaking is produced, the breaking of the global gauge invariance is spontaneous, as will be discussed in the next section.

4. Generalized Mean Field Phases

We are now in a position to include the constraint at finite temperatures, within the saddle point approximation. The dimer phase and the flux phase are still found as stationary points and these are the two phases we concentrate on. They are obtained by specializing Eq. (35) to a given choice of the order parameter $d_i (i = 1, \ldots, 4)$.

(a) *Dimer phase*

This phase is a bond-centered charge density wave in which each site forms a dimer with one of its nearest neighbours and in fact breaks the original translational symmetry. The dimer phase considered here is alternating on the bonds, so that the translational symmetry along the diagonals of the lattice is preserved according to the ansatz of Eq. (26).

Here only one of the d_i's fields is different form zero and it may be made real by a gauge transformation ($d_1 = d$ and $d_2 = d_3 = d_4 = 0$).

Then the resulting x_k to be substituted into Eqs. (31) and (35) is $x_k = d/t$. Equation (35) becomes

$$2d = \tanh \frac{d}{2t} + \frac{1}{2} D_P \tag{36}$$

where $D_P = \frac{\partial}{\partial x} \ln B_P(x)|_{x=d/2t}$. Here is

$$B_P(x) = 1 - \frac{1}{4}\left(\frac{\tanh x}{x} + \frac{1}{\cosh^2 x}\right) \tag{37}$$

according to Eq. (29) and D_P is the limit of Eq. (34) for $x \to y$.

The effect of the constraint on the temperature dependence of the order parameter d is all included in the extra term $D_P/2$ of Eq. (36). The mean field transition temperature is found to be higher ($t_c = 5/12$), than that found in the absence of the constraint ($t_{co} = 1/4$). However the zero temperature value for the order parameter is found to be equal in both cases: $d(0) = d_0(0) = 1/2$. This is probably not consistent with the increase of the critical temperature and follows from the fact that $B_P \to 1$ for $T \to 0$ and that D_P vanishes in this limit. We discuss this point further in Sec. 6.

(b) *Flux phase*

The flux phase carries half a quantum flux per plaquette: $\prod_i d_i = d_1 d_2 d_3 d_4 = |d_1||d_2||d_3||d_4|e^{i\pi}$. A special choice of the gauge which makes the phases equal among the link variables is: $d_i = de^{i\pi/4}$ (i=1,...,4) so that $d_k = 2d(\cos k_x - i\cos k_y)$.

Now is $x_k = 2d\epsilon_k$ with $\epsilon_k = (\cos k_x^2 + \cos k_y^2)^{1/2}$. In this case the self-consistency equation for the amplitude of the order parameter d reads

$$4d = \int_{\mathrm{RBZ}} \frac{d^2k}{2\pi^2}\epsilon_k \tanh\frac{d\epsilon_k}{t} + \frac{t}{2}\frac{\partial \ln B}{\partial d} \tag{38}$$

where Eq. (69) of Appendix A, specialized to the flux phase order parameter, becomes

$$\frac{\partial B}{\partial d} = \int_{\mathrm{RBZ}} \frac{d^2k}{2\pi^2}\left(\frac{t}{d^2}\int_{\mathrm{RBZ}} \frac{d^2k'}{2\pi^2}\frac{\epsilon_k}{\epsilon_k^2 - \epsilon_{k'}^2}\tanh\frac{\epsilon_k d}{t} + \frac{1}{d}\int_{\mathrm{RBZ}} \frac{d^2k'}{2\pi^2}\frac{\epsilon_k^2}{\epsilon_k^2 - \epsilon_{k'}^2}\tanh^2\frac{\epsilon_k d}{t} - \frac{1}{2d}\right) . \tag{39}$$

The transition temperature is found to be equal to that of the dimer phase, both in the presence and in the absence of the constraint. Again here $d(0) = d_o(0) = \bar{\epsilon}/4$ with $\bar{\epsilon} = \int \frac{d^2k}{2\pi^2}\epsilon_k = 0.918$, because at the mean field level the constraint is ineffective at $T = 0$ within the static approximation.

It follows that at zero temperature the total effective action of Eq. (31), when evaluated at the stationarity points, gives back the values of AM for the energies of the two phases

$$f^0_{\mathrm{eff}}(t=0) = -1/4 \qquad \text{(dimer phase)}$$
$$f^0_{\mathrm{eff}}(t=0) = -\bar{\epsilon}^2/4 = -0.2295 \qquad \text{(flux phase)}$$

where $f_{\mathrm{eff}} = \mathcal{F}_{\mathrm{eff}}/NJ$ is the dimensionless free energy per particle.

We add one-loop corrections to Eq. (31) in order to get meaningful results for an approximated temperature dependent free energy.

To this end one has to analyze the second variation of the action around the dimer and flux phase saddle points.

As a first step we have kept only time independent gaussian fluctuations in the functional integral of Eq. (30), restricting ourselves to the fluctuations which conserve the spatial symmetry. Therefore, the variation of $\lambda(k)$ is assumed to be

$$\delta\lambda(k) = \delta\mathcal{U}_1 e^{ik_x} + \delta\mathcal{U}_2^\star e^{-ik_y} + \delta\mathcal{U}_3 e^{-ik_x} + \delta\mathcal{U}_4^\star e^{ik_y} . \tag{40}$$

Thus, the choice of $\delta\mathcal{U}_i (i = 1, \ldots, 4)$ is the same for each of the $N/2$ vectors k. In the case of the dimer phase, being the excitation spectrum dispersionless, the fluctuations on different sites are independent and this assumption is not a limitation.

We expand the effective action to second order, $\mathcal{F}_{\text{eff}} = \mathcal{F}^0_{\text{eff}} + \mathcal{F}^{(2)}$, where $\mathcal{F}^0_{\text{eff}}$ is the effective action of Eq. (31) evaluated at the stationarity point, and $\mathcal{F}^{(2)}_{\text{eff}}$ is the second variation which is worked out in Appendix A.

Then, Eq. (30) becomes

$$\mathcal{Z} \approx e^{-\beta \mathcal{F}^0_{\text{eff}}} \left[\int \prod_{i=1}^{4} d^2 \delta\mathcal{U}_i e^{-\frac{2}{N}\beta \mathcal{F}^{(2)}_{\text{eff}}} \right]^{N/2} \tag{41}$$

with

$$\frac{\beta \mathcal{F}^{(2)}}{N} \equiv \pi y_i M_{ij} y_j = \beta J \left\{ \sum_{i=1}^{4} |\delta d_i|^2 + \frac{t}{N} S^{(2)}_{\text{eff}} - \frac{t}{2} \left(\frac{\delta^2 B}{B} - \frac{(\delta B)^2}{B^2} \right) \right\} . \tag{42}$$

This equation defines the curvature matrix M for the vector y, whose components are the real and imaginary parts of $\delta\mathcal{U}_i$. (These, in turn, are related to δd_i by $\delta\mathcal{U}_i = (2\beta J/\pi)^{1/2} \delta d_i$.) The second variation of the action is

$$S^{(2)}_{\text{eff}} = \frac{1}{2}\delta^2 \mathcal{S}_{\text{eff}} = 2t \sum_k \left(Q(|d_k|)|\delta d_k|^2 + \Re \left[\delta d_k \left(\frac{d^*_k}{|d_k|} \right)^2 q(|d_k|) \delta d_k \right] \right) \tag{43}$$

where

$$\begin{aligned} Q(|d_k|) &= -\frac{1}{4|d_k|} \tanh \frac{|d_k|}{2t} - \frac{1}{8t \cosh^2(\frac{|d_k|}{2t})} \\ q(|d_k|) &= \frac{1}{4|d_k|} \tanh \frac{|d_k|}{2t} - \frac{1}{8t \cosh^2(\frac{|d_k|}{2t})} . \end{aligned} \tag{44}$$

The full expressions for δB and $\delta^2 B$ can be found in Appendix A (Eq. (69) and Eq. (71) respectively).

The analysis of the results leads to the following conclusions. Our order parameter has four complex components. Therefore, the dynamical matrix M around the stationary point solutions is an 8×8 matrix. Its diagonalization gives us eight normal modes. In the case of the flux phase four of them are amplitude modes while the other four are phase modes. For the dimer phase instead, two of them can be denoted as pure phase and amplitude modes respectively, while the remaining six are mixed ones.

The total effective action is invariant with respect-to any special choice of gauges in the order parameter as reported at length in Appendix B. This implies that there are zero modes which appear as zero eigenvalues of the curvature matrix M.

In the case of the dimer phase only one zero mode exists which corresponds to a global gauge transformation

$$d_k \to d_k e^{i\theta} \ . \tag{45}$$

This is immediately seen if the constraint is excluded. In fact direct substitution of Eq. (45) into Eq. (43) and Eq. (42) (with $B = 0$) yields

$$f_{\text{eff}}^2 = \frac{\mathcal{F}_{\text{eff}}^{(2)}}{NJ} = \frac{1}{2}\left(1 - \frac{1}{2d}\tanh\frac{d}{2t}\right)(\delta\theta)^2 \ . \tag{46}$$

This vanishes identically, due to the gap equation Eq. (36).

Apart from this mode there is one non-degenerate amplitude mode whose corresponding eigenvalue we denote by λ_2 and six degenerate modes which correspond to the eigenvalue λ_1. While the first one is associated with a change in the amplitude of d_1, the remaining six eigenmodes are associated to changes of d_2, d_3, d_4, both in amplitude and phase.

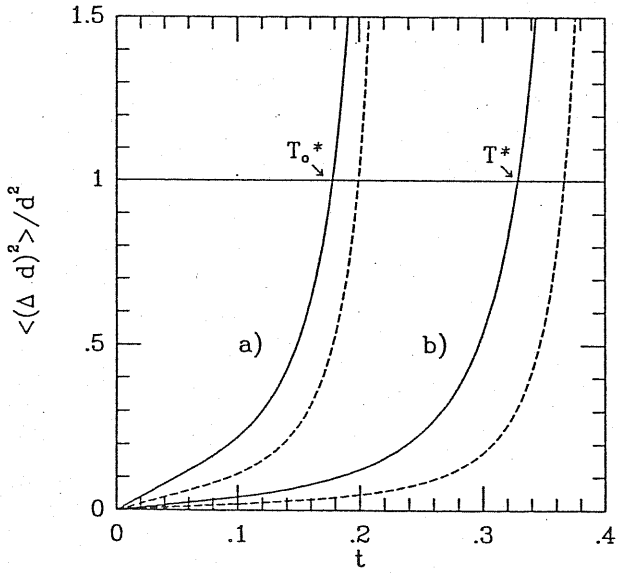

Fig. 3. Plot of $\left(\langle(\Delta d)^2\rangle/d^2\right)_{1,2} = t/4d^2\lambda_{1,2}$ versus temperature $t = (\beta J)^{-1}$ for the dimer phase. Here $\lambda_{1,2}$ are the eigenvalues of the curvature matrix M of the free energy around the saddle point, with the constraint included (b) and without (a). The broken curve corresponds to the non-degenerate amplitude mode (λ_1), while the full curve refers to the other six times degenerate modes.

In Fig. 3 the quantities $\left(\frac{\langle(\Delta d)^2\rangle}{d^2}\right)_i = \frac{t}{4\lambda_i d^2}$ $(i = 1, 2)$ are plotted, as a function of the reduced temperature t. This ratio is a measure of the mean square fluctuations

in the Gaussian approximation. While the curves on the l.h.s. (labeled by a) do not include the effect of the constraint, the ones on the r.h.s. (b) refer to fluctuations with the constraint taken into account. They diverge at the two critical temperatures T_{co} and T_c, respectively. The broken curves in Fig. 3, which are lower, refer to the fluctuations of $|d_1|$ which are smaller than those of d_2, d_3 and d_4 due to the fact that they affect the amplitude of the order parameter in a direct way.

We have also reported T_o^* and T^* as indicative temperatures at which fluctuations become of the order of the amplitude of the mean field order parameter itself, so that one enters the critical region.

In the case of the flux phase, there are three zero eigenvalues of the curvature matrix, which correspond to relative changes of the phases of the four U_i's without altering the total flux in the plaquette. One of these is again a global gauge transformation as in Eq. (45). The other two affect the energies ϵ_k according to

$$\epsilon_k \rightarrow \epsilon'_k = \sqrt{\cos^2(k_x - \theta_2) + \cos^2(k_y - \theta_3)} \tag{47}$$

with $\theta_{2,3} \in (0, 2\pi)$. They are extensively discussed in Appendix C. The energies ϵ_k are not gauge invariant and are not to be related with the quasiparticle energy spectrum as it is usually done in the spirit of the usual mean field approximation. In particular it should already be clear from the form of the free energy of Eq. (31) that there is no resemblance to a non-interacting gas of quasiparticles of energies ϵ_k, due to the presence of the constraint which depends on the ϵ_k's themselves.

Examining the non-zero eigenvalues the corresponding collective excitations are listed below:

(i) One amplitude mode which changes the modulus of the order parameter with $\delta d_1 = \delta d_2 = \delta d_3 = \delta d_4$(of energy denoted by λ_3);
(ii) one phase mode which changes the total flux in the plaquette (λ_2);
(iii) three degenerate modes which change the relative amplitude of d_1, d_2, d_3, d_4 for a given $\delta|d_k|$ (λ_1).

These are plotted in Fig. 4 as a function of temperature. They are such that $\lambda_3 > \lambda_2 > \lambda_1$, which implies increasing stiffness of the mean field solution with respect to these fluctuations. Careful inspection of Fig. 4 shows that while the constraint strongly stabilizes the flux phase in the same way for the first two modes it is less effective on the remaining three degenerate ones.

Changes of the order parbe integrated over at the outset in evaluating the partition function, give rise to an overall factor which is the volume of the group that leaves the action invariant.[34] Otherwise the integration of the quadratic term of the expansion would show meaningless divergences. Following a standard procedure,[35] we define $M_\perp$ as the projection of the matrix M on the subspace orthogonal to the zero modes, each of which is parametrized by an angle θ_i. In the case of ν zero

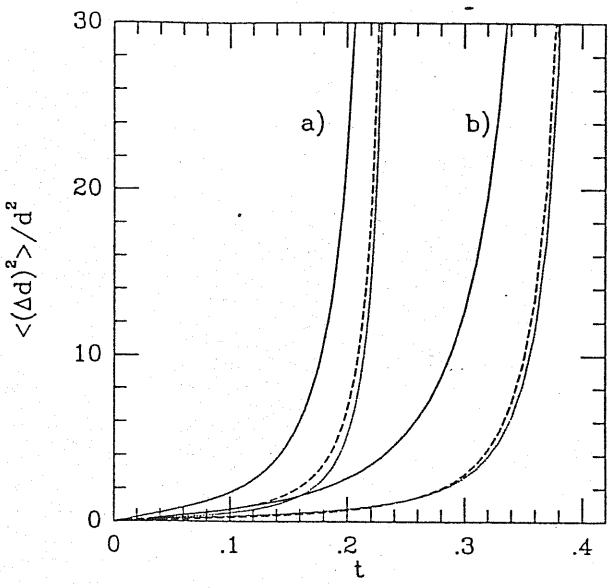

Fig. 4. Same as Fig. 3, but for the flux phase: the dotted curve refers to the amplitude mode (λ_3), the broken curve refers to the phase mode (λ_2), the full curve refers to the other three times degenerate modes (λ_1), with the constraint included (b) and without (a).

modes ($\nu = 1$ for the dimer phase and $\nu = 3$ for the flux phase) we have

$$\mathcal{Z} = e^{-\beta \mathcal{F}^{\circ}_{\text{eff}}} \frac{1}{\sqrt{\det M_{\perp}}} \prod_{i=1}^{\nu} \int \frac{d\theta_i}{2\pi} (\det \mathcal{L})^{1/2} \tag{48}$$

where $\mathcal{L}$ is a $\nu \times \nu$ matrix with elements given by

$$\mathcal{L}_{ij} = \sum_{l=1}^{4} \left(\frac{\partial d_l}{\partial \theta_i} \right)^{*} \cdot \frac{\partial d_l}{\partial \theta_j} \, . \tag{49}$$

The free energy for the dimer phase, which follows from Eq. (48), is

$$f^{P}_{\text{eff}} = (f^{0}_{\text{eff}})_P - \frac{t}{2} \ln \left(\frac{d}{\sqrt{\lambda_1^6 \lambda_2}} \right) \, . \tag{50}$$

The factor d arises from the integral over the angular variable θ, parametrizing the zero mode. An extra term in $t \ln t$ has been omitted which is canceled when quantum fluctuations are also included.[31] The free energy of the constrained system is obviously higher than the one without the constraint.

Finally, the free energy for the flux phase is

$$f^{F}_{\text{eff}} = (f^{0}_{\text{eff}})_F - \frac{t}{2} \ln \left(\frac{3.403 d^3}{\sqrt{\lambda_1^3 \lambda_2 \lambda_3}} \right) \, . \tag{51}$$

The free energies for the two phases, which include the constraint and the one loop static corrections (classical fluctuations around the mean field solution) are plotted in Fig. 5. The one for the flux phase is found to be always well above that for the dimer phase. We discuss its temperature dependence, together with that of the specific heat in Sec. 6.

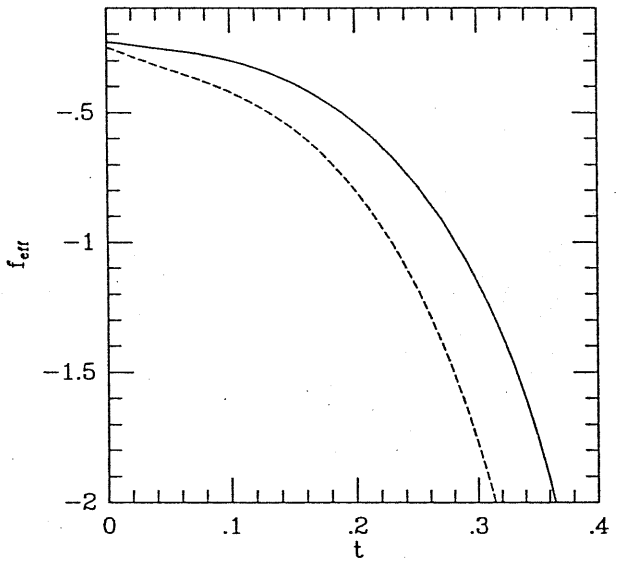

Fig. 5. Dimensionless effective free energy $f_{\text{eff}} = \mathcal{F}_{\text{eff}}/NJ$ as a funtion of temperature $t = (\beta J)^{-1}$ for the dimer phase (broken curve) and the flux phase (full curve) with the constraint included.

5. Analysis of the Constraint

Crucial check of our method to include the single occupancy constraint is the evaluation of the mean occupation number $\langle n_i \rangle$ and of its mean square fluctuations.

We can easily prove that the average of the occupation number operator on the site i is exactly equal to one in the case of a square lattice also when just including static auxiliary fields U_{ij}.

Besides, were the constraint enforced exactly, one should find that the mean square fluctuations of the occupation number at site i, $\langle n_i^2 \rangle - 1$ vanish. Although this is not the case within the saddle point approximation, we have found that the deviations are relatively small.

Let us first discuss the average site occupancy

$$\langle n_i \rangle = \mathcal{Z}^{-1} \left\langle -\frac{\partial}{\partial z_i} e^{-\Sigma(z)} \right\rangle \Bigg|_{z=0} . \tag{52}$$

Here

$$\Sigma(z) = -S_{\text{eff}} + \sum_k \ln(4\tilde{B}_k) \tag{53}$$

is the constrained effective action to be evaluated with the Gaussian weight according to Eqs. (9), (10)

$$\langle \ldots \rangle \equiv \int \prod_{(i,j)} d^2\mathcal{U}_{i,j} e^{-\frac{\pi}{2} \operatorname{Tr} \mathcal{U}^2} (\ldots) \tag{54}$$

and $\mathcal{Z}$, the constrained partition function, is given by Eq. (16). The derivative implies an extra factor in the average, with respect to the evaluation of $\mathcal{Z}$ itself

$$-\left.\frac{\partial \Sigma}{\partial z_i}\right|_{z=0} = \left[-\frac{\partial S_{\text{eff}}}{\partial z_i} + \sum_{k=1}^{N} B_k^{-1} \frac{\partial B_k}{\partial z_i}\right]_{z=0} \tag{55}$$

where

$$\frac{\partial B_k}{\partial z_i} = \frac{\partial^3 S_{\text{eff}}}{\partial z_i \partial z_k^2} - 2\frac{\partial^2 S_{\text{eff}}}{\partial z_i \partial z_k}\left(1 + \frac{\partial S_{\text{eff}}}{\partial z_k}\right) . \tag{56}$$

From Eq. (21) we know that $\partial S_{\text{eff}}/\partial z_i|_{z=0} = -1$. Therefore, to prove that $\langle n_i \rangle = 1$ we have to prove that Eq. (56) is zero, what is evident once we have shown that the third derivative of the effective action vanishes. This reads (see Appendix B)

$$\frac{\partial^3 S_{\text{eff}}}{\partial z_i^2 \partial z_k} = -4 \sum_n Sp\{\chi_n P_i \chi_n P_i \chi_n P_k\} \tag{57}$$

where $\chi_n = (i\omega_n + \tilde{U})^{-1}$, so that the third derivative is explicitly an odd function of $\tilde{U}$. We now show that this derivative is always zero when calculated at $z = 0$ (i.e., $\tilde{U} = -c\mathcal{U}$). The expansion of Eq. (57) gives:

$$\frac{\partial^3 S_{\text{eff}}}{\partial z_i^2 \partial z_k} = -4 \sum_n \left(\frac{1}{i\omega_n}\right) \sum_{h,q,l} \left(\frac{1}{i\omega_n}\right)^{h+q+l} \times c^{h+q+l} Sp\{\mathcal{U}^h P_i \mathcal{U}^q P_i \mathcal{U}^l P_k\} . \tag{58}$$

The sum over frequencies forces $h + q + l$ to be odd. But

$$Sp\{\mathcal{U}^h P_i \mathcal{U}^q P_i \mathcal{U}^l P_k\} = (\mathcal{U}^h)_{ki} (\mathcal{U}^q)_{ii} (\mathcal{U}^l)_{ik} \tag{59}$$

where no summation on i and k is implied. On a square lattice, $(\mathcal{U}^q)_{ii}$ must contain an even number of $\mathcal{U}$'s so that q must be an even number. To go from site i to site k the number of steps is of course even or odd whatever the path in the lattice is chosen. Therefore, h and l should be both even or odd. But then $h + q + l$ cannot be odd. This proves that the third derivative of the effective action is equal to zero

and consequently that

$$\left.\frac{\partial \Sigma}{\partial z_i}\right|_{z=0} = -1 \tag{60}$$

so that the average on-site occupation number is exactly equal to one.

Next, the mean value of the squared occupation number is

$$\begin{aligned}\langle n_i^2 \rangle &= \mathcal{Z}^{-1} \left\langle \frac{\partial^2}{\partial z_i^2} e^{-\Sigma(z)} \right\rangle \Bigg|_{z=0} \\ &= \mathcal{Z}^{-1} \left\langle \left[\left(\frac{\partial \Sigma}{\partial z_i} \right)^2 - \frac{\partial^2 \Sigma}{\partial z_i^2} \right] e^{-\Sigma(z)} \right\rangle \Bigg|_{z=0}\end{aligned} \tag{61}$$

or using Eq. (60)

$$\langle n_i^2 \rangle - 1 = -Z^{-1} \left\langle \left.\frac{\partial^2 \Sigma}{\partial z_i^2}\right|_{z=0} e^{-\Sigma(0)} \right\rangle . \tag{62}$$

Because of the vanishing of Eq. (56) when calculated at $z = 0$, we have

$$\frac{\partial^2 \Sigma}{\partial z_i^2} = \frac{\partial^2 S_{\text{eff}}}{\partial z_i^2} - \sum_j \frac{1}{B_j} \left[\frac{\partial^4 S_{\text{eff}}}{\partial z_j^2 \partial z_i^2} - 2 \left(\frac{\partial^2 S_{\text{eff}}}{\partial z_i \partial z_j} \right) \right]_{z=0} . \tag{63}$$

In the limiting case of zero interaction ($c = 0$) is

$$S_{\text{eff}} = \sum_i [-z_i - 2 \ln \cosh(z_i/2)] \tag{64}$$

which is diagonal in i and j, and Eq. (63) vanishes, when evaluated at $z_i = 0$, as expected.

In the general case, we have not succeeded in proving that the average at the r.h.s. of Eq. (62) is zero, unfortunately, but we have evaluated it at the saddle point. The discrepancy of the result with respect to the expected value provides a direct measure of the reliability of our method at this level of approximation.

The manipulations are lengthy but straightforward and are summarized in Appendix B. Inspection of the results shows that at zero temperature and at T_c, $\partial^2 \Sigma / \partial z_i^2$ vanishes. In fact $\langle n_i^2 \rangle$ is one at zero temperature, because the saddle point satisfies the constraint and no classical (static) fluctuations survive at zero temperature. Besides we have again $\langle n_i^2 \rangle = 1$ at T_c in the constrained case for both the dimer and the flux phase, because we can interpret the $\mathcal{U}_i$'s as effective hopping amplitudes and these tend to zero at the critical temperature. This is at striking difference with the non constrained case, when we expect $\langle n_i^2 \rangle = 3/2$ at the critical temperature for both phases. Infact, let $P(1)$ be the probability that site i is occupied just once and $P(2)$ be the probability that it is doubly occupied. In the absence of the constraint and above the critical temperature, when the particles no longer interact, they are both equal to 1/4, so that we expect $\langle n_i^2 \rangle = 2P(1) + 4P(2) = 3/2$.

The results of $\langle n_i^2 \rangle - 1$ are plotted in Fig. 1 for the dimer and the flux phases, both in the presence and in the absence of the constraint, for comparison. At intermediate temperatures we get at most a deviation of 10% from the desired result.

6. Results and Conclusions

Non-magnetic phases for the spin-1/2 Heisenberg model in 2–D (BZA phase, AM phases, chiral phases etc.) are estimated to be very close in energy to the AF phase which is the ground state of the system. Because this model is obtained from the Hubbard model at half-filling when the U interaction goes to infinity, these phases could be relevant for the cuprate compounds, particularly at low doping.

However the constraint of single site occupancy is crucial both for transforming the Hubbard model into the t-J model, and for using a fermion representation of the spins.

Mean field theory on the resulting effective action automatically satisfies the constraint at zero temperature, so that the mean field ground state energy can be evaluated for these phases. But, zero temperature quantum fluctuations do not fulfill the constraint anyhow and its implementation via a slave boson method is unsatisfactory, unless one introduces an arbitrary small expansion parameter ($1/N$ expansion), which, in the end is put equal to 1/2. Of course, the mean field approximation does not conserve the constraint also when temperature is finite.

In this paper we introduce a new method to take into account the constraint of single site occupancy which is exact also at finite temperatures, till the moment when saddle point approximation or loop expansion has to be undertaken. In estimating fluctuations of the site occupation number around $n_i = 1$, we find that the mean field result accounts for the constraint fairly well, because these are reduced to less than 10% of their value.

We have studied the dimer and the flux phase of AM at finite temperatures, including the constraint and adding static Gaussian fluctuations around these saddle points. This corresponds to taking into account the contribution to the entropy due to the classical fluctuations, which are only effective at finite temperature.

After inclusion of the constraint the flux phase remains higher in energy than the dimer phase and the critical temperature is found to be the same for both phases ($T_c = 5/12$), but higher than the one without the constraint ($T_{co} = 1/4$) (see Fig. 5).

The critical region around T_c is found to be much enlarged by classical fluctuations. A rough estimate of the temperature at which the mean field approximation breaks down due to the overwhelming fluctuations is given by the Ginzburg criterion: $\frac{\langle (\Delta d)^2 \rangle}{d^2} \sim 1$. This defines an upper temperature which moves, for example, in the case of the dimer phase, from $T^\star = 0.22$ to $T^\star = 0.33$ by adding the constraint, to be compared with $T_{co} = 0.25$ and $T_c = 0.42$ respectively. Therefore the critical region grows by about 9%, what is also the case of the flux phase.

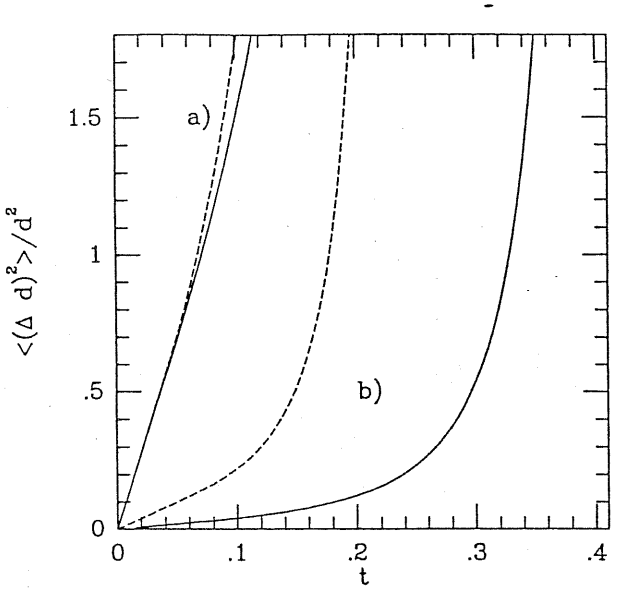

Fig. 6. Comparison between the largest fluctuations $\lambda_1^{D,F}$ for the flux phase (curves *a*) and the dimer phase (curves *b*) versus temperature. Full curves include the constraint, while broken curves do not.

In Fig. 6 we compare the most divergent fluctuations of the dimer (*b*) and flux (*a*) phases including and excluding the constraint (taken from Figs. 3, 4). Fluctuations diverge at the corresponding critical temperatures, as expected. This forces the ones with the constraint (full curve) to keep lower than the free ones (broken curves) at least close to T_c. As it appears from the picture, the large fluctuations are much more affected by the presence of the constraint in the dimer phase than they are in the flux phase. This allows to think that the effect of the temperature is to destabilize the flux phase more easily than the dimer one.

These results seem to be consistent as long as the temperature is not too low.

This is clearly seen in the temperature dependence of the specific heat reported in Fig. 7 for the dimer phase, and Fig. 8 for the flux phase.

The gaussian fluctuations constitute the dominant contribution to the specific heat. This is reduced heavily by the constraint, and becomes unphysically negative for $T \leq 0.08$ in our approximations. This is because quantum fluctuations have been ignored. Their inclusion, in the form of frequency dependent fluctuations will be discussed elsewhere.[32] When these are taken into account the free energy tends to a lower value at zero temperature and its temperature derivatives are corrected.

The evaluation of the fluctuations has led us to the analysis of the zero modes due to the broken symmetries of the action. It is interesting to note that the volume of the configurational space which is covered by the symmetry group also contributes with a term $t \ln t$ to the free energy, a feature typical of two dimensions. It can be shown, however, that this term is exactly canceled when integrating also frequency dependent fluctuations.

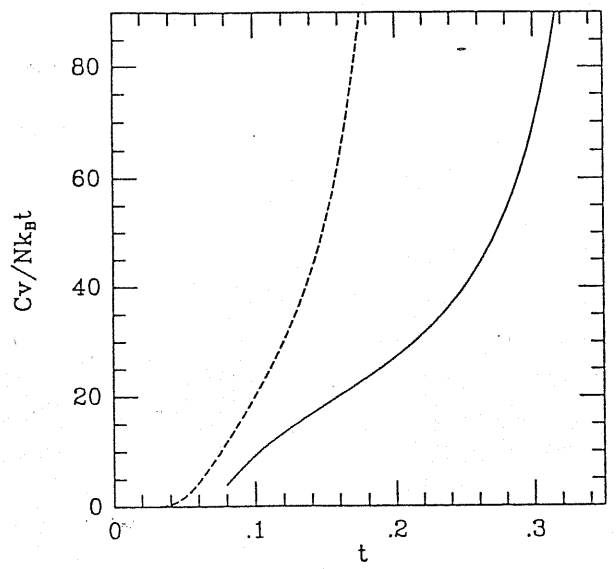

Fig. 7. Specific heat per particle over temperature C_v/k_BNt versus reduced temperature $t = (\beta J)^{-1}$ for the dimer phase. The full curve includes the constraint, while the broken one does not.

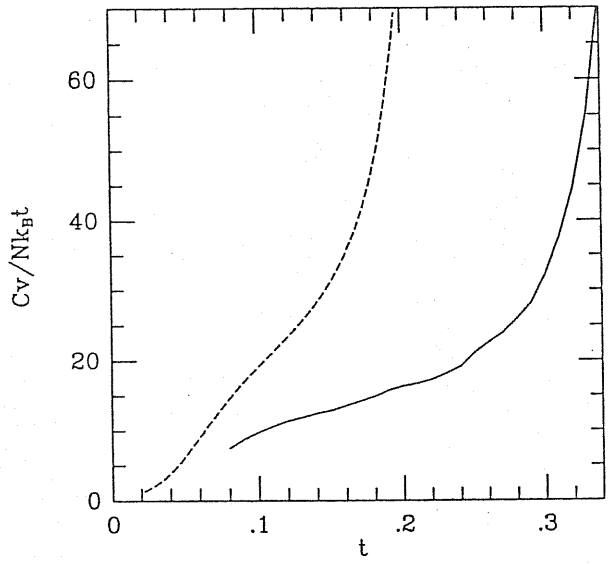

Fig. 8. Specific heat per particle over temperature C_v/k_BNt versus reduced temperature $t = (\beta J)^{-1}$ for the flux phase. The full curve includes the constraint, while the broken one does not.

In conclusion, we have studied the nature of the fluctuation modes around the dimer and flux mean field solutions and their contribution to the free energy at finite temperatures. Fluctuations of the site occupancy number can be controlled with our method of including the constraint and are consistently reduced. Our calculation shows that the inclusion of the constraint within the mean field approximation has

the effect that the temperature destabilizes the flux phase more easily than the dimer phase.

The method presented here can be extended to the case when the filling is no longer one electron per site, which is presently under investigation. Away from half-filling the full Gutzwiller projector has to be implemented so that two auxiliary variables are needed, which should be coupled to the particle density for each spin at each site. However these source terms no longer commute with the t-J hamiltonian which would be used in this context. This requires that the interaction representation is used and that functional derivatives are performed each time.

Acknowledgments

This work is partly supported by MURST. Suggestions and discussions with E. Tosatti are gratefully aknowledged. One of us (G.M.) would like to thank E. Tosatti and Yu Lu (ICTP) for their hospitality at Trieste where this work was completed.

Appendix A: Variation of the Total Effective Action

Our starting point is the effective free energy of Eq. (31)

$$f_{\text{eff}} \equiv \frac{\mathcal{F}_{\text{eff}}}{NJ} = \sum_i |d_i|^2 + \frac{t}{N} S_{\text{eff}} - t \ln 4B \tag{A1}$$

where S_{eff} and B are given by Eqs. (28) and (29), respectively. The first variation of the effective action, with respect to the fields $\delta\mathcal{U}$ is

$$\delta S_{\text{eff}} = \delta(-2 \,\text{Tr}\, \ln[G_0^{-1} - c\mathcal{U}]) = -cSp\left[\tanh \frac{c\mathcal{U}}{2} \delta\mathcal{U}\right] . \tag{A2}$$

The function B due to the constraint takes the form

$$B = 1 + 2 \sum_n Sp[\chi_n P_i \chi_n P_i] \tag{A3}$$

where Sp denotes the trace over site indices only, and $\chi_n = (i\omega_n - c\mathcal{U})^{-1}$, so that one gets

$$\delta B = 4c \sum_n Sp[\chi_n P_i \chi_n P_i \chi_n \delta\mathcal{U}] . \tag{A4}$$

Due to the static approximation, the frequency summation does not mix with the sum over site configurations. Also, the trace over site indices can be expressed as sums over the reduced Brillouin zone. Finally we get, in a fashion that is described

in Appendix C, the constraint contribution to the first variation of the action

$$\delta B = \left(\frac{2}{N}\right)^2 \sum_{k,k'} A_1 \left(\frac{2(x_k^2 + x_{k'}^2)}{(x_k^2 - x_{k'}^2)^2} \tanh \frac{x_k}{2} \right.$$
$$\left. - \frac{x_k x_{k'}}{(x_k^2 - x_{k'}^2)^2} \tanh \frac{x_{k'}}{2} - \frac{x_k}{x_k^2 - x_{k'}^2} (1 - \tanh^2 \frac{x_k}{2}) \right) \tag{A5}$$

where we have defined: $A = A_1 + iA_2 = \left\{ \frac{d_k}{|d_k|} \delta d_k^* \right\} / t$.

In terms of these quantities, the first variation of the total effective action is

$$\delta\beta \mathcal{F}_{\text{eff}}[\mathcal{U}] = \pi Sp[\mathcal{U}\delta\mathcal{U}] + c \sum_n Sp[\tanh \frac{\mathcal{U}}{2} \delta\mathcal{U}] - \frac{N}{B} \delta B \ . \tag{A6}$$

In the same way we have for the second variation of the effective action

$$f_{\text{eff}}^{(2)} = \frac{\mathcal{F}_{\text{eff}}^{(2)}}{NJ} = \sum_{i=1}^{4} |\delta d_i|^2 + \frac{t}{N} S_{\text{eff}}^{(2)} - \frac{t}{2} \left(\frac{\delta^2 B}{B} - \frac{(\delta B)^2}{B^2} \right) \tag{A7}$$

where

$$S_{\text{eff}}^{(2)} = \frac{1}{2} \delta^2 S_{\text{eff}} = -c^2 \sum_n Sp[\chi_n \delta\mathcal{U} \chi_n \delta\mathcal{U}] \ . \tag{A8}$$

Its expression in the wave vector representation is reported in Eqs. (43, 44) of the text. On the other hand while the second variation of B is given by

$$\delta^2 B = 4c^2 \sum_n 2Sp[\chi_n P_i \chi_n P_i \chi_n \delta\mathcal{U} \chi_n \delta\mathcal{U}]$$
$$+ Sp[\chi_n \delta\mathcal{U} \chi_n P_i \chi_n \delta\mathcal{U} \chi_n P_i] \ . \tag{A9}$$

Here the trace has to be evaluated explicitly. We obtain three contributions which we denote as follows

$$\delta^2 B = B_1[A_1 A_1'] + B_2[A_1^2] + B_3[A_2^2] \ . \tag{A10}$$

Here $A_{1,2}$ are the real and imaginary part of the complex function A defined previously and the prime is a short-hand notation for the k' dependence. Their explicit expression is

$$B_1[A_1 A_1'] = 2 \left(\frac{2}{N}\right)^2 \sum_{k,k'} \frac{x_k x_{k'}}{(x_k^2 - x_{k'}^2)^2} [\frac{(3x_k^2 + x_{k'}^2)}{(x_k^2 - x_{k'}^2)} \frac{2}{x_k} \tanh x_k/2$$
$$- \frac{(3x_{k'}^2 + x_k^2)}{(x_k^2 - x_{k'}^2)} \frac{2}{x_{k'}} \tanh x_{k'}/2 - 2 + \tanh^2 x_k/2 + \tanh^2 x_{k'}/2] A_1 A_1'$$

$$B_2[A_1^2] = \left(\frac{2}{N}\right)^2 \sum_{k,k'} [\frac{4x_k(x_k^2+3x_{k'}^2)}{(x_k^2-x_{k'}^2)^2} \tanh\frac{x_k}{2} - \frac{4x_{k'}(x_{k'}^2+3x_k^2)}{(x_k^2-x_{k'}^2)^2} \tanh\frac{x_{k'}}{2}$$
$$- \frac{2(x_k^2+x_{k'}^2)}{(x_k^2-x_{k'}^2)}(1-\tanh^2\frac{x_k}{2}) - x_k \tanh\frac{x_k}{2}(1-\tanh^2\frac{x_k}{2})] \frac{-1}{x_k^2-x_{k'}^2} A_1^2$$
$$B_3[A_2^2] = \left(\frac{2}{N}\right)^2 \sum_{k,k'} \frac{1}{x_k^2-x_{k'}^2} \left[\frac{2(x_k^2+x_{k'}^2)}{x_k(x_k^2-x_{k'}^2)} \tanh x_k/2\right.$$
$$\left. - \frac{4x_{k'}}{x_k^2-x_{k'}^2} \tanh x_{k'}/2 - 1 + \tanh^2 x_k/2\right] A_2^2 \,. \tag{A11}$$

These complete the evaluation of the second variation of the total effective action.

Appendix B: Averages of the occupation number

We outline here the procedure to evaluate the derivatives of the effective action of Eq. (15) with respect to z_i. These are required to evaluate the average number $\langle n_i \rangle$ and the average fluctuation $1 - \langle n_i^2 \rangle$, in particular Eq. (63)

$$\frac{\partial^2 \Sigma}{\partial z_i^2} = \frac{\partial^2 S_{\text{eff}}}{\partial z_i^2} - \sum_j \frac{1}{B_j} \left[\frac{\partial^4 S_{\text{eff}}}{\partial z_j^2 \partial z_i^2} - 2\left(\frac{\partial^2 S_{\text{eff}}}{\partial z_i \partial z_j}\right)\right]_{z=0} . \tag{B1}$$

The first derivative of the action $\partial S_{\text{eff}}/\partial z_i$ given by Eq. (18) can be written formally as

$$\frac{\partial S_{\text{eff}}[\tilde{U}]}{\partial z_i} = -2\,\text{Tr}\,\{\chi P_i\} \tag{B2}$$

where $\chi = (i\omega_n + \tilde{U})^{-1}$ and $\tilde{U} = \sum_i z_i P_i - c\mathcal{U}$. The trace symbol refers to the sum over frequencies and sites. Each further derivative can be performed by noting that $\partial\chi/\partial z_k = -\chi P_k \chi$ so that

$$\frac{\partial^2 S_{\text{eff}}[\tilde{U}]}{\partial z_i \partial z_j} = 2\,\text{Tr}\,\{\chi P_i \chi P_j\} \tag{B3}$$

which coincides with Eq. (19) of the text when j is put equal to i. For the third derivative one gets Eq. (57). Similarly one obtains

$$\frac{\partial^4 S_{\text{eff}}[\tilde{U}]}{\partial^2 z_i \partial^2 z_j} = 4\,\text{Tr}\,\{\chi P_i \chi P_j \chi P_i \chi P_j + 2\chi P_i \chi P_i \chi P_j \chi P_j\} \,. \tag{B4}$$

We exemplify the procedure by evaluating Eq. (A1). To express the trace explicitly we choose the basis in which the matrix U is diagonal and label these states generically by the indices μ, ν

$$|\mu\rangle \equiv |\vec{k}\pm\rangle \text{ such that } U|\vec{k}\pm\rangle = \pm E(\vec{k})|\vec{k}\pm\rangle$$

i.e.

$$\left.\frac{\partial^2 S_{\text{eff}}[\tilde{U}]}{\partial z_i \partial z_j}\right|_{z=0} = 2\sum_n \sum_{\mu\nu} \frac{1}{i\omega_n - cU_\nu}\langle\nu|P_j|\mu\rangle \frac{1}{i\omega_n - cU_\mu}\langle\mu|P_i|\nu\rangle \ . \tag{B5}$$

The sum over frequencies can be performed easily

$$\sum_n \frac{1}{i\omega_n - cU_\mu}\frac{1}{i\omega_n - cU_\nu} = \frac{1}{2c}\frac{\tanh(cU_\mu/2) - \tanh(cU_\nu/2)}{U_\nu - U_\mu} \ . \tag{B6}$$

The matrix elements of the projectors depend on whether the site is even or odd

$$\begin{aligned} \langle\vec{k}\alpha|P_i|\vec{k'}\beta\rangle &= 1 \ , && i \text{ odd} \\ &= \alpha\beta\frac{\lambda_k \lambda^*_{k'}}{|\lambda_k||\lambda_{k'}|} \ , && i \text{ even} \end{aligned} \tag{B7}$$

where α, β are plus or minus and so is the product $\alpha\beta$ depending on whether they are equal or opposite.

The result for the two site indices belonging to the same sublattice is

$$\frac{\partial^2 S_{\text{eff}}}{\partial z_i \partial z_j} = \left(\frac{2}{N}\right)\sum_{k,k'} e^{i(k-k')(R_i - R_j)}\frac{x_k \tanh(x_k/2) - x_{k'}\tanh(x_{k'}/2)}{x_k^2 - x_{k'}^2} \ , \tag{B8}$$

while if i belongs to the even sublattice and j to the odd one is

$$\frac{\partial^4 S_{\text{eff}}}{\partial z_i^2 \partial z_j^2} = \left(\frac{2}{N}\right)\sum_{k,k'} e^{i(k-k')(R_i - R_j)}\frac{\lambda_k}{|\lambda_k|}\frac{\lambda^*_{k'}}{|\lambda_{k'}|}\frac{(x_{k'}\tanh(x_k/2) - x_k \tanh(x_{k'}/2)}{x_k^2 - x_{k'}^2} \ . \tag{B9}$$

when i belongs to the even sublattice and j to the odd one the two indices can be exchanged (here again $x_k = cE(k)$ and λ_k is given by Eq. (26).

The result of $\partial^2\Sigma/\partial z_i^2$ for the dimer case is site independent and can be put into closed form as follows

$$\begin{aligned} \frac{\partial^2\Sigma}{\partial z_i^2} = &-\frac{1}{4\cosh^2(\frac{x}{2})}\left[\frac{1+\sinh x}{x}\right] - \frac{4\cosh^2(\frac{x}{2})}{4\cosh^2(\frac{x}{2}) - \frac{\sinh x}{x} - 1} \\ &\times [3p(x) + 4q(x) + 5r(x)] - \frac{1}{4\cosh^4(\frac{x}{2})}\left(\frac{1+\sinh^2 x}{x^2}\right) \end{aligned} \tag{B10}$$

where is $x = d/t$ and the functions have been defined

$$p(x) = \frac{1}{48\cosh^4(x/2)[1-2\sinh^2(x/2)]}$$
$$q(x) = \frac{1}{16x^3\cosh^2(x/2)[x^2\tanh(x/2)-\sinh x + x]}$$
$$r(x) = \frac{1}{8x^3\cosh^2(x/2)[\sinh x - x]} \,. \tag{B11}$$

It is immediately seen that at zero temperature and at T_c, that is when $x \to 0$, the functions p, q, r tend to $1/48$ and $\partial^2\Sigma/\partial z_i^2 \to 0$ as well. In fact we expect to have $\langle n_i^2 \rangle = 1$ in the constrained case for both the dimer and the flux phase, as explained in the text.

Appendix C: Zero Modes of the Dimer and the Flux Phase

The global gauge transformation of Eq. (45) is the only zero mode of the dimer phase. This can be checked immediately if the contraint is omitted, because Eq. (42) (with $B = 0$) becomes

$$f_{\text{eff}}^{(2)} = \frac{2}{N}\sum_k |d_k|^2 \left(1 + Q(|d_k|) - \{q(|d_k|)\}\right)(\delta\theta)^2 \tag{C1}$$

where the functions Q and q are defined in Eq. (40) of the text. In the dimer phase is $|d_k| = d$ and we have

$$f_{\text{eff}}^{(2)} = \frac{1}{2}\left(1 - \frac{1}{2d}\tanh\frac{d}{2t}\right)(\delta\theta)^2 \tag{C2}$$

which vanishes due to the gap equation Eq. (36).

The same mode is found for the flux phase. Again, it can be seen in one line in the absence of the constraint that this mode leaves the effective action invariant. In fact, putting $|d_k| = 2d\epsilon_k$ in Eq. (66) we have

$$f_{\text{eff}}^{(2)} = \frac{1}{N}\sum_k \left(4d^2\epsilon_k^2 - d\epsilon_k \tanh\frac{d\epsilon_k}{t}\right)(\delta\theta)^2 = 0 \tag{C3}$$

and the gap equation enforces the identity, because $\bar{\epsilon^2} = \int \frac{d^2k}{2\pi^2}\epsilon_k^2 = 1$.

In the case of the flux phase there are two more phase modes for which is $f_{\text{eff}}^{(2)} = 0$. These are the modes in which three phases of the order parameter are

changed arbitrarily, provided that the total phase in the elementary plaquette is kept constant to the value of π.

They are

$$\begin{aligned} d_1 &\to d\, e^{-i\theta_2}\,, \qquad d_2 \to d\, e^{-i\theta_3} \\ d_3 &\to d\, e^{i\theta_2}\,, \qquad d_4 \to d e^{i\theta_3} \\ d_{2,4} &\to d\,, \qquad\quad d_{1,3} \to d \end{aligned} \tag{C4}$$

which gives $|d_k| \to 2\, d\tilde{\epsilon}_k$, with $\tilde{\epsilon}_k = |\cos(k_x - \theta_2) - i\cos(k_y)|$ and $\tilde{\epsilon}_k = |\cos(k_x) - i\cos(k_y - \theta_3)|$ respectively.

Because the free energy is integrated over the full RBZ, it is obviously invariant with respect to these transformations of ϵ_k. This is easily seen analytically if the constraint is neglected. The first mode gives the change of d_k

$$\delta d_k = d_k \frac{\sin k_x}{\epsilon_k^2}(\cos k_x + i\cos k_y)\delta\theta_2 \tag{C5}$$

which implies

$$\begin{aligned} f_{\text{eff}}^{(2)} &= \frac{2}{N}\sum_k 4d^2 \sin^2 k_x (\delta\theta_2)^2 \left(1 + Q + q\Re e\left(1 + 2i\cos k_y \frac{(\cos k_x + i\cos k_y)}{\epsilon_k^2}\right)\right) \\ &= 4d^2(\delta\theta_2)^2 \frac{2}{N}\sum_k \sin^2 k_x \left(1 + Q + q - q\frac{2\cos^2 k_y}{\epsilon_k^2}\right)\,. \end{aligned} \tag{C6}$$

Using the identity

$$\frac{2}{N}\sum_k \frac{2\cos^2 k_x \cos^2 k_y}{\epsilon_k^2} q = \frac{2}{N}\sum_k Q(2\cos^2 k_x - 1) \tag{C7}$$

we find

$$f_{\text{eff}}^{(2)} = 4d^2(\delta\theta_2)^2 \frac{2}{N}\sum_k \left(\frac{1}{2} + (Q - q)\cos^2 k_x\right)\,. \tag{C8}$$

This is exactly equal to zero due to the gap equation (38) which can be rewritten as

$$\frac{2}{N}\sum_k (Q - q)\cos^2 k_x = -\frac{2}{N}\sum_k \frac{\epsilon_k^2}{2}\frac{1}{2|d_k|}\tanh\frac{d\epsilon_k}{t} = -\frac{1}{2} \tag{C9}$$

The proof for the third mode is obtained just by interchanging k_x and k_y.

When the constraint is included, the analytical expressions for the elements of the 8×8 curvature matrix M can be written down starting from the results of Appendix A and this can be diagonalized giving rise to analytical expressions for the eigenvalues λ_i which we omit for brevity.[36] The related quantities $t/4\lambda_i d^2$, defined in Sec. 6 as relative fluctuations of the order parameter for each eigenmode are plotted in Fig. 4 and discussed in the text.

References

1. See, e.g., the Proceedings of the International Conference on *Materials and Mechanism of Superconductivity, High-temperature Superconductors III* in *Physica* **C185-189** (1991).
2. P. W. Anderson, *Science* **235**, 1196 (1987).
3. F. C. Zhang, T. M. Rice, *Phys. Rev.* **B37**, 3759 (1988).
4. J. E. Hirsch and S. Tang, *Phys. Rev. Lett.* **62**, 591 (1989); D. A. Huse and V. Elser, *Phys. Rev. Lett.* **60**, 2531 (1988).
5. W. Stephan and P. Horsch, *Phys. Rev. Lett.* **66**, 2258 (1991).
6. G. Baskaran, Z. Zou and P. W. Anderson, *Solid State Comm.* **63**, 973 (1987); S. Liang, B. Douçot and P. W. Anderson, *Phys. Rev. Lett.* **61**, 365 (1988).
7. N. Nagaosa and P. A. Lee, *Phys. Rev. Lett.* **64**, 2450 (1990); *Phys. Rev.* **B1233** (1991).
8. C. Gros, *Ann. of Phys. (N.Y.)* **189**, 53 (1989).
9. E. Manousakis, *Rev. Mod. Phys.* **63**, 1 (1991).
10. M. Takahashi, *Phys. Rev.* **B40**, 2494 (1989).
11. S. Chakravarty, B. Halperin and D. R. Nelson, *Phys. Rev. Lett.* **60**, 1057 (1988); *Phys. Rev.* **B39**, 2344 (1989).
12. I. D. Reger and A. P. Young, *Phys. Rev.* **B37**, 5493 (1988); *Phys. Rev.* **B37**, 5978 (1988); Narayanan and Singh, *Phys. Rev.* **B42**, 10305 (1990).
13. Ding and Makivic, *Phys. Rev.* **B43**, 3562 (1991).
14. D. P. Arovas and A. Auerbach, *Phys. Rev.* **B38**, 316 (1988).
15. N. Read and S. Sachdev, *Phys. Rev.* **B42**, 4568 (1990).
16. G. Kotliar, *Phys. Rev.* **B37**, 3664 (1988).
17. I. Affleck and J. B. Marston, *Phys. Rev.* **B37**, 3774 (1988); J. B. Marston and I. Affleck, *Phys. Rev.* **B39**, 11538 (1989).
18. N. Read and S. Sachdev, *Nucl. Phys.* **B316**, 609 (1989).
19. N. Read and S. Sachdev, *Phys. Rev. Lett.* **66**, 1773 (1991).
20. I. Affleck, Z. Zou, T. Hsu, P. W. Anderson, *Phys. Rev.* **B38**, 745 (1988).
21. T. Dombre and G. Kotliar, *Phys. Rev.* **B39**, 855 (1989).
22. T. K. Lee and S. P. Feng, *Phys. Rev.* **B38**, 11809 (1988).
23. G. J. Chen, R. Joynt, F. C. Zang, and C. Gros, *Phys. Rev.* **B42**, 2662 (1990).
24. X. G. Wen, F. Wilczek and A. Zee, *Phys. Rev.* **B39**, 11413 (1989).
25. M. Di Stasio, *Phys. Rev.* **B46**, 9825 (1992).
26. I. J. R. Aitchison and N. E. Mavromatos, *Phys. Rev.* **B39**, 6544 (1989); *Mod. Phys. Lett.* **A4**, 521 (1989); *Phys. Rev. Lett.* **63**, 2684 (1989).
27. For a review see e.g., A. P. Balachandran, E. Ercolessi, G. Morandi, and A. M. Srivastava, *Int. J. Mod. Phys.* **B4**, 2057 (1990).
28. M. Gross, E. Sanchez Velasco and E. Siggia, *Phys. Rev.* **B39**, 2484 (1989); N. Trivedi and D. Ceperly, *Phys. Rev.* **B41**, 4552 (1990).
29. T. C. Hsu, *Phys. Rev.* **B41**, 11379 (1990).
30. M. U. Ubbens and P. A. Lee, *Phys. Rev.* **B46**, 8434 (1992).

31. M. Di Stasio, E. Ercolessi, G. Morandi, A. Tagliacozzo, and F. Ventriglia, *Phys. Rev.* **B45**, 1939 (1992).
32. M. Di Stasio, E. Ercolessi, G. Morandi, A. Tagliacozzo and F. Ventriglia (in preparation).
33. S. Elitzur, *Phys. Rev.* **D12**, 3978 (1975).
34. V. N. Popov, *Functional Integrals in Quantum Field Theory and Statistical Physics* (Reidel, 1983).
35. J. W. Negele and H. Orland, *Quantum Many-particle Systems* (Addison-Wesley, 1988).
36. M. Di Stasio, thesis, SISSA-ISAS (unpublished).

Paper IV

Effects of quantum fluctuations in the large U Hubbard model at half-filling

M.Di Stasio[(1)], E.Ercolessi[(2)], G.Morandi[(3)] and A.Tagliacozzo[(1,4)]

(1) S.I.S.S.A.-I.S.A.S.,v. Beirut2,I-34100 Miramare,Trieste,Italy

(2) Physics Dept.,Syracuse University, Syracuse,N.Y. 13244-1130,USA

(3) Dipartimento di Fisica, Universita' di Bologna,
INFM and INFN,v.Irnerio 46,I-40126 Bologna, Italy,

(4) Dipartimento di Scienze Fisiche,Universita' di Napoli
INFM,Mostra d'Oltremare Pad.19, I-80125 Napoli,Italy

Abstract

A quantitative estimate of the role of quantum fluctuations is given at zero and finite temperatures within the one loop approximation around the antiferromagnetic and the dimer saddle points. Our results include the constraint of single occupancy of sites also for thermodynamical quantities.

SISSA: 55/93/CM/MB

The limit of the large U Hubbard model at half filling is the spin 1/2 AFM (antiferromagnetic) Heisenberg model. In this work we report results of thermal and quantum fluctuations on an AFM background, and in dimer ordered phases starting from a fermionic representation of the hamiltonian[1]. Here the constraint of single site occupancy is a crucial ingredient.

While Quantum Monte Carlo approaches are restricted to relatively small systems [2], analytical methods to include the constraint originate from the Gutzwiller projection[3].

The constraint is often implemented within the saddle point approximation by a Lagrange multiplier (or slave bosons away from half-filling[4]). However it is hard to control its fluctuations both at zero and at finite temperatures. We have implemented it, at all temperatures, with a new method[5], by means of a local chemical potential.

The fluctuations are calculated within the one-loop approximation around the chosen saddle point for an effective action.

We find that, in the AFM case, because the magnetization acts as a local mean field, our method guarantees that the constraint is fully satisfied at the mean field level. In fact the mean square fluctuations of the occupancy $< n_i^2 - 1 >$ vanish at all temperatures when the constraint is evaluated by saddle point approximation. At zero temperature, the results of spin wave theory for the AFM ground state energy are recovered.

Zero point fluctuations in the staggered and columnar dimer phases were first discussed by Read and Sachdev[6] within the $SU(N)$ model. We show that their results in the $N = 2$ limit do not differ from a fermionized theory in the absence of the constraint. In this case the fluctuations are unrealistically large. This is because unconstrained fermionization of spin operators enlarges the Hilbert space enormously in the case of the dimer phases, due to the opportunity given to the bond field of building up couplings to states which change the site occupancy. This implies that the mean field free energy of the dimer phases is lowered too much, unless the constraint is enforced.

We show that addition of the constraint raises up the mean field energy and reduces the fluctuations. However our approximations in dealing with it depress the mean average thermal fluctuations of the occupancy number in the dimer phase only up to 10% of the unconstrained value[7]. Evidently this is not enough because the energies we obtain are still too low with respect to what is expected[8].

On the other hand while the saddle point effective action cannot be promoted to a free energy when the constraint is added, we show that by including fluctuations a physically meaningful temperature dependence is recovered. Fig.(2) reports our results for the specific heat versus temperature.

At half filling the spin 1/2 AFM Heisenberg hamiltonian can be rewritten,

in the restricted Hilbert space with single site occupancy, as:

$$H_o = -\frac{J}{2}\sum_{(i,j)}\sum_{\alpha\beta} c^{\dagger}_{i,\alpha}c_{j,\alpha}c^{\dagger}_{j,\beta}c_{i,\beta} - \frac{NJ}{2} \tag{1}$$

where the sum is over ordered n.n. pairs of sites in the lattice and N is the number of sites.

The partition function within the subspace of singly occupied states is:

$$\mathcal{Z} = Tr\left\{\prod_i n_i(2-n_i)e^{-\beta H_o}\right\} \tag{2}$$

($n_i = n_{i\uparrow} + n_{i\downarrow}; n_{i\sigma} = c^{\dagger}_{i\sigma}c_{i\sigma}, \sigma = \uparrow, \downarrow$). To implement the constraint we add a source term [5] to the Hamiltonian H_o and define: $H[z_i] = H_o - \beta^{-1}\sum_i z_i n_i$ (the z_i's are real variables). We call $\mathcal{Z}[z_i]$ the generating functional of averages of the occupation numbers. The partition function of eq.(2) can be recovered as:

$$\mathcal{Z} = \prod_i \frac{\partial}{\partial z_i}(2 - \frac{\partial}{\partial z_i})\mathcal{Z}[z_i]\Big|_{z=0}. \tag{3}$$

The advantage is that the evaluation of $\mathcal{Z}[z_i]$ only requires standard techniques because the trace is unrestricted and the source term commutes with H_o. The last feature is lost when one goes away from half filling.

The Hubbard Stratonovich decoupling of H_o requires an auxiliary field in imaginary time (denoted generically by $\mathcal{U}$ in the following), depending on

the saddle point chosen:

$$\sum_{\beta} c^{\dagger}_{j,\beta} c_{i,\beta} \rightarrow \mathcal{U}_{ij}(\tau) \quad \text{Flux and Dimer Phases}$$
$$c^{\dagger}_{i,\alpha} c_{i,\beta} \rightarrow \sum_{q} \gamma_q^{1/2}\, e^{iqR_i} \vec{\mathcal{M}}_q(\tau) \cdot \vec{\sigma}_{\alpha\beta} \quad \text{AFM Phase} \tag{4}$$

Here: $\mathcal{U}^{\star}_{ij}(\tau) = \mathcal{U}_{ji}(\tau)$, the components of $\vec{\sigma}$ are the Pauli matrices and $\gamma_q = \sum_{n.n.} e^{iqR} = \cos q_x + \cos q_y$.

The $\pi-$ Flux Phase[9] has been discussed by us elsewhere[7]. We have found that temperature destabilizes it more easily than the Dimer ones due to the lower lying excitations. However this phase, together with an AFM background was found to be a good starting point of Monte Carlo calculations for low doping[10]. The order parameter $\mathcal{U}_{ij}$ of the staggered and columnar dimer phases are sketched in Fig.(1). Integrating out the fermions one arrives at the intermediate result:

$$\mathcal{Z}[z_i] = \int \prod_{(i,j)} \mathcal{D}\mathcal{U}_{ij} \exp\left\{ -\pi \sum_{(i,j)} \sum_{m} \mid \mathcal{U}_{i,j}(\Omega_m) \mid^2 + Tr \ln[1 + G_o \tilde{\mathcal{U}}] \right\} \tag{5}$$

Where: $\Omega_m = \omega_{n'} - \omega_n$ is a Bose-like Matsubara frequency,

$$\left(\tilde{\mathcal{U}}^{AF}\right)^{\alpha\beta}_{ij}(\Omega_m) = \delta_{i,j} \left\{ z_i \delta_{m,0} \delta_{\alpha\beta} - 2 \sum_{q} e^{iqR_i} \left(\frac{-\pi\beta J \gamma_q}{N} \right)^{1/2} \vec{\mathcal{M}}_q(\Omega_m) \cdot \vec{\sigma}_{\alpha\beta} \right\}. \tag{6}$$

for the AFM phase, while:

$$\left(\tilde{\mathcal{U}}^d\right)_{ij}^{\alpha\beta}(\Omega_m) = \delta_{\alpha,\beta}\left\{z_i\delta_{m,0}\delta_{i,j} - \left(\frac{\pi\beta J}{2}\right)^{1/2}\mathcal{U}_{i,j}(\Omega_m)\right\} \tag{7}$$

for the dimer phases. Also, G_o is the Green function in the absence of $\mathcal{U}$ ($(G_o)_{ij}^{nn'} = (i\omega_n)^{-1}\delta_{i,j}\delta_{n,n'}$). Inserting this result into eq.(3), we obtain eventually:

$$\mathcal{Z} = \int \prod_{(i,j)} \mathcal{D}\mathcal{U}_{ij} e^{\left\{-\pi\sum_{(i,j)}\sum_m |\mathcal{U}_{ij}(\Omega_m)|^2 + Tr\ln[1+G_o\tilde{\mathcal{U}}] + \sum_i \ln 4B_i[\tilde{\mathcal{U}}]\right\}_{z_i=0}} \tag{8}$$

The contribution of the constraint is represented by the last term of eq.(8) with:

$$B_i[\mathcal{U}] = Tr\left\{[\chi G_o P_i]^2\right\} + 2Tr\left\{\chi G_o P_i\right\} - \left(Tr\left\{\chi G_o P_i\right\}\right)^2 \tag{9}$$

Here: $\chi = (1 - G_o\tilde{\mathcal{U}})^{-1}\Big|_{z_i=0}$ and we have introduced the projector P_i onto the $i-th$ site of the lattice, whose matrix elements are $(P_i)_{jk} = \delta_{jk}\delta_{ij}$.

We now expand the action to second order around the mean field saddle point: $\mathcal{F} = \mathcal{F}^0 + \mathcal{F}^{(2)}$. The second variation $\mathcal{F}^{(2)}$ is given by:

$$\beta\mathcal{F}^{(2)} = \pi\int_0^1 d\tau Tr\left\{(\delta\mathcal{U})^2\right\} - \frac{1}{2}Tr\left\{\chi\delta\mathcal{U}\chi\delta\mathcal{U}\right\} - \frac{1}{2}\sum_i\left(\frac{\delta^2 B_i}{B_i} - \frac{(\delta B_i)^2}{B_i^2}\right) \tag{10}$$

The eigenvalues $\lambda(m)$ of the quadratic form are listed in Table I, for the case without the constraint, together with their degeneracy and the component

admixture which is present in the eigenvector. They are functions of Ω_m and are expressed in terms the mean field order parameters M(magnetization) and d(dimer bond). The functions $E(m)$, $F(m)$ also appear, defined as:

$$F(m) = \frac{2M|\gamma_q|}{\sqrt{\Omega_m^2 t^2 + (4M)^2}} \;\; ; \;\; E(m) = \frac{4d^2}{\Omega_m^2 t^2 + 4d^2} \tag{11}$$

where: $t = 1/\beta J$. In the case of the AFM phase, the longitudinal mode decouples with respect to the transverse ones. The collective excitation spectrum can be obtained from the latter. In fact one has to continue analytically the product $\lambda_+^{AF} \cdot \lambda_-^{AF}$ for $i\Omega_m \rightarrow \beta\omega + i0$ and look for the zeros. The spin waves dispersion is recovered in this way, that is: $\omega_q = 2MJ\sqrt{(1-(\gamma_q/2)^2)}$.

In the case of the dimer phase, the second variation $\mathcal{F}^{(2)}$ can be expressed in terms of the complex variations: $u_l(\mathrm{Q})$ $(l = 1,4)$ for the staggered and $v_l(\mathrm{Q})$ for the columnar phase which are the Fourier transforms of $\mathcal{U}_l(i,\tau)$ and are taken to depend on site and time (with $\mathrm{Q} \equiv (\vec{Q}, \Omega_m)$). Here i spans just one of the sublattices , according to Fig.(1). In this case there is no $\vec{Q}$ dependence of the eigenmodes.

In Table I the zero modes are also indicated in the absence of the constraint. However, the features that we will discuss in the following are preserved by the inclusion of the constraint. The AFM phase has a vanishing eigenvalue for $\vec{q} = 0$ and $\vec{q} = (\pi, \pi) = \vec{\pi}$ due to the self-consistent equation for the magnetization M. For the dimer phases there is one zero mode which

corresponds to an overall change of the phase of the component of the order parameter $d =< \mathcal{U}_1 >$. In addition to this, the second variation of the action around the columnar phase saddle point is found to be flat versus two more amplitude deviations which add a small opposite weight on vertical bonds (mixing of the real or imaginary parts of v_3 and v_4), leading to a ladder pattern for the order parameter. Quartic terms in the deviations, that are here neglected, would guarantee that the columnar phase minimum is stable.

The free energy per particle of the AFM phase, in units of J, is:

$$f^{AF} = f_0^{AF} + \frac{2t}{N} \sum_q^{RBZ} \sum_{m\geq 0} \ln \lambda_+^{AF}(m)\lambda_-^{AF}(m) + \frac{t}{N} \sum_q^{RBZ} \sum_{m\geq 0} \ln \lambda_l^{AF}(m) \quad (12)$$

The zero temperature limit is the well known result of the first $(1/S)$ correction:

$$f^{AF}(t=0) = f_0^{AF} + \frac{2}{N} \sum_q^{RBZ} \left[\sqrt{(1-(\gamma_q/2)^2)} - 1\right] \quad (13)$$

where $f_0^{AF} = 2(M^2 - M) = -0.5$, $(M = 1/2)$ and the correction due to the fluctuations is -0.158 . Addition of the constraint does not change the zero temperature results but the thermodynamical quantities (see Fig.(2)).

In the case of the staggered dimer phase, the closed form for the free energy is:

$$f^s = f^0 - \frac{t}{2} \ln \mathcal{C}^s + \frac{t}{4} \sum_{m\geq 0} \ln \lambda_1^s(m) + \frac{3t}{2} \sum_{m\geq 0} \ln \lambda_2^s(m) + \frac{t}{4} \sum_{m>0} \ln \lambda_3^s(m) \quad (14)$$

where the constant $\mathcal{C}^s = 2d(2\pi/t)^{1/2}$ arises from the zero mode integration.

For the columnar phase we get:

$$f^c = f^0 - \frac{t}{2}\ln C^c + \frac{3t}{4}\sum_{m>0}\ln\lambda_1^c(m) + \frac{t}{2}\sum_{m\geq 0}\ln\lambda_2^c(m) + \frac{3t}{4}\sum_{m\geq 0}\ln\lambda_3^c(m) \quad (15)$$

where $C^c = 2^3 d(2\pi/t)^{3/2}$. The saddle point free energy f^0 is equal for the two phases. Its zero temperature value is: $f^0 = d^2 - d - 1/2 = -3/4$ $(d = 0.5)$ without the constraint. Imposing the constraint this value raises up to $f^0 = -0.375$, that is the energy per particle of a collection of spin singlets.

The contribution of quantum fluctuations to the free energy at zero temperature, in the absence of the constraint, is :

$$\begin{aligned} \Delta f^s(t=0) &= -\frac{d}{4} - 6\cdot\frac{d}{4}(1-1/\sqrt{2}) \quad \text{staggered} \\ \Delta f^c(t=0) &= -3\cdot\frac{d}{4} - 2\cdot\frac{d}{4}(1-1/\sqrt{2}) \quad \text{columnar} \end{aligned} \quad (16)$$

The factors $6, 3$ and 2 come from the degeneracies of the eigenvalues. This result, derived first by Read and Sachdev[6] within the $1/N$ expansion, implies that the degeneracy of the staggered and the columnar phases is broken by quantum fluctuations and that the last one is favoured energetically.

The eigenvalues mostly contributing to lower the energy for both periodicities are $\lambda_1^{s,c}(m \neq 0)$. The presence of two extra amplitude modes of this kind in the columnar phase implies that the energy is lower in this case.

We report here just the analytical zero temperature result with the con-

straint included:

$$\Delta f^s(t=0) = -2d(1-1/\sqrt{2}) \quad \text{staggered}$$
$$\Delta f^c(t=0) = -\frac{d}{2} - d(1-1/\sqrt{2}) \quad \text{columnar} \tag{17}$$

In the $t = 0$ limit the constraint affects only the contribution of the zero mode eigenvalues and lifts partially the degeneracy of $\lambda_1^c(m)$. Summing up, the constraint rises the zero temperature energies including one-loop corrections from the values of -1.095 (staggered phase) and -1.198 (columnar phase) up to -0.668 and -0.771 respectively. Although these values become comparable with the AFM result, within the same approximations, they are still lower than the AFM one, what is commonly accepted to be wrong[8]. We believe that fluctuations can be further depressed when the constraint is dealt with at an higher level of approximation.

At finite temperatures, we have calculated the constraint violation within mean field, which is found to be about 10% . Its action is evident in the temperature dependence of the specific heat, as can be seen from Fig.2 (a,b). Spin waves dominate the specific heat of the AFM phase, which remains therefore quadratic in temperature close to $t = 0$, while the gapped spectrum of the dimer phase gives an exponential temperature dependence as seen in the inset of Fig.2(b). The zero modes, being dispersionless in the dimer phases, do not change the gapped nature of the excitation spectrum.

The figures show that our way of including the constraint up to one loop corrections gives consistent finite temperature results.

References

[1] D.P.Arovas and A.Auerbach, Phys.Rev. B **38**,316 (1988)

[2] E.Y.Loh, J.E Gubernatis, in " Electron phase transitions" ed. by W.Hanke and Y.V. Kopaeve (North Holland , NY, 1990)

[3] C.Gros Ann.Phys. (NY) **189**,53(1989)

[4] G.Kotliar, A.E.Ruckenstein Phys.Rev.Lett.**57**,1362 (1986)

[5] M.Di Stasio, E.Ercolessi, G.Morandi, A.Tagliacozzo and F.Ventriglia, Phys.Rev. B **45**,1939 (1992)

[6] N.Read and S.Sachdev, Nucl.Phys.B **316**,609 (1989)

[7] M.Di Stasio, E.Ercolessi, G.Morandi, A.Tagliacozzo and F.Ventriglia, Int. J. Mod. Phys. B **7**,3281 (1993)

[8] E.Manousakis, Rev.Mod.Phys. **63**,1 (1991)

[9] I.Affleck and J.B.Marston, Phys.Rev.B **37**,3774 (1988), J.B.Marston and I.Affleck, Phys.Rev.B **39**,11538 (1989)

[10] T.C.Hsu, Phys.Rev.B **41**, 11379 (1990)

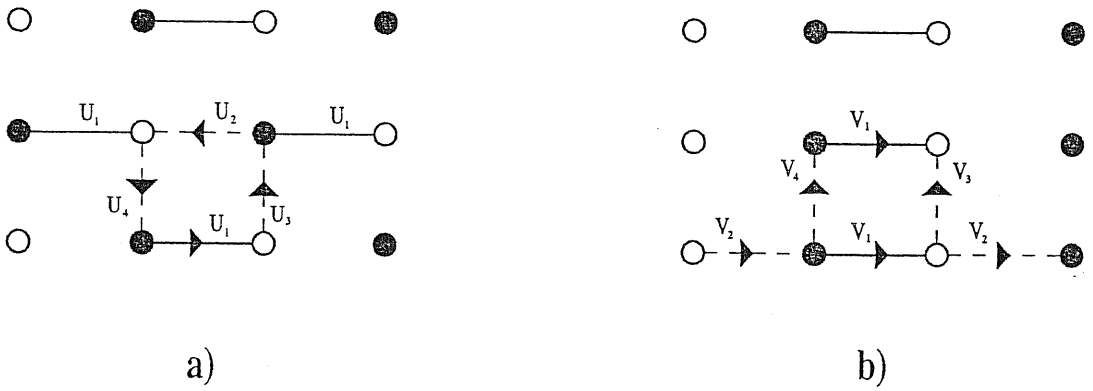

figure 1 Pictorial representation of the link order parameter U in terms of a) U_1, U_2, U_3, U_4 for the staggered dimer phase (periodicity is along the diagonals) and b) V_1, V_2, V_3, V_4 for the columnar dimer phase (periodicity is doubled on the x axes). Reversing the arrows implies complex conjugation

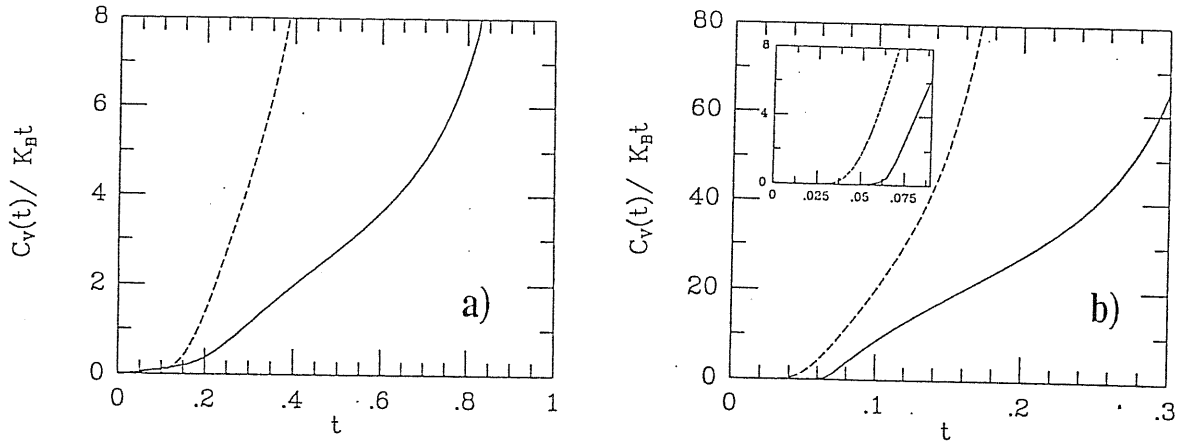

figure 2 Temperature dependence of the specific heat $c(T)$ for the AFM phase (a) and the staggered dimer phase (b). Full curves include the constraint while the broken ones do not.

	λ ($m \neq 0$)	$\lambda(m=0)$		deg.	mixture
ANTIFERROMAGNETIC PHASE	$\lambda_+^{AF} = 1 - F(m)$	$1 - \frac{\gamma(\vec{q}) \tanh M\, t}{4M}$	'zero modes $\vec{q}$=0,$\vec{\pi}$'	2	$m_x(\vec{q}), m_y^\star(\vec{q}+\vec{\pi})$
	$\lambda_l^{AF} = 1$	$1 + \frac{\gamma(\vec{q})}{2t \cosh^2 M/t}$		2	$m_x(\vec{q})$
	$\lambda_-^{AF} = 1 + F(m)$	$1 + \frac{\gamma(\vec{q}) \tanh M/t}{4M}$		2	$m_x^\star(\vec{q}+\vec{\pi}), m_y(\vec{q})$
STAGGERED DIMERS	$\lambda_1^S = 1 - E(m)$	$1 - \frac{1}{2d} \tanh \frac{d}{2t} = 0$	'zero mode'	1	$u_1(\vec{Q}), u_1(-\vec{Q})$
	$\lambda_2^S = 1 - \frac{E(m)}{2}$	$1 - \frac{1}{2}\left(\frac{1}{2d} \tanh \frac{d}{2t} + \frac{1}{4t \cosh^2 d/2t}\right)$		6	$u_i(\vec{Q})$ i = 2,3,4
	$\lambda_3^S = 1$	$1 - \frac{1}{4t \cosh^2 d/2t}$		1	$u_1(\vec{Q}), u_1(-\vec{Q})$
COLUMNAR DIMERS	$\lambda_1^C = 1 - E(m)$	$1 - \frac{1}{2d} \tanh \frac{d}{2t} = 0$	'zero mode'	1	$v_1(\vec{Q}), v_1(-\vec{Q})$
			'flat second variation'	2	v_3^R, v_4^R v_3^I, v_4^I
	$\lambda_2^C = 1 - \frac{E(m)}{2}$	$1 - \frac{1}{2}\left(\frac{1}{2d} \tanh \frac{d}{2t} + \frac{1}{4t \cosh^2 d/2t}\right)$		2	$v_2(\vec{Q})$
	$\lambda_3^C = 1$	$1 - \frac{1}{4t \cosh^2 d/2t}$		3	$v_1(\vec{Q}), v_1(-\vec{Q})$ v_3^R, v_4^R v_3^I, v_4^I

Table I Eigenvalues of the second variation of the effective action, as functions of the Matsubara frequencies Ω_m, for the dimer and antiferromagnetic phases together with their degeneracy and the corresponding admixture of the fluctuating fields. The constraint is not included. Modes that vanish for $\Omega = 0$ are explicitly indicated. All the quantities are defined in the text.

Paper V

Finite temperature results from constrained fermionization in the 2-D spin 1/2 Heisenberg antiferromagnet. I: the Néel phase

M.Di Stasio[(1)], E.Ercolessi[(2)], G.Morandi[(3)]
and A.Tagliacozzo[(1,4)]

(1) S.I.S.S.A.-I.S.A.S.,v. Beirut2,I-34100 Miramare,Trieste,Italy

(2) Physics Dept.,Syracuse University, Syracuse,N.Y. 13244-1130,USA

(3) Dipartimento di Fisica, Universita' di Bologna,
INFM and INFN,v.Irnerio 46,I-40126 Bologna, Italy,

(4) Dipartimento di Scienze Fisiche,Universita' di Napoli
INFM,Mostra d'Oltremare Pad.19, I-80125 Napoli,Italy

Abstract

The antiferromagnetic saddle point is studied up to one-loop corrections, including, within the same approximation, the constraint of single site occupancy in the fermionization procedure, at all temperatures. The resulting spin wave spectrum and zero point fluctuations are the same as those of the spin wave theory. The effect of the constraint on the temperature dependence of the specific heat is discussed.

SISSA: 134/93/CM/MB
SYRACUSE: SU-4240-541

1 Introduction

General consensus has been reached on the statement that the ground state of the spin 1/2 antiferromagnetic (AFM) Heisenberg model on a two dimensional square lattice is the Néel state[1], [2], [3], [4].

Various techniques led to the analytical results which confirm the previous numerical work, e.g. large spin expansion and Schwinger boson representation[5], [6].

Fermionization of the spin operators also has been applied mostly within the saddle point approximation. However emphasis is laid on the non magnetic saddle points rather than on the antiferromagnetic one[7]. It is also not evident how fermionization can give the spin-wave results to the same level of approximation.

On the other hand fermionization can be a useful tool to discuss frustrated antiferromagnetic (FAFM) models as well as doped antiferromagnets (AFM). The latter are often described by means of the $t-J$ hamiltonian [8] which is the limiting case of the Hubbard hamiltonian in the strongly correlated regime below half-filling.

The physics of FAFM models is exciting in view of the search for the so called spin liquid state. However numerical results are not conclusive[9], [10].

On the other hand models including hole doping in the Heisenberg quan-

tum antiferromagnet are currently extensively studied because of their relevance to the high T_c cuprate superconductors. A small amount of doping destroys the Néel ordering and phases characterized by singlet pair bonds on the lattice have been considered as competing with the antiferromagnetically ordered phase[11].

The representation of spin operators by means of fermion annihilation and creation operators requires that the Hilbert space of states, on which the latter act, includes the singly occupied ones only.

The constraint of no double site-occupancy is also needed when the limit of the Hubbard model for large U is considered, which leads to the $t-J$ model.

This work is aimed to discuss the thermal properties of the magnetic and non magnetic phases in the $S = 1/2$ AFM Heisenberg model on the same footing at all temperatures, within the fermion representation. The essential feature of our calculation is the addition of the constraint of single site-occupancy by means of a new method[12]. Our analysis concerns mostly the effect of the constraint on the fluctuations around the saddle point. The fluctuations are considered at the one-loop approximation level. By means of our fermionization scheme we were also able to discuss some features of the $S = 1/2$ FAFM Heisenberg model which we report elsewhere.

The present work consists of two parts.

In part I the AFM saddle point is chosen. The main result of our method is that,at the mean field level, the constraint is fully implemented. In fact the average occupancy is one while its mean square fluctuations vanish at all temperatures. As a consequence the fermionization procedure is exact at this level of approximation and the mean field results coincide with those of other techniques which deal directly with spin Hamiltonians.

We evaluate also the contribution of the fluctuations at zero and finite temperature and show the role of the constraint in the one-loop correction. This is governed by the usual spin wave excitation spectrum and we show that one-loop corrections to the saddle point in a path integral description is equivalent to the linear spin wave theory. At finite temperature, due to the presence of the constraint, there is a marked reduction of the specific heat, because traces are taken on a restricted Hilbert space.

In part II of this work we deal with the (non magnetic) dimer phases (staggered and columnar dimer phase[15]) using the same method. Quantum fluctuations around the dimer saddle point contribute substantially to lowering their energies. However, it is widely accepted that a fully constrained calculation would give a final energy for the dimer phases, which is higher than the AFM one. Unfortunately, our approximations in implementing the constraint are only partly satisfactory in reducing the weight of quantum fluctuations. As a consequence we are unable to produce such a result.

In our method the average site occupancy is one for all temperatures, but unlike the AFM phase, its mean square fluctuations are not completely suppressed at the mean field level, from $T = 0$ to the transition temperature. Still they are within less than 10% of their unconstrained value [14].

By inclusion of the one loop contribution, it is possible to define a free energy for the constrained problem, as we will show, which has the correct thermodynamical behavior, both in the case of the AFM saddle point and of the dimer phases.

In section 2 of the present paper we briefly review the fermionization procedure and the AFM mean field results. Appendix 1 includes the evaluation of the mean square fluctuation of the occupation number, which vanishes at all temperatures at the mean field level.

In section 3 we show how it is possible to recover the spin wave spectrum from the one-loop corrections and we obtain an expression for the free energy which includes gaussian fluctuations. The temperature dependence of the specific heat is also discussed.

Finally, we briefly comment on our results in the last section.

2 Antiferromagnetic decoupling

In this section we adopt the fermion representation on the spin 1/2 AFM Heisenberg model, described by the hamiltonian:

$$H_o = J \sum_{(i,j)} \vec{S}_i \cdot \vec{S}_j \tag{1}$$

Here the sum runs over ordered n.n. pairs of sites on a square lattice. If one considers this hamiltonian as the limiting case of the large U Hubbard model at half filling, then J equals $4t^2/U$ (with t the hopping parameter). To obtain this limit the constraint of single site occupancy is required, as well as by the fermionization procedure itself.

Given the wave vector $\vec{q}$ in reciprocal space, the spin 1/2 operators are represented as:

$$\vec{S}(q) = \frac{1}{\sqrt{N}} \sum_i e^{-i\vec{q}\cdot\vec{R}_i} c^\dagger_{i\alpha} \vec{\sigma}_{\alpha\beta} c_{i\beta} \tag{2}$$

where $2\vec{\sigma}$ are the Pauli matrices. The partition function is:

$$\mathcal{Z} = Tr \left\{ \prod_i n_i(2 - n_i) e^{-\beta H_0} \right\} \tag{3}$$

($n_i = n_{i\uparrow} + n_{i\downarrow}; n_{i\sigma} = c^\dagger_{i\sigma} c_{i\sigma}, \sigma = \uparrow, \downarrow$) and the prefactor restricts the trace to states with single occupancy of sites.

We adopt the Hubbard-Stratonovich decoupling in terms of an auxiliary vector field which plays the role of the staggered magnetization:

$$e^{-\beta J\ \gamma_q \vec{S}(q)\cdot\vec{S}(-q)} =$$

$$= \int \mathcal{D}^2\vec{\mathcal{M}}(q,\tau) e^{-\int_0^1 d\tau\left\{\pi|\vec{\mathcal{M}}(q,\tau)|^2+\sqrt{-\pi\beta J\gamma_q}\left(\vec{\mathcal{M}}(q,\tau)\cdot\vec{S}(q,\tau)+h.c.\right)\right\}} \qquad (4)$$

where $\gamma_q = \cos k_x + \cos k_y$.

To implement the constraint we add a source term to the Hamiltonian H_o and define the generating functional:

$$\mathcal{Z}[z_i] = Tr\{\exp(-\beta H_o + \sum_i z_i n_i)\} \qquad (5)$$

(the z_i's are real variables). The original partition function is recovered as:

$$\mathcal{Z} = \prod_i \frac{\partial}{\partial z_i}(2 - \frac{\partial}{\partial z_i})\mathcal{Z}[z_i]\Big|_{z_i=0} . \qquad (6)$$

The advantage is that the evaluation of $\mathcal{Z}[z_i]$ requires only standard techniques because the trace is unrestricted and the source term commutes with H_o. Using eq.(4) the fermionic trace can be represented in terms of Grassmann fields ψ and $\psi^\star$ as:

$$\mathcal{Z}[z_i] = \int \prod_{q,m} \mathcal{D}^2\vec{\mathcal{M}}(q,\Omega_m) \prod_{i,\alpha} \mathcal{D}\psi^*_{i,\alpha}\mathcal{D}\psi_{i,\alpha}\ \ e^{-\pi\sum_{q,m}|\vec{\mathcal{M}}(q,\Omega_m)|^2}$$

$$\exp\left\{\sum_{i,\alpha,\beta}\sum_{n,n'} \psi^*_{i,\alpha}(\omega_n)\left[i\omega_n\delta_{n,n'}\delta_{\alpha,\beta} + \mathcal{A}^{nn'}_{\alpha\beta}(i,i)\right]\psi_{i,\beta}(\omega_{n'})\right\} \qquad (7)$$

Here ψ and $\psi^\star$ have been transformed to Fermi Matsubara frequencies $\omega_n = (2n+1)\pi$. The matrix $\mathcal{A}$ depends only on $\omega_{n'} - \omega_n = \Omega_m$ (Bose frequencies) and its matrix elements are:

$$\mathcal{A}^{nn'}_{\alpha\beta}(i,j) = \delta_{i,j}\left\{ z_i \delta_{n,n'}\delta_{\alpha\beta} - 2\sum_q e^{iqR_i}\left(\frac{-\pi\beta J\gamma_q}{N}\right)^{1/2} \vec{\mathcal{M}}_q(\Omega_m)\cdot\vec{\sigma}_{\alpha\beta}\right\} \quad (8)$$

The path integral over the Grassmann fields can now be performed, and we obtain:

$$\mathcal{Z}[z_i] = \mathcal{Z}_0 \int \prod_{q,m} \mathcal{D}^2\vec{\mathcal{M}}(q,\Omega_m) \exp\left\{-\pi\sum_{q,m} \mid \vec{\mathcal{M}}(q,\Omega_m)\mid^2 - S_{eff}[\mathcal{A}]\right\} \quad (9)$$

with

$$S_{eff}[\mathcal{A}] = -Tr\ln[1 + G_o\mathcal{A}] \quad (10)$$

and $\mathcal{Z}_0 = \exp\{Tr\ln G_o\}$. We have defined here $(G_o)^{n,n'}_{\alpha,\beta}(i,j) = (i\omega_n)^{-1}\delta_{i,j}\delta_{n,n'}\delta_{\alpha,\beta}$. Eq.(6) yields then the partition function. The resulting extra factors can be re-exponentiated to give:

$$\begin{aligned} \mathcal{Z} &= \int \prod_{q,m} \mathcal{D}^2\vec{\mathcal{M}}(q,m) \exp\{-\beta\mathcal{F}\} \\ \beta\mathcal{F} &= \pi\sum_{q,m} \mid \vec{\mathcal{M}}(q,m)\mid^2 + S_{eff}[\mathcal{A}] - \sum_i \ln 4B_i[\mathcal{A}] \end{aligned} \quad (11)$$

The contribution of the constraint is:

$$B_i[\mathcal{A}] = Tr\left\{\chi P_i \chi P_i\right\} + 2Tr\left\{\chi P_i\right\} - \left(Tr\left\{\chi P_i\right\}\right)^2 \tag{12}$$

Here we have defined the operator $\chi = (G_o^{-1} + \mathcal{A})^{-1}$ and the projector P_i, onto the $i-th$ site of the lattice, whose matrix elements in the Wannier representation are $(P_i)_{jk} = \delta_{j,k}\delta_{i,j}$.

To isolate the static saddle point corresponding to the AFM phase we make the choice $\vec{\mathcal{M}}(q,m) = \hat{z}\mathcal{M}^z(\vec{\pi},0)\delta_{m,0}\delta_{q,\vec{\pi}}$ where: $\vec{\pi} \equiv (\pi,\pi)$. At the saddle point we have:

$$(\chi)_{\alpha\beta}^{n,n'}(i) = \left(i\omega_n - \alpha(-1)^i 2M/t\right)^{-1}\delta_{n,n'}\delta_{\alpha,\beta} \tag{13}$$

and we have introduced the rescaled order parameter $M = \sqrt{\frac{\pi}{2N\beta J}}\mathcal{M}^z$ and the dimensionless temperature $t = 1/\beta J$.

The evaluation of the effective action of eq.(10) at the saddle point can be performed with the usual procedure of inserting a coupling constant g to multiply the matrix $\mathcal{A}$ and integrating over the derivative:

$$\frac{dS_{eff}}{dg} = -Tr\left\{\chi_g \mathcal{A}\right\} = -N\frac{2M}{t}\tanh g\frac{M}{t} \tag{14}$$

which leads to:

$$S_{eff} = -2N\ln\cosh M/t \tag{15}$$

The saddle point approximation to the free energy is:

$$f^0 = \mathcal{F}/NJ = 2M^2 - 2t \ln \cosh M/t - t \ln B \tag{16}$$

where the constraint B, which turns out to be site independent, reads:

$$B = 1 - \frac{1}{2 \cosh^2 M/t} \tag{17}$$

This implies that the final result becomes:

$$f^0 = 2M^2 - t \ln \cosh 2M/t + t \ln 2 \tag{18}$$

Minimization of this expression yields the mean field magnetization:

$$M = \frac{1}{2} \tanh \frac{2M}{t} \tag{19}$$

with critical temperature $t_c = 1$ and $f^0_{eff}(t = 0) = -1/2$. This is exactly what is found in the mean field approach to the $S = 1/2$ Heisenberg and/or Ising model, when traces are performed directly over spin states. In fact, as will be shown below (see Appendix 1), the constraint is satisfied exactly at all temperatures at the mean field level, because using eq.(9) we find $< n_i >= 1$ and $< n_i^2 >= 1$ at all temperatures. This implies that at the mean field level the fermionization procedure is exact due to the inclusion of the constraint, leading to results that are equivalent to those obtained directly from spin

hamiltonians.

It is worthwhile to mention that when the constraint is ignored the mean field critical temperature becomes: $t_c^0 = 0.5$ and the equation for the magnetization reads:

$$M = \frac{1}{2} \tanh \frac{M}{t} \tag{20}$$

this is not the right result, nor is $< n_i^2 >$ equal to one anymore. The temperature dependence of the magnetization according to eq.(19) (full curve) and to eq.(20) (broken curve) are depicted in fig.1.

3 One loop corrections

The total effective action from eq.(11), evaluated at the stationary point to give eq.(18), is a poor approximation to the free energy. By including the one loop corrections in the evaluation of the path integral, we take into account field configurations that allow for fluctuations of the order parameter around its mean field value, at the gaussian level.

We write:

$$\vec{\mathcal{M}}(\vec{q}, \Omega_m) = \mathcal{M}^z(\vec{\pi}, 0)\hat{z} + \delta\vec{\mathcal{M}}(\vec{q}, \Omega_m) \tag{21}$$

This changes $\mathcal{A}$ into $\mathcal{A}_o + \delta\mathcal{A}$ with:

$$\delta\mathcal{A}_{\alpha\beta}(i,\Omega_m) = -2\sum_q e^{iqR_i}\left(\frac{-\pi\gamma_q}{Nt}\right)^{1/2}\delta\vec{\mathcal{M}}(\mathbf{Q})\cdot\vec{\sigma}_{\alpha\beta} \tag{22}$$

Here we have introduced $(\mathbf{Q}) = (\vec{q},\Omega_m)$ and we will write $(\mathbf{Q}+\pi) = (\vec{q}+\vec{\pi},\Omega_m)$ for brevity. The effective action can be approximated as: $\mathcal{F} = \mathcal{F}^0 + \mathcal{F}^{(2)}$ with $S_{eff} = S^0_{eff} + S^{(2)}_{eff}$, where the superscript (0) denotes the mean field value and the superscript (2) the second variation.

Understanding χ as the one particle propagator evaluated at the saddle point ($\chi = (G_o^{-1} + \mathcal{A}_o)^{-1}$), we get:

$$S^{(2)}_{eff} = \frac{1}{2}Tr\{[\chi\delta\mathcal{A}]^2\}. \tag{23}$$

The second variation $\mathcal{F}^{(2)}$ is therefore:

$$\beta\mathcal{F}^{(2)} = \pi Tr\{\mid\delta\vec{\mathcal{M}}\mid^2\} + S^{(2)}_{eff} - \frac{1}{2}\sum_i\left[\frac{\delta^2B_i}{B_i} - \left(\frac{\delta B_i}{B_i}\right)^2\right] \tag{24}$$

where δB_i is given by:

$$\delta B_i = 2Tr\{\chi P_i\chi P_i\chi\delta\mathcal{A}\} \tag{25}$$

and

$$\delta^2 B_i = 4Tr\{\chi P_i\chi P_i\chi\delta\mathcal{A}\chi\delta\mathcal{A}\} + 2Tr\{\chi P_i\chi\delta\mathcal{A}\chi P_i\chi\delta\mathcal{A}\} \tag{26}$$

Writing down the trace for $S^{(2)}_{eff}$ of eq.(23) explicitly we have:

$$S^{(2)}_{eff} = \frac{1}{2}\sum_{i,\alpha,\beta}\sum_{m}\Theta^{11}_{\alpha\beta}(i,m)$$
$$< i\alpha \mid \delta\mathcal{A}(m) \mid i\beta >< i\beta \mid \delta\mathcal{A}(-m) \mid i\alpha > \qquad (27)$$

which is sketched in fig.2(a). Here:

$$\Theta^{11}_{\alpha\beta}(i,m) = \sum_{n} < i\alpha \mid \chi(\omega_n) \mid i\alpha >< i\beta \mid \chi(\omega_n - \Omega_m) \mid i\beta > \qquad (28)$$

because χ is diagonal in the basis chosen. The function $\Theta^{11}_{\alpha\beta}$ is a particular case of the following function:

$$\Theta^{lr}_{\alpha\beta}(i,m) = \sum_{n} \frac{1}{[i\omega_n - \alpha(-1)^i 2M/t]^l} \frac{1}{[i\omega_n - i\Omega_m - \beta(-1)^i 2M/t]^r} \qquad (29)$$

We define also (with $\bar{\alpha} \neq \alpha$):

$$\Theta^{lr}_{z}(m) = \sum_{\alpha} \Theta^{lr}_{\alpha\alpha}(i,m)$$
$$\Theta^{lr}_{+}(m) = \sum_{\alpha} \Theta^{lr}_{\alpha\bar{\alpha}}(i,m)$$
$$\Theta^{lr}_{-}(m) = (-1)^i \sum_{\alpha} \alpha\Theta^{lr}_{\alpha\bar{\alpha}}(i,m) \qquad (30)$$

to be used in what follows. Explicitly, when $l = r = 1$, we get:

$$\Theta^{11}_{\alpha\alpha}(i,m) = -\delta_{m,0}\frac{1}{4\cosh^2 M/t} \qquad (31)$$

$$\Theta^{11}_{\bar{\alpha}\alpha}(i,m) = \frac{\tanh M/t}{i(-1)^i\alpha\Omega_m - 4M/t} \qquad (32)$$

In particular, due to eq.(31) the term of eq.(27) with $\alpha = \beta$, describing fluctuations in the longitudinal direction, contributes only to the thermal fluctuations (that is $\Omega_m = 0$ only), giving:

$$S_L^{(2)} = \pi\beta J\Theta_z^{11}(0) \sum_q^{(RBZ)} \frac{|\gamma_q|}{2} [-\delta\mathcal{M}^z(\vec{q},0)\delta\mathcal{M}^z(-\vec{q},0)+ \\ +\delta\mathcal{M}^z(\vec{q}+\vec{\pi},0)\delta\mathcal{M}^z(-\vec{q}-\vec{\pi},0)] \tag{33}$$

The terms with $\alpha \neq \beta$ in eq.(27), give:

$$S_T^{(2)} = \pi\beta J \sum_m \sum_q^{(RBZ)} \frac{|\gamma_q|}{2} \Big\{ \Big(- \mid \delta\mathcal{M}^x(\mathbf{Q}) \mid^2 + \mid \delta\mathcal{M}^x(\mathbf{Q}+\pi) \mid^2 + \\ - \mid \delta\mathcal{M}^y(\mathbf{Q}) \mid^2 + \mid \delta\mathcal{M}^y(\mathbf{Q}+\pi) \mid^2 \Big) \cdot \Theta_+^{11} + \\ -2i\Im m \left[\delta\mathcal{M}^x(\mathbf{Q})\delta\mathcal{M}^y(-\mathbf{Q}-\pi) - \delta\mathcal{M}^y(\mathbf{Q})\delta\mathcal{M}^x(-\mathbf{Q}-\pi)\right] \cdot \Theta_-^{11}(m) \Big\} \tag{34}$$

In the absence of the constraint eqn.s (33,34) represent the full second variation of the free energy.

Let us ignore for the moment the contribution of the constraint to eq.(24). The second variation of the total action $\mathcal{F}^{(2)}$ relative to the longitudinal fluctuation modes described by eq.(33) is readily diagonalized giving the eigenvalue:

$$\lambda_z = \pi \left(1 - \Theta_z^{11}(0)\frac{\gamma_q}{2t}\right) \tag{35}$$

The quadratic form for $\mathcal{F}^{(2)}$ relative to the transverse fluctuations consists of four equal 2×2 blocks for each $\vec{q}$ vector, mixing the real and imaginary

components of $\delta\mathcal{M}^x$ and $\delta\mathcal{M}^y$ at $\vec{q}$ and $\vec{q}+\vec{\pi}$ in pairs. We denote them symbolically by: $(Re\delta\mathcal{M}^x(q), Im\delta\mathcal{M}^y(q+\pi))$, $(Im\delta\mathcal{M}^x(q), Re\delta\mathcal{M}^y(q+\pi))$,

$(Re\delta\mathcal{M}^y(q), Im\delta\mathcal{M}^x(q+\pi))$, $(Im\delta\mathcal{M}^y(q), Re\delta\mathcal{M}^x(q+\pi))$. The matrix corresponding to each block is given by:

$$\begin{pmatrix} \pi-\theta(m) & \eta(m) \\ \eta(m) & \pi+\theta(m) \end{pmatrix} \tag{36}$$

where:

$$\begin{aligned} \theta(m) &= \pi\frac{|\gamma_q|}{2t}\Theta_+^{11}(m) \\ \eta(m) &= -\pi i\frac{|\gamma_q|}{2t}\Theta_-^{11}(m) \end{aligned} \tag{37}$$

We denote the eigenvalues of the matrix (36) by λ_+ and λ_-. Using eq.(20), they are given by:

$$\lambda_\pm = \pi\left[1 \pm \frac{2M|\gamma_q|}{\sqrt{\Omega_m^2 t^2 + (4M)^2}}\right] \tag{38}$$

It follows that the eigenmodes vanish at $\Omega_m = 0$ when $\vec{q} = 0$ and $\vec{q} = \vec{\pi}$. They include the Goldstone modes (spin waves) corresponding to the spontaneously broken symmetry of the AFM state.

Let us now consider the contribution due to the constraint. Going back to eq.(24), $\delta^2 B_i$, as given by eq.(26) can be expressed in terms of the functions:

$$\Theta_\nu^4(m) = 2\Theta_\nu^{31}(m) + \Theta_\nu^{22}(m) \qquad \nu = z, +, - \tag{39}$$

according to the definitions of eq.s (29) and (30) and is represented diagrammatically in fig.2(b). The wiggly line is the fluctuation $\delta\vec{\mathcal{M}}(\mathbf{Q})$, the full lines are χ functions while the broken line represents the effect of the projector viewed as an external perturbation. Similarly, eq.(25) for (δB_i) is depicted in fig.2(c). Note that $\Theta^4_z(m)$ of eq.(39) vanishes identically when is $m \neq 0$.

The symmetry of the modes is not affected by the constraint. The longitudinal fluctuating mode described by eq.s (33) and (35) requires the substitution:

$$\Theta^{11}_z(0) \to \Theta^{11}_z(0) - \frac{2}{B}\Theta^4_z(0) + \frac{4}{B^2}\left(\Theta^{30}_-(0)\right)^2 \tag{40}$$

where, written explicitly, is :

$$\Theta^{30}_-(0) = \tanh M/t \frac{1}{2\cosh^2 M/t}$$
$$\Theta^4_z(0) = \frac{1}{8\cosh^4 M/t}\left[1 - \frac{1}{2}\cosh 2M/t\right] \tag{41}$$

At the one-loop level of approximation, no frequency dependent longitudinal fluctuation is induced by the constraint. In fact terms with $\alpha = \beta$ and $m \neq 0$ are absent in the second variation of eq.(24).

The transverse part of the second variation of the action given by eq.(34), requires the substitutions:

$$\Theta^{11}_\pm(m) \to \Theta^{11}_\pm(m) - \frac{2}{B}\Theta^4_\pm(m) \quad . \tag{42}$$

Here is:

$$\Theta^4_+(m) = -\frac{\tanh M/t}{2\cosh^2 M/t}\frac{4M/t}{(i\Omega_m)^2-(4M/t)^2}$$
$$\Theta^4_-(m) = -\frac{\tanh M/t}{2\cosh^2 M/t}\frac{i\Omega_m}{(i\Omega_m)^2-(4M/t)^2} \qquad (43)$$

Diagonalization of the quadratic form for $\mathcal{F}^{(2)}$ can be performed along the same lines as before with the obvious generalization of the functions θ and η of eq.(37) that follows from eq.(42).

It is remarkable that, making use of the explicit expressions of eqs. (43) and of the order parameter equation (19) in presence of the constraint, we get again eq.(38) for the eigenmodes.

These eigenvalues determine the collective excitation spectrum. Indeed, by analytically continuing the product $\lambda_+ \cdot \lambda_-$ for $i\Omega_m \to \beta\omega + i0$, the zeroes yield the usual spin waves dispersion, that is $\omega_q = 2MJ\sqrt{(1-(\gamma_q/2)^2)}$.

It follows that the spin wave spectrum is unchanged with respect to the unconstrained case, except for a different temperature dependence of the order parameter M (see fig.1).

The contribution of the fluctuations to the ground state energy can be derived from the full expression of the free energy per particle (in units of J), including the one loop correction:

$$f = f^0 + \frac{2t}{N}\sum_q^{RBZ}\sum_{m\geq 0}\ln\lambda_+(m)\lambda_-(m) + \frac{t}{N}\sum_q^{RBZ}\ln\lambda_z \qquad (44)$$

where f^0 is given by eq.(18). The last term doesn't contribute to the limiting expression for zero temperature, which reads :

$$f(t=0) = f^0(0) + \frac{2}{N}\sum_{q}^{RBZ}\left[\sqrt{(1-(\gamma_q/2)^2)}-1\right] \tag{45}$$

(with $(M(0)=1/2)$ and $f^0(0) = 2(M^2(0)-M(0)) = -1/2$) The correction due to the zero point fluctuations is: $\Delta f = -0.158$. This is the well known result of the first $(1/S)$ correction of the spin wave theory.

On the contrary, the presence of the constraint affects the finite temperature dependence of the free energy in two ways: by changing the temperature dependence of M and by changing λ_z.

The temperature dependence of the specific heat is plotted in fig.3, which is obtained by numerical derivation of eq.(44). There we compare our result with the one in which the constraint is not accounted for. In the latter case the curve rises much faster with temperature. At low temperatures, the specific heat goes as $C_V = at^\alpha$ with $\alpha = 2$, as expected, and $a = 0.174K_B$ both in presence and in absence of the constraint.

4 Concluding remarks

We have studied the AFM phase of the spin 1/2 Heisenberg model at all temperatures within the saddle point approximation by fermionization of the spin operators.

The constraint is already fully saturated at the mean field level, because we obtain $< n_i >= 1$ and $< n_i^2 >= 1$, where n_i is the occupation number of the i-th site in the lattice. This procedure gives rise to the correct mean field critical temperature and magnetization.

One-loop corrections to the saddle point approximation lead to the spin wave spectrum and to zero point fluctuations that are identical to those obtained within linear spin wave theory. This was also found within a response function formalism but no care of the constraint was taken there[17]. We have shown that consistent use of the equation for the magnetization (eq.(19)) and of the quadratic effective free energy of eq.(24) gives the same result for these quantities as the corresponding ones when the constraint is disregarded. However, the thermodynamics is heavily changed to the same level of approximation, when the constraint is accounted for. This is because, when the partition function is evaluated including the quadratic fluctuations around the static saddle point, the contribution due to the constraint acts as an entropy term, to account for the restriction of the allowed configurations.

One of the outcomes of our calculation is that, although no variational principle is valid for the saddle point action in presence of the constraint, by including one-loop corrections we obtain a free energy which has the correct temperature behavior. Our free energy accounts for the depression of the longitudinal thermal fluctuations due to the constraint. The power

law temperature dependence of the specific heat for t approaching zero is conserved, as expected from the spin wave spectrum.

5 Appendix 1

Mean square occupation number $< n_i^2 >$.

A crucial check of our method to include the single site-occupancy constraint is the evaluation of the mean occupation number $< n_i >$ and of its mean square fluctuation $< n_i^2 >$. It can be easily proved that $< n_i >= 1$ at all temperatures[14], but we cannot in general prove the corresponding relation: $< n_i^2 >= 1$. Here we show that, at the saddle point, when the constraint is taken into account, the mean square occupation number $< n_i^2 >_{s.p.}$ is exactly equal to one.

According to eq.(11) we write symbolically this quantity as:

$$< n_i^2 >_{s.p.}= \left\langle \frac{\partial^2}{\partial z_i^2} e^{-\Sigma(z)} \Big|_{z=0} \right\rangle_{s.p.} \tag{46}$$

where

$$\Sigma(z) = S_{eff}(z) - \sum_i \ln 4B_i(z). \tag{47}$$

S_{eff} is defined in eq.(10), while the full expression for the constraint is

$$B_i(z_i) = \frac{\partial^2 S_{eff}}{\partial z_i^2} - 2\frac{\partial S_{eff}}{\partial z_i} - \left(\frac{\partial S_{eff}}{\partial z_i}\right)^2 \tag{48}$$

which becomes eq.(12) when z_i is set equal to zero, due to the fact that $\frac{\partial S_{eff}}{\partial z_i}\Big|_{z=0} = -Tr\{\chi P_i\} = -1$ and that $\frac{\partial^2 S_{eff}}{\partial z_i^2}\Big|_{z=0} = Tr\{\chi P_i \chi P_i\}$.

In the absence of the constraint we have:

$$< n_i^2 >_{s.p.}^0 = 1 - \langle \frac{\partial^2 S_{eff}}{\partial z_i^2}\Big|_{z=0} \rangle = 1 + \frac{1}{\cosh^2 M/t} \tag{49}$$

$< n_i^2 >$ is one only at zero temperature because the saddle point satisfies the constraint and no classical (static) fluctuations survive. At the critical temperature, when M is zero, it reaches the value 3/2 due to the equiprobability of occupations.

Including the constraint we have: $\langle \frac{\partial^3 S_{eff}}{\partial z_i^2 \partial z_j}\Big|_{z=0} \rangle = 0$ and consequently $\langle \frac{\partial B}{\partial z_i}\Big|_{z=0} \rangle = 0$, so that:

$$< n_i^2 >_{s.p.} = 1 - \left\langle \left(\frac{\partial^2 S_{eff}}{\partial z_i^2} - \sum_j \frac{1}{B_j} \frac{\partial^2 B_j}{\partial z_i^2} \right) \Big|_{z=0} \right\rangle_{s.p.} = 1 \ . \tag{50}$$

The last identity follows from the saddle point evaluation evaluation of:

$$\frac{\partial^2 B_j}{\partial z_i^2} = \frac{\partial^4 S_{eff}}{\partial z_i^2 \partial z_j^2} - 2 \left(\frac{\partial^2 S_{eff}}{\partial z_i \partial z_j} \right)^2 \ . \tag{51}$$

In fact:

$$\left\langle \frac{\partial^4 S_{eff}}{\partial z_i^2 \partial z_j^2}\Big|_{z=0} \right\rangle = \delta_{ij} \left\langle \frac{\partial^4 S_{eff}}{\partial z_i^4}\Big|_{z=0} \right\rangle = 4\Theta_z^4(0) \ , \tag{52}$$

$$\left\langle \frac{\partial^2 S_{eff}}{\partial z_i \partial z_j}\Big|_{z=0} \right\rangle = \left\langle \delta_{ij} \frac{\partial^2 S_{eff}}{\partial z_i^2}\Big|_{z=0} \right\rangle = B - 1 \ . \tag{53}$$

and eq.(41) has been used together with the explicit expression of B (eq.(17)).

References

[1] J.D.Reger,A.P.Young Phys.Rev B**37**,5978(1988)

[2] N.Trivedi,D.Ceperly Phys.Rev B**40**,2737(1989)

[3] S.D.Liang Phys.Rev B**42**,6555(1990)

[4] B.Bernu, C.Lhuillier, L.Pierre Phys.Rev.Lett. **69**,2590 (1992)

[5] A.Auerbach,D.P.Arovas, J.Appl.Phys.**67**,5734(1990)

[6] E.Manousakis Rev.Mod.Phys. **63**,1 (1991)

[7] I.Affleck, J.B.Marston Phys.Rev.B **37**, 3774 (1988); J.B.Marston, I.Affleck Phys.Rev.B **39**, 11538 (1989)

[8] F.C.Zhang, T.M.Rice Phys.Rev.B **37**,3759 (1988)

[9] Q.F.Zhong,S.Sorella Europhys. Lett. **21**,629(1993)

[10] E.Dagotto,A.Moreo Phys.Rev.Lett. **63**,2148(1989)

[11] S.Liang B.Doucot P.W.Anderson Phys.Rev.Lett. **61**, 2585 (1988)

[12] M.Di Stasio, E.Ercolessi, G.Morandi, A.Tagliacozzo, F.Ventriglia Phys.Rev.B **45**, 1939(1992)

[13] P.W.Anderson Phys.Rev. **86**, 694 (1952)

[14] M.Di Stasio, E.Ercolessi, G.Morandi, A.Tagliacozzo, F.Ventriglia Int.Jou.Mod.Phys.B (1993) (in press)

[15] N.Read, S.Sachdev Nucl.Phys.B **316**, 609 (1989)

[16] M.Di Stasio, E.Ercolessi, G.Morandi, A.Tagliacozzo Euro.Phys.Lett.(submitted)

[17] A.Singh, Z.Tesanovic Phys.Rev.B **41**,614 (1990)

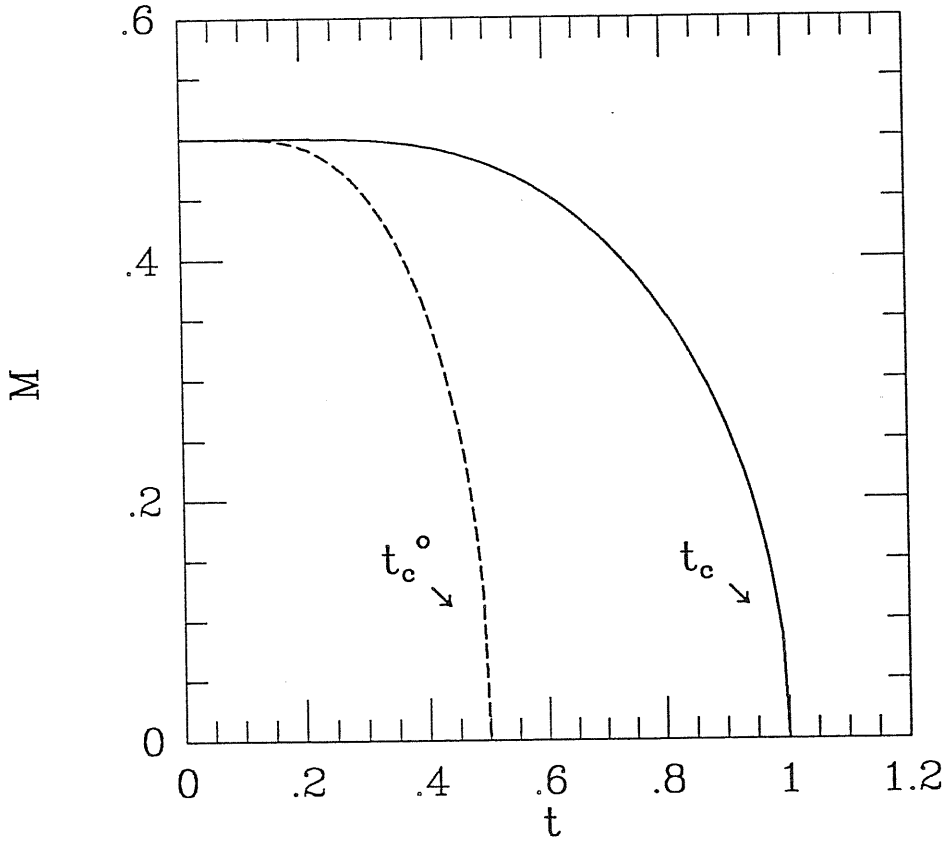

Figure 1

Temperature dependence of the magnetization. The full curve is in the presence of the constraint. The broken one is for the unconstrained case. The mean field critical temperatures are indicated by the arrows.

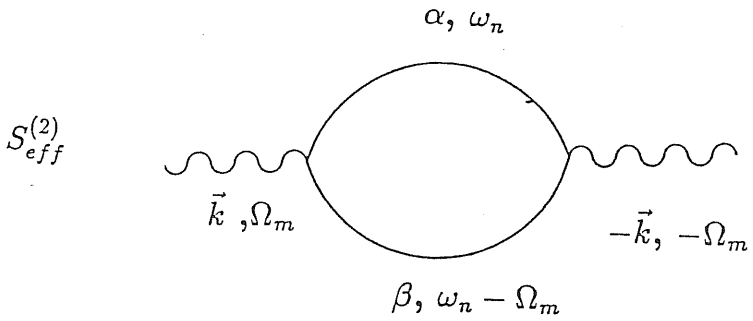

(a)

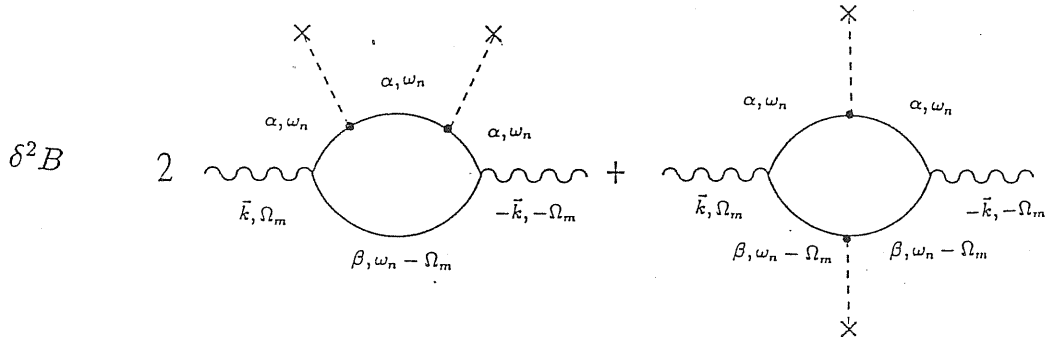

(b)

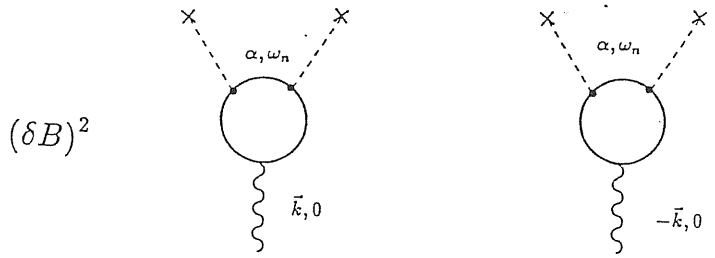

(c)

Figure 2

One-loop corrections. Diagramatic representation of: (a) $S^{(2)}_{eff}$; (b)second variation of the constraint contribution, $\delta^2 B$; (c) first variation,δB. The symbols are explained in the text.

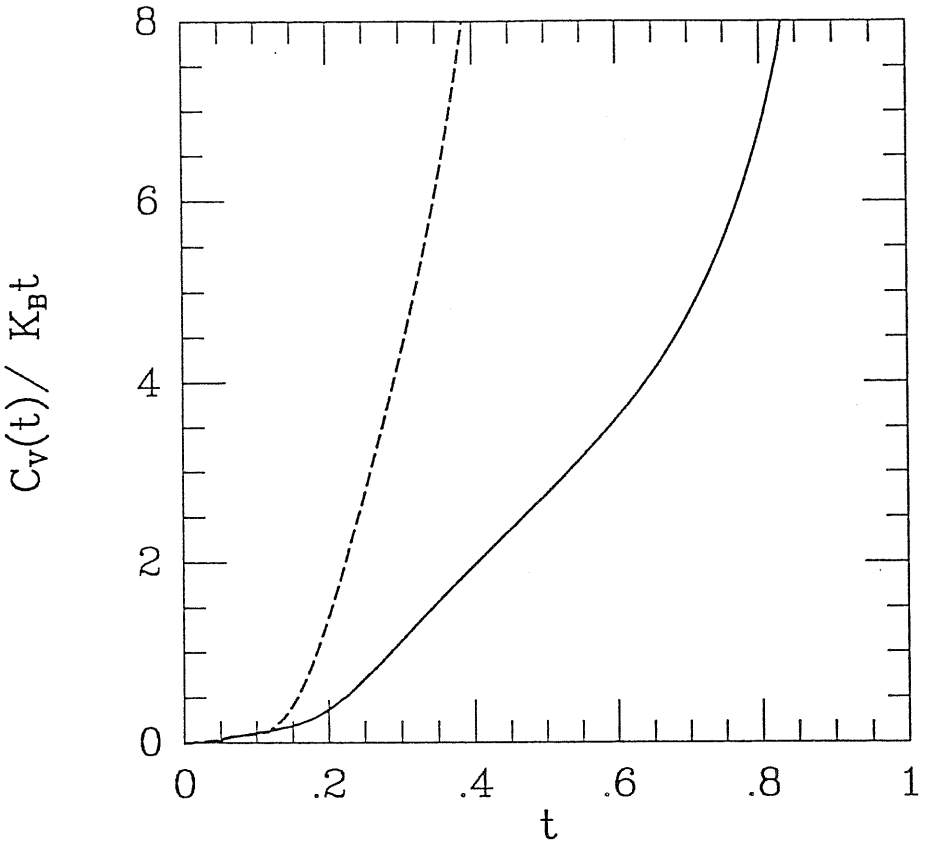

Figure 3

Temperature dependence of the specific heat for the AF phase. The full curve includes the constraint while the broken ones does not.

Paper VI

Finite temperature results from constrained fermionization in the 2-D spin 1/2 Heisenberg antiferromagnet. II: fluctuations in the dimer phases

M.Di Stasio[(1)], E.Ercolessi[(2)], G.Morandi[(3)]
and A.Tagliacozzo[(1,4)]

(1) S.I.S.S.A.-I.S.A.S.,v. Beirut2,I-34100 Miramare,Trieste,Italy

(2) Physics Dept.,Syracuse University, Syracuse,N.Y. 13244-1130,USA

(3) Dipartimento di Fisica, Universita' di Bologna,
INFM and INFN,v.Irnerio 46,I-40126 Bologna, Italy,

(4) Dipartimento di Scienze Fisiche,Universita' di Napoli
INFM,Mostra d'Oltremare Pad.19, I-80125 Napoli,Italy

Abstract

The constraint of single site occupancy is implemented in the fermionization of the model, within the saddle point approximation. The columnar and the staggered dimer phases are studied and the contribution of the fluctuations to the zero point energy and the specific heat is analyzed.

SISSA: 135/93/CM/MB
SYRACUSE: SU-4240-542

1 Introduction

Non magnetic phases have been proposed as metastable states of the spin 1/2 antiferromagnetic (AFM) Heisenberg hamiltonian on a square lattice in two dimensions $(2 - D)$. In these phases the spin rotation symmetry is unbroken, but a discrete lattice symmetry is broken.

Since the work by Fazekas and Anderson[1], [2], [3] dimer phases[4] and valence bond phases are widely studied, together with the flux [5] and chiral phases[6] which could be relevant particularly when frustrating interactions are added to the hamiltonian.

Numerical calculations[7] and series expansions [8] ,[9] of the spin 1/2 frustrated antiferromagnetic (FAFM) Heisenberg model seem to confirm that dimers can be stabilized. The interest in these phases has been triggered by the physics of doped antiferromagnets, as is the case of the high T_c superconducting cuprates.

In fact doping or frustration disfavour the AFM ordering and could lead to a realization of the so called "spin liquid" state[6], which is actively searched for.

In the unfrustrated case, there is various evidence[10] by now that quantum fluctuations are not strong enough to destroy the AFM long range order in the square lattice system, at zero temperature. However, it has been

claimed that dimer phases can play an important role in the $SU(N)$ extension of the Heisenberg antiferromagnet with n.n. exchange interactions[11].

Among the various solid superstructure of dimers, the staggered dimer phase keeps the translational symmetry along the diagonals of the square lattice, while the columnar dimer phase arranges the dimers into columns (see Fig.1). The two arrangements are degenerate at the mean field level, but quantum fluctuations lift the degeneracy in favour of the columnar phase.

In the $SU(2)$ case, link variables like the ones describing dimer phases are most easily represented if fermionization of the spin variables is performed[12]. However this requires the restriction of the Hilbert space to states in which each site is singly occupied. This restriction is also crucial when the Hubbard model is considered in the limit of large correlation U .

In Part I of this work we have discussed the finite temperature properties of the Néel phase using fermionization and implementing the constraint within the saddle point approximation. It is found that, while the spin wave spectrum that is obtained from one-loop corrections is not affected by the constraint, the thermal fluctuations are strongly depressed by it. This is apparent in the temperature dependence of the specific heat.

In this Part II we consider the temperature properties of the dimer phases within the same approximations. It is shown that there is a large contribution due to fluctuations to the saddle point energy value, although their size is

reduced also at $T = 0$, when the constraint is taken into account. The last feature is at difference with the AFM case and is intimately connected with the breaking of the $U(1)$ gauge symmetry which follows from the non vanishing of a dimer order parameter.

The zero mode are accompanied by finite frequency modes for which the correction due to the constraint is present also at $T = 0$.

Because the degeneracy of these modes is different between the the columnar and the staggered phase, the quantum fluctuations lower the energy of the first one with respect to the other.

Unfortunately we find that the quantitative result is unsatisfactory. This is because fluctuations shift the zero energies of the dimer phases to values that are lower than the accepted AFM ground state.

In fact, were the Hilbert space of available states properly restricted, the zero point fluctuations would be further depressed and final energies would be higher as expected. This confirms that the constraint is even more crucial in studying the dimer phases than the AFM phase and shows that the saddle point approximation gives unreliable quantitative results expecially at zero temperature.

At finite temperatures the presence of the constraint is quite effective in reducing the thermal fluctuations. The mean field critical temperature is increased and the curve of the specific heat versus temperature is much lower

than the corresponding one when the constraint is disregarded (see Fig.3).

Consequently, addition of the one-loop corrections to the saddle point action provides a physically meaningful approximation to the free energy at finite temperatures.

In sect.2 the mean field results are summarized[13]. In sect.3 (and the Appendices) the one-loop corrections are evaluated for the staggered and the columnar phase and the free energy is presented. In sect.4 the quantitative results are analyzed and discussed.

2 Non-magnetic decouplings: dimer phases

We start from the Hamiltonian:

$$H_o = J \sum_{(i,j)} \vec{S}_i \cdot \vec{S}_j \quad . \tag{1}$$

The sum is over ordered n.n. pairs of sites in the lattice. Altogether there will be 2N such pairs for a 2D square lattice with N sites.

Fermionization of the spin 1/2 operators ($\vec{S}_i = \sum_{\alpha\beta} c^\dagger_{i\alpha} \vec{\sigma}_{\alpha\beta} c_{i\beta}$) directly leads to:

$$H_o = -\frac{J}{2} \sum_{(i,j)} \sum_{\alpha\beta} c^\dagger_{i,\alpha} c_{j,\alpha} c^\dagger_{j,\beta} c_{i,\beta} - \frac{J}{2} N \quad . \tag{2}$$

The last term in the Hamiltonian will be ignored for the time being.

The representation of eq.(2) is exact provided that the fermionic Hilbert space is restricted to states with single site occupancy.

Following the method of Part I, the projected partition function is:

$$\mathcal{Z} = \prod_i \frac{\partial}{\partial z_i}(2 - \frac{\partial}{\partial z_i})\mathcal{Z}[z]\Big|_{z=0} . \tag{3}$$

with

$$\mathcal{Z}[z] = Tr\{e^{-\beta H_o + \sum_i z_i n_i}\} \tag{4}$$

Our task is now to evaluate $\mathcal{Z}$ within the saddle point approximation.

In view of discussing the non uniform phases first introduced by Affleck and Marston[5] we single out the operators:

$$\mathcal{U}_{ij}(\tau) = \sum_\beta c^\dagger_{j,\beta}(\tau) c_{i,\beta}(\tau) \tag{5}$$

and use the Hubbard Stratonovich decoupling to integrate out the fermionic fields by means of auxiliary fields $\mathcal{U}_{ij}(\tau)$ that obey both periodic boundary conditions in τ and the hermiticity condition:

$$\mathcal{U}^*_{ij}(\tau) = \mathcal{U}_{ji}(\tau) \quad \forall \tau \in [0,1] \tag{6}$$

After Fourier transforming with respect to the time variable, the generating function becomes:

$$\begin{aligned} \mathcal{Z}[z] = \mathcal{N} \int \prod_{(i,j)} \mathcal{D}\mathcal{U}_{ij} \exp\{-\pi \sum_{(i,j)} \sum_m \mid \mathcal{U}_{ij}(\Omega_m) \mid^2\} \\ \cdot \exp\{2Tr \ln[1 + G_o \mathcal{U}^d]\} \end{aligned} \tag{7}$$

where $\Omega_m = \omega_n - \omega_{n'}$, with $\omega_n = (2n+1)\pi$. The trace appearing in eq.(7) sums over site and frequency indices and the factor of two in front of it comes from the sum over spins.

The matrix $\mathcal{U}^d$ has elements:

$$\left(\mathcal{U}^d\right)_{ij}^{nn'} = z_i \delta_{n,n'} \delta_{i,j} - \left(\frac{\pi\beta J}{2}\right)^{1/2} \mathcal{U}_{i,j}(\Omega_m) \,, \tag{8}$$

$\mathcal{U}^d$ is hermitian (i.e. $(\mathcal{U}^d)_{ij}^{n,n'} = \left((\mathcal{U}^d)_{ji}^{n',n}\right)^\star$), what restricts the independent variables of the functional integration only to those with non negative frequencies Ω_m. Using eq.(3) and re-exponentiating the extra factors appearing in the path integral, we obtain the following expression for the partition function:

$$\mathcal{Z} = \int \prod_{(i,j)} \prod_{m \geq 0} \mathcal{D}^2 \mathcal{U}_{ij}(\Omega_m) \quad e^{-\beta \mathcal{F}_{eff}} \tag{9}$$

and the total effective action $\mathcal{F}_{eff}$ is given by:

$$\beta \mathcal{F}_{eff} = \pi \sum_{(i,j)} \sum_{m \geq 0} \mid \mathcal{U}_{ij}(\Omega_m) \mid^2 + S_{eff}[\mathcal{U}] - \sum_i \ln 4 B_i[\mathcal{U}] \tag{10}$$

where the effective action in the absence of the constraint is given as a functional of the Gaussian random fields $\mathcal{U}$ as:

$$S_{eff}[\mathcal{U}] = -2Tr \ln[1 + G_o \mathcal{U}^d] \tag{11}$$

with $(G_o^{-1})_{ij}^{nn'} = i\omega_n \delta_{i,j} \delta_{n,n'}$. The contribution of the constraint, $B_i[\mathcal{U}]$ is expressed in terms of $\chi = (G_o^{-1} + \mathcal{U}^d)^{-1}$ as:

$$B_i[\mathcal{U}] = 2Tr\left\{\chi P_i \chi P_i\right\} + 4Tr\{\chi P\} - 4\left(Tr\{\chi P_i\}\right)^2 \qquad (12)$$

Here we have introduced the projector P_i onto the $i-th$ site of the lattice whose matrix elements are: $(P_i)_{jk} = \delta_{jk}\delta_{ij}$.

The static mean field columnar and staggered dimer phases [4],[5],[13] can be described in terms of four complex (oriented) link variables which we call $\mathcal{U}_i$ for the staggered phase and $\mathcal{V}_i$ for the columnar phase. They are depicted in Fig.1. Complex conjugation of one link variable implies reversing the arrow of the corresponding link. They are found as saddle points of eq.(10)as reported in the rest of this Section.

For a static $\mathcal{U}$ the traces in eq.(11) and eq.(12) can be performed by means of a suitable basis as shown in Appendix 1. All the relevant quantities turn out to depend only on the eigenvalues $E_\pm$ of the matrix $\mathcal{U}$ that are defined in Appendix 1. In particular, eq.(12) becomes site independent. From eq.(10) the total effective action, which takes the same form for both phases, reads:

$$\begin{aligned} f_{eff} &= \frac{\mathcal{F}_{eff}}{NJ} \\ &= \sum_i \mid d_i \mid^2 - \frac{2}{N}\sum_k \frac{2}{\beta J}\ln[e^{cE_+/2} + e^{cE_-/2}] - \frac{1}{\beta J}\ln B \end{aligned} \qquad (13)$$

where: $d_i = c\mathcal{U}_i/\beta J$ $(c\mathcal{V}_i/\beta J)$ $(i = 1,...,4)(\ c = \sqrt{\pi\beta J/2})$. The static configurations that minimize the r.h.s. of eq.(13) correspond to having just

one of the d_i's fields different form zero ($d_1 = d$, $d_2 = d_3 = d_4 = 0$, e.g.). In this case the saddle point is degenerate for the two phases.

The degeneracy is lifted however when one loop corrections are included. That is what we will do in the next section.

The temperature dependence of the order parameter d is given by:

$$d = \frac{1}{2}\tanh d/2t + \frac{1}{2}\frac{\partial}{\partial x}\ln B(x)\Big|_{x=d/t} \tag{14}$$

with $cE(k) = d/t$ ($t = 1/\beta J$) and

$$\begin{aligned} B(x) &= 1 + 2Tr\{\chi P \chi P\} = \\ &= 1 - \frac{1}{2}\left(\frac{\tanh(x/2)}{x} + \frac{1}{2\cosh^2(x/2)}\right) \quad . \end{aligned} \tag{15}$$

The mean field transition temperature to the dimer ordered phase is increased by the second term on the r.h.s. of eq.(14) from $t_c = 1/4$ to $t_c = 5/12$ [13]. At zero temperature the total effective action of eq.(13), when evaluated at the stationary points, gives back the values of Ref.([5]) for the energies of the two phases: $f^0_{eff}(t = 0) = -1/4$. Because $B \to 1$ in the zero temperature limit, it is apparent from eq.(13) that the unconstrained value for the free energy is not changed at the mean field level at $t = 0$. This is because the saddle point satisfies the constraint in the average automatically. Adding back the extra constant term appearing in the hamiltonian, the energy, when the constraint is satisfied only in the average, becomes $f^0_{dimers} = -3/4$.

However this does not correspond to strictly projecting out empty and doubly occupied states. At zero temperature this can be done by hand as shown in Ref.([5]), noticing that the independent dimers of the mean field configuration, when projected, become a collection of spin singlets with a total energy per particle $f_{singlets} = -S(S+1)/2 = -3/8$.

This is half the value of the previous estimate, at the same level of approximation. This shows already that, if the constraint is taken into account only in the average, the variational energy lowers too much.

3 One-loop corrections

By including the one-loop corrections in the evaluation of the path integral, we take into account field configurations that allow for fluctuations of the order parameter around its mean field value, at the gaussian level. We find that the resulting free energy has the correct temperature dependence. On the contrary eq.(13) increases with temperature at low temperature and cannot be considered as an approximation to the thermodynamical potential.

From now on we denote by u the variation $\delta\mathcal{U}$ of $\mathcal{U}$ (we tacitly refer also to $\mathcal{V}$ for the columnar phase whenever no confusion arises). The second variation $\mathcal{F}^{(2)}$ can be expressed in terms of the complex deviations: $u_l(\vec{R}_i, \tau)$ $(l = 1, 4)$ of the $\mathcal{U}$'s from the saddle point value and of their Fourier transforms $u_l(\vec{Q}, \Omega_m)$. Here $\vec{R}_i$ spans just one of the sublattices (e.g. the "black" sites

of Fig.1) while $\vec{Q}$ is in the corresponding reduced Brillouin zone.

Instead of varying all the $\mathcal{U}_{i,j}$'s for every pair of sites, we choose to vary the $\mathcal{U}_l$ only, so that variations with any frequency Ω_m and transferred momentum $\vec{Q}$ are allowed but they are only restricted to nearest neighbor couplings. Complex Fourier transformation implies that: $\left(u_l(-\vec{Q},-\Omega_m)\right)^* = u_l^*(\vec{Q},\Omega_m)$, where $u_l^*(\vec{Q},\Omega_m)$ is the Fourier transform of $(u_l(i,\tau))^*$. This can be viewed as a definition of $u_l^*(Q,\Omega_m)$. Moreover, the hermiticity condition $u_l(Q,\Omega_m) = (u_l(Q,-\Omega_m))^*$ restricts the independent variables to those with non negative frequencies. Expanding up to second order in the deviations the total effective action in eq.(9), we find:

$$Z = e^{-\beta\mathcal{F}^0}\int \prod_{\vec{Q},m\geq 0}\prod_{i=1,4} du_i^R(\mathrm{Q})du_i^I(\mathrm{Q})e^{-\beta\mathcal{F}^{(2)}} \tag{16}$$

where u_i^R and u_i^I are the real and imaginary parts of u_i, $\mathrm{Q} =: (\vec{Q},\Omega_m)$, $\mathcal{F} \approx \mathcal{F}^{(0)} + \mathcal{F}^{(2)}$ and

$$\beta\mathcal{F}^{(2)} = \pi\sum_{Q}\sum_{m\geq 0}\sum_{l} \mid u_l(Q,m)\mid^2 + S_{eff}^{(2)} - \frac{1}{2}\sum_i\left(\frac{\delta^2 B_i}{B_i} - \left(\frac{\delta B_i}{B_i}\right)^2\right) \quad . \tag{17}$$

The first term in $\mathcal{F}^{(2)}$ becomes:

The one loop correction to the effective action (see Fig.2(a)) is given by:

$$\begin{aligned} S_{eff}^{(2)} &= Tr\{[\chi\delta\mathcal{U}^d]^2\} = \frac{\pi\beta J}{2}\sum_{k,q}\sum_{m}\sum_{\mu,\nu}\Phi_{\mu\nu}(m)\cdot \\ &\cdot < k\mu \mid u(\Omega_m) \mid q\nu >< q\nu \mid u(-\Omega_m) \mid k\mu > \end{aligned} \tag{18}$$

Here we have defined the function $\Phi_{\mu\nu}(m)$ as:

$$\Phi_{\mu\nu}(m) = \sum_n \frac{1}{i\omega_n - \mu d/t} \; \frac{1}{i\omega_n - i\Omega_m - \nu d/t} \tag{19}$$

and we have chosen the basis in which χ is diagonal. This is the one in which $\mu(\nu) = \pm$ labels the energy eigenvalues, $E_\pm$, of the matrix $\mathcal{U}$ $(\mathcal{V})$ which are reported in Appendix 1. They correspond to the eigenstates:

$$\mid k\pm >= \left[\mid k, b > \pm e^{-ik_x} \mid k, w >\right] / \sqrt{2} \tag{20}$$

The indices b and w label the "black" and "white" sites according to Fig.1 (see Appendix 1).

The sums in eq.(19) over the internal Fermi frequencies can be performed easily. The result is:

$$\Phi_{\mu,\mu}(m) = -\delta_{m,0} \frac{1}{4\cosh^2 d/2t} \tag{21}$$

$$\Phi_{+-}(m) = \Phi_{-+}(-m) = \frac{\tanh d/2t}{i\Omega_m - 2d/t} \; . \tag{22}$$

The matrix elements of u for the staggered and the columnar phase and the wave vector sums are given in Appendix 2. The latter depend only on $\vec{Q} = \vec{k} - \vec{q}$.

The result is:

$$S^{(2)}_{eff} = \pi\beta J \sum_Q \Big\{ \Phi_{++}(0) G_+(\vec{Q}, [u]) + \frac{1}{2} \sum_m \left(\Phi_{+-}(m) + \Phi_{-+}(m)\right) G_-(\mathbf{Q}, [u]) \Big\} \tag{23}$$

For the staggered phase, $G_{\pm}$ is given by:

$$G^s_{\pm}(\mathbf{Q},[u]) = \frac{1}{4}\left\{ \sum_{i=1,4} \left(\mid u_i(\mathbf{Q}) \mid^2 + \mid u_i(-\mathbf{Q}) \mid^2 \right) + \right.$$
$$\left. \pm \left(u_1(\mathbf{Q}) u_1(-\mathbf{Q}) + u_1(\mathbf{Q})^\star u_1(-\mathbf{Q})^\star \right) \right\} , \qquad (24)$$

while, for the columnar phase we have:

$$G^c_{\pm}(\mathbf{Q},[v]) = G^s_{\pm}(\mathbf{Q},[v]) \pm \{ v_4(\mathbf{Q}) v_3(\mathbf{Q})^\star + v_4(-\mathbf{Q})^\star v_3(-\mathbf{Q}) +$$
$$+ v_3(\mathbf{Q}) v_4(\mathbf{Q})^\star + v_3(-\mathbf{Q})^\star v_4(-\mathbf{Q}) \} \qquad (25)$$

As it appears from eq.(25) the columnar phase shows an additional mixing of the third and fourth component of the order parameter with respect to the staggered phase.

Because both functions $G_{\pm}$ are symmetrical under the interchange of $\mathbf{Q} \leftrightarrow -\mathbf{Q}$ one can express the prefactor of the second term on the r.h.s. of eq.(23) by means of the real quantity :

$$E(|m|) = -\frac{1}{2t} \left(\Phi_{+-}(m) + \Phi_{-+}(m) \right) = 2d \frac{\tanh d/2t}{\Omega_m^2 t^2 + 4d^2} \quad . \qquad (26)$$

thus yielding:

$$S^{(2)}_{eff} = 2\pi \sum_{\vec{Q} \geq 0} \left\{ \beta J \Phi_{++}(0) G_+(\vec{Q},[u]) - 2 \sum_{m \geq 0} E(m) G_-(\mathbf{Q},[u]) \right\} \qquad (27)$$

We postpone the evaluation of the effect of the constraint until the end of this Section.

The result of the gaussian integrals of eq.(16) can be immediately expressed in terms of the eigenvalues of the quadratic form $\mathcal{F}^{(2)}$. There are 8 eigenvalues of the matrix of the complex components of the fluctuation for each frequency[15]. They are independent of $\vec{Q}$.

Due to its block form, it is very easy to diagonalize the matrix. We list the eigenvalues in Table I, for both the staggered and the columnar phases. Their expressions for the two phases coincide but the degeneracies and the admixtures of components of the fluctuations change. In Table I the degeneracy is also reported as well as the admixture of components which characterizes the fluctuations.

There is one zero mode for both the staggered and the columnar phase, which corresponds to an overall change of the phase of the component of the order parameter $u_1(v_1)$. In addition to this, the columnar phase has a flat second variation of the action for two modes which imply small changes of the real (imaginary) part of v_3, v_4 in an opposite way. Quartic corrections should be added to stabilize the effective action with respect to these variations.

The zero mode integration[16] gives raise to the prefactor $\mathcal{C}^s = \left(2d(2\pi\beta J)^{1/2}\right)^{N/2}$ to the partition function. In terms of these eigenvalues the result for the partition function of the staggered dimer phase is:

$$Z = e^{-\beta\mathcal{F}^0}\mathcal{C}^s \prod_{\vec{Q}\geq 0} \left(\lambda_2^s(m=0)\right)^{-6} \left(\lambda_3^s(m=0)\right)^{-1} \prod_{\vec{Q}\geq 0, m>0} \left(\lambda_2^s(m)\right)^{-6} \left(\lambda_1^s(m)\right)^{-1} \tag{28}$$

The free energy per particle in units of J is:

$$f = f^0 - \frac{t}{N}\ln \mathcal{C}^s + \frac{3t}{2}\sum_{m\geq 0}\ln\lambda_2^s(m) + \frac{t}{4}\sum_{m>0}\ln\lambda_1^s(m) + \frac{t}{4}\ln\lambda_3^s(m=0)\ . \quad (29)$$

The prefactors are the degeneracies of each eigenvalue, divided by 4 . The frequency sums are easily performed, yielding:

$$\sum_{m\geq 0}\ln\lambda_2^s(m) = \sum_{m\geq 0}\ln\left(1 - \frac{2d^2}{\Omega_m^2 t^2 + 4d^2}\right) = \ln\left(\frac{\sinh d/\sqrt{2}t}{\sqrt{2}\sinh d/t}\right)$$
$$\sum_{m>0}\ln\lambda_1^s(m) = \sum_{m>0}\ln\left(1 - \frac{4d^2}{\Omega_m^2 t^2 + 4d^2}\right) = \ln\left(\frac{d/t}{\sinh d/t}\right) \quad (30)$$

Note that the term $t\ln t$ due to $t\ln\mathcal{C}^s$ is compensated by an analogous term in eq.(30). Therefore, the specific heat is well behaved for temperatures going to zero.

The contribution of quantum fluctuations at zero temperature to the free energy is :

$$\Delta f^s(t=0) = -\frac{d}{4} - 6\cdot\frac{d}{4}(1 - 1/\sqrt{2}) \quad (31)$$

Going through similar steps, one gets for the columnar phase :

$$f = f^0 - \frac{t}{N}\ln\mathcal{C}^c + \frac{3t}{4}\sum_{m>0}\ln\lambda_1^c(m) + \frac{t}{2}\sum_{m\geq 0}\ln\lambda_2^c(m) + \frac{3t}{4}\ln\lambda_3^c(m=0) \quad (32)$$

with $\mathcal{C}^c = \left(2^3 d(2\pi/t)^{3/2}\right)^{N/2}$. The flat modes, being indistinguishable from the zero mode at this level of approximation, have been integrated out in the same way. This is the origin of the power of three in $\mathcal{C}^c$.

The zero temperature limit of $\Delta f = f - f^0$ for the columnar phase is:

$$\Delta f^c(t=0) = -\frac{3d}{4} - 2 \cdot \frac{d}{4}(1 - 1/\sqrt{2}) \tag{33}$$

This result, first derived by Read and Sachdev[4] within the $1/N$ expansion, implies that the degeneracy of the staggered and the columnar phase is lifted by quantum fluctuations and that the last one becomes energetically favoured.

The eigenvalues that contribute most to lower the energy for both periodicities are $\lambda_1^{s,c}(m \neq 0)$. These correspond to the zero mode, when $m = 0$ for both phases. However, in the case of the columnar phase there are two more flat modes at $m = 0$, which have the same eigenvalues at $m \neq 0$. Essentially, they are responsible of the lifting of the degeneracy and of the fact that the columnar phase is lower in energy than the staggered one.

Now we come to the discussion of quantum fluctuations of the constraint. The latter appears in the free energy expression of Eq.(10) in the form of $\sum_i \ln B_i$ so that its second variation is given by:

$$\frac{1}{2}\delta^2 \sum_i \ln B_i = \frac{1}{2} \sum_i \left(\frac{\delta^2 B_i}{B_i} - \left(\frac{\delta B_i}{B_i} \right)^2 \right) \tag{34}$$

where:

$$\delta B_i = 4Tr\{\chi P_i \chi P_i \chi \delta \mathcal{U}^d\} \ , \tag{35}$$

$$\delta^2 B_i = 4\left(2Tr\{\chi P_i \chi P_i \chi \delta\mathcal{U}^d \chi \delta\mathcal{U}^d\} + Tr\{\chi P_i \chi \delta\mathcal{U}^d \chi P_i \chi \delta\mathcal{U}^d\}\right) \quad . \qquad (36)$$

Because there is a single $\delta\mathcal{U}^d$ in eq.(35), the trace does not allow for any change of frequency, so that the second contribution to eq.(34) is static ($\Omega_m = 0$). In Fig.2(b) the diagrammatic representation of δB_i is sketched. The wavy line represents $\delta\mathcal{U}^d$, each full line is a propagator χ and the broken lines represent the projector P_i viewed as an external perturbation. The first and second contribution to the r.h.s. of eq.(36) are sketched in Fig.2(c) and Fig.2(d) respectively, while Fig.2(a) is the representation of the second variation of the effective action $S^{(2)}_{eff}$. The corresponding analytical expressions of eq.(35) and eq.(36) are reported in the Appendix 3.

Following the same lines as in the evaluation of the second variation of the effective action we end up with a fluctuation matrix to be diagonalized. The full expressions of the eigenvalues including the constraint are listed in Appendix 3. The contribution of the constraint to each eigenvalue takes the same form for the staggered and the columnar phase. In particular, the second term of the r.h.s. of eq.(34) just contributes to λ_3 for $m = 0$.

We report here just the zero temperature results. For the staggered phase we get:

$$\Delta f^s(t=0) = -2d(1 - \frac{1}{\sqrt{2}}) \qquad (37)$$

For the columnar phase the result is:

$$\Delta f^c(t=0) = -\frac{d}{2} - d(1-1/\sqrt{2}) \tag{38}$$

Comparing these results with those of eq.s(31,33), we note that fluctuations are depressed due to the presence of the constraint, which, in the zero temperature limit affects only the contribution of the singly degenerate eigenvalue λ_1.

4 Discussion and conclusion

In this paper we have shown how to implement, at all temperatures, the single site-occupancy projector needed to represent the spin 1/2 operators in terms of fermion operators and Pauli matrices. This representation is a very natural one in describing non magnetic phases of Heisenberg hamiltonians such as the dimer phases studied here or the flux or chiral phases[5], [6].

At the saddle point level of approximation we have shown[14] that our method guarantees that $< n_i >= 1$ and that $< n_i^2 - 1 >$ deviates from zero less then 10% in the whole range of temperature $t \in [0, t_c]$ when the dimer phases are considered.

The relevance of the projector can be easily seen from the zero temperature mean field results for the free energy. In fact the isolated spin singlet free energy value is recovered only when the single site-occupancy projector is taken into account.

Quantum and thermal fluctuations around the dimer saddle point have been evaluated within one-loop approximation. The need of accounting for quantum fluctuations is a very well known fact in the study of the $2-D$ $S=1/2$ Heisenberg model. As previously shown in Ref.([4]) they lift the degeneracy between the columnar and the staggered dimer phase.

By including the one-loop corrections to the free energy in the presence of the constraint, we obtain corrections to the mean field energy that are $\Delta f^s = 0.293$ for the staggered phase and $\Delta f^c = 0.396$ for the columnar phase, to be compared with the unconstrained results, $\Delta f_0^s = 0.345$ and $\Delta f_0^c = 0.448$ respectively. While there is an improvement of the result, in that zero point fluctuations are reduced appreciably due to the constraint, the quantitative result is still unsatisfactory. In fact, the energy of these phases turns out to be lower than the energy of the AFM phase[10] which is accepted as the ground state.

This is due to the fact that while in the AFM case, in which the magnetization acts as a local order parameter, our method guarantees that the constraint is fully satisfied at the mean field level ($< n_i^2 - 1 >= 0$ at all temperatures (see Part I of this work)), this is not the case in the dimer phases. Here the unconstrained mean field hamiltonian would be an hopping hamiltonian and our method to implement the single site-occupancy constraint only guarantees a variation of less than 10%. One-loop corrections,

even in the presence of the constraint, are not enough to compare ground state energies when different decoupling schemes are adopted.

On the other hand, in our method the constraint behaves as an entropy corrector at finite temperatures, giving origin to a well behaved free energy only if one-loop corrections are added to the saddle point total action. This corrects the fact that, as one can see from Fig.3, the specific heat obtained from the saddle point approximated free energy goes negative at low temperatures (broken curve). The specific heat is strongly reduced due to the constraint inclusion. Lowering the temperature, it exponentially decays to zero due to the presence of a gap d in the excitation spectrum, as expected.

5 Appendix 1

The non vanishing order parameter changes the periodicity in the lattice. In Fig.1 the filled circles are denoted as black sites (b), the empty ones as white sites (w). The single particle states $\mid l,k >$ are eigenfunctions of the translation operators $T_{\vec{a}(\vec{b})}$:

$$T_{\vec{a}(\vec{b})}|l,k>= e^{-i\vec{k}\vec{a}(\vec{b})}\ |l,k> \tag{39}$$

Here k is in the RBZ and l takes the two values "black" or "white" ($l = b, w$), labeling the two sublattices respectively. Their projection onto the Wannier

states labeled by the site index i $(i = b, w)$ is:

$$< i|l, k >= \sqrt{\frac{2}{N}} e^{-ikR_i} \delta_{i,l} \ . \tag{40}$$

In this basis the matrix elements of the projector P_i are:

$$< l, \vec{k} \mid P_i \mid r, \vec{h} >= \frac{2}{N} e^{i(\vec{h}-\vec{k})R_i} \delta_{l,r} \delta_{l,i} \tag{41}$$

that is, they are diagonal in the l indices.

The appropriate periodicity has to be chosen according to each phase. Here we follow the notations of Ref.([13],[5]).

Staggered Phase :

Periodicity in the direct lattice is along the diagonals: $\vec{a} = \vec{x}+\vec{y}, \vec{b} = \vec{x}-\vec{y}$.

The matrix elements of $\mathcal{U}$ in the $\mid l, k >$ basis are:

$$< b, \vec{k} \mid \mathcal{U} \mid b, \vec{h} >=< w, \vec{k} \mid \mathcal{U} \mid w, \vec{h} >= 0$$

$$< b, \vec{k} \mid \mathcal{U} \mid w, \vec{h} >= \delta_{\vec{k},\vec{h}} \lambda(\vec{k})$$

where:

$$\lambda(\vec{k}) = \mathcal{U}_1 e^{ik_x} + \mathcal{U}_2^\star e^{-ik_y} + \mathcal{U}_3 e^{-ik_x} + \mathcal{U}_4^\star e^{ik_y} \ . \tag{42}$$

The lattice constant is taken to be unity. The eigenvalues of the matrix $\mathcal{U}$ are $E_\pm = \pm \mid \lambda(\vec{k}) \mid^2$.

Columnar Phase :

In this case the translation vectors are: $\vec{a} = 2\vec{x}$, $\vec{b} = \vec{y}$.

The matrix elements of $\mathcal{V}$ can be deduced from Fig.1b):

$$< b,\vec{k} \mid \mathcal{V} \mid b,\vec{h} >= \delta_{\vec{k},\vec{h}}\lambda_3(k_y) = \delta_{\vec{k},\vec{h}}(\mathcal{V}_3 e^{ik_y} + \mathcal{V}_3^\star e^{-ik_y})$$

$$< w,\vec{k} \mid \mathcal{V} \mid w,\vec{h} >= \delta_{\vec{k},\vec{h}}\lambda_4(k_y) = \delta_{\vec{k},\vec{h}}(\mathcal{V}_4 e^{ik_y} + \mathcal{V}_4^\star e^{-ik_y})$$

$$< b,\vec{k} \mid \mathcal{V} \mid w,\vec{h} >= \delta_{\vec{k},\vec{h}}\lambda_0(k_x) = \delta_{\vec{k},\vec{h}}(\mathcal{V}_1 e^{ik_x} + \mathcal{V}_2^\star e^{-ik_x})$$

$$< w,\vec{k} \mid \mathcal{V} \mid b,\vec{h} >= \delta_{\vec{k},\vec{h}}\lambda_0^\star(k_x) \qquad (43)$$

The eigenvalues of the matrix $\mathcal{V}$ are $E_\pm = (\lambda_3+\lambda_4 \pm \sqrt{(\lambda_3-\lambda_4)^2 + \mid \lambda_0 \mid^2})/2$.

6 Appendix 2

When performing the traces to evaluate the fluctuations, it is convenient to choose as working basis the one that diagonalizes the propagator χ . This is here denoted by $|k\alpha >$ of eq.(20), with $\alpha = \pm$ corresponding to the eigenvalue $E_\pm$ of the matrix $\mathcal{U}\,(\mathcal{V})$ (see Appendix 1) and is given in eq.(20) of the text:

$$\mid k\pm >= \left[\mid k,b > \pm e^{-ik_x} \mid k,w >\right]/\sqrt{2} \qquad (44)$$

The matrix elements of the fluctuation $\delta\mathcal{U}$ in this basis are $(\alpha,\beta = \pm)$:

$$< k\alpha \mid \delta\mathcal{U}(m) \mid q\beta >= \frac{1}{2}(< kb \mid + \alpha e^{ik_x} < kw \mid)\delta\mathcal{U}(m)(\mid qb > + \beta e^{-iq_x} \mid qw >) \qquad (45)$$

The matrix elements of any matrix U in the site indices become:

$$< k\alpha \mid U \mid q\beta >=$$

$$= \beta \frac{1}{2} \sum_{i,j} e^{-iq_x} < kb \mid i > U_{ij} < j \mid qw > \delta_{i,black}\delta_{j,white} +$$
$$+\alpha e^{ik_x} < kw \mid i > U_{ij} < j \mid qb > \delta_{i,white}\delta_{j,black}$$
$$= \frac{1}{N} \sum_{i\ black} \beta e^{-i(k-q)R_i} \Big\{ (U_{i,i+a} + U_{i,i-a}e^{-2iq_x}$$
$$+U_{i,i+b}e^{-i(q_x-q_y)} + U_{i,i-b}e^{-i(q_x+q_y)} \Big\}$$
$$+\frac{1}{N} \sum_{j\ black} \alpha e^{-i(k-q)R_j} \Big\{ (U_{j+a,j} + U_{j-a,j}e^{2ik_x}$$
$$+U_{j+b,j}e^{i(k_x-k_y)} + U_{j-b,j}e^{i(k_x+k_y)} \Big\}$$

Now we assume that the only non vanishing matrix elements are those connecting nearest neighbors. To proceed, we specialize the matrix elements of the fluctuations of the link variables $U_l(i)$ $(l = 1, .., 4)$ for the staggered and the columnar phase according to Fig.1. Collecting the two sums together we have:

Staggered Phase:

$$< k\alpha|U|q\beta > \quad = \frac{1}{N} \sum_{i\ black} e^{-i(k-q)R_i} \beta \Big\{ (U_1^\star(i) + U_3^\star(i)e^{-2iq_x}$$
$$+ U_4(i)e^{-i(q_x-q_y)} + U_2(i)e^{-i(q_x+q_y)} \Big\} +$$
$$+\alpha \Big\{ U_1(i) + U_3(i)e^{2ik_x} + U_4^\star(i)e^{i(k_x-k_y)} + U_2^\star(i)e^{i(k_x+k_y)} \Big\}$$

Defining the symbol $\mathbf{Q} = (\vec{Q}, \Omega_m)$, where $\vec{Q} = \vec{k} - \vec{q}$ is the transferred momentum, we introduce the Fourier transformed fields:

$$u_l(\mathbf{Q}) = \sqrt{\frac{2}{N}} \sum_{i\ black} e^{-iQR_i} U_l(i, m). \tag{46}$$

They are complex and we will use $u_l(\mathbf{Q}) = u_l^R(\mathbf{Q}) + iu_l^I(\mathbf{Q})$ as well as $u_l(\mathbf{Q})^* \equiv (u_l(\mathbf{Q}))^* = u_l^R(\mathbf{Q}) - iu_l^I(\mathbf{Q})$. We obtain:

$$
\begin{aligned}
&< k\alpha \mid \delta\mathcal{U}(m) \mid q\beta >= \beta\frac{1}{\sqrt{2N}}\Big\{u_1(-\mathbf{Q})^* + +u_3(-\mathbf{Q})^* e^{-2ik_x} e^{2iQ_y} \\
&+ u_4(\mathbf{Q}) e^{-i(k_x-k_y)} e^{i(Q_x-Q_y)} + u_2(\mathbf{Q}) e^{-i(k_x+k_y)} e^{i(Q_x+Q_y)}\Big\} \\
&+\alpha\Big\{u_1(\mathbf{Q}) + u_3(\mathbf{Q}) e^{2ik_x} + u_4(-\mathbf{Q})^* e^{i(k_x-k_y)} + u_2(-\mathbf{Q})^* e^{i(k_x+k_y)}\Big\}
\end{aligned}
$$

Performing the sum that appears in eq.(18) of the text, over the internal momentum $\vec{k}$ of the product matrix elements, only the terms that are diagonal in the component indices i survive due to the orthogonality of the plane waves, yielding for the staggered phase:

$$
\begin{aligned}
&\sum_{k,q} < k\alpha \mid \delta\mathcal{U}(m) \mid q\beta >< q\beta \mid \delta\mathcal{U}(-m) \mid k\alpha >= \\
&= \frac{1}{4}\sum_{\vec{Q}}\Bigg\{\sum_{i=1,4}\Big(\mid u_i(\mathbf{Q}) \mid^2 + \mid u_i(-\mathbf{Q}) \mid^2\Big) + \\
&+ \alpha\cdot\beta\,[u_1(\mathbf{Q})u_1(-\mathbf{Q}) + u_1(\mathbf{Q})^* u_1(-\mathbf{Q})^*]\Big\} \\
&= \sum_{\vec{Q}} G^s_{\alpha\cdot\beta}(\mathbf{Q}, [u])
\end{aligned}
\tag{47}
$$

where $\alpha, \beta = \pm$. Hence eq.(24) of the text follows.

Columnar phase:

In the case of the columnar phase, the same steps as before can be followed, obtaining finally:

$$< k\alpha \mid \delta\mathcal{V}(m) \mid q\beta >=$$

$$\frac{1}{\sqrt{2N}}\left\{v_4(\mathbf{Q})e^{iq_y}+v_4^\star(\mathbf{Q})e^{-ik_y}+\beta\left(v_2(\mathbf{Q})e^{2iq_x}+v_1^\star(\mathbf{Q})\right)+\right.$$
$$\left.+\alpha\left(v_2^\star(\mathbf{Q})e^{-2ik_x}+v_1(\mathbf{Q})\right)+\alpha\beta\left(v_3(\mathbf{Q})e^{iq_y}+v_3^\star(\mathbf{Q})e^{-ik_y}\right)\right\}$$

which implies that:

$$\sum_{k,q}<k\alpha\mid\delta\mathcal{V}(m)\mid q\beta><q\beta\mid\delta\mathcal{V}(-m)\mid k\alpha>=$$
$$=\frac{1}{4}\sum_{\vec{Q}}\left\{\sum_{i=1,4}\left(\mid v_i(\mathbf{Q})\mid^2+\mid v_i(-\mathbf{Q})\mid^2\right)+\right.$$
$$+\alpha\cdot\beta\left[v_4(\mathbf{Q})v_3(\mathbf{Q})^\star+v_4(-\mathbf{Q})^\star v_3(-\mathbf{Q})\right.$$
$$+v_3(\mathbf{Q})v_4(\mathbf{Q})^\star+v_3(-\mathbf{Q})^\star v_4(-\mathbf{Q})+$$
$$\left.\left.+v_1(\mathbf{Q})v_1(-\mathbf{Q})+v_1(\mathbf{Q})^\star v_1(-\mathbf{Q})^\star\right]\right\}$$

This suggests the definition of eq.(25) where eq.(24) is also used.

7 Appendix 3

The contribution of the constraint to the fluctuations is given by eq.(34) of the text:

$$\frac{1}{2}\delta^2\sum_i\ln B_i=\frac{1}{2}\sum_i\left(\frac{\delta^2B_i}{B_i}-\left(\frac{\delta B_i}{B_i}\right)^2\right)\qquad(48)$$

with δB_i given by eq.(35) and sketched in Fig.2(b) and with $\delta^2B_i=\delta^2B_i^{(1)}+\delta^2B_i^{(2)}$ given by eq.(36)and sketched in Fig.2(c) and Fig.2(d). We give here their analytical expression.

The following functions are required:

$$\psi_{\alpha\gamma}(0) = \sum_n \chi_\alpha(\omega_n)\left(\sum_\zeta \chi_\zeta(\omega_n)\right)\chi_\gamma(\omega_n)$$

$$\psi^\delta_{\alpha\beta\gamma}(m) = \sum_n \chi_\alpha(\omega_n)\chi_\beta(\omega_n)\chi_\gamma(\omega_n)\chi_\delta(\omega_n - \Omega_m)$$

$$\psi^{\gamma\delta}_{\alpha\beta}(m) = \sum_n \chi_\alpha(\omega_n)\chi_\beta(\omega_n)\chi_\gamma(\omega_n - \Omega_m)\chi_\delta(\omega_n - \Omega_m)$$

where we have defined $\chi_\alpha(\omega_n) = [i\omega_n - \alpha d/t]^{-1}$ $(\alpha = \pm)$ .In terms of these functions we have:

$$\begin{aligned}\sum_i (\delta B_i)^2 &= \frac{\pi}{t}\sum_{\alpha\beta\gamma\delta}\sum_Q (1+\alpha\beta\gamma\delta)\psi_{\alpha\gamma}\,\psi_{\beta\delta}\cdot \\ &\cdot\frac{1}{4}[\alpha\cdot u_1(-Q)^* + \gamma\cdot u_1(Q)][\beta\cdot u_1(Q)^* + \delta\cdot u_1(-Q)]\end{aligned} \tag{49}$$

and dividing the two contributions to $\delta^2 B_i = \delta^2 B_i^{(1)} + \delta^2 B_i^{(2)}$:

$$\begin{aligned}\delta^2 B_i^{(1)} &= 8Tr\{\chi P_i \chi P_i \chi \delta\mathcal{U}^d \chi \delta\mathcal{U}^d\} = \\ &= \frac{\pi}{t}\sum_{\alpha\delta}\sum_\beta \Phi^\delta_{\alpha\beta\alpha}(m) G^{s,c}_{\alpha\cdot\delta}\end{aligned}$$

where $G_{\alpha\cdot\delta}$ $(\alpha\cdot\delta = \pm)$ is given in the text and the superscript s,c refer to the staggered (eq.(24)) and the columnar phase (eq.(25)) respectively.

Finally:

$$\begin{aligned}\delta^2 B_i^{(2)} &= 4Tr\{\chi P_i \chi \delta\mathcal{U}^d \chi P_i \chi \delta\mathcal{U}^d\} = \\ &= \frac{\pi}{2t}\sum_{\alpha\beta\gamma\delta}(1+\alpha\beta\gamma\delta)\Phi^{\gamma\delta}_{\alpha\beta}(m)\cdot \\ &\cdot\frac{1}{4}\sum_Q [\gamma\cdot u_1(-Q)^* + \beta\cdot u_1(Q)][\alpha\cdot u_1(Q)^* + \delta\cdot u_1(-Q)]\end{aligned}$$

We list here in the following the eigenvalues λ including the constraint of single site occupancy, corresponding to those of Table I. We omit a factor of π in each eigenvalue, as we do in Table I . Use will be done in the following of the definitions (with $x = d/t$) :

$$
\begin{aligned}
a &= \frac{1}{2x^2}\tanh x/2 \\
b &= (4x\cosh^2 x/2)^{-1} \\
\Delta(m) &= (2x)^2 - (i\Omega_m)^2 \\
B &= 1 - \frac{1}{2}\left[\frac{\tanh x/2}{x} + \frac{1}{2\cosh^2 x/2}\right] \\
E(m) &= \frac{2x}{t}(\tanh x/2)/\Delta(m)
\end{aligned}
\tag{50}
$$

The last two eq.s coincide with eq.(15) and eq.(26) of the text, respectively. The gap equation reads:

$$
1 - xa - \frac{1}{2dB}\frac{\partial B}{\partial x} = 0 \tag{51}
$$

with $\partial B/\partial x = a - b + 2x^3 ab$.

We get:

$$
\begin{aligned}
&\lambda_1(m) = 1 - E(m) - \frac{1}{2tB}\left[\frac{4x}{\Delta(m)}\frac{\partial B}{\partial x} + \frac{8x}{(\Delta(m))^2}(i\Omega_m)^2 a\right] = \\
&= (i\Omega_m)^2\frac{((i\Omega_m)^2 - \gamma^2)}{\Delta^2}
\end{aligned}
$$

where $\gamma^2 = 4x^2\left[2 - xa\left(1 + \frac{4}{tB}\right) + \frac{2x}{tB}\frac{\partial B}{\partial x}\right]$ and the gap equation has been

used in the last identity. The eigenvalue $\lambda_2(m)$ is:

$$\lambda_2(m) = 1 - \frac{1}{2}E(m) - \delta_{m,0}\frac{1}{8t\cosh^2 x/2} - \frac{x}{tB}R(m) \qquad (52)$$

with:

$$R(m) = \frac{b}{(i\Omega_m)^2} - \frac{a}{\Delta(m)}(1-2x^3b) + 2b\frac{(i\Omega_m)^2}{(\Delta(m))^2} - 4x^2\frac{a}{(\Delta(m))^2} - 4\frac{a(2xi\Omega_m)^2}{(\Delta(m))^3}$$

Finally:

$$\lambda_3(m) = 1 + \frac{2\tanh x/2}{dB\Delta(m)} \quad (m \neq 0)$$

$$\lambda_3(0) = 1 - xb - \frac{3x}{tB}R(0) + \frac{1}{xtB}\frac{\partial B}{\partial x} + \frac{1}{2tB^2}\left(\frac{\partial B}{\partial x}\right)^2$$

In the limit of zero temperature the last two eigenvalues are unaffected by the constraint. $\lambda_3(m)$ becomes unity while $\lambda_2(m) \to (2x^2 - (i\Omega_m)^2)\,/\,(4x^2 - (i\Omega_m)^2)$. Next $\lambda_1(m) \to (i\Omega_m)^2\left((i\Omega_m)^2 - 8x^2\right)/\Delta^2$ while it goes to $(i\Omega_m)^2/\Delta$ when the constraint is not included.

References

[1] P.Fazekas, P.W.Anderson, Phil. Mag.**30**,432 (1974)

[2] S.A.Kivelson,D.S.Rokhsar,J.P.Sethna, Phys.Rev.**B35**,8865 (1987)

[3] P.W.Anderson, Science **235**,1196 (1987)

S.Liang, B.Douçot and P.W.Anderson, Phys.Rev.Lett.,**61**,365 (1988)

[4] N.Read and S.Sachdev, Nucl.Phys.B **316**,609 (1989)

[5] I.Affleck and J.B.Marston, Phys.Rev.B **37**,3774 (1988), J.B.Marston and I.Affleck, Phys.Rev.B **39**,11538 (1989)

[6] X.G.Wen, F.Wilczek, A.Zee Phys.Rev.B **38**,9335 (1989)

[7] E.Dagotto, A.Moreo Phys.Rev.Lett. **63**,2148 (1989)
D.Poilblanc, E.Gagliano, S.Bacci, E.Dagotto Phys.Rev.B **43**,10970 (1991)
H.Schulz, T.Ziman Europhys.Lett. **18**,355 (1992)

[8] M.P.Gelfand, R.R.P.Singh, D.A.Huse Phys.Rev.B **40**,10801 (1989)

[9] R.R.P.Singh, D.A.Huse Phys.Rev.Lett. **68**,1766 (1992)

[10] E.Manousakis, Rev.Mod.Phys. **63**,1 (1991)

[11] N.Read and S.Sachdev, Phys.Rev.Lett. **66**,1773 (1991)

[12] D.P.Arovas and A.Auerbach, Phys.Rev. B **38**,316 (1988)

[13] M.Di Stasio, E.Ercolessi, G.Morandi, A.Tagliacozzo and F.Ventriglia, Phys.Rev. B **45**,1939 (1992)

[14] M.Di Stasio, E.Ercolessi, G.Morandi, A.Tagliacozzo and F.Ventriglia, Int. Jou. of Mod. Phys. B **7**,3281 (1993)

[15] Diagonalization is achieved by means of four real functions of Q (with $\vec{Q} \geq 0,\ \Omega_m \geq 0$), $\xi_{lr}(Q)$, for each l $(l, r = 1, 4)$:

$$u_l(\pm\vec{Q}, \Omega_m) = \frac{1}{\sqrt{2}} \{(\xi_{l1}(Q) \mp \xi_{l2}(Q)) + i\,(\xi_{l3}(Q) \pm \xi_{l4}(Q))\} \ .$$

[16] J.W. Negele and H. Orland, "Quantum many-particle systems", Addison-Wesley (1988)

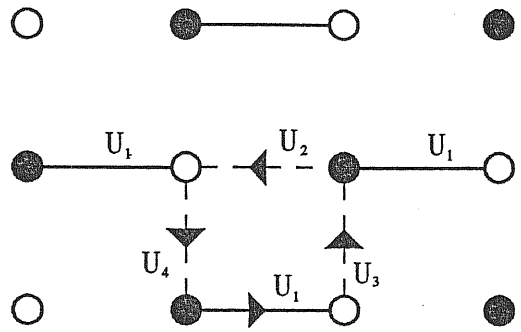

a)

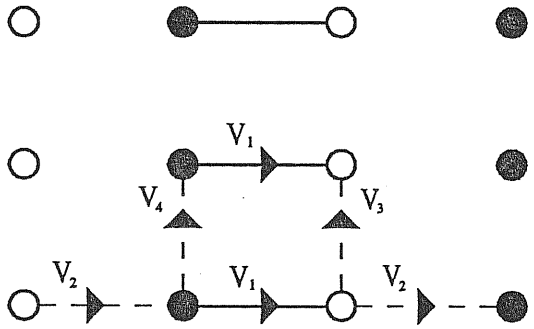

b)

figure 1

a) Pictorial representation of the link order parameter in terms of $\mathcal{U}_1, \mathcal{U}_2, \mathcal{U}_3, \mathcal{U}_4$. Periodicity is along the diagonals. Reversing the arrows implies complex conjugation. Black filled sites are named "even" in the text.

b) Pictorial representation of the link order parameter in terms of $\mathcal{V}_1, \mathcal{V}_2, \mathcal{V}_3, \mathcal{V}_4$. Periodicity is doubled on the x axes. Reversing the arrows implies complex conjugation. Black filled sites are named "even" in the text.

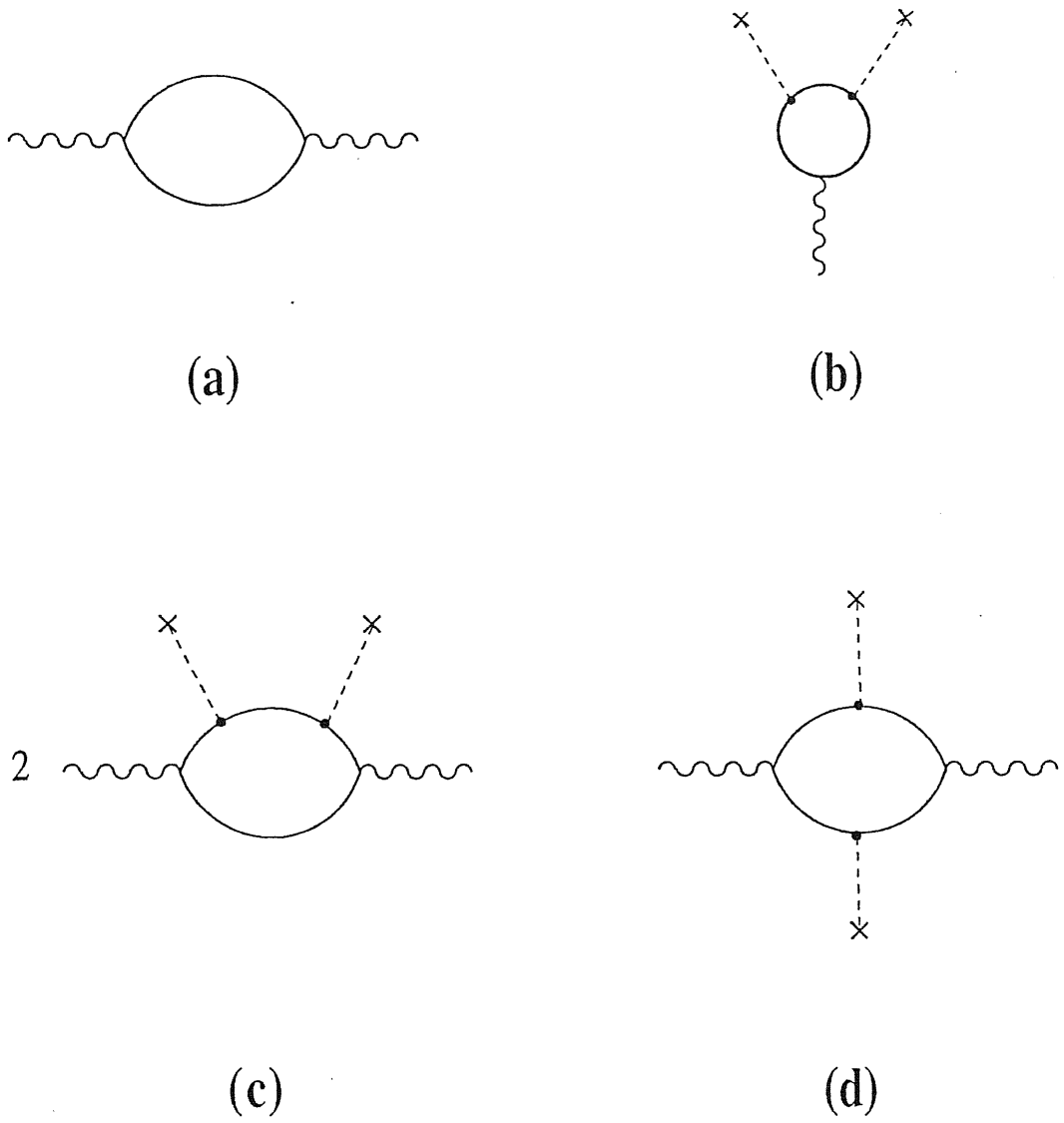

figure 2

Diagrammatic picture of the one loop expansion. Wavy lines are for the fluctuating fields and continuous lines for the propagators χ defined in the text. The on-site projector P_i is depicted as an external potential with a dashed cross line. (a) effective action contribution ; (b) δB contribution ; (c) and (d) $\delta^2 B$ constraint contributions

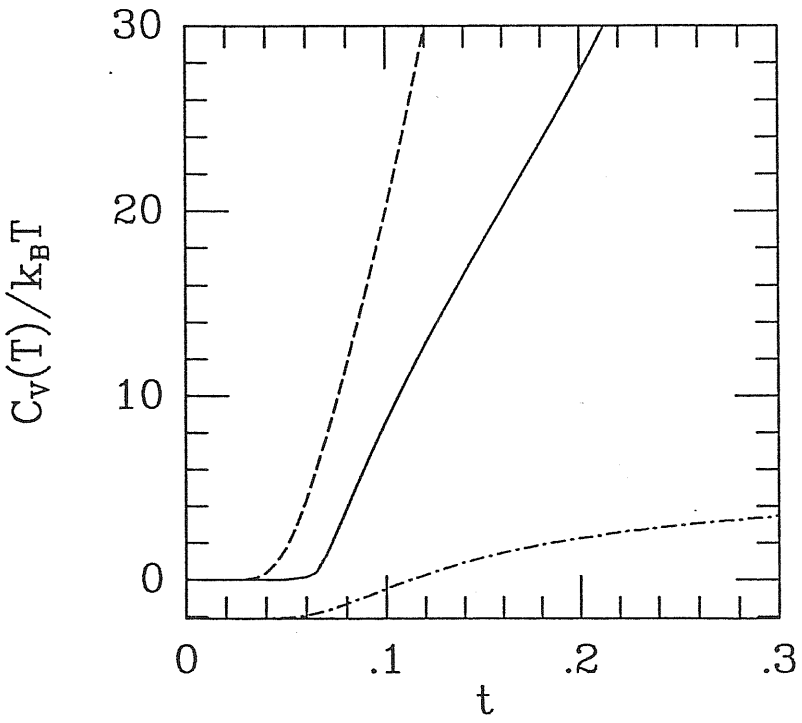

figure 3

Specific heat over temperature vs. temperature. The solid curve is in presence of the constraint and adding quantum fluctuations. The dotted dashed curve is without quantum fluctuations and shows the wrong behavior at low t described in the text. The dashed curve, reported for comparison, is in absence of the constraint and adding quantum fluctuations.

λ ($m \neq 0$)	$\lambda(m=0)$		deg.	mixture
STAGGERED DIMERS				
$\lambda_1^S = 1 - E(m)$	$1 - \frac{1}{2d}\tanh\frac{d}{2t} = 0$ 'zero mode'		1	$u_1(\vec{Q}), u_1(-\vec{Q})$
$\lambda_2^S = 1 - \frac{E(m)}{2}$	$1 - \frac{1}{2}\left(\frac{1}{2d}\tanh\frac{d}{2t} + \frac{1}{4t\cosh^2 d/2t}\right)$		6	$u_i(\vec{Q})$ i = 2,3,4
$\lambda_3^S = 1$	$1 - \frac{1}{4t\cosh^2 d/2t}$		1	$u_1(\vec{Q}), u_1(-\vec{Q})$
COLUMNAR DIMERS				
$\lambda_1^C = 1 - E(m)$	$1 - \frac{1}{2d}\tanh\frac{d}{2t} = 0$	'zero mode'	1	$v_1(\vec{Q}), v_1(-\vec{Q})$
		'flat second variation'	2	v_3^R, v_4^R v_3^I, v_4^I
$\lambda_2^C = 1 - \frac{E(m)}{2}$	$1 - \frac{1}{2}\left(\frac{1}{2d}\tanh\frac{d}{2t} + \frac{1}{4t\cosh^2 d/2t}\right)$		2	$v_2(\vec{Q})$
$\lambda_3^C = 1$	$1 - \frac{1}{4t\cosh^2 d/2t}$		3	$v_1(\vec{Q}), v_1(-\vec{Q})$ v_3^R, v_4^R v_3^I, v_4^I

Table I

Eigenvalues of the second variation of the effective action, as a function of the Matsubara frequencies Ω_m, for the dimer phases together with their degeneracy and the corresponding admixture of the fluctuating fields. The constraint is not included. Modes that vanish at $\Omega = 0$ are explicitly indicated.All the quantities are defined in the text.

Paper VII

Fluctuations around the magnetic and non-magnetic saddle points in the 2-D spin 1/2 frustrated Heisenberg model

M.Di Stasio[(1)], E.Ercolessi[(2)], G.Morandi[(3)]
and A.Tagliacozzo[(1,4)]

(1) S.I.S.S.A.-I.S.A.S.,v. Beirut2,I-34100 Miramare,Trieste,Italy

(2) Physics Dept.,Syracuse University, Syracuse,N.Y. 13244-1130,USA

(3) Dipartimento di Fisica, Universita' di Bologna,
INFM and INFN,v.Irnerio 46,I-40126 Bologna, Italy,

(4) Dipartimento di Scienze Fisiche,Universita' di Napoli
INFM,Mostra d'Oltremare Pad.19, I-80125 Napoli,Italy

Abstract

Fermionization of the spin operators is allowed only in the restricted Hilbert space of singly occupied sites. A new method to implement this single site-occupancy constraint is applied to the frustrated Heisenberg model. This method allows to study either magnetic or non-magnetic phases at finite temperatures. A quantitative estimate of the relative weight of quantum fluctuations around the disordered dimer phases and the antiferromagnetic phase is given.

SISSA: 136/93/CM/MB
SYRACUSE: SU-4240-543

1 Introduction

In the recent past remarkable evidences for antiferromagnetic correlations have been presented for the unfrustrated two dimensional (2D) spin 1/2 antiferromagnetic Heisenberg model (with interaction J_1 between nearest neighbor (NN) spins) on a square lattice[1]. As one can easily see, the Néel state has a non conserved order parameter. This means that the antiferromagnetic phase could get disordered even at zero temperature due to quantum fluctuations. Moreover, the presence of a next nearest neighbour (NNN) antiferromagnetic interaction (J_2) that introduces frustration in the antiferromagnetic order, enhances the effects of the quantum fluctuations. Many different methods have been applied to the study of the $J_1 - J_2$ model. Classically, this model exhibits a Néel ordered phase for $J_2/J_1 = \alpha^2 < 0.5$ and independent Néel order in the two sublattices when $\alpha^2 > 0.5$. It is generally agreed that there is a cross-over region, around $\alpha^2 \simeq 0.5$, in which the ground state gets disordered by quantum fluctuations[2], [3], [4], [5], [6]. The nature of the disordered state (or disordered states) is quite controversial. Among the disordered states proposed there are dimerized phases in which spin singlets are formed between nearest neighbor sites filling all the links in the lattice. Their generalization to RVB states have been proposed as competitive ground state candidates for the HTCS in their normal phase[7].

A method that allows for a study of ordered and non ordered phases in quantum spin systems has been recently proposed[8],[9] and is applied here to the $J_1 - J_2$ model. Starting with a fermionic representation of the spin operators, the partition function has to be evaluated as a trace over the restricted Hilbert space of singly occupied sites. This constraint can be implemented via an appropriate combination of derivatives of a suitable generating function. Within this framework, we have studied the effects of quantum fluctuations in dimer phases for both the columnar and staggered orders. In presence of frustration, the inclusion of the link diagonal fluctuating fields (see Fig.1) gives relevant contributions to the free energy. In particular we find that in the strongly frustrated limit, i.e. when $J_1 = J_2$ the two dimer phases become degenerate just as they are in the saddle point approximation. Concerning the antiferromagnetically ordered phase the linear spin wave results[2] are recovered at zero temperature and the constraint is found to act only at finite temperatures.

2 Generalized mean field solutions

The frustrated Heisenberg Hamiltonian we are dealing with is:

$$H = J_1 \sum_{(ij)_{NN}} \vec{S}_i \cdot \vec{S}_j + J_2 \sum_{(ij)_{NNN}} \vec{S}_i \cdot \vec{S}_j \qquad (1)$$

where $(ij)_{NN}((ij)_{NNN})$ stands for not repeated nearest (next nearest) neighbor pairs of sites. The spin operators can be represented in terms of fermion operators $(c^{\dagger}_{i,\sigma},c_{i,\sigma})$ and Pauli matrices $(\vec{\sigma})$ as:

$$\vec{S}_i = c^{\dagger}_{i,\alpha}\vec{\sigma}_{\alpha\beta}c_{i,\beta} \tag{2}$$

acting on the restricted Hilbert space of singly occupied sites whose projector is:

$$\mathbf{P} = \prod_i n_i(2-n_i) \tag{3}$$

(n_i being the occupation number operator). Due to the fact that $\mathbf{P}$ and H commute, the exact partition function can be written as:

$$\mathcal{Z} = Tr\left\{e^{-\beta H}\mathbf{P}\right\} \tag{4}$$

and can be calculated performing the appropriate derivatives of a generating function $\mathcal{Z}[z_i]$ as:

$$\begin{aligned}\mathcal{Z} &= \prod_i \frac{\partial}{\partial z_i}\left(2-\frac{\partial}{\partial z_i}\right)\mathcal{Z}[z_i]\Big|_{z_i=0} = \\ &= \prod_i \frac{\partial}{\partial z_i}\left(2-\frac{\partial}{\partial z_i}\right) Tr\left\{e^{-\beta H+\sum_i z_i n_i}\right\}\Big|_{z_i=0}\end{aligned}, \tag{5}$$

the last equality defining the generating function. We have introduced local chemical potentials z_i as source terms. The advantage is that $\mathcal{Z}[z_i]$ can

be evaluated with the usual techniques for unconstrained path integrals. In particular, introducing the anticommuting Grassmann fields $\psi^{\star}_{i\alpha}(\tau)$ and $\psi_{i\alpha}(\tau)$ ($\tau \in [0,1]$) we can decouple the four fermion terms via an Hubbard-Stratonovich transformation. Preparing for the magnetic and non-magnetic mean field solutions we adopt two different decoupling schemes. In the magnetic case we introduce auxiliary vector fields which play the role of the staggered magnetization:

$$\vec{\mathcal{M}}(q,\tau) = \frac{1}{\sqrt{N}} \sum_i e^{i\vec{q}\cdot\vec{R}_i} \psi^{\star}_{i\alpha}(\tau) \vec{\sigma}_{\alpha\beta} \psi_{i\beta}(\tau) \quad . \tag{6}$$

These are used to decouple the Fourier transformed four fermion terms of the Hamiltonian that is: $J_1 \bar{\gamma}(q) \vec{S}(q) \cdot \vec{S}(-q)$ where $\bar{\gamma}(q) = \gamma(q) + 2\alpha^2 \cos q_x \cos q_y$ and $\gamma(q) = \cos q_x + \cos q_y$.

In order to study the dimer link phases we single out instead the auxiliary fields:

$$\begin{aligned} \mathcal{U}_{ij}(\tau) &= \sum_{\alpha} \psi^{\star}_{i\alpha}(\tau) \psi_{j\alpha}(\tau) \quad i,j = NN \\ \mathcal{U}'_{ij}(\tau) &= \sum_{\alpha} \psi^{\star}_{i\alpha}(\tau) \psi_{j\alpha}(\tau) \quad i,j = NNN \end{aligned} \tag{7}$$

Now we can integrate out exactly the fermions and end up with a multi-dimensional integral over the auxiliary fields (called generically X). The resulting effective action depends on the auxiliary fields X and on the local

chemical potential z_i. The following relations holds:

$i) X(0) = X(1)$,

$ii) X(\tau) = \sum_m X(\Omega_m) e^{-i\Omega_m \tau} \quad (\Omega_m = 2m\pi)$,

$iii) Tr\{\mid X \mid^2\} = \sum_m Sp\{X(\Omega_m)X(-\Omega_m)\}$

and finally

$$Sp\{X(\Omega_m)X(-\Omega_m)\} = \begin{cases} \sum_{\vec{q}} \mid \vec{\mathcal{M}}(\vec{q}, \Omega_m) \mid^2 & \text{AFM case} \\ \sum_{(ij)} \mid \mathcal{U}_{ij}(\Omega_m) \mid^2 & \text{Dimer case} \end{cases}$$

The generating function reads:

$$\mathcal{Z}[z_i] = \int \mathcal{D}X \exp\left\{-\pi Tr\{\mid X \mid^2\} - S_{eff}[X, z_i]\right\} \quad . \tag{8}$$

The original partition function is then recovered as:

$$\mathcal{Z} = \int \mathcal{D}X \exp\left\{-\pi Tr\{\mid X \mid^2\} - S_{eff}[X] + \sum_i \ln 4B_i[X]\right\} \tag{9}$$

where:

$$S_{eff}[X] = -Tr\{\ln[1 + G_o\tilde{X}]\} \tag{10}$$

and

$$B_i = Tr\left\{[\chi G_o P_i]^2\right\} - 2Tr\left\{\chi G_o P_i\right\} - \left(Tr\left\{\chi G_o P_i\right\}\right)^2 \quad . \tag{11}$$

Here we have introduced the free Green function G_o whose matrix elements are: $(G_o)^{n,n'}_{\alpha,\beta}(ij) = (i\omega_n)^{-1}\delta_{i,j}\delta_{n,n'}\delta_{\alpha,\beta}$ ($\omega_n = (2n+1)\pi$) and the projector

P_i, onto the $i-th$ site of the lattice, whose matrix elements in the Wannier representation are $(P_i)_{jk} = \delta_{jk}\delta_{ij}$. Finally we have defined $\chi = (G_o^{-1} + \tilde{X})^{-1}$.

For the magnetic phase the matrix $\tilde{X}$ is:

$$\left(\tilde{X}_{AFM}\right)^{n,n'}_{\alpha\beta}(i,j) = -2\delta_{i,j}\sum_q \sqrt{\frac{-\pi\beta J_1\bar{\gamma}(q)}{N}} e^{i\vec{q}\cdot\vec{R}_i}\vec{\mathcal{M}}(q,\Omega_m)\cdot\vec{\sigma}_{\alpha\beta} \qquad (12)$$

($\Omega_m = \omega_n - \omega_{n'}$) and because it is diagonal in site indices the traces will be performed in direct space. For the non magnetic phases we have:

$$\left(\tilde{X}_{DIM}\right)^{n,n'}_{\alpha\beta}(i,j) = -\delta_{\alpha,\beta}\sqrt{\frac{\pi\beta J_1}{2}}\left[\mathcal{U}_{ij}(\Omega_m)\delta_{i-j,NN} + \alpha\mathcal{U}'_{ij}(\Omega_m)\delta_{i-j,NNN}\right] \qquad (13)$$

The staggered dimer phase, breaks translational invariance down to a $\sqrt{2}\times\sqrt{2}$ periodicity with two sites (black and white in Fig.1) per unit cell. For the columnar dimer phase, the elementary cell is 2×1 with two other black and white sites per cell as in Fig.1. In the two cases we have 8 different link fields. $\tilde{X}_{DIM}$ can be easily diagonalized in Fourier space where the traces will be performed.

Saddle point solutions are found as in Ref.([10]), and we discuss them briefly now.

1) Antiferromagnetic solution:

$$\vec{\mathcal{M}}(q,m) = \sqrt{\frac{2N}{\pi t}(1-\alpha^2)}M(\vec{\pi},0)\hat{z}\delta_{q,\pi}\delta_{m,0} \tag{14}$$

($t = 1/\beta J_1$ being the dimensionless temperature). The saddle point approximation to the free energy is:

$$f^o_{AFM} = 2M^2(1-\alpha^2) - 2t\ln\cosh x - t\ln 4\left(1 - \frac{1}{2\cosh^2 x}\right) \tag{15}$$

where $x = \frac{M}{t}(1-\alpha^2)$ and $M(t=0) = 1/2$. The last term is the contribution of the constraint. The inclusion of the constraint is exact at this level of approximation. In fact we find $< n_i >_{s.p.} = < n_i^2 >_{s.p.} = 1$ as required by the fermionization procedure.

2) Dimer solutions:

Dimer phases correspond to the choice of $\mathcal{U}_1 = d\sqrt{\frac{2}{\pi t}}$ and all the other $\mathcal{U}$'s equal to zero as depicted in Fig.1. They are degenerate and the saddle point free energy is:

$$f^o_{DIM} = d^2 - 2t\ln\cosh\frac{d}{2t} - t\ln 4B \tag{16}$$

where $B = 1 - \frac{1}{4}\left(\frac{\tanh x}{x} + \frac{1}{\cosh^2 x}\right)_{x=d/2t}$ and $d(t=0) = 1/2$. As one can see the dimer saddle point free energies are totally unaffected by the frustrating J_2 interaction. Constraint fermionization is not exact: $< n_i >_{s.p.} = 1$ but $< n_i^2 >_{s.p.} \neq 1$ when evaluated at the dimer saddle point. However, fluctu-

ations in the occupation number are always within 10% [11] in the whole range of temperature. We will come back to this point in the final discussion.

3 Quantum fluctuations

The effects of the frustration can be seen by evaluating the second variation of the total saddle point action. Here we describe in detail the unconstrained case and report only the changes that are brought about by the inclusion of the constraint. We denote by U the complex variations of the auxiliary fields. The Fourier transformed fields will be denoted by $u_l(\mathbf{Q})$ $(u'_l(\mathbf{Q}))$ and $v_l(\mathbf{Q})$ $(v'_l(\mathbf{Q}))$ for the staggered and columnar dimer phases respectively and by $m^{x(y,z)}(\mathbf{Q})$ for the antiferromagnetic case. Here $\mathbf{Q} = (\vec{Q}, \Omega_m)$ and $(U(-\mathbf{Q}))^* = U^*(\mathbf{Q})$. The second variation of the free energy is:

$$\beta\mathcal{F}^{(2)} = \pi Tr\{|U|^2\} + S^{(2)}_{eff} - \frac{1}{2}\sum_i \left(\frac{\delta^2 B_i}{B_i} - \left(\frac{\delta B_i}{B_i}\right)^2\right) \tag{17}$$

where:

$$\begin{aligned} S^{(2)}_{eff} &= \frac{1}{2} Tr\{\chi U \chi U\} \\ \delta B_i &= 2Tr\{\chi U \chi P_i \chi P_i\} \\ \delta^2 B_i &= 2Tr\{\chi U \chi P_i \chi U \chi P_i\} + 4Tr\{\chi U \chi U \chi P_i \chi P_i\} \end{aligned} \tag{18}$$

We analyze now in more details $\mathcal{F}^{(2)}$for the various phases.

1) Antiferromagnetic phase. We find:

$$S_{eff}^{(2)} = -\frac{\pi}{2t}\sum_{Q,m>0}\Big\{\Phi_+(m)\bar{\gamma}(Q)\left[|m^x(\mathbf{Q})|^2+|m^y(\mathbf{Q})|^2\right]$$
$$-i\Phi_-(m)\sqrt{\bar{\gamma}(Q)\bar{\gamma}(Q+\pi)}\left[m^x(\mathbf{Q})m^y(-\mathbf{Q})-m^y(\mathbf{Q})m^x(-\mathbf{Q})\right]\Big\}$$
$$+\frac{\pi}{2t}\Phi_z(0)\sum_Q\bar{\gamma}(Q)|m^z(Q,0)|^2 \qquad (19)$$

Here: $\Phi_+(m) = 8x\frac{\tanh x}{(i\Omega_m)^2-(4x)^2}$, $\Phi_-(m) = 2i\Omega_m\frac{\tanh x}{(i\Omega_m)^2-(4x)^2}$ and $\Phi_z(0) = \frac{1}{2\cosh^2 x}$ with $x = M/t(1-\alpha^2)$.

Adding the free part we can easily diagonalize the fluctuation matrix and perform the gaussian integration over $\mathcal{D}m = \prod_{Q,m}\prod_{i=x,y,z} d\Re m^i(\mathbf{Q})d\Im m^i(\mathbf{Q})$. In the absence of the constraint, the fluctuations parallel to $\hat{z}$ do not contribute to the $t=0$ free energy while the transverse fluctuations m^x and m^y mix as the usual spin waves thus yielding:

$$\Delta f_{AFM}(t=0) = 2M\frac{1}{N}\sum_q\left[\left(1-\alpha^2(1-\cos q_x\cos q_y)\right)^2-\left(\frac{\gamma(q)}{2}\right)^2\right]^{1/2}+$$
$$-2M(1-\alpha^2) \qquad (20)$$

The constraint affects only the temperature dependence of the free energy. The presence of the constraint does not affect the spin waves spectrum except for the different temperature dependence of the magnetization. The eigenvalue of the m^z mode is given by:

$$\lambda_z(m=0) = \pi \left[1 + \frac{\bar{\gamma}(q)}{4t\cosh^2 x} \left(1 - \frac{1}{B} \left(2M \tanh x - \frac{1}{2\cosh^2 x} \right) \right) \right]_{x=M/t(1-\alpha^2)} \tag{21}$$

where the last term comes from the constraint. The total zero temperature free energy is plotted in Fig.2. Note that the spin wave corrections to the free energy give an instability for $\alpha^2 \geq 0.5$. When the corrections to the magnetization are taken into account the instability is found for $\alpha^2 \simeq 0.4$.

2a) Staggered dimer phase. We have:

$$S^{(2)}_{eff} = \frac{\pi}{2t} \sum_{kq} \sum_{m} \sum_{\mu\nu} \Phi_{\mu\nu}(m)$$
$$< k\mu \mid U(m) + U'(m) \mid q\nu >< q\nu \mid U(-m) + U'(-m) \mid k\nu > \tag{22}$$

where $\mu, \nu = \pm$ and $|q\nu>$ is the basis where U is diagonal[10]. The functions $\Phi_{\mu\nu}(m)$ have the same expression as for the unfrustrated case because they depend only on the choice of the saddle point ($\Phi_{\mu\nu}(m) = \sum_n \frac{1}{i\omega_n - i\Omega_m - \mu 2d/t} \frac{1}{i\omega_n - \nu 2d/t}$).

Here we report explicitly only the $\Omega_m > 0$ fluctuating modes. These quantum fluctuations give all the zero temperature contribution to the free energy. The second variation of the effective action is:

$$S^{(2)}_{eff} = \frac{\pi}{2t} \sum_{Q} \sum_{m>0} \sum_{\mu\nu} \left\{ \sum_{i=1,4} \left[\mid u_i(\mathbf{Q}) \mid^2 + \mid u'_i(\mathbf{Q}) \mid^2 \right] + \right.$$

$$+\frac{\mu\nu}{2}\left[u_3(\mathbf{Q})u_3(-\mathbf{Q})+u_3^*(\mathbf{Q})u_3^*(-\mathbf{Q})\right]$$
$$+\mu\nu\left[u_1'(\mathbf{Q})u_2'(\mathbf{Q})^*+u_1'(\mathbf{Q})^*u_2'(\mathbf{Q})\right]$$
$$+\mu\nu\left[u_3'(\mathbf{Q})u_4'(\mathbf{Q})^*+u_3'(\mathbf{Q})^*u_4'(\mathbf{Q})\ \right]\ \Big\}\Phi_{\mu\nu}(m) \qquad (23)$$

Adding the free part for the auxiliary fields we can easily diagonalize the second variation matrix. The resulting eigenvalues for the $u_i(\mathbf{Q})$ fields are the same as in the absence of frustration[10]. The real and imaginary parts of u_1' and u_2' mix in the same way as the real and imaginary parts of u_3' and u_4' yielding finally the eigenvalues divided by π: $\lambda_3'=1$ and $\lambda_1'=1-\alpha^2E(m)$ (here: $E(m)=\frac{2d}{t^2}\frac{\tanh d/2t}{(i\Omega_m)^2+4d^2/t^2}$). They are four times degenerate for each value of $\vec{Q}$ in the reduced Brillouin zone. In Table I we report the eigenvalues, their degeneracies and admixtures.

The inclusion of the constraint does not change the symmetry of the eigenmodes and moreover does not change the zero temperature contribution to the free energy due to the diagonal link modes. We get:

$$\Delta f_{STA}(t=0)=-2d(1-1/\sqrt{2})-d\left(1-\sqrt{1-\alpha^2}\right) \qquad (24)$$

where the last term comes from the link diagonal auxiliary fluctuating fields. The only effect of the constraint on these diagonal fields contribution is at finite temperature. The free energy changes according to the following modification of the eigenvalues (divided by π):

$$\lambda_3' = 1 - \alpha^2 \tilde{\Phi}^-(m)$$

$$\lambda_1' = 1 - \alpha^2 E(m) - \alpha^2 \tilde{\Phi}^+(m) \qquad (25)$$

where $\tilde{\Phi}^- = -\frac{t^2}{2Bd^2} E(m)$, $\tilde{\Phi}^+ = \frac{d}{Bt^2} \frac{(2d/t)^2+5(\Omega_m)^2}{((2d/t)^2+(\Omega_m)^2)^3}$ and B is the constraint evaluated at the dimer saddle point.

2b) Columnar dimer phase.

Analyzing the second variation of the effective action we have found that the v_3' and v_4' modes do not mix leading to the fourfold degenerate eigenvalue $\lambda_2' = 1 - \alpha^2 E(m)/2$. On the contrary, the v_1' and v_2' modes mix with each other in the following way:

$$S_{eff}^{(2)}[v_1', v_2'] = \frac{\pi\alpha^2}{4} \sum_{m>0} \sum_{Q} E(m) \Big\{ \mid v_1'(\mathbf{Q}) \mid^2 + \mid v_2'(\mathbf{Q}) \mid^2 - \Big[v_1'(\mathbf{Q}) v_2'(-\mathbf{Q}) e^{-iQ_y} + v_1'(\mathbf{Q})^\star v_2'(-\mathbf{Q})^\star e^{iQ_y} \Big] \Big\} \qquad (26)$$

The resulting 4×4 matrix is (defining $W = \alpha^2 \frac{E(m)}{4}$):

$$\begin{pmatrix} \frac{1}{2} - W & 0 & -W\cos Q_y & -W\sin Q_y \\ 0 & \frac{1}{2} - W & -W\sin Q_y & W\cos Q_y \\ -W\cos Q_y & -W\sin Q_y & \frac{1}{2} - W & 0 \\ -W\sin Q_y & W\cos Q_y & 0 & \frac{1}{2} - W \end{pmatrix} \qquad (27)$$

Its eigenvalues are: $\lambda_3' = 1$ and $\lambda_1' = 1 - \alpha^2 E(m)$ and they are both doubly degenerate. The zero temperature contribution to the free energy is:

$$\Delta f_{COL}(t=0) = -\frac{d}{2} - d(1-1/\sqrt{2}) +$$
$$-\frac{d}{2}\left(1-\sqrt{1-\alpha^2}\right) - d\left(1-\sqrt{1-\frac{\alpha^2}{2}}\right) \qquad (28)$$

where the last two terms come from the four link diagonal modes. In Fig.3 we have plotted the zero temperature free energies including the quantum fluctuations for the staggered and columnar dimer phases (broken and full lines respectively) as a function of the frustration parameter α^2. The dotted line is the mean field free energy which is degenerate for the two phases.

4 Concluding remarks

We have studied the magnetic and non-magnetic phases of the 2D frustrated $J_1 - J_2$ Heisenberg hamiltonian starting from a Fermionic representation of the spin 1/2 operators. This can be done only if the fermion operators act on the restricted Hilbert space of singly occupied sites. Implementing this projection with a method recently proposed[8], we have studied the AFM phase and the columnar and staggered dimer phases in presence of frustration. In particular we have studied the effects of quantum fluctuations around these generalized mean field phases. The relevance of the inclusion of quantum fluctuations in order to obtain the correct thermodynamical behavior has been pointed out recently in the unfrustrated case[10].

By including the constraint of single site-occupancy at this level of approximation (saddle point and one-loop corrections), we are unable to overcome completely the drawbacks of unconstrained fermionization which makes the estimate of the ground state energies unsatisfactory. In fact while numerical studies suggest strongly an AFM ground state in the unfrustrated case[12] we have found lower energies for the dimer phases. We believe that even if the entropy correction term ($\ln B$) strongly depresses the fluctuations, one-loop corrections are not enough to provide a reliable quantitative estimate of the relative ground state energies when different decouplings are adopted[10].

Here we have reported the effects of frustration on the antiferromagnetic phase and on the non magnetic dimer phases when quantum corrections are added.

The dimer phases are degenerate and the free energy does not depend on α at the mean field level. Including the quantum corrections the degeneracy lifts in favour of the columnar ordered phase. As one can see from Fig.(3), in the extremely frustrated limit of $\alpha = 1$ the two dimer phases are again degenerate. This is the limiting case above which the curvature matrix of the fluctuations acquires negative eigenvalues and the saddle points become simultaneously unstable. Of course at this limit point a cross-over is expected towards other dimer saddle points defined on the diagonal lattice.

At this level of approximation we have found the spin wave results for

the zero temperature corrections to the AFM free energy and consequently the instability of this saddle point for $\alpha^2 \geq 0.5$.

Finally, as expected from numerical studies[3], [4], the magnetic and the non-magnetic phases show opposite trends for the free energies as a function of the frustrating parameters α. While the AFM free energy increases (see Fig.2) the free energies of the dimer phases decrease substantially, thus giving a good chance to these phases to be stabilized in the intermediate range of frustration, i.e. $\alpha^2 \sim 0.5$.

References

[1] For a recent review see: E.Manousakis Rev.Mod.Phys. **63**,1 (1991)

[2] Spin waves approaches: P.Chandra, B.Doucot Phys.Rev. B **38**,9335 (1988); M.Takahashi Phys.rev.B **40**,2494 (1989); C.Burder, F.Mila Europhys.Lett. **17**,463 (1992); Q.F.Zhong, S.Sorella Europhys.Lett. **21**,629 (1992)

[3] Exact diagonalizations: E.Dagotto, A.Moreo Phys.Rev.Lett. **63**,2148(1989); D.Poilblanc, E.Gagliano, S.Bacci, E.Dagotto Phys.Rev.B **43**,10970 (1991); H.Schulz, T.Ziman Europhys.Lett. **18**,355 (1992)

[4] Series expansions: M.P.Gelfand, R.R.P.Singh, D.A.Huse Phys.Rev.B **40**,10801 (1989); R.R.P.Singh, N.Narajanan Phys.Rev.Lett. **65**,1072 (1990); R.R.P.Singh, D.A.Huse Phys.Rev.Lett. **68**,1766 (1992)

[5] Large N expansion: N.Read, S.Sachdev Phys.Rev.Lett. **66**,1773 (1991)

[6] Non Linear σ model approach: T.Einarsson, H.Johannesson Phys.Rev.B **43**,5867 (1991)

[7] P.W. Anderson Science **235**,1196 (1987)

[8] M.Di Stasio, E.Ercolessi, G.Morandi, A.Tagliacozzo, F.Ventriglia Phys.Rev.B **45**,1939 (1992)

[9] M.Di Stasio Phys.Rev.B **46**,9825 (1992)

[10] M.Di Stasio, E.Ercolessi, G.Morandi, A.Tagliacozzo Europhys.Lett.(submitted)

[11] M.Di Stasio, E.Ercolessi, G.Morandi, A.Tagliacozzo, F.Ventriglia Int.Jou.Mod.Phys.B **7**,3281 (1993)

[12] J.D.Reger,A.P.Young Phys.Rev. B**37**,5978(1988); N.Trivedi,D.Ceperly Phys.Rev. B**40**,2737(1989); S.D.Liang Phys.Rev. B **42**,6555(1990); B.Bernu, C.Lhuillier, L.Pierre Phys.Rev.Lett. **69**,2590 (1992)

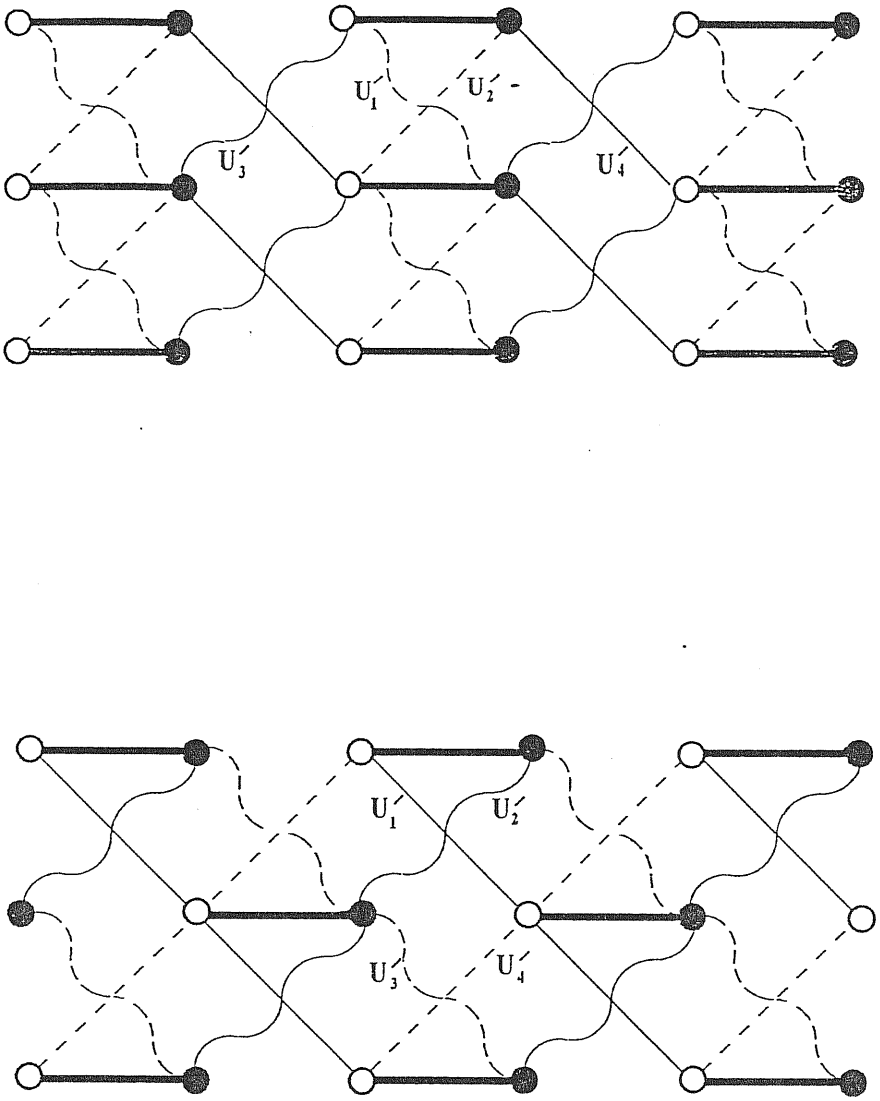

Fig.1 Pictorial representation of the link order parameter (heavy line) and of the diagonal fluctuating bond fields in the columnar and staggered dimer phases.

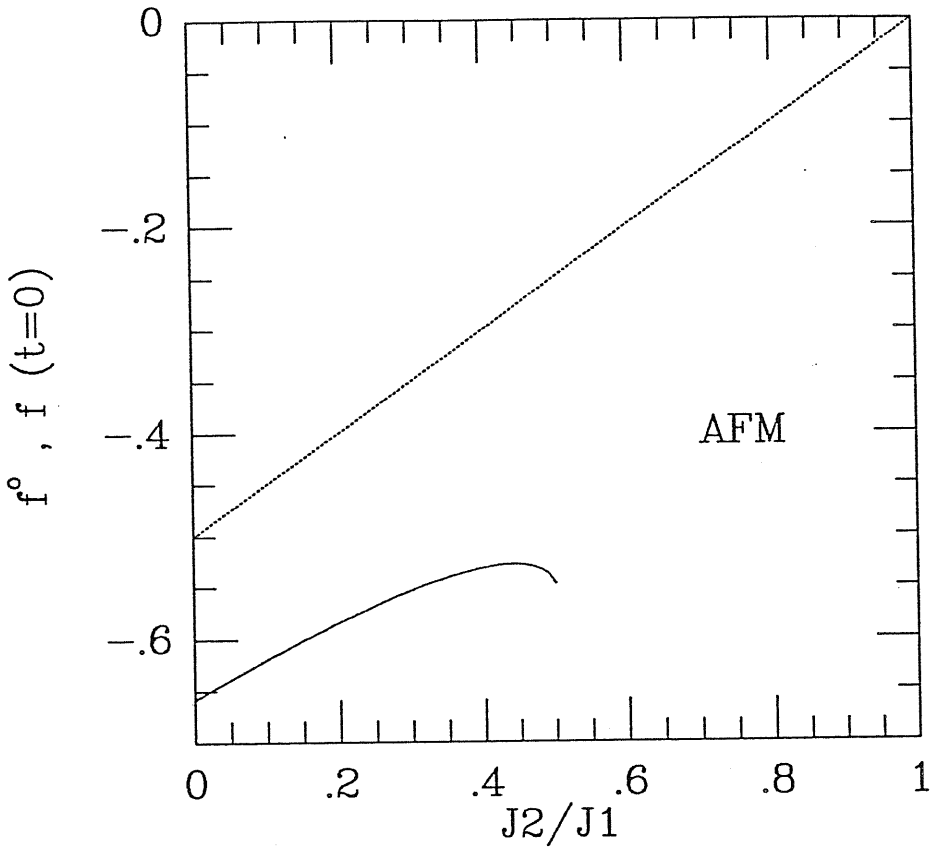

Fig.2 Zero temperature results for the mean field free energy (dotted curve) and for the one-loop corrected free energy (continuous curve) of the antiferromagnetic phase vs. α^2.

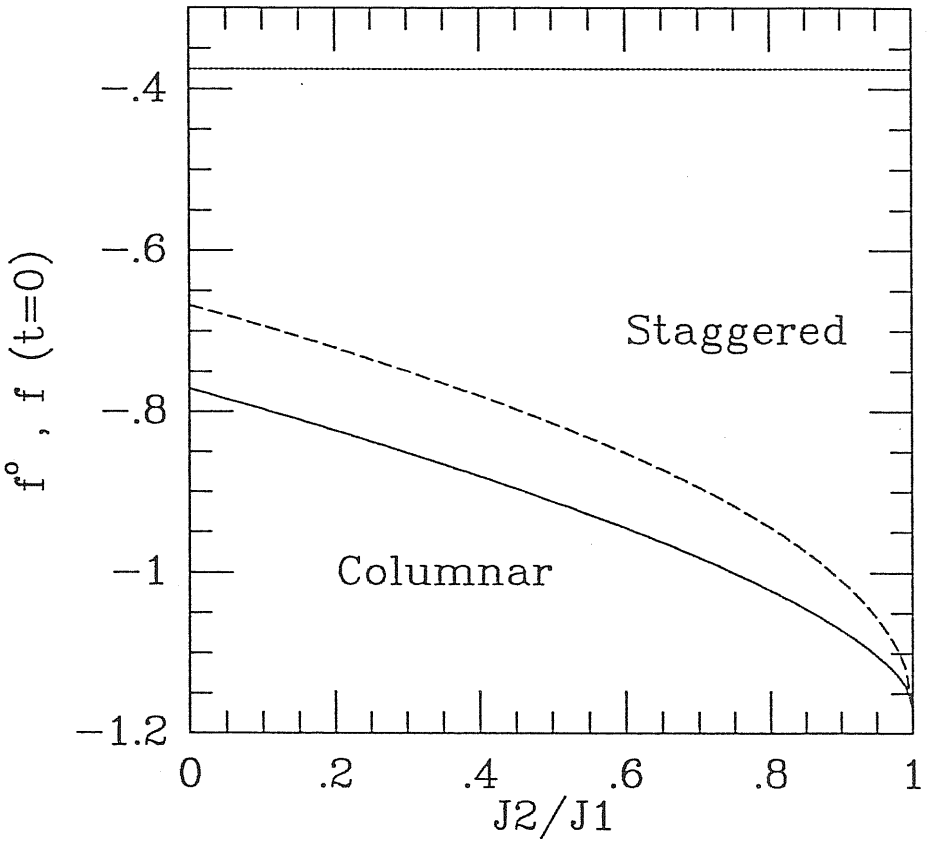

Fig.3 Zero temperature results for the staggered (dashed curve) and columnar (continuous curve) dimer free energy vs. α^2. The mean field degenerate free energy of both phases is given by the dotted curve.

	STAGGERED		COLUMNAR	
λ $(m \neq 0)$	degeneracy	mixture	degeneracy	mixture
$\lambda_1 = 1 - E(m)$	1	$u_1(Q), u_1(-Q)$	3	$v_1(Q), v_1(-Q)$ v_3^R, v_4^R v_3^I, v_4^I
$\lambda_2 = 1 - \frac{E(m)}{2}$	6	$u_i(Q)$ i = 2,3,4	2	$v_2(Q)$
$\lambda_3 = 1$	1	$u_1(Q), u_1(-Q)$	3	$v_1(Q), v_1(-Q)$ v_3^R, v_4^R v_3^I, v_4^I
$\lambda_1' = 1 - \alpha^2 E(m)$	4	$u_1'^{R(I)}(Q), u_2'^{R(I)}(-Q)$ $u_3'^{R(I)}(Q), u_4'^{R(I)}(-Q)$	2	$v_1'^R(Q), v_2'^R(Q)$ $v_1'^I(Q), v_2'^I(Q)$
$\lambda_2' = 1 - \alpha^2 \frac{E(m)}{2}$	0		4	v_3' v_4'
$\lambda_3' = 1$	4	$u_1'^{R(I)}(Q), u_2'^{R(I)}(-Q)$ $u_3'^{R(I)}(Q), u_4'^{R(I)}(-Q)$	2	$v_1'^R(Q), v_2'^R(Q)$ $v_1'^I(Q), v_2'^I(Q)$

Table I

Eigenvalues of the second variation of the effective action, as a function of Matsubara frequencies Ω_m, for the staggered and columnar dimer phases together with their degeneracy and the corresponding admixture of the fluctuating fields. The constraint is not included. All the quantities are defined in the text.

Paper VIII

Effective Action and Adiabatic Expansions for the 1-D and 2-D Hubbard models at half-filling

M.Di Stasio[(1)], E.Ercolessi[(2)], G.Morandi[(3),(⋆)]
R.Righi[(4)], A.Tagliacozzo[(1,5)] and G.P.Zucchelli[(5)]

(1) S.I.S.S.A.-I.S.A.S.,v. Beirut2,I-34100 Miramare,Trieste,Italy

(2) Physics Dept.,Syracuse University, Syracuse,N.Y. 13244-1130,USA

(3) Jawaharlal Nehru Centre for Advanced Scientific Research
and Centre for Theoretical Studies. Indian Institute of Science,
Bangalore.India. INFM and INFN, Bologna, Italy.

(4) Dipartimento di Fisica, Universita' di Bologna,
v.Irnerio 46,I-40126 Bologna, Italy.

(5) Dipartimento di Scienze Fisiche,Universita' di Napoli
INFM,Mostra d'Oltremare Pad.19, I-80125 Napoli,Italy

(⋆) Permanent address: (4) Dipartimento di Fisica, Universita' di Bologna, v.Irnerio 46,I-40126 Bologna, Italy.

SISSA 138/93/CM/MB

SU-4240-544

Abstract

We analyze here the occurrence of antiferromagnetic (AFM) correlations in the half filled Hubbard model in one and two space dimensions using a natural fermionic representation of the model and a newly proposed way of implementing the half-filling constraint. We find that our way of implementing the constraint is capable of enforcing it exactly already at the lowest levels of approximation. We discuss how to develop a systematic adiabatic expansion for the model and how Berry's phase contributions arise quite naturally from the adiabatic expansion. At low temperatures and in the continuum limit the model gets mapped onto an O(3) nonlinear sigma model (NLσ). A topological, Wess-Zumino term is present in the effective action of the 1D NLσ as expected, while no topological terms are present in 2D. Some specific difficulties that arise in connection with the implementation of an adiabatic expansion scheme within a thermodynamic context are also discussed, and we hint at possible solutions.

Since its inception in the early Sixties the Hubbard model [1],[2] has proved to be one of the most challenging playgrounds for theoretical Solid State Physics. Devised originally to provide a model for the Mott transition [3], i.e. for the fact that systems like the time-honoured oxide V_2O_3 (a classical "Mott insulator") that ought to be "bona fide" metals having a half filled band are instead insulators *and* antiferromagnets, the model, despite its apparent and deceptive simplicity, has become to be considered as some kind of a paradigm for problems involving strongly correlated electrons in which one cannot single out any kind of small parameter and hence no straightforward weak-coupling expansions (perturbation theory, e.g.) can give any reasonable answer to the relevant physical problems the model is supposed to embody.

The simplest, one-band, version of the Hubbard model is described by the Hamiltonian:

$$\mathcal{H} = -\sum_{ij\sigma} t_{ij} c^{\dagger}_{i\sigma} c_{j\sigma} + U \sum_{i} \hat{n}_{i\uparrow} \hat{n}_{i\downarrow} \qquad (1)$$

where Latin indices label lattice sites on an arbitrary lattice, $\sigma = \uparrow, \downarrow$ is a spin index (we consider here only spin-1/2 fermions), the $c_{i\sigma}$'s are Fermion annihilation operators and: $\hat{n}_{i\sigma} =: c^{\dagger}_{i\sigma} c_{i\sigma}$.

The parameters of the model are the on-site Coulomb repulsion U and the hopping integral t_{ij} [2]. Usually, although not necessarily, the hopping integral is taken as a constant: $t_{ij} = const. = t$ if i and j are nearest neighbor sites and zero otherwise.

That for positive U the Hubbard model can exhibit AFM correlations and insulating behavior when there is one electron per site and for large values of the ratio $U/|t|$ has been known for quite some time from approximate treatments of the Hamiltonian (1) [1],[4] as well as of more sophisticated versions thereof. Actually, if one restricts (projects) the Hubbard Hamiltonian to the *half-filled* subspace of the full Hilbert space, which is characterized by the *operator* condition:

$$\hat{n}_i = \sum_\sigma \hat{n}_{i\sigma} = 1 \ \ \forall i \tag{2}$$

then it can be shown [2],[5],[6] that to lowest (second) order in $|t|/U$ the Hubbard Hamiltonian can be mapped onto an AFM Heisenberg Hamiltonian. The hopping term is completely quenched by the projection and the system is AFM and an insulator.

The procedure of Refs.[5] and [6] can be extended to higher orders in $|t|/U$, and it has been shown [7] that one obtains to all orders in the expansion an effective AFM spin Hamiltonian.

Below half-filling, i.e. if one changes Eqns.(2) into the set of inequalities: $\hat{n}_i \leq 1 \ \forall i$, then one obtains the so-called "t-J" model [8]. A discussion of the latter is however beyond the scopes of the present paper, that will be concerned only with some features of the Hubbard model at exact half-filling.

In recent years, and after the discovery of high-T_c superconductivity in cuprous oxides [9], the Hubbard model has been advocated, mainly by the

Princeton group [10],[11],[12],[13] as the most adequate model for the description of the dynamics of electrons in the $Cu-O$ planes of the cuprates. In this context one is led to consider the Hubbard model on a $2D$ lattice and in the limit of strong coupling.

Since the early studies of the model in restricted subspaces [14] it has become evident that one of the major difficulties resides in a consistent implementation of the relevant projections. In the case of exact half-filling, the projector that implements the constraint of Eq. (2) is:

$$\mathrm{P}_{hf} =: \prod_i \hat{n}_i(2-\hat{n}_i) \tag{3}$$

We are thus led to consider a partition function defined by a restricted trace of the form:

$$\mathcal{Z} = Tr\left\{\exp[-\beta\mathcal{H}]\cdot \mathrm{P}_{hf}\right\} \tag{4}$$

In the strong-coupling limit we can take for $\mathcal{H}$ the effective Heisenberg-type Hamiltonian [2]:

$$\mathcal{H} = \frac{1}{2}\sum_{ij} J_{ij}\vec{S}_i\cdot\vec{S}_j \;\;;\;\; J_{ij} = 4|t_{ij}|^2/U \tag{5}$$

where the $\vec{S}_i$'s are spin operators given in the following fermionic representation:

$$\vec{S}_i =: \frac{1}{2}\sum_{\alpha,\beta=\uparrow\downarrow} c^\dagger_{i\alpha}\vec{\sigma}_{\alpha\beta}c_{i\beta} \tag{6}$$

where: $\vec{\sigma} = (\sigma_1,\sigma_2,\sigma_3)$ are the Pauli matrices.

The $\vec{S}_i$'s close on the Lie algebra of SU(2), and they represent [2] a spin 1/2 on the doublet of states with single occupancy (on each site) and, separately, spin 0 on the states with zero and double occupancy respectively. They represent therefore "bona fide" spin 1/2 operators when and only when the half-filling projection is implemented correctly.

Some of us [15], [16], [17] have devised recently a novel way of implementing the half-filling constraint that we will briefly summarize here.

Taking advantage of the fact that the on-site number operators $\hat{n}_i$ commute with the Hamiltonian (5) for both values (S_i=0 or S_i=1/2) of the local spins, we can introduce a *generating function* $\mathcal{Z}[z]$ defined by the unrestricted trace:

$$\mathcal{Z}[z] = Tr\left\{\exp\left[-\beta(\mathcal{H} - \beta^{-1}\sum_i z_i\hat{n}_i)\right]\right\} \tag{7}$$

The z_i's resemble local chemical potentials. However, they are considered here simply as real numbers with no further physical implications, and the restricted trace (4) is recovered as:

$$\mathcal{Z} = \prod_i \frac{\partial}{\partial z_i}\left\{2 - \frac{\partial}{\partial z_i}\right\}\mathcal{Z}[z_i]\Big|_{z_i=0} \tag{8}$$

The advantage of working with the generating function (7) is that, as already mentioned, the trace is now unrestricted, and we can (and will in the sequel) employ the full machinery of finite-temperature many-body and functional integral techniques [18] for its evaluation.

Our method of implementing the constraint is in principle exact. However, its actual effectiveness when one resorts to specific approximations has to be tested in each case separately.

The constraint will be implemented exactly iff:

$$< \hat{n}_i >=< \hat{n}_i^2 >= 1 \ \ \forall i \tag{9}$$

In all the cases that we have studied up to now [17] we have found: $< \hat{n}_i >= 1$ already at the level of the saddle-point approximation to the functional integral expression [18] of the partition function, while, at the same level of approximation, $< \hat{n}_i^2 >$ was found to deviate from its exact value by at most 10% and in a rather narrow temperature range in the study of the staggered dimer phase [17],[19].

For reasons that will become apparent shortly, we will rewrite the partition function as:

$$\mathcal{Z} = \exp\left[\frac{3N}{8}\beta J'\right] Tr\left\{\exp\left[-\beta\left(\mathcal{H} + \frac{3NJ'}{8}\right)\right] \cdot \mathbf{P}_{hf}\right\} \tag{10}$$

for some constant J'.

This is of course a trivial identity. However, in the half-filled, spin 1/2 subspace where: $\vec{S}_i^2 = S_i(S_i+1) = 3/4$, we can rewrite the constant term inside the trace as:

$$\frac{3NJ'}{8} = \frac{1}{2}J' \sum_i \vec{S}_i \cdot \vec{S}_i \tag{11}$$

All in all, this amounts to redefining the Hamiltonian as:

$$\mathcal{H} = \frac{1}{2}\sum_{ij} \tilde{J}_{ij}\vec{S}_i \cdot \vec{S}_j \tag{12}$$

where:

$$\tilde{J}_{ij} =: J_{ij} + J'\delta_{i,j} \tag{13}$$

The additional on-site coupling J' will be assumed to be such that the *matrix* $||\tilde{J}_{ij}||$ be *negative-definite*, a property that will turn out to be essential later on. The constant $(\exp[3N\beta J'/8])$ that we have just introduced in front of the trace will be neglected henceforth.

The generating function of Eq.(7) can be expressed as a functional integral over Grassmann variables [18], thus being given by:

$$\begin{aligned} &\mathcal{Z}[z] = \int [\mathcal{D}\psi^\star \mathcal{D}\psi] \\ &\exp\left\{ -\sum_{i\alpha} \int_0^1 d\tau \psi^\star_{i\alpha}(\tau)(\partial_\tau - z_i)\psi_{i\alpha}(\tau) - \beta \int_0^1 d\tau \mathcal{H}(\tau) \right\} \end{aligned} \tag{14}$$

where the Hamiltonian $\mathcal{H}$ is expressed now in terms of the Grassmann variables.

We want now to decouple the quartic fermionic Hamiltonian by using a Hubbard-Stratonovich transformation [20],[21], [22]. To this effect, let us recall some elementary facts concerning multidimensional Gaussian identities.

Let A be a *negative-definite* $N \times N$ symmetric matrix with real entries.

Then:

$$\exp\left[-\frac{1}{4} < h, Ah >\right] =$$
$$= \left\{\pi^N |\det A|\right\}^{-1/2} \int_{-\infty}^{\infty} \{\prod_i dx_i\} \exp\left[< x, (A^{-1})x > - < h, x >\right] \quad (15)$$

where h and x are N-dimensional real vectors.

If, in addition, h (and hence x) carries an additional index: $h \to h^\alpha$, $\alpha = 1, ..., n$ for some n, then:

$$\exp\left[-\frac{1}{4}\sum_\alpha < h^\alpha, Ah^\alpha >\right] = \left\{\pi^N |\det A|\right\}^{-n/2} \int_{-\infty}^{\infty} \{\prod_{i\alpha} dx_i^\alpha\}$$
$$\exp\left[\sum_\alpha \left\{< x^\alpha, (A^{-1})x^\alpha > - < h^\alpha, x^\alpha >\right\}\right] \quad (16)$$

Setting now:

$$n = 3 \ , \ h_i^\alpha = S_i^\alpha \ , \ A = 2\beta\tilde{J} \ , \ x_i^\alpha = \beta\phi_i^\alpha \quad (17)$$

we obtain:

$$\exp\left[-\frac{\beta}{2}\sum_{ij} \tilde{J}_{ij}\vec{S}_i \cdot \vec{S}_j\right] = \left\{\left(\frac{2\pi}{\beta}\right)^N |\det \tilde{J}|\right\}^{-\frac{3}{2}} \int \{\prod_i d\vec{\phi}_i\}$$
$$\exp\left\{\frac{\beta}{2}\sum_{ij}(\tilde{J}^{-1})_{ij}\vec{\phi}_i \cdot \vec{\phi}_j - \beta\sum_i \vec{\phi}_i \cdot \vec{S}_i\right\} \quad (18)$$

The r.h.s. of Eq.(18) makes sense only if $\tilde{J}$ (and hence $\tilde{J}^{-1}$) is negative definite, which clarifies why previously we had to renormalize J to $\tilde{J}$.

Functional integrals are usually evaluated by performing a "time slicing" of the imaginary time interval $[0, 1]$. The Gaussian identity (18) can then be applied to each slice.

Lumping all multiplicative constants into a normalization factor $\mathcal{N}$, the generating function of Eq.(14) can be rewritten as a functional integral over auxiliary fields in the following form:

$$\mathcal{Z}[z] = \mathcal{N} \int \{\prod_{i\tau} d\vec{\phi}_i(\tau)\} \exp\left\{\frac{\beta}{2} \sum_{ij} \int_0^1 d\tau (\tilde{J}^{-1})_{ij} \vec{\phi}_i(\tau) \cdot \vec{\phi}_j(\tau)\right\} \mathcal{Z}[z; \{\vec{\phi}(\tau)\}] \tag{19}$$

where:

$$\mathcal{Z}[z; \{\vec{\phi}(\tau)\}] = \int [\mathcal{D}\psi^* \mathcal{D}\psi] \exp\left\{-\sum_i \int_0^1 d\tau d\tau' \sum_{\mu\nu} \psi^*_{i\mu}(\tau) A^{(i)}_{\mu\nu}(\tau, \tau') \psi_{i\nu}(\tau')\right\} \tag{20}$$

and the operators $A^{(i)}$ are given by:

$$A^{(i)}_{\mu\nu}(\tau, \tau') =: \left\{(\partial_\tau - z_i)\delta_{\mu\nu} + \frac{\beta}{2} \vec{\phi}_i(\tau) \cdot \vec{\sigma}_{\mu\nu}\right\} \delta(\tau - \tau') \ , \ i = 1, ..., N \tag{21}$$

while the auxiliary, and normally distributed, random fields $\vec{\phi}_i(\tau)$ obey the Bose-type boundary conditions:

$$\vec{\phi}_i(0) = \vec{\phi}_i(1) \ , \ i = 1, ..., N \tag{22}$$

The prefactor $\mathcal{N}$ can be determined by the requirement that the Gaussian functional average be normalized, i.e. by:

$$\mathcal{N}^{-1} = \int \{\prod_{i\tau} d\vec{\phi}_i(\tau)\} \exp\left\{\frac{\beta}{2} \sum_{ij} \int_0^1 d\tau (\tilde{J}^{-1})_{ij} \vec{\phi}_i(\tau) \cdot \vec{\phi}_j(\tau)\right\} \tag{23}$$

According to the well known rules of Grassmann integration [18]:

$$\mathcal{Z}[z; \{\vec{\phi}(\tau)\}] = \prod_i \det A^{(i)} = \exp\left\{\sum_i Tr(\ln A^{(i)})\right\} \tag{24}$$

or, explicitly:

$$\mathcal{Z}[z;\{\vec{\phi}(\tau)\}] = \exp\left\{\sum_i Sp\int_0^1 d\tau[\ln A^{(i)}](\tau,\tau^+)\right\} \tag{25}$$

where "Sp" stands for a trace over the spin indices alone.

Everything acquires a more familiar appearance if we introduce the Fourier transforms, namely if we expand both the $\psi_{i\alpha}$'s and the $A^{(i)}$'s as:

$$\psi_{i\alpha}(\tau) = \sum_n \exp[-i\omega_n\tau]\psi_{i\alpha}(n) \tag{26}$$

and:

$$A^{(i)}(\tau,\tau') = \sum_{nn'} \exp[-i(\omega_n\tau - \omega_{n'}\tau')]A^{(i)}(n,n') \tag{27}$$

where: $\omega_n = (2n+1)\pi$, $-\infty < n < +\infty$ are fermionic Matsubara frequencies. Then it is easily seen that:

$$A^{(i)}(n,n') = (-i\omega_n - z_i)\delta_{\mu\nu}\delta_{nn'} + \frac{\beta}{2}\vec{\sigma}_{\mu\nu}\cdot\vec{\phi}_i(\Omega_m)\ ;\ \Omega_m =: \omega_n - \omega_{n'} \tag{28}$$

and:

$$Sp\int_0^1 d\tau[\ln A^{(i)}](\tau,\tau^+) = \sum_n \exp[i\omega_n 0^+]Sp[\ln A^{(i)}](n,n) \tag{29}$$

Before proceeding, let's pause a moment and examine the simplest approximation to the functional integral, namely the *static approximation*, corresponding to the restriction of the functional integral to time independent fields, i.e.:

$$\vec{\phi}_i(\tau) = const. \ \Leftrightarrow\ \vec{\phi}_i(\Omega_m) = \vec{\phi}_i\cdot\delta_{m,0} \tag{30}$$

In such a case, $A^{(i)}$ becomes diagonal in the Matsubara indices and the frequency sum on the r.h.s. of Eq.(29) is easily evaluated by standard contour-integration techniques, yielding:

$$\mathcal{Z}_{st.}[z;\{\vec{\phi}\}] = \exp\left\{\sum_i \ln\left[1 + e^{2z_i} + 2e^{z_i}\cosh(\beta|\vec{\phi}_i|/2)\right]\right\} \tag{31}$$

Using then Eq.(8) to enforce the constraint, we find eventually that the static partition function is given by:

$$\mathcal{Z}_{st.} = \mathcal{N}\int\{\prod_i d\vec{\phi}_i\}\exp\left\{S_{eff}[\vec{\phi}]\right\} \tag{32}$$

where:

$$S_{eff}[\vec{\phi}] =: \frac{\beta}{2}\sum_{ij}\left(\tilde{J}^{-1}\right)_{ij}\vec{\phi}_i\cdot\vec{\phi}_j + \sum_i \ln[2\cosh(\beta|\vec{\phi}_i|/2)] \tag{33}$$

The mean field approximation is obtained, as usual, by evaluating the multiple integral on the r.h.s. of Eq.(32) by the saddle point method. The saddle points are determined by the equations:

$$\frac{\partial S_{eff}}{\partial \phi_i^\alpha} = 0 \tag{34}$$

Using Eq.(13), we get the explicit form of Eqns.(34) as:

$$\phi_i^\alpha\left\{1 + \frac{J'}{2|\vec{\phi}_i|}\tanh\left(\beta|\vec{\phi}_i|/2\right)\right\} = -\frac{1}{2}\sum_j J_{ij}\frac{\phi_j^\alpha}{|\vec{\phi}_j|}\tanh\left(\beta|\vec{\phi}_j|/2\right) \tag{35}$$

$(\alpha = 1,2,3)$.

For the standard case in which $J_{ij} = J > 0$ if i and j are nearest neighbors and zero otherwise, and defining:

$$\vec{\psi}_i =: J^{-1}\vec{\phi}_i \quad \text{and:} \quad \beta J = \frac{1}{t} \tag{36}$$

we find easily:

$$\psi_i^\alpha \left\{ 1 + \frac{J'}{2J|\vec{\psi}_i|} \tanh\left(\frac{|\vec{\psi}_i|}{2t}\right) \right\} = -\frac{1}{2} \sum_{j,n.n.} \frac{\psi_j^\alpha}{|\vec{\psi}_j|} \tanh\left(\frac{|\vec{\psi}_j|}{2t}\right) \qquad (37)$$

Considering, for the sake of definiteness, a bipartite lattice, we can look for AFM solutions of the form say:

$$\psi_i^\alpha = \delta^{\alpha,3}(-1)^{||i||} m \ , \ m = m(t) \geq 0 \qquad (38)$$

where: $||i|| =: |i_x + i_y|$ for a 2D lattice.

Then, we obtain the self-consistency equation for m in the form:

$$m(t) \left\{ 1 + \frac{J'}{2Jm(t)} \tanh\left(\frac{m(t)}{2t}\right) \right\} = \frac{\delta}{2} \tanh\left(\frac{m(t)}{2t}\right) \qquad (39)$$

where δ is the coordination number of the lattice. This predicts, e.g., a transition at:

$$t = t_c = \frac{1}{4}\left(\delta - \frac{J'}{J}\right) \qquad (40)$$

while, near t_c, $m(t)$ behaves as:

$$m(t) \approx \sqrt{12 t_c}(t_c - t)^{1/2} \ , \ t \lesssim t_c \qquad (41)$$

These expressions are regular functions of J' (as long as $J' \leq 0$) that can therefore be continued to $J' = 0$, yielding the standard results for the mean field theory of a spin 1/2 AFM Heisenberg Hamiltonian.

The fact that we recover exactly the mean field treatment of a *spin* Hamiltonian implies that our way of enforcing the constraint of half-filling is exact already at this simple level of approximation.

We turn now to the general, time-dependent case. In order to evaluate the fermionic determinants in Eqns.(24) and (25) we need to find the eigenvalues of the operators $A^{(i)}$.

Dropping, for the time being, the site index, we consider therefore the eigenvalue problem:

$$(\partial_\tau - \zeta)|u(\tau) > + M(\tau)|u(\tau) >= 0 \tag{42}$$

where: $\zeta = z + \lambda$, λ being the eigenvalue, and:

$$M(\tau) =: \frac{\beta}{2}\vec{\phi}(\tau)\cdot\vec{\sigma}\ ,\ M(0) = M(1) \tag{43}$$

while the eigenvector $|u(\tau) >$ will be assumed to be a two-component spinor obeying antiperiodic (Fermi-type) boundary conditions, i.e.:

$$|u(1) >= -|u(0) > \tag{44}$$

Denoting by λ_k the eigenvalues (as will be seen later, k is actually a multi-index), the fermionic determinant can be evaluated (under reserve of convergence) as:

$$\det A = \exp\left\{\sum_k \ln(\lambda_k)\right\} \tag{45}$$

For example, in the static case it is easy to see that:

$$\lambda_k = \lambda_{nm} = -i\omega_n - z + m\frac{\beta|\vec{\phi}|}{2}\ ,\ m = \pm 1 \tag{46}$$

and the sum over the fermionic frequencies (with the convergence factor of Eq.(23)) as well as over the spin index m yields back the static result of Eq.(31).

It is well known that, due to the fact that the "time" derivative ∂_τ is an *anti-hermitian* operator, "time" evolution in the imaginary time domain is not unitary. Therefore, the norm of the spinor $|u(\tau)>$ need not to be preserved by the time evolution defined by Eq.(42), although, in view of the boundary condition of Eq.(44), which determines the eigenvalues of the problem, the eigenvalues will take care of the fact that the initial and final norms have to be the same.

A formal solution of the problem can be written down rather easily. Indeed, the general solution of Eq.(42) is:

$$|u(\tau)>= e^{\zeta\tau}\tilde{U}(\tau)|u(0)> \tag{47}$$

where, denoting by T the "time" ordering operator in the imaginary time domain, $\tilde{U}(\tau)$ is the (non-unitary) evolution operator:

$$\tilde{U}(\tau) =: T\exp\left\{-\int_0^\tau d\tau' M(\tau')\right\} \tag{48}$$

The boundary condition of Eq.(44) yields then the equation:

$$\det||1 + e^{\zeta}\tilde{U}(1)|| = 0 \tag{49}$$

determining the eigenvalues. For example, in the static approximation:

$$\tilde{U}(\tau) = \exp\{-\tau M\} \; ; \; M = \frac{\beta}{2}\vec{\phi}\cdot\vec{\sigma} \; ; \; \vec{\phi} = const. \tag{50}$$

and it is a simple exercise to show that Eq.(49) yields the spectrum of Eq.(46).

In the general case, however, the previous approach, although exact in principle, is of rather limited use, and we will resort here to a somewhat different strategy following an approach that is due essentially to Berry [23],[24].

Let's begin by making a brief geometrical digression.

A normalized two-component spinor can be represented as:

$$|u>= \left| \begin{array}{c} z_1 \\ z_2 \end{array} \right| \; , \; z_1, z_2 \in C \; , \; |z_1|^2 + |z_2|^2 = 1 \tag{51}$$

Therefore: $|u> \in S^3 \approx SU(2)$. As an element of SU(2), it can be parameterized in a standard way [25] as:

$$\begin{aligned} & z_1 = \cos(\theta/2)\exp[i\chi] \; , \; z_2 = \sin(\theta/2)\exp[i(\chi+\delta)] \; , \\ & 0 \leq \theta \leq \pi \quad , \quad 0 \leq \chi, \delta \leq 2\pi \end{aligned} \tag{52}$$

As is well known, there is a standard fibration, the Hopf fibration [25]-[27]:

$$U(1) \rightarrow S^3 \rightarrow S^2 \tag{53}$$

associated with SU(2), with typical fiber U(1) and projection map:

$$\pi : S^3 \rightarrow S^2 \; , \; |u> \rightarrow \hat{n} \text{ by } : \; \hat{n} = < u|\vec{\sigma}|u > \tag{54}$$

Explicitly: $n_i = \sum_{\alpha,\beta=1,2} z^*_\alpha (\sigma_i)_{\alpha\beta} z_\beta$, and the components of the unit vector $\hat{n} \in S^2$ are given by:

$$\begin{aligned} n_1 &= 2\Re(z_1^* z_2) = \sin\theta\cos\delta \\ n_2 &= 2\Im(z_1^* z_2) = \sin\theta\sin\delta \ , \\ n_3 &= |z_1|^2 - |z_2|^2 = \cos\theta \end{aligned} \tag{55}$$

Coming back to our problem, whenever $\vec{\phi}(\tau) \neq 0$, we can write $M(\tau)$ as:

$$M(\tau) = \Gamma(\tau)\hat{n}(\tau)\cdot\vec{\sigma} \ , \ \Gamma(\tau) =: \frac{\beta|\vec{\phi}(\tau)|}{2} \tag{56}$$

The unit vector $\hat{n}(\tau) \in S^2$ specifies then the direction of $\vec{\phi}(\tau)$ and, as τ varies over the interval $[0,1]$, it will trace a closed path γ on S^2. We will parametrize $\hat{n}$ with polar angles $\theta(\tau)$ and $\delta(\tau)$ as in Eq.(55). In view of the boundary conditions obeyed by $\vec{\phi}(\tau)$, we may assume:

$$\theta(1) = \theta(0) \ \text{ and : } \ \delta(1) = \delta(0) \tag{57}$$

As the eigenvalues of a matrix of the form $\hat{n}\cdot\vec{\sigma}$, with $\hat{n}$ a unit vector, are ± 1, the instantaneous eigenvalues of $M(\tau)$ will be given by: $m\Gamma(\tau)$, $m = \pm 1$. The corresponding *instantaneous* eigenvectors will be denoted by: $|m(\tau)>$, $m = \pm$. Explicitly:

$$|+(\tau)> = e^{i\chi_+} \begin{vmatrix} \cos(\theta/2) \\ e^{i\delta}\sin(\theta/2) \end{vmatrix} \ ; \ |-(\tau)> = e^{i\chi_-} \begin{vmatrix} \sin(\theta/2) \\ -e^{i\delta}\cos(\theta/2) \end{vmatrix} \tag{58}$$

where: $\theta = \theta(\tau)$ and $\delta = \delta(\tau)$ are the polar angles of $\hat{n}(\tau)$, while: $\chi_+ = \chi_+(\tau)$ and $\chi_- = \chi_-(\tau)$ are as yet unspecified overall phases that are not determined by the instantaneous eigenvalue equation for $M(\tau)$.

The instantaneous eigenvectors of $M(\tau)$ are therefore *normalized* spinors. As such, they belong to $S^3 \approx SU(2)$. From now on we will omit explicit mention of the time argument of the instantaneous eigenvectors whenever it is not strictly necessary.

We recall that the Hopf bundle is endowed [25], [27] with a natural connection one-form $\tilde{\Omega}$ defined by:

$$\tilde{\Omega} =: -i < u|d|u > \tag{59}$$

($\tilde{\Omega} = -i \sum_\alpha z_\alpha^\star dz_\alpha$). The proof that $\tilde{\Omega}$ is indeed a connection one-form on a U(1) bundle is standard [26],[27] and will not be repeated here. Explicitly:

$$\tilde{\Omega} = \sin^2(\theta/2) d\delta + d\chi \tag{60}$$

The associated curvature two-form will be:

$$F = d\tilde{\Omega} = \frac{1}{2} \sin\theta d\theta \wedge d\delta \tag{61}$$

F is therefore *projectable* [26] on the base manifold S^2, and represents the field strength of a magnetic monopole of "charge" 1/2 located at the origin of S^2. In other words, the connection form $\tilde{\Omega}$ correspond to the *Pancharatnam connection* [25],[28] on the Hopf bundle.

Following Berry [23], we fix now completely the phases of the instantaneous eigenstates of $M(\tau)$ *by requiring that* $|m(\tau)>$ *be the parallel transported along the path* γ *on* S^2 *of* $|m(0)>$, i.e. that:

$$< m(\tau)|\partial_\tau|m(\tau)>= 0 \tag{62}$$

Explicitly:

$$\begin{aligned} < +|\partial_\tau|+ >&= i\{\partial_\tau\chi_+ + \sin^2(\theta/2)\partial_\tau\delta\} \\ < -|\partial_\tau|- >&= i\{\partial_\tau\chi_- + \cos^2(\theta/2)\partial_\tau\delta\} \end{aligned} \tag{63}$$

For completeness, we report also the remaining matrix elements of ∂_τ, namely:

$$< +|\partial_\tau|- >= -[< -|\partial_\tau|+ >]^* = \frac{1}{2}\exp[i(\chi_- - \chi_+)]\{\partial_\tau\theta - i\sin\theta(\partial_\tau\delta)\} \tag{64}$$

The matrix elements (64) will become useful later.

The parallel transport condition leads therefore to the differential equations:

$$\begin{aligned} \partial_\tau\chi_+ + \sin^2(\theta/2)\partial_\tau\delta &= 0 \\ \partial_\tau\chi_- + \cos^2(\theta/2)\partial_\tau\delta &= 0 \end{aligned} \tag{65}$$

Integrating now from $\tau = 0$ to $\tau = 1$ we find at once:

$$\begin{aligned} \Delta\chi_+ = \chi_+(1) - \chi_+(0) &= -\int_0^1 d\tau \sin^2(\theta/2)\partial_\tau\delta = -\oint_\gamma \sin^2(\theta/2)d\delta \\ \Delta\chi_- &= -\Delta\chi_+ \end{aligned} \tag{66}$$

Finally, using Stoke's theorem, we find:

$$\Delta\chi_+ = -\Delta\chi_- = -\frac{1}{2}\Omega(\gamma) \tag{67}$$

$\Omega(\gamma)$ being the solid angle subtended by the portion of S^2 that is bounded by γ in the positive sense.

In this way we find that the parallel transport condition leads to:

$$|m(1)>= \exp[-im\Omega(\gamma)/2]|m(0)> \tag{68}$$

$\Omega(\gamma)$ (or, better, $\Omega(\gamma)/2$) is of course the *holonomy* [26], or the *Berry phase* [28]-[31], associated with the connection form (59).

The matrix $M(\tau)$ is diagonalized by the unitary matrix:

$$U(\tau) = \begin{vmatrix} e^{-i\chi_+}\cos(\theta/2) & e^{-i(\chi_+ + \delta)}\sin(\theta/2) \\ e^{-i\chi_-}\sin(\theta/2) & -e^{-i(\chi_- + \delta)}\cos(\theta/2) \end{vmatrix} \tag{69}$$

($\theta = \theta(\tau)$, $\delta = \delta(\tau)$, $\chi_\pm = \chi_\pm(\tau)$), i.e.:

$$U(\tau)\cdot M(\tau)\cdot U^\dagger(\tau) = \Gamma(\tau)\sigma_3 \tag{70}$$

It follows from the parallel transport condition that:

$$U(1) = \exp[i\Omega(\gamma)\sigma_3/2]\cdot U(0) \tag{71}$$

Defining now:

$$|\psi(\tau)>=: U(\tau)|u(\tau)> \tag{72}$$

we find that $|\psi>$ obeys the differential equation:

$$(\partial_\tau - \zeta + \Gamma(\tau)\sigma_3)|\psi(\tau)>=[(\partial_\tau U(\tau))\cdot U^\dagger(\tau)]|\psi(\tau)> \tag{73}$$

with the boundary condition:

$$|\psi(1)>=-\exp[i\Omega(\gamma)\sigma_3/2]|\psi(0)> \tag{74}$$

Explicitly, we find:

$$(\partial_\tau U(\tau))\cdot U^\dagger(\tau) = -\begin{vmatrix} 0 & <+|\partial_\tau|->\\ <-|\partial_\tau|+> & 0\end{vmatrix} \tag{75}$$

where the matrix elements $<\pm|\partial_\tau|\mp>$ are given by Eq.(64) and the diagonal matrix elements vanish by virtue of the parallel transport condition.

The *adiabatic approximation* amounts to neglecting the off-diagonal terms, and hence altogether the r.h.s. of Eq.(73). Within this approximation the general solution of the equation is easily found to be:

$$|\psi(\tau)>=\exp\left\{\zeta\tau-\int_0^\tau d\tau'\Gamma(\tau')\sigma_3\right\}|\psi(0)> \tag{76}$$

Imposing the boundary condition (74), we find the equation determining the eigenvalues in the form:

$$\det||1+\exp[\zeta-\tilde{\Gamma}\sigma_3]|| = 0 \tag{77}$$

where 1 is the identity 2×2 matrix and:

$$\tilde{\Gamma} =: \int_0^1 d\tau\Gamma(\tau)+\frac{1}{2}i\Omega(\gamma) \tag{78}$$

The eigenvalues are then easily found to be:

$$\lambda_{nm} = -i\omega_n - z + m\tilde{\Gamma} \; ; \; -\infty < n < +\infty \; , \; m = \pm 1 \tag{79}$$

It is apparent from Eqns. (76) and (79) that the norm of $|\psi(\tau)>$ (and hence of $|u(\tau)>$, which is unitarily related to $|\psi(\tau)>$) will not be a constant except in the static approximation, when: $\vec{\phi}(\tau) = const. = \vec{\phi}$ implies that γ reduces to a point, $\Omega(\gamma) = 0$ and: $\Gamma(\tau) = const. = \beta|\vec{\phi}|/2$.

We can perform now the summation over the Matsubara frequencies and the spin indices just as in the case of the static approximation, thus finding:

$$\sum_{nm} e^{i\omega_n 0^+} \ln \lambda_{nm} = \ln\{1 + e^{2z} + 2e^z \cosh(\tilde{\Gamma})\} \tag{80}$$

Implementing then the constraint, the final result for the partition function, within the adiabatic approximation, is:

$$\mathcal{Z} = \mathcal{N} \int \{\prod_{i\tau} d\vec{\phi}_i(\tau)\}$$
$$\exp\left\{\frac{\beta}{2}\sum_{ij}\left(\tilde{J}^{-1}\right)_{ij}\int_0^1 d\tau \vec{\phi}_i(\tau)\cdot\vec{\phi}_j(\tau)\right\}\prod_i\left\{2\cosh\left(\tilde{\Gamma}_i\right)\right\} \tag{81}$$

Again, after the implementation of the constraint, this result is the same that would be obtained, at the same level of approximation, starting directly from a spin 1/2 Heisenberg Hamiltonian [22].

Now we can try to iterate the scheme that has led to the adiabatic approximation.

Eq.(73) can be rewritten as:

$$[\partial_\tau - \zeta + \tilde{M}(\tau)]|\psi(\tau)>= 0 \tag{82}$$

where:

$$\tilde{M} = \begin{vmatrix} \Gamma & \eta \\ -\eta^\star & -\Gamma \end{vmatrix} \quad \eta =:< +|\partial_\tau|- > \quad . \tag{83}$$

Note that in view of Eqns.(55,64):

$$|\eta|^2 = |\partial_\tau \hat{n}|^2/4 \tag{84}$$

The nonunitarity of the "time" evolution brings about one major difference with the previous step as well as with Berry's iteration scheme. Indeed, $\tilde{M}$ is manifestly *non-hermitian*. We will see in a short while what are the consequences of this fact.

As (cfr. Eqns.(64,67)) $\eta(1) = \exp(i\Omega(\gamma))\eta(0)$, $\tilde{M}$ obeys now the boundary conditions:

$$\tilde{M}(1) = e^{i\Omega(\gamma)\sigma_3/2}\tilde{M}(0)e^{-i\Omega(\gamma)\sigma_3/2} \tag{85}$$

(while, previously, $M(\tau)$ was periodic over the interval $[0,1]$).

The eigenvalues of $\tilde{M}$ are easily found to be given by:

$$\Lambda_m(\tau) = m\Lambda(\tau)\ ; m = \pm\ ,\ \Lambda = \sqrt{\Gamma^2 - |\eta|^2} \tag{86}$$

Now we argue (see,e.g.,Ref.[22] for a discussion of this point) that paths that are relevant in the functional integral correspond to non-vanishing Hubbard-Stratonovich fields. We will also limit our analysis to the low temperature regime of the model. This leads us to assume that: $\Gamma >> |\eta|$ for all relevant paths, and therefore that the eigenvalues of $\tilde{M}$ are real and distinct.

The main reason for restricting ourselves to the low temperature region is that β is the "time" the auxiliary field takes to come back to its initial value. In an adiabatic expansion it is therefore β that plays the role of the adiabatic parameter, and the expansion is expected to possibly make sense only in the asymptotic region $\beta \sim \infty$.

Up to now we have obtained contributions to the effective action that are $\mathcal{O}(\beta)$ (the first term in Eq.(78)) and $\mathcal{O}(1)$ (the Berry phase). Our aim in what follows will be to obtain in a consistent way all the contributions up to terms that are $\mathcal{O}(\beta^{-1})$.

The instantaneous eigenvectors of $\tilde{M}$ will be denoted by $|\xi_m(\tau)>$. Omitting again for brevity the explicit mention of the time argument, they are given by:

$$|\xi_m >= e^{i\tilde{\chi}_m} \left| \begin{array}{c} -\eta a_m \\ b_m \end{array} \right| \tag{87}$$

where:

$$a_m = [2\Gamma(\Gamma - \Lambda_m)]^{-1/2} \ , \ b_m = \left[\frac{\Gamma - \Lambda_m}{2\Gamma}\right]^{1/2} \tag{88}$$

and the $\tilde{\chi}_m$'s are again as yet undetermined phases.

It is very easy to check that the eigenvectors are normalized,i.e.:

$$< \xi_m | \xi_m >= a_m^2 |\eta|^2 + b_m^2 = 1 \ , \ m = \pm \tag{89}$$

while:

$$\mu =:< \xi_+ | \xi_- >= \frac{|\eta|}{\Gamma} \exp[i(\tilde{\chi}_- - \tilde{\chi}_+)] = \exp[i(\tilde{\chi}_- - \tilde{\chi}_+)](|\eta|^2 a_+ a_- + b_+ b_-) \tag{90}$$

The nonorthogonality of the eigenvectors follows directly from the non-hermiticity of $\tilde{M}$. Indeed, with real eigenvalues, orthonormality of the eigenvectors implies hermiticity and viceversa.

It is easy to prove that, with:

$$\Delta\tilde{\chi}_m = \tilde{\chi}_m(1) - \tilde{\chi}_m(0) \tag{91}$$

the $|\xi_m >$'s obey the boundary conditions:

$$|\xi_m(1) >= \exp[i(\Delta\tilde{\chi}_m + \Omega(\gamma)/2)] \exp[i\Omega(\gamma)\sigma_3/2] |\xi_m(0) > \tag{92}$$

The boundary conditions depend therefore on the way the phases $\tilde{\chi}_m$ are determined.

Together with the non-orthogonal basis of the eigenvectors of $\tilde{M}$, we can introduce the dual basis $\{|\eta_m>\}$ defined, as usual, through:

$$<\eta_m|\xi_n>=\delta_{m,n} \tag{93}$$

this fixes the $|\eta_m>$'s uniquely, and they turn out to be given by:

$$\begin{aligned} |\eta_+>&=\frac{1}{1-|\mu|^2}(|\xi_+>-\mu^*|\xi_->) \\ |\eta_->&=\frac{1}{1-|\mu|^2}(|\xi_->-\mu|\xi_+>) \end{aligned} \tag{94}$$

Also:

$$<\eta_m|\eta_m>=\frac{1}{1-|\mu|^2}\ ,\ <\eta_+|\eta_->=-\frac{\mu}{1-|\mu|^2} \tag{95}$$

It is easy to prove that the following properties holds, namely:

i) The $|\eta_m>$'s are eigenvectors of $\tilde{M}^\dagger$, i.e.:

$$\tilde{M}^\dagger|\eta_m>=\Lambda_m|\eta_m>\ ,\ m=\pm \tag{96}$$

ii) Though endowed with a nonorthogonal basis, $\tilde{M}$ has a *resolution of the identity* associated with it, i.e.:

$$\sum_m |\eta_m><\xi_m| = \mathbf{1} \tag{97}$$

$\mathbf{1}$ being the identity matrix.

We try now to diagonalize $\tilde{M}$ via a similarity transformation. We look therefore for a nonsingular matrix V such that:

$$V^{-1}\tilde{M}V=\Lambda\sigma_3 \tag{98}$$

Denoting by $\{|x_m>\}$ the standard basis $\left(|x_+>=\begin{pmatrix}1\\0\end{pmatrix}\ ,\ |x_->=\begin{pmatrix}0\\1\end{pmatrix}\right)$, it is again not difficult to check that we can choose:

$$V=\sum_m |\xi_m><x_m|$$
$$V^{-1}=\sum_m |x_m><\eta_m| \tag{99}$$

Note that the solution (99) is not unique. Indeed, if: $V=V(\tau)$ is a solution of (98), then any other matrix of the form $V(\tau)\exp(\lambda(\tau)\sigma_3)$, with λ an arbitrary (real or complex) function of τ will solve (98) as well.

We are now ready to iterate the previous scheme. Defining a new spinor $|\varphi(\tau)>$ via:

$$|\psi(\tau)>=V(\tau)|\varphi(\tau)> \tag{100}$$

eq.(82) yields the following equation for $|\varphi>$:

$$(\partial_\tau-\zeta+\Lambda\sigma_3)|\varphi>=-(V^{-1}\partial_\tau V)|\varphi> \tag{101}$$

with the boundary conditions:

$$|\varphi(1)>=-\left[V^{-1}(1)e^{i\Omega\sigma_3/2}V(0)\right]|\varphi(0)> \tag{102}$$

Explicitly the matrix on the r.h.s. of eq.(101) is given by:

$$V^{-1}\partial_\tau V=\begin{pmatrix}<\eta_+|\partial_\tau|\xi_+> & <\eta_+|\partial_\tau|\xi_->\\ <\eta_-|\partial_\tau|\xi_+> & <\eta_-|\partial_\tau|\xi_->\end{pmatrix} \tag{103}$$

Eq.(103) suggests that we try to generalize the parallel transport condition by requiring the λ_m's to be determined by the equations:

$$<\eta_m|\partial_\tau|\xi_m>=0\ ,\ m=\pm \tag{104}$$

We can show however that imposing the conditions (104) leads to inconsistencies. Indeed, we have:

$$< \eta_+|\partial_\tau|\xi_+ >= \frac{1}{1-|\mu|^2}\{< \xi_+|\partial_\tau|\xi_+ > -\mu < \xi_-|\partial_\tau|\xi_+ >\} \qquad (105)$$

and a similar equation for $< \eta_-|\partial_\tau|\xi_- >$, that can be obtained form (105) by changing pluses into minuses (and viceversa), and replacing μ with $\mu^\star$.

The conditions (104) lead therefore to the would-be parallel transport equations:

$$\begin{aligned} &< \xi_+|\partial_\tau|\xi_+ > -\mu < \xi_-|\partial_\tau|\xi_+ >= 0 \\ &< \xi_-|\partial_\tau|\xi_- > -\mu^\star < \xi_+|\partial_\tau|\xi_- >= 0 \end{aligned} \qquad (106)$$

With some algebra and a careful use of Eqns.(89,90), we obtain:

$$< \xi_m|\partial_\tau|\xi_m >= i(\partial_\tau\tilde{\chi}_m) + \frac{1}{2}a_m^2(\eta^*\partial_\tau\eta - \eta\partial_\tau\eta^*) \ , \ m = \pm \qquad (107)$$

and:

$$\begin{aligned} &< \xi_+|\partial_\tau|\xi_- >= i(\partial_\tau\tilde{\chi}_-) < \xi_+|\xi_- > + \\ &+e^{i(\tilde{\chi}_- - \tilde{\chi}_+)}\{|\eta|^2 a_+\partial_\tau a_- + b_+\partial_\tau b_- + a_-a_+\eta^*\partial_\tau\eta\} \\ &< \xi_-|\partial_\tau|\xi_+ >= i(\partial_\tau\tilde{\chi}_+) < \xi_-|\xi_+ > + \\ &e^{i(\tilde{\chi}_+ - \tilde{\chi}_-)}\{|\eta|^2 a_-\partial_\tau a_+ + b_-\partial_\tau b_+ + a_-a_+\eta^*\partial_\tau\eta\} \end{aligned} \qquad (108)$$

Putting things together, the explicit form of Eqns.(106) turns out to be:

$$i(\partial_\tau\tilde{\chi}_+)(1-|\mu|^2) + \frac{1}{2}a_+^2(\eta^*\partial_\tau\eta - \eta\partial_\tau\eta^*) =$$

$$= |\mu|(|\eta|^2 a_- \partial_\tau a_+ + b_- \partial_\tau b_+ + a_- a_+ \eta^* \partial_\tau \eta)$$

$$i(\partial_\tau \tilde{\chi}_-)(1 - |\mu|^2) + \frac{1}{2} a_-^2 (\eta^* \partial_\tau \eta - \eta \partial_\tau \eta^*) =$$

$$= |\mu|(|\eta|^2 a_+ \partial_\tau a_- + b_+ \partial_\tau b_- + a_- a_+ \eta^* \partial_\tau \eta) \qquad (109)$$

Defining now $X = \tilde{\chi}_+ + \tilde{\chi}_-$, we obtain for X the equation:

$$i(\partial_\tau X)(1 - |\mu|^2) + \frac{1}{2}(a_+^2 + a_-^2 - 2|\mu| a_- a_+)(\eta^* \partial_\tau \eta - \eta \partial_\tau \eta^*) = \frac{1}{2} \partial_\tau |\mu|^2 \quad (110)$$

If the phases are real, as they should, then the l.h.s. of eq.(110) is purely imaginary, and eq.(110) will make sense only for $|\mu| = const.$, which is not likely (to say the least) to be true for a generic path.

We conclude therefore that we are not allowed to impose the parallel transport conditions in the form (104), and that we have to resort to the more conventional ones, namely:

$$< \xi_m | \partial_\tau | \xi_m >= 0 \ , \ m = \pm \qquad (111)$$

The explicit form of Eqns.(111) is:

$$i(\partial_\tau \tilde{\chi}_m) + \frac{1}{2} a_m^2(\tau)(\eta^* \partial_\tau \eta - \eta \partial_\tau \eta^*) = 0 \ , \ m = \pm \qquad (112)$$

and they integrate to:

$$\Delta \tilde{\chi}_m = \frac{i}{2} \int_0^1 d\tau a_m^2(\tau)(\eta^* \partial_\tau \eta - \eta \partial_\tau \eta^*) \ , \ m = \pm \qquad (113)$$

Up to now everything has been exact. We will discuss now the low temperature expansion that has been alluded to previously. We have argued already

that, at low temperatures, we expect $\Gamma >> |\eta|$ for all relevant paths. One can argue furthermore that, at low temperatures and hence at low energies, the functional integral over $|\vec{\phi}(\tau)|$ will be dominated by a nonzero saddle point with fluctuations around it being high in energy and hence unimportant ([32], [33] for a similar discussion and [2], Ch.6 for a review). This implies that we can consider: $\Gamma(\tau) = \beta|\vec{\phi}(\tau)|/2$ as approximately constant, and that we can use an expansion in inverse powers of Γ as a power-counting device to single out the dominant contributions at low temperatures. Proceeding then as outline above, we obtain:

$$a_+^2 = \frac{1}{2\Gamma(\Gamma - \Lambda)} \simeq \frac{1}{|\eta|^2}(1 + \mathcal{O}(|\mu|^2)) \; ; \; |\mu| = \frac{|\eta|}{\Gamma} \tag{114}$$

$$a_-^2 = \frac{1}{2\Gamma(\Gamma + \Lambda)} \simeq \frac{1}{4\Gamma^2}(1 + \mathcal{O}(|\mu|^2)) = \mathcal{O}(\beta^{-2}) \tag{115}$$

Neglecting then a_-^2, we obtain: $\Delta\tilde{\chi}_- \simeq 0$ and:

$$\Delta\tilde{\chi}_+ \simeq \frac{i}{2}\int_0^1 d\tau \frac{\eta^\star\partial_\tau\eta - \eta\partial_\tau\eta^\star}{|\eta|^2} = -\oint_\gamma d(\arg\eta) = -\Delta(\arg\eta) \tag{116}$$

But we see from Eq.(64) that: $\eta = \exp[i(\chi_- - \chi_+)]\times$ (a periodic function of τ). Hence: $\Delta(\arg\eta) = \Omega(\gamma)$, and we obtain:

$$\Delta\tilde{\chi}_+ = -\Omega(\gamma) \; , \; \Delta\tilde{\chi}_- = 0 \tag{117}$$

upto correction terms that are at least $\mathcal{O}(\beta^{-2})$. Using this result in the boundary condition (102) we find:

$$V^{-1}(1)e^{i\Omega(\gamma)\sigma_3/2}V(0) = \sum_{m,n} |x_m >< \eta_n(1)|e^{i\Omega(\gamma)\sigma_3/2}|\xi_n(0) >< x_n| \tag{118}$$

and, upon using Eqns.(92) and (117):

$$V^{-1}(1)e^{i\Omega(\gamma)\sigma_3/2}V(0) = e^{i\Omega(\gamma)\sigma_3/2} \tag{119}$$

again up to corrections that are $\mathcal{O}(\beta^{-2})$.

If we turn now back to Eqns.(109), we see that the $|\mu|^2$ on the l.h.s. can be neglected. Also, some simple power counting shows that the r.h.s. of both equations is of order $\Gamma^{-2} \sim \beta^{-2}$, and hence can be neglected as well. Incidentally, this is consistent with the r.h.s. of Eq.(110) being $(\partial_\tau|\mu|^2)/2 = \mathcal{O}(\Gamma^{-2})$.

We conclude then that, to leading order in an expansion in $1/\beta$ (i.e. up to order β^{-1}), Eqns. (104) and (111) are actually equivalent. Therefore, and to the same order, the parallel transport condition leads to the vanishing of the diagonal elements of $V^{-1}\partial_\tau V$.

We can now proceed by iteration. Neglecting off-diagonal elements, the r.h.s. of Eq.(101)can be ignored altogether and we obtain:

$$|\varphi(\tau)>= \exp\left\{\zeta\tau - \sigma_3\int_0^\tau \Lambda(\tau')d\tau'\right\}|\varphi(0)> \tag{120}$$

Imposing then the boundary conditions, we easily find the eigenvalues to be:

$$\lambda_{n,m} = -i\omega_n - z + m\left(\int_0^1 d\tau\Lambda(\tau) + i\Omega(\gamma)/2\right) \tag{121}$$

To be consistent, we have to expand $\Lambda(\tau)$ as well in powers of $|\mu|$. This

yields:

$$\int_0^1 d\tau \Lambda(\tau) = \int_0^1 d\tau \Gamma(\tau) - \frac{1}{8}\int_0^1 d\tau \frac{|\partial_\tau \hat{n}|^2}{\Gamma(\tau)} + ... \tag{122}$$

where we have used Eq.(84). Note that the last term in Eq.(122) is $\mathcal{O}(\Gamma^{-1}) \approx \mathcal{O}(\beta^{-1})$

Defining then:

$$\hat{\Gamma} = \int_0^1 d\tau \Gamma(\tau) + i\Omega(\gamma)/2 - \frac{1}{8}\int_0^1 d\tau \frac{|\partial_\tau \hat{n}|^2}{\Gamma(\tau)} \tag{123}$$

we see that we can write the partition function as in Eq.(81) by simply replacing $\tilde{\Gamma}_i$ there with $\hat{\Gamma}_i$. As, in the low temperature limit: $2\cosh\hat{\Gamma}_i \simeq \exp\hat{\Gamma}_i$, we obtain eventually, after implementing the constraint:

$$\mathcal{Z} = \mathcal{N}\int \{\prod_{i,\tau} d\vec{\phi}_i(\tau)\} \exp\left\{\frac{\beta}{2}\sum_{i,j}(\tilde{J}^{-1})_{ij}\int_0^1 d\tau \vec{\phi}_i(\tau)\cdot\vec{\phi}_j(\tau)\right\} \exp\left\{\sum_i \hat{\Gamma}_i\right\} \tag{124}$$

To make more contact with the results of the literature [22],[24], let us remark that, by introducing the (instantaneous) transverse projector:

$$M_{\mu\nu}(\tau) = \frac{1}{2|\vec{\phi}(\tau)|^3}(\delta_{\mu,\nu} - n_\mu n_\nu) \ , \ \mu,\nu = 1,2,3 \tag{125}$$

we can recast the integrand in the last term of $\hat{\Gamma}$ as:

$$\frac{1}{8}\frac{|\partial_\tau \hat{n}|^2}{\Gamma(\tau)} = \frac{1}{2\beta} M_{\mu\nu}(\partial_\tau \phi^\mu)(\partial_\tau \phi^\nu) \tag{126}$$

Rewriting Eq.(124) in the form:

$$\mathcal{Z} = \mathcal{N}\int \{\prod_{i,\tau} d\vec{\phi}_i(\tau)\} \exp\left\{S_{eff}[\vec{\phi}_i(\tau)]\right\} \tag{127}$$

we may conclude that the effective action we have obtained, i.e.:

$$S_{eff}[\vec{\phi}_i(\tau)] = \frac{\beta}{2}\sum_{i,j}(\tilde{J}^{-1})_{ij}\int_0^1 d\tau\vec{\phi}_i(\tau)\cdot\vec{\phi}_j(\tau) + \sum_i \hat{\Gamma}_i \qquad (128)$$

contains all the contributions up to order β^{-1} to the action. Again, after implementing the constraint, we obtain a result that matches exactly those that are obtained by starting directly from a spin Hamiltonian ([22]). In view of this, we can simply borrow from the analysis of the latter that has already been done by other authors. In particular, a continuum limit followed by a gradient expansion ([18], [22],[31]) will yield a map of the low-energy, low-temperature sector of the Hubbard model onto an O(3) nonlinear σ-model. As long as one considers fluctuations around an ordered AFM background, the Berry phase term will contribute a topological, Wess-Zumino term to the action in 1D. It is well known (see [25] and literature quoted therein) that the topological term is of the form:

$$2\pi i S Q \ , \ Q = \frac{1}{8\pi}\int d^2x\epsilon^{\mu\nu}\hat{n}\cdot(\partial_\mu\hat{n}\times\partial_\nu\hat{n}) \qquad (129)$$

where S is the spin and Q, the Pontrjagin index [27] is an integer labeling the homotopy classes of paths from compactified spacetime, i.e. S^2, to the space of fields values, S^2 again, and that are classified by $\pi_2(S^2) = Z$ [25],[27]. As, in the present case,$S = 1/2$, the topological term (129) will impart opposite signs to the contributions to the functional integral (127) coming from odd and even homotopy classes respectively. According to Haldane [34] this im-

plies that the spectrum of elementary excitations in the low energy sector of the 1D Hubbard model will be gapless, and that the model will be disordered at low temperatures with only (or at most) algebraic LRO. According to Eq. (123) we expect the wave velocity of the elementary excitations (the "speed of light" of the NLσ model) to scale as the square root of Γ, and hence to go "soft" at the transition point predicted by the saddle-point approximation, where Γ vanishes.

Affleck [35] has also analyzed the 1D Hubbard model at half filling. He finds both a gapless spectrum for spin excitations *and* a gapped spectrum for charge excitations in the continuum limit. However, Affleck's definition of half filling is that there should be *as many electrons as lattice sites.* As such, it corresponds to a *weak* half filling condition, namely to:

$$< n_i >= 1 \tag{130}$$

and *not* to the stronger operator condition (2). As, in our approach, we are *strictly* projecting out all double occupancies, we are projecting out the charge excitations as well, which belong in a higher energy sector.

Again in the continuum limit, the topological term will vanish in 2D when considering fluctuations around an ordered AFM background, as can be inferred from related treatments [22], [36]-[41] of spin models. As our results match exactly those of the above references, a separate proof of the

vanishing of the topological (Hopf) term seems to be superfluous. From Refs.[38]-[41] it can be inferred also that frustration and/or doping are not likely to help in stabilizing a Hopf term in the effective action of the 2D model. Parenthetically, this seems to shed a negative light on the hopes that have been nourished for quite some time (see [2] for a review) that the elementary excitations of the (doped) 2D Hubbard model might obey anyon statistics [25],[42] and hence that the model might also exhibit anyonic superconductivity [43],[44]. That the model at half filling should show no presence of topological terms in the effective action had also been argued previously [45] in a rather different context (that of the so-called "s-wave flux phases"). However, below half filling the Hubbard Hamiltonian contains, besides the hopping term and the Heisenberg term (the two together making up for the t-J model [8]), a three-site hopping term ([2] Ch.2) that is usually neglected mainly on the grounds that it is proportional to a higher power of the doping fraction than the hopping term itself. The authors of Refs.[45] have argued that it is precisely this term that could provide in the continuum limit the missing Hopf term in the effective action. The rather preliminary analysis of Ref.[45] has not been pursued any further, though, and therefore the existence of a Hopf (or Abelian Chern-Simons) term in the effective action of the 2D Hubbard model is still to some extent an open question.

It is certainly rewarding that the analysis presented here matches rather

well results that have been obtained on related models and/or by different techniques. However, we would like to make some concluding remarks concerning some serious problems that seem to emerge from what we have done up to now and that cannot be overlooked, namely:

i) Immediately after the adiabatic approximation, i.e. already at the stage of Eq.(81) and presumably even more at further stages, we have been forced to deal with *non−hermitian* matrices. That we should be able to diagonalize a matrix such as $\tilde{M}$ is a crucial step in in any adiabatic (or "superadiabatic" [23]) step of approximation but, of course, that a non-hermitian matrix can be diagonalized is by no means granted "a priori". Should at some step the equivalent of $\tilde{M}$ fail to be diagonalizable, then the entire iteration scheme would break down and we would be either lost or would have to resort to some other kind of approach. On the other hand, let's recall that the fact that $\tilde{M}$ had distinct eigenvalues (which is in turn a sufficient condition for diagonalizability) stemmed from the assumption that $\Gamma >> |\eta|$, i.e. it was granted in the low temperature regime. As we expect the adiabatic iteration procedure to produce a series expansion (actually an asymptotic series [23]) in β^{-1}, we may expect also that this low temperature expansion will avoid the occurrence of such catastrophes as the one envisaged before.

It seems quite clear to us that this difficulty that may or may not show up at some stage, is not to be blamed on the specific model we are using nor

on the fermionization procedure. It rather stems directly from the already stressed fact that evolution in the imaginary-time domain is non-unitary. As such the same difficulty should be present (or hidden somewhere) also in other related models in Statistical Mechanics that start directly from spin Hamiltonians without going through fermions.

ii) The second point which looks a bit puzzling to us concerns the status of a purely imaginary term like the Berry phase in an effective (Euclidean type) action which should be eventually inserted into a functional integral to yield a partition function. After all, in a thermodynamic context every respectable partition function is supposed to be *real and positive*, as its logarithm should yield a "bona fide" (real) free energy. It is true that in the continuum limit the Berry phase contribution either disappears altogether (thus making the problem a nonexistent one) or gives rise (as in 1D) to a topological action. The latter being quantized, there are no complex contributions to the partition function. However, contributions from different topological sectors may came with different signs. We can only argue that the functional integral should be dominated by the positive contributions (in particular by the trivial topological sector), but this has to be checked at least on specific models and/or approximations.

Worse than that, if we do *not* insist on the continuum limit and stick to a lattice, the Berry phase is there and gives geometrical but not topological

contributions to the effective action and to the partition function.

Fortunately, as can be easily demonstrated, Berry's phase is *odd* (mod 4π) under parity ($\vec{\phi}_i \to -\vec{\phi}_i$ for all i's), while the gaussian term in the effective action is manifestly even. It follows then that only the contributions from the real part of the Berry phase term will survive in the partition function. A sign problem remains here too, though. Concerning this, we can only argue as follows: the functional integral is most often evaluated by performing a saddle point expansion around the saddle point, mean field solutions, i.e. by adding one-loop, two-loop corrections and so forth.

The saddle point solution, being static, will have of course a vanishing Berry phase, and we may expect that the solid angle subtended by the path spanned by $\hat{n}(\tau)$ will increase with the order of approximation, so that the loop expansion of the partition function should be dominated by contributions coming from small enough solid angles to ensure positivity of the final result.

All in all, we have pointed out some interesting results that come out from our approach to the half-filled Hubbard model as well as some (at least for us) conceptual difficulties that are connected with the method employed here and that other, related models should share as well. We have been able to put forward only at best slightly more than hand-waving arguments towards a solution in the positive of the aforementioned difficulties. To the best of

our knowledge, neither kind of difficulty has been discussed in the available literature, and we believe that both of them deserve further attention and investigation.

ACKNOWLEDGEMENTS. One of the authors (GM) would like to thank the JNCASR, and especially Profs. V. Krishnan and N.Mukunda, for inviting him as a guest scientist, and the CTS for the hospitality that was extended to him during his stay in Bangalore where part of this work was carried on.

Work partially supported by CNR, INFM, INFN and the Italian MURST.

References

[1] J.Hubbard, Proc. Roy. Soc. A**276**, 238 (1963); A**277**, 237 (1964); A**281**, 401 (1964)

[2] For a recent review, see: A.P.Balachandran, E.Ercolessi, G.Morandi, A.M.Srivastava: "Hubbard Model and Anyon Superconductivity". Lect. Notes in Physics vol. 38. World Scientific, Singapore, 1990.

[3] N.F.Mott, Adv. Math. Phys. **3**, 76 (1952); Canad. J. Phys. **34**, 1356 (1956)

[4] M.Cyrot, J. Phys. (Paris) **33**, 125 (1972)

[5] K.A.Chao, J.Spalek, A.M.Oles, J. Phys. C **10**, L271 (1977); Phys. Rev. B **18**, 3453 (1978)

[6] J.Spalek, Phys. Rev. B**37**, 539 (1978)

[7] A.H.Mac Donald, S.M.Girvin, D.Yoshioka, Phys. Rev. B**37**, 9573 (1988)

[8] F.C.Zhang, T.M.Rice, Phys. Rev. B**37**, 3759 (1988)

[9] J.G.Bednorz, K.A.Müller, Z. Phys. B**64**, 188 (1986)

[10] P.W.Anderson, in: "Frontiers and Borderlines in Many-Particle Physics". North-Holland, 1987.

[11] P.W.Anderson, G.Baskaran, Z.Zou, T.Hsu, Phys. Rev. Letters **58**, 2790 (1987)

[12] G.Baskaran, P.W.Anderson, Phys. Rev. B**27**, 580 (1987)

[13] G.Baskaran, Z.Zou, P.W.Anderson, Solid State Comm. **63**, 973 (1987)

[14] M.Gutzwiller, Phys. Rev. A**137**, 1726 (1965)

[15] M.Di Stasio, E.Ercolessi, G.Morandi, A.Tagliacozzo, F.Ventriglia, Phys. Rev. B**45**, 1939 (1992)

[16] M.Di Stasio, Phys. Rev. B**46**, 9825 (1992)

[17] M.Di Stasio, E.Ercolessi, G.Morandi, A.Tagliacozzo, F.Ventriglia, Int. J. Mod. Phys. B **7**,3281 (1993)

[18] J.W.Negele, H.Orland: "Quantum Many-Particle Systems". Addison Wesley, 1988.

[19] N.Read, S.Sachdev Nucl.Phys.B **316**, 609 (1989)

[20] R.L.Stratonovich, Sov. Phys. Doklady **2**, 416 (1958)

[21] J.Hubbard, Phys. Rev. Lett. **3**, 77 (1959)

[22] A.Angelucci, G.Jug, Int. J. Mod. Phys. B**3**, 1069 (1989)

[23] M.V.Berry, Proc. Roy. Soc. A**414**, 31 (1987)

[24] R.Jackiw, Int. J. Mod. Phys. A**3**, 285 (1988)

[25] G.Morandi: "The Role of Topology in Classical and Quantum Physics". Lect. Notes in Physics vol. m7. Springer-Verlag, 1992.

[26] Y.Choquet-Bruhat, C.DeWitt-Morette: "Analysis, Manifolds and Physics". Part I, 2nd Ed.. North-Holland, 1982.

[27] R.Bott, L.Tu: "Differential Forms in Algebraic Topology". Springer-Verlag, 1982.

[28] M.V.Berry, in: "Geometric Phases in Physics". A.Shapere and F.Wilczek Eds. World Scientific, 1989

[29] M.V.Berry, Proc. Roy. Soc. A**392**, 45 (1984)

[30] M.V.Berry, in: "Anomalies, Phases, Defects...". M.Bregola, G.Marmo and G.Morandi Eds. Bibliopolis, Naples, 1990

[31] E.Fradkin: "Field Theories of Condensed-Matter Systems". Addison Wesley, 1991

[32] I.Affleck, Z.Zou, T.Hsu and P.W.Anderson, Phys. Rev. **B38**, 745 (1988)

[33] Z.Zou, Phys. Letters **A131**, 197 (1988)

[34] F.D.M.Haldane, Phys.Rev.Lett. **50**, 1153 (1983) and: Phys.Lett. **A93**, 464 (1983).

[35] I.Affleck, in:"Fields, Strings and Critical Phenomena". E.Brezin and J.Zinn-Justin Eds. North-Holland, 1989.

[36] A.Muramatsu, R.Zeyher, Nucl. Phys. B**346**, 387 (1990)

[37] A.Muramatsu, Phys. Rev. Lett. **65**, 2909 (1990)

[38] C.Kubert, A.Muramatsu, Phys. Rev. B**47**, 787 (1993)

[39] T.B.Einarsson,H.Johannesson, Phys.Rev.B **43**, 5867 (1991)

[40] T.Dombre, N.Read, Phys.Rev.B **38**, 7281 (1988)

[41] E.Fradkin, M.Stone, Phys. Rev.B **38**, 7215 (1988)

[42] R.Lerda: "Anyons". Springer, 1993.

[43] F.Wilczek (Ed.): "Fractional Statistics and Anyon Superconductivity". World Scientific, 1991. See also: F.Wilczek in: "Anomalies, Phases, Defects..." (Ref. ([30]).

[44] A.Fetter: "Anyons and Anyon Superconductivity". Lectures delivered at the School on:"Low Dimensional QFT for Condensed Matter Physicists". ICTP, Trieste, Summer 1992.

[45] I.J.R. Aitchison, N.E.Mavromatos, Phys.Rev.B **39**, 6544 (1989); Mod.Phys.Lett.A 4, 521 (1989), and: Phys. Rev. Lett. **63**, 2684 (1989).